Vol. 45, No. 1 / 2015

e: ISSN 2068 – 2239
p: ISSN 2068 – 4215

INMATEH – AGRICULTURAL ENGINEERING

JANUARY - APRIL

Editorial

The National Institute of Research-Development for Machines and Installations designed to Agriculture and Food Industry - INMA Bucharest has the oldest and most prestigious research activity in the field of agricultural machinery and mechanizing technologies in Romania.

Short History

- In 1927, the first research **Center for Agricultural Machinery** in Agricultural Research Institute of Romania - ICAR (Establishing Law was published in O.D. no. 97/05.05.1927) was established;
- In 1930, was founded **The Testing Department of Agricultural Machinery and Tools** by transforming Agricultural Research Centre of ICAR - that founded the science of methodologies and experimental techniques in the field (Decision no. 2000/1930 of ICAR Manager - GHEORGHE IONESCU ŞIŞEŞTI);
- In 1952, was established the Research Institute for Mechanization and Electrification of Agriculture - ICMA Băneasa, by transforming the Department of Agricultural Machines and Tools Testing;
- In 1979, the Research Institute of Scientific and Technological Engineering for Agricultural Machinery and Tools – ICSITMUA was founded - subordinated to Ministry of Machine Building Industry - MICM, by unifying ICMA subordinated to MAA with ICPMA subordinated to MICM;
- In 1996 the National Institute of Research-Development for Machines and Installations designed to Agriculture and Food Industry – INMA was founded – according to G.D. no.1308/25.11.1996, by reorganizing ICSITMUA, G.D no. 1308/1996 coordinated by the Ministry of Education and Research G.D. no. 823/2004;
- In 2008 INMA has been accredited to carry out research and developing activities financed from public funds under G.D. no. 551/2007, Decision of the National Authority for Scientific Research - ANCS no. 9634/2008.

As a result of widening the spectrum of communication, dissemination and implementation of scientific research results, in 2000 was founded the institute magazine, issued under the name of SCIENTIFIC PAPERS **(INMATEH)**, ISSN 1583 – 1019.

Starting with volume 30, no. 1/2010, the magazine changed its name to **INMATEH - Agricultural Engineering**, appearing both in print format (ISSN 2068 - 4215), and online (ISSN online: 2068 - 2239). The magazine is bilingual, being published in Romanian and English, with a rhythm of three issues / year: January-April, May-August, September-December and is recognized by CNCSIS – with B^+ category. Published articles are from the field of AGRICULTURAL ENGINEERING: technologies and technical equipment for agriculture and food industry, ecological agriculture, renewable energy, machinery testing, environment, transport in agriculture etc. and are evaluated by specialists inside the country and abroad, in mentioned domains.

Technical level and performance processes, technology and machinery for agriculture and food industry increasing, according to national requirements and European and international regulations , as well as exploitation of renewable resources in terms of efficiency, life, health and environment protection represent referential elements for the magazine „**INMATEH - Agricultural Engineering**".

We are thankful to all readers, publishers and assessors.

Editor in chief,
Ph. D. Eng. Pirnă Ion

Managing Editorial Board - INMA Bucharest

In the present, *INMATEH - Agricultural Engineering* journal is indexed in the next international databases:
ULRICHSWeb: Global Serials Directory, CABI, SCIPIO, ELSEVIER /SciVerse SCOPUS, Index COPERNICUS International, EBSCO Publishing, Elektronische Zeitschriftenbibliothek

INMATEH - Agricultural Engineering
vol. **45**, no. **1** / **2015**
NATIONAL INSTITUTE OF RESEARCH-DEVELOPMENT FOR MACHINES AND INSTALLATIONS DESIGNED TO AGRICULTURE AND FOOD INDUSTRY - INMA Bucharest
6 Ion Ionescu de la Brad Blvd., sector 1, Bucharest
Three issues per year,
e ISSN: 2068 – 2239
p ISSN: 2068 – 4215
Edited by: INMA Bucharest

CUPRINS / *CONTENTS*

A MECHANIZED TECHNIQUE OF ECOLOGICAL SOIL PLANTING FOR THE ANNUAL DOUBLE CROPPING OF WHEAT AND MAIZE WITH A FIVE-YEAR CYCLE
/
适合小麦玉米一年两熟五年一周期的机械化生态沃土种植技术研究

Ph.D. Guohai Zhang, Prof. Ruicheng Du, Prof. Ph.D. Peisong Diao, Prof. Ph.D. Duanyang Geng
School of Agricultural Engineering and Food Science, Shandong University of Technology, Zibo / China
Tel: +86 533 2789896; Email: guohz@163.com

Abstract: *An ecological soil planting method was proposed for the annual double cropping of wheat and maize with a five-year cycle. This method is suitable for Huang-Huai-Hai Region and aims to address the problems of reduced crop yield and soil crust as a result of soil and water loss, deteriorated land fertility, and protective tillage in intensive cultivation. Moreover, the planting specifications of the annual double-cropping rotation patterns of wheat and maize were unified, and the key agricultural equipment was designed for full mechanization. Research results on the test demonstration base showed that the return of straw to the field and scientific fertilization can limit the emissions of harmful gas and the use of fertilizer. Furthermore, these steps can enhance ecological agricultural production. The return of straw to the field and suitable cultivation can increase the content of organic matters in soil, improve the aggregate structure, and enhance soil fertility. Finally, the implementation of the ecological fertile soil planting technique can overcome the disadvantages of intensive cultivation and protective tillage, thereby facilitating stable and high crop yield.*

Keywords: *Intensive cultivation; protective tillage; planting specification; Agricultural mechanization*

INTRODUCTION

The population of China comprises 18.84% of the world population. However, its arable land constitutes only 8.7% of that of the world. As a result, the development pattern of high agricultural yield involves a gradual increase in labor input-intensive cultivation. Intensive cultivation is essentially for a comprehensive technological system of traditional agriculture. In line with this knowledge, a series of studies has been conducted on intensive cultivation technology and its development. The results indicate that although intensive cultivation improves crop yield and solves the employment problem, it also induces soil erosion, environmental degradation, and other problems [1], [3], [5-7], [12], [20]. This process can also significantly reduce the earthworm population[6-7], as well as affect organic matter content, enzyme activities, microbial quantity, the abundance of fungal mycelium, the functional diversity of microbes, the abundance of bacterial species, and other soil properties[3],[7]. The increase in cropping intensity eliminated the self-protection function and activity of soil. In addition, straw burning enhanced atmospheric pollution.

Strong black storms hit the western US and the former Soviet Union in the 20th century. Many experiments have been conducted on sandstorm treatment, and they confirmed that protective tillage is the most successful suppression method [10]. Research on this method

摘要: *提出了一种合适小麦玉米一年两熟的五年一周期的生态土壤种植方法。本方法适合黄淮海地区，目的是解决精耕细作存在的水土流失、土地肥力减退和保护性耕作导致的农作物减产、土壤板结等问题。统一了小麦玉米一年两熟种植模式的种植规格，设计了全程机械化的关键农业装备。通过在试验示范基地的研究表明：秸秆还田及科学施肥，能够减少有害气体的排放和化肥的使用量，实现生态化农业生产；秸秆还田及适量耕作，可以增加土壤有机质含量、改善土壤团粒结构，提高土地肥力；生态沃土种植技术的实施，可以克服精耕细作和保护性耕作的缺点，实现农作物的稳产高产。*

关键词: *精耕细作, 保护性耕作, 种植规格, 农业机械化*

引言

中国人口数量为世界人口总数的 18.84%，而耕地面积只有世界耕地面积的 8.7%，因此逐渐形成了通过增加劳动力投入换取农业高产量的发展模式——精耕细作。精耕细作是对中国传统农业精华的一种概括，是传统农业的一个综合技术体系。围绕精耕细作技术及其发展进行了一系列的研究，结果表明精耕细作虽然提高了农产品的产量，解决了劳动力就业问题，但同时带来了水土流失、环境恶化等问题 [1], [3], [5-7], [12], [20]。精耕细作能大幅减少蚯蚓种群[6-7]，影响有机质含量、酶活性、微生物量、真菌菌丝体丰富度、微生物功能多样性、细菌物种丰富度等土壤性质[3],[7]。耕作强度增大使得土壤失去了自我保护功能，土壤慢慢失去活性，同时秸秆焚烧加重了大气污染。

美国西部和前苏联曾在二十世纪发生了巨大的黑色风暴，针对治理沙尘暴进行了大量的实验研究，证明保护性耕作方法是最成功的抑制方法[10]。保护性耕作研究主要集中在对土壤性质的影响[2], [11], [13-17], [21-24], 土壤

mainly focused on its influence on soil properties[2], [11], [13-17], [21-24], the composition of soil species [4], and the microbial quantity and fungi abundance in soil [19], [25]. Protective tillage can limit soil erosion and water loss [8], increase the contents of organic matters in soil, improve soil structure, control soil loss, reduce wind and water erosion, and shorten tillage times. In addition, straw residue cover can limit dust hazard. Thus, its implementation can prevent the loss of dust, water, and soil in farmlands. It can also store and preserve water, promote the productivity of fertilized land, save costs, increase efficiency, reduce emissions from straw burning and greenhouse gas, and enhance the sustainable development of agriculture. However, many researchers believe that simple protective tillage is not conducive to high yield given that the overuse of chemical fertilizers, pesticides, and other chemicals has generated ecological issues and problems with soil crust.

Based on a survey of the annual double-cropping patterns of wheat and maize in the Huang-Huai-Hai Region and on the advantages of intensive cultivation and protective tillage following years of field experiment research, a new method of ecological soil planting is proposed in the current study for these patterns. This mechanized ecological soil planting technique is investigated by determining the representative dry area, well irrigation area, and saline land. The results suggest that scientific and reasonable soil cultivation can enhance ecological agricultural production, soil structure, and the contents of organic matters in soil to ensure the stable and high yield of grain, as well as to realize the sustainable development of agriculture.

MATERIAL AND METHOD

Description of the Mechanized Ecological Soil Planting Technique

The so-called ecological soil planting technique guides scientific development. It focuses on the stable and sustainable development of agriculture in the long term, as well as on ecological agriculture construction and soil fertility cultivation. Crops are planted using ecological and mechanized techniques and methods. Furthermore, straw is treated scientifically to increase the contents of organic matters in soil, to improve soil structure, and to reduce the use of chemical fertilizers, pesticides, and other chemicals. Ultimately, it achieves the purpose of ecology, which is to facilitate high-quality, low-consumption, and high-efficiency agricultural production.

Key Techniques of Mechanized Ecological Soil Planting

Scientific Tillage Method

Tillage method is a general term for all techniques and measures that recirculate several crop systems in a region, including planting, soil tillage, fertilization, and weed control methods. The ecological soil planting technique is an establishment of the ecological soil tillage method, which combines tillage and protection with the ecological planting method. Agricultural machinery and agronomy are integrated as well.

Soil Tillage Method

The ecological soil tillage method with a five-year cycle (ploughing in the first year, digging the soil in the

物种组成的影响[4]、土壤微生物量和菌类丰富度的影响[19], [25] 等几个方面。保护性耕作，可以减少侵蚀和水土流失[8], 增加土壤有机质，改善土壤结构，控制水土流失，减少风蚀和水蚀，减少土壤耕作次数，秸秆残茬覆盖可以减轻粉尘危害。实施保护性耕作具有防治农田扬尘和水土流失、蓄水保墒、培肥地力、节本增效、减少秸秆焚烧和温室气体排放、促进农业可持续发展等作用，但许多人认为单纯的保护性耕作不利于高产，由于化肥、农药等化学物品的过度使用，带来了一系列生态和土壤板结等问题。

在对黄淮海地区小麦玉米一年两熟种植模式调研基础上，综合精耕细作和保护性耕作的优点，经过多年田间试验研究，提出了适合黄淮海地区小麦玉米一年两熟种植模式的一种新的生态型土壤耕作方法——机械化生态沃土种植技术。对机械化生态沃土种植技术进行了研究，选取具有代表性的旱作区、井灌区和盐碱地块，对该技术进行了实验研究，结果表明通过科学合理的土壤耕作，可以实现农业生产生态化，可以改善土壤结构，增加土壤有机质含量，从而保证粮食的稳产高产，实现农业的可持续发展。

材料与方法

机械化生态沃土种植技术的含义

所谓机械化生态沃土种植技术，是以科学发展观为指导，着眼于农业长期稳定可持续发展，将建立生态型农业和土地肥力培育作为两大重要目标，用生态型机械化技术和方法耕作，配合秸秆科学处理以不断增加土壤有机质含量、改善土壤结构，逐步减少化肥、农药等化学物质的使用，最终达到农业生产生态、优质、低耗、高效的目的。

机械化生态沃土种植关键技术

科学耕作方法

耕作方法是一个地区循环种植几种作物系统采取的全部农田技术措施的统称。它主要包括种植方法、土壤耕作方法、施肥和杂草防除方法等。生态沃土种植技术建立了耕作与保护并重的生态型土壤耕作方法、农机农艺融合的生态型种植方法。

土壤耕作方法

建立“一耕三四松，二五间隔停”的五年一周期生态

third and fourth years, and no ploughing or digging in the second and fifth years) was developed to emphasize both soil tillage and protection equally. Thus, the tillage and protective measures complement each other.

Ploughing in the first year: Ploughing can improve soil structure, the capacity of water storage and preservation, and crop root growth and nutrient absorption. It can also adjust nutrient distribution, loosen the organic matters accumulated on the soil surface, continuously improve the fertility of the tilth layer of soil, enhance the soil ecosystem, and promote the balance of the biological population in soil. Finally, it buries weed seeds, pathogen spores, and pest eggs deep into the soil to inhibit diseases and pests.

Digging deeply into the soil in the third and fourth years: This process mainly protects the soil surface and its dynamic configuration. Its main role is to break the plough pan to help the roots of crops adhere to the soil, to improve water storage and preservation capabilities, to enhance soil porosity, to improve air and water operation in soil, to generate conditions for the decomposition of organic matters by soil microorganisms, and to promote soil fertility and nutrient absorption.

No ploughing or digging in the second and fifth years: Over-tillage has many disadvantages, and the most serious is water and soil loss. No ploughing after tillage and complete digging is conducive to shortening the times of mechanized farming and to protecting the soil surface.

Planting Specification

The unification of planting specifications is the premise of the scientific design of mechanized agronomy. Planting specification mainly includes row width, line quantity and spacing, as well as the strip width and line spacing of deep digging. The parameters are agricultural machinery, agronomy, and irrigation methods. For convenient machine configuration, planting specifications must be unified, such as line spacing and row width. To adapt to the annual double-cropping patterns of wheat and maize in the well irrigation area of the Huang-Huai-Hai Region, a planting specification is designed as shown in Fig.1.

型土壤耕作方法，使土壤耕作与保护并重、耕作措施与保护措施相辅相成。

“一耕”是指在耕作周期第一年进行翻耕。翻耕可以改善土壤结构，增强蓄水保墒能力，利于作物根系发育和营养吸收；调整养分分布，将土壤表层积累的有机质翻入深层，持续提高耕层土壤肥力；改善土壤生态，利于土壤生物种群平衡，并将杂草种子、病菌孢子、害虫卵块等埋入深层，抑制病虫害发生。

“三四松”是指在耕作周期第三、四年间隔深松。采用间隔深松主要是考虑土壤表层保护和动力配置。深松的主要作用是打破犁底层，利于作物根系深扎，提高蓄水保墒能力，提高土壤孔隙度，改善土壤内部气、水运行状态，创造土壤微生物分解有机质的条件，利于土地肥力发挥和作物营养吸收。

“二五间隔停”是在耕作周期第二年和第五年既不耕也不松。过度耕作有很多弊端，最严重的是造成水土流失。在耕后的一年和完成全面深松后的一年不进行耕、松作业，有利于减少机器进地次数、保护土壤表层。

种植规格

统一种植规格是科学设计机械化农艺的前提，种植规格主要包括畦宽、行数、行距、苗带宽、深松行距等参数。这些参数既有农机的也有农艺的，甚至与灌溉方式紧密相关。为了便于机器配套，应当尽量统一，比如统一行距、统一畦宽等。为适应黄淮海井灌区小麦玉米一年两熟种植模式，设计了如图 1 所示的种植规格。

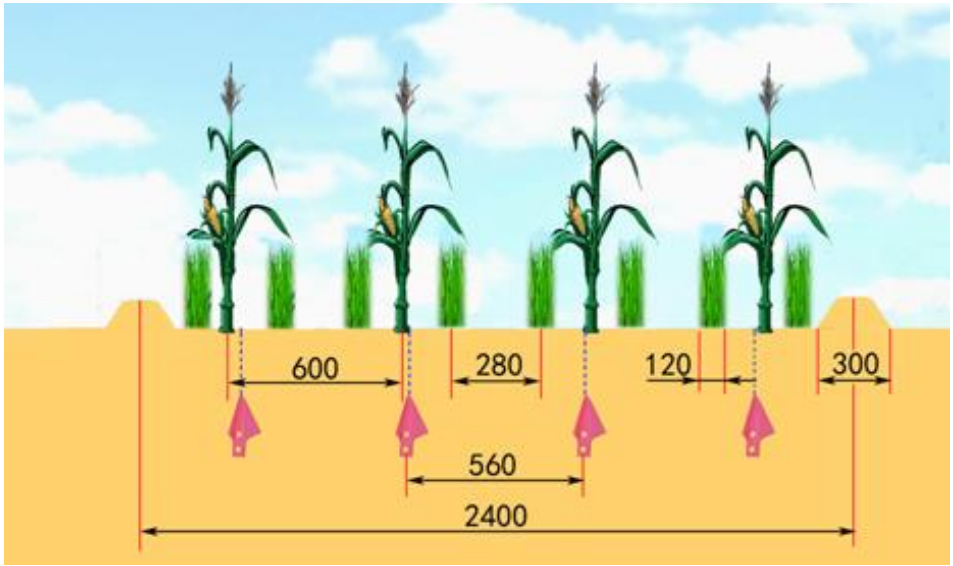

Fig. 1 - Planting Specification in the Well Irrigation Area (Unit: mm)

Key Agricultural Equipment

The mechanized ecological soil planting technique emphasizes the heavy integration of agricultural machinery and agronomy, enhances standardized planting procedures, and regards high efficiency, low consumption, and low investment as the goals of the system configuration and of machine operation. The tillage and planting requirements of this technique are presented in Table 1.

关键农业装备

机械化生态沃土种植技术，强调农机农艺深度融合，推行规格化种植，把高效、低耗、低投入作为机器系统配置和运行的目标。生态沃土种植技术的耕作及种植要求如表 1 所示。

Table 1

Requirements of the Mechanized Agronomic System

Item Name	Requirements of Agronomy
Ploughing depth (mm)	200～250
Digging depth (mm)	230～300
Wheat planting depth (mm)	30～50
Fertilization depth for wheat planting (mm)	80～100
Interval width between wheat seeds and fertilizer(mm)	50～60
Suppression strength for wheat sowing (N/cm^2)	20～30
Maize planting depth (mm)	30～40
Fertilization depth for maize sowing (mm)	100～120
Interval width between maize seeds and fertilizer (mm)	60～80
Suppression strength for maize sowing (N/cm2)	20～50
Cutting length of maize straw (mm)	<100

Given the annual double-cropping patterns of wheat and maize, the key agricultural equipment and techniques include:

小麦玉米一年两熟种植模式下，涉及的关键农业装备及关键技术主要有：

Fig. 2 - Sowing by Wheat Deep Digging and Fertilization Seeder and Seedlings

Wheat Seeder

The deep-digging wheat seeder performs six processes, namely, deep digging, rotary tilling, fertilizing, sowing, covering, and suppressing. Two rows of deep digging spades are staggered to prevent grass entangling and plugging effectively and to enhance the stability of deep digging [18] On October 12, 2012, the Shandong Agricultural Machinery Test Evaluation Station assessed the performance of the deep-digging wheat seeder. The main parameters are displayed in Table 2.

小麦播种机

小麦深松播种机由深松、旋耕、施肥、播种、覆土和镇压 6 部分组成，深松铲前后两排交错排列，有效避免了铲间缠草、堵塞问题，提高了深松的稳定性[18]。2012 年 10 月 12 日山东省农业机械试验鉴定站对小麦深松施肥播种机进行了性能检测，主要参数如表 2 所示。

Table 2

Performance Parameters of Wheat Deep Digging Fertilization Seeder

Performance Index	Parameter	Performance Index	Parameter
Supporting Dynamics (kW)	≥73.5	Fertilization spacing qualified rate (%)	≥98
Number of sowing Lines	8	Sowing rate error (%)	±0.4
Productivity (hm2/h)	≥0.8	Linking spacing qualified rate (%)	≥90
Sowing depth qualified rate (%)	≥80	Digging depth (cm)	≥30
Sowing uniformity variation coefficient (%)	≤45	Digging depth stability (%)	≥85

The wide strip sowing technique can improve the effective tillage of seeds and assist in ventilation, lighting, and crop growth. Wheat seeds are distributed in the field uniformly, and yield increases by 6% to 8% in comparison with that obtained with conventional sowing.

采用宽苗带播种技术，可提高种子有效分蘖、有利于通风、采光和作物生长，小麦种子在田间分布更加均匀，比常规播种增产 6％至 8%。

(a) 2BYMZ-8 monomer copying maize seeder (b) Strip grooming device

Fig. 3 - Maize Seeder and Its Strip Grooming Device

Maize Seeder and Dynamic Anti-plugging Device

The strip grooming device depicted in Fig. 3(b) is adopted to solve the plugging problem of the furrow opener on the no-tillage maize seeder when straw coverage is large (more than 0.6 kg/m2) or when straws are long (more than 22 cm) and scattered unevenly. This device exhibits the functions of dynamic anti-plugging and stubble ploughing. The number of the rotating knives is similar to that of furrow openers. In this device, a group of rotating knives is placed in front of the pillar of each furrow opener. Each group of rotating knives contains two rotating knives that are installed symmetrically at 180° [26].

The strip grooming device not only clears straw residues but also breaks the dry and hard soil layer on the surface, thus generating a good seeding bed and increasing the seedling rate by 2.5%. The monomer copying technique reduces the leakage sowing rate caused by uneven ground and enhances the consistency of seedlings.

Maize Straw Returning Machine

Given that the spacing of maize does not match the wheel tread of the harvester, the maize straws may be crushed during harvest. This phenomenon strongly affects the returning quality. To solve this problem, the technique employed by the crushing machine is improved by installing a stubble digging device in front of the machine (as exhibited in Fig. 4). This device digs maize straws up from the surface of the ground slowly and returns them to the straw returning machine. The straw returning machine crushes the straws rapidly to prevent its blade from hitting the earth, to reduce dynamic consumption, and to slow the onset of blade wear. Thus, the problem wherein maize straws cannot be returned to the field as a result of wheel rolling is solved.

玉米播种机及动力防堵装置

针对玉米免耕播种机在秸秆覆盖量较大（大于 0.6kg/m2）或秸秆长度较长（大于 22cm）和秸秆抛撒不均匀时，开沟器易被堵塞的技术难题，采用图 3(b)所示的苗带清整装置。该装置具有动力防堵和灭茬功能，旋刀组数与种肥开沟器数量相同，每个种肥开沟器的立柱前端均设有一组旋刀，每组旋刀包括呈 180º 对称安装的两把旋刀[26]。

苗带清整装置既清理了苗带的秸秆残茬，又破除地表干硬土层，营造良好种床，提高发苗率 2.5%。采用的单体仿形技术，减少了因地面不平导致的漏播率，提高了出苗的一致性。

玉米秸秆还田机

由于玉米行距与收获机轮距不匹配，在收获的时候玉米秸秆可能被压倒，严重影响还田质量，为此，对粉碎还田机进行了技术改进，在还田机前方安装挖茬机构（如图 4 所示）。挖茬机构以较低的速度将玉米秸秆贴地表挖起，向后抛向还田机，还田机以较高的速度将玉米秸秆打碎还田，防止还田机刀片打土，减小动力消耗，减缓刀片磨损，解决了因车轮碾压引起的部分秸秆无法还田的问题。

Fig. 4 - Stubble Digging, Crushing and Returning Machine

The comprehensive crushing and returning of maize straws and roots after harvest not only limits the dynamic harvest but also gathers the remaining ears in the harvesting process to reduce harvest loss and the cleaning of emerging wheat seedlings.

RESULT ANALYSIS

The representative dry area, well irrigation area, and saline land were selected as per the proposed mechanized ecological soil planting technique to determine the test demonstration bases (as indicated in Table 3).

在玉米收获后对秸秆和根系进行一次综合性粉碎还田处理，这样不仅减少了收获过程的动力消耗，而且能够使收获过程出现的果穗遗落损失得到及时捡拾，降低了果穗的收获损失，减少了小麦出苗后的玉米苗清理问题。

结果分析

根据提出和设计的机械化生态沃土种植技术，选取旱作区、井灌区、盐碱地等较为典型的地域建设试验示范基地（如表 3 所示）。

Table 3

Test Demonstration Bases

Serial No.	Item Name	Cooperation Unit	Construction Time
1	Dry Area Test Demonstration Base	Longyi Village in Zichuan District, Zibo	2011
2	Well Irrigation Area Test Demonstration Base	Donglai Agricultural Machinery Cooperative in Changshan Town, Zhouping County, Bingzhou	2012
3	Saline Land Test Demonstration Park	Jin Fu Xiang Peasant Planting Cooperative in Mingji Village, Lijin County, Dongying	2012
4	Well Irrigation Area Test Demonstration Base	Fujia Village, Zhangdian, Zibo	2005

The protective tillage system has been implemented in test demonstration base no. 4 since 2005. The mechanized planting technique has been adopted since 2011. After 10 years of returning straw to the field and of scientific and reasonable soil tillage, significant effects have been observed.

Ecological Production Mode

In the case in which all straws were returned to the field, 11 t/hm2 to 15 t/hm2 of maize straws were recovered annually. The amount of wheat straws returned ranged from 7.5 t/hm2 to 9 t/hm2. The concentrations of gas emissions reduced directly by straw returning per hm2 are displayed in Table 4 based on the data reported in the literature [9].

在 4 号试验示范基地上，从 2005 年开始实施保护性耕作制度，从 2011 年开始采用机械化种植技术进行土壤耕作，经过长达近 10 年的秸秆还田及科学合理的土地翻耕，取得了较为明显的效果。

生产方式生态化

秸秆全部还田情况下，每年还田的玉米秸秆为 11～15t/hm^2,小麦秸秆为 7.5～9 t/hm^2。根据文献[9]所提供的数据，采用秸秆还田每公顷直接减少的气体排出量如表 4 所示。

Table 4

Directly Reduced Gas Emissions per hm^2 (unit:kg)

Chemical Name	Quality
CO	2413.45～3150.3
CO_2	26598.15～34722
NO	15.07～19.5
NO_2	6.75～8.67
NO_x	21.92～28.32

The return of straw to the field can reduce air pollution and prevent damage to the soil structure as a result of straw burning. It can also improve the efficiency of fertilizer use and reduce usage by 40%. Root stubble crushing loosens and stirs the topsoil, thereby changing the physical and chemical properties of the soil and destroying the parasitic environment of insects and other pests on the surface. This process inhibits the onset of plant diseases and pest invasion.

Organic Soil Fertilization

The scientific processing of crop straws increases the content of organic matters in soil consistently every year, improves the aggregate structure of soil, enhances soil permeability, balances soil microorganisms, and improves the microenvironment of the field, thus realizing stable and high yields. The changes in the contents of organic matters, the increment of water content, and the volume-to-weight ratio reduction in the soil of test demonstration base no. 4 are shown in Fig. 5.

秸秆还田可以减少大气污染，并且可以避免因秸秆焚烧而带来的土壤结构破坏问题。合理施肥，提高了化肥的使用效率,可以减少 40%的化肥使用量。由于根茬粉碎疏松和搅动表土，能改变土壤的理化性能，破坏表层害虫及其他地下害虫的寄生环境，故能抑制病虫害的发生。

培肥地力有机化

通过科学处理作物秸秆，逐年稳步增加土壤有机质含量，改善土壤团粒结构，增加种床土壤透气性，平衡土壤微生物，改善农田微环境，实现稳产高产。在 4 号实验示范基地，其土壤有机质含量、土壤含水量增量和土壤容重比下降量变化如图 5 所示。

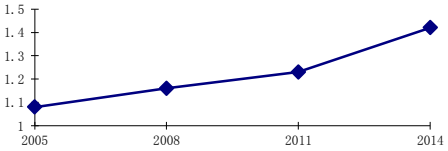

a) The Content of Organic Matters in Soil (%)

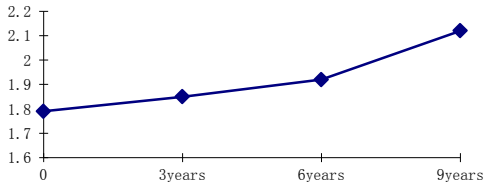

b) Water Content Increment in Soil (%)

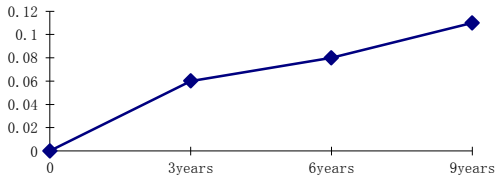

c) The Volume-to-weight Ratio Reduction of Soil

Fig. 5 - Influence of the return of straw to the field on soil

Since 2011, soil tillage has strictly accorded with the requirements of the ecological soil planting project, thereby steadily increasing the yields of wheat and corn. Scientific fertilization limits the use of fertilizer and fundamentally weakens the adverse influence of fertilizer production and use on soil and ecology. The yields of wheat and corn, as well as the amount of fertilizer used in test demonstration base no. 4, are depicted in Fig. 6(Note: The crops in Shandong were frozen because of the low temperature, snow, and rain in the spring of 2013). Late in May, rare rainstorms and strong winds resulted in a severe loss of wheat. Moreover, droughts in the late summer and early autumn affected sowing. In the middle of September, Luzhong experienced hail, which intensified the disaster and reduced yield.

从 2011 年以来，严格按照生态沃土种植工程要求，进行土地的耕作，小麦玉米产量得到了稳步提高，通过科学施肥，减少了化肥的用量，从根本上减少化肥生产和使用对土壤和生态的不利影响。4 号试验示范基地小麦玉米产量及化肥使用量如图 6 所示（说明：山东省 2013 年春季低温雨雪使农作物受冻，5 月下旬罕见的大风暴雨气候导致小麦倒付严重，夏末秋初少雨干旱影响秋播，9 月中旬鲁中遭受风雹袭击令灾害严重，导致粮食减产）。

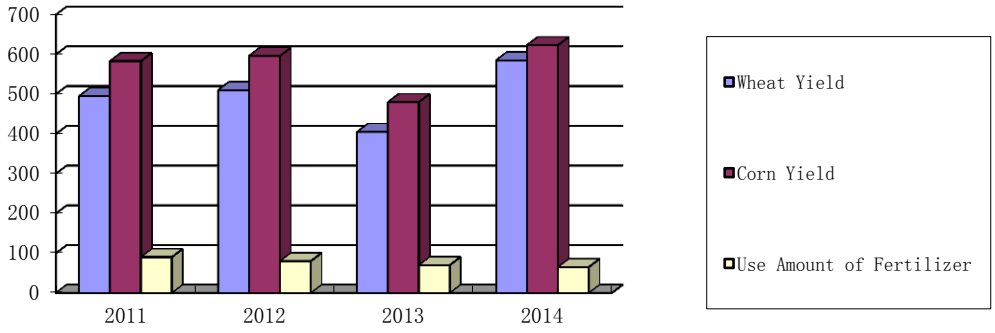

Fig. 6 - Yields of wheat and corn and the amount of fertilizer used (unit: kg/mu)

CONCLUSIONS

Based on the analysis of the two typical planting patterns of intensive cultivation and protective tillage and according to several years of testing and research, a mechanized ecological soil planting technique was proposed for the annual double cropping of wheat and maize. This method is suitable for the Huang-Huai-Hai Region. The characteristics of the planting technique were explained, and the planting specification was designed. This specification was appropriate for the ecological soil tillage method employed in the mechanized ecological soil planting technique and for the combination of agricultural machinery and agronomy. The corresponding key agronomic equipment was designed to mechanize the operation of the annual double cropping of wheat and maize fully. The proposed technique was applied, and the results showed that it reduced the emissions of polluted gases and the amount of fertilizer used through scientific fertilization to establish the ecological production mode. In addition, it increased the contents of organic matters in soil, improved the microenvironment of farmland, and enhanced the organic fertilization through the return of straw to the field and through suitable soil tillage. Thus, the implementation of this tillage method ensured stable and high crop yields, as well as the sustainable development of agricultural production.

ACKNOWLEDGEMENT

This research was supported by the Young Teachers Program of Shandong University of Technology and the Maize Industry Innovation Team Program of Shandong Modern Agricultural Industrial Technique System (SDAIT-01-022-10).

REFERENCES

[1]. Adepetu J. A., Corey R. B., (1997) - *Changes in N and P availability and P fractions in soil from Nigeria under intensive cultivation,* Plant and Soil, vol. 46, pp. 309-316;
[2]. Afzalinia S., Zabihi J., (2014) - *Soil compaction variation during corn growing season under conservation tillage,* Soil and Tillage Research, vol. 137, pp. 1-6;
[3]. Bonanomia G., D'Ascolic R., Antignania V., et al. (2011) - *Assessing soil quality under intensive cultivation and tree orchards in Southern Italy,* Applied Soil Ecology,

结论

在分析精耕细作和保护性耕作两种经典种植模式基础上，根据多年的试验研究，提出了一种适合黄淮海地区小麦玉米一年两熟种植模式的机械化生态沃土种植技术，阐述了该种植技术的内涵特点。提出了适合机械化生态沃土种植技术的生态型土壤耕作方法和农机农艺融合的种植规格，设计了适合该种植技术的关键农艺装备，实现了小麦玉米一年两熟全程机械化作业，并对提出的机械化生态沃土种植技术进行了试验示范。结果表明，机械化生态沃土种植技术通过秸秆还田减少污染气体的排放，通过科学施肥减少化肥使用量，建立了生态化的生产方式；通过秸秆还田和适当土壤耕作，提高了土壤有机质含量，改善了农田微环境，实现了有机化地力培育；通过该耕作方法的实施，保证了农作物产量稳产丰产和农业生产可持续发展。

致谢

本研究得到山东理工大学青年教师支持计划和山东省现代农业产业技术体系玉米产业创新团队项目（SDAIT-01-022-10）的资助。

参考文献

[1]. Adepetu J. A., Corey R. B. (1997) - *精细耕作对尼日利亚伊沃土壤中 N 和 P 的利用率和 P 分数的改变,* 植物和土壤, 第 46 卷, 309-316;
[2]. Afzalinia S., Zabihi J. (2014) - *保护性耕作下在玉米生长期土壤板结变化研究,* 土壤耕作研究, 第 137 卷, 1-6;
[3]. Bonanomia G., D' Ascolic R., Antignania V. 等. (2011) - *意大利南部精耕细作和树果园土壤质量评估,* 应用

vol. 47, no.3, pp. 184–194;
[4]. Boscutti F., Sigura M., et al. (2015) - *Conservation Tillage Affects Species Composition But Not Species Diversity: A Comparative Study in Northern Italy,* Environmental Management, vol.55, no.2, pp.443-452;
[5]. Coote D. R., Ramsey. J. F. (1983) - *Quantification of the effects of over 35 years of intensive cultivation on four soils,* Canadian journal of soil science, vol. 63, no.1, pp. 1-14;
[6]. Curry P.J., Byrne D., Schmidt O., (2002) - *Intensive cultivation can drastically reduce earthworm populations in arable land,* European Journal of Soil Biology, vol. 38, no.2, pp. 127−130;
[7]. Fraser P.M., Haynes R.J., Williams P.H., (1994) - *Effects of pasture improvement and intensive cultivation on microbial biomass, enzyme activities, and composition and size of earthworm populations,* Biology and Fertility of Soils, vol. 17, no.3, pp. 185-190;
[8]. Gebhardt R. M., Daniel C. T., Schweizer E., Allmaras R., (1985) - *Conservation Tillage,* Science, vol. 230, no.4726, pp. 625-630;
[9]. Hefeng Zhang, Xingnan Ye, Tiantao Cheng, et al. (2008) - *Emission simulation of gaseous pollutants and GIS analysis from agricultural crop residue combustion in China,* The 26th CCS Congress, Division of Environmental Chemistry, July, Tianjin, China.
[10]. Huanwen Gao, Wenying Li, Hongwen Li. (2003) - *Conservation tillage technology with Chinese characteristrics,* Transactions of the CSAE, vol. 19, no. 3, pp. 1-4;
[11]. Jiantao Du, WenQing He, Vinary Nangia, et al. (2008) - *Effects of conservation tillage on soil water content in northern arid regions of China,* Transactions of the CSAE, vol. 24, no. 11, pp. 25-29;
[12]. Ketcheson J. W., (1980) - *Long-range effects of intensive cultivation and monoculture on the quality of southern Ontario soils,* Canadian journal of soil science, vol. 60, no.3, pp. 403-410;
[13]. Ketema H., Yimer F., (2014) - *Soil property variation under agroforestry based conservation tillage and maize based conventional tillage in Southern Ethiopia,* Soil & Tillage Research, vol. 141, pp. 25–31;
[14]. Lal R., Kimble J.M., (1997) - *Conservation tillage for carbon sequestration,* Nutrient Cycling in Agroecosystems, vol. 49, no.1-3, pp. 243–253;
[15]. Lixue Wang, Xi Jiang, et al. (2014) - *Effects of conservation tillage on soil water erosion and soil compaction degree,* Journal of Irrigation and Drainage, vol. 33, no. 2, pp. 83-85;
[16]. López-Garrido R., Madejón E., Moreno F., and Murillo J. M., (2014) - *Conservation tillage influence on carbon dynamics under Mediterranean conditions*, Pedosphere, vol. 24, no. 1, pp. 65–75;
[17]. Page K., Dang Y., Dalal R., (2013) - *Impacts of conservation tillage on soil quality, including soil-borne crop diseases, with a focus on semi-arid grain cropping systems,* Australasian Plant Pathology, vol. 42, no.3, pp. 363–377;
[18]. Peisong Diao, Ruicheng Du, Fuhui Li, et al. (2013) – *Development of Wheat Subsoiling and No-tillage Fertilization Planter,* Journal of Agricultural Mechanization Research, no. 11, pp. 103-106;
[19]. Plaza C, Courtier-Murias D, et al. (2013) - *Physical, chemical, and biochemical mechanisms of soil organic matter stabilization under conservation tillage systems: A*

土壤生态学, 第 47 卷, 第 3 期, 184 – 194;
[4]. Boscutti F., Sigura M. 等. (2015) - *保护性耕作对物种组成, 非物种多样性的影响:在意大利北部的比较研究,* 环境管理, 第 55 卷, 第 2 期, 443-452;
[5]. Coote D. R., Ramsey. J. F. (1983) - *对超过 35 年的精耕细作四个土壤的量化影响,* 加拿大土壤杂志, 第 63 卷, 第 1 期, 1-14;
[6]. Curry P.J., Byrne D., Schmidt O. (2002) - *精耕细作可以大大减少耕地蚯蚓群体,* 欧洲土壤生物学报, 第 38 卷, 第 2 期, 127−130;
[7]. Fraser P.M., Haynes R.J., Williams P.H. (1994) - *草场改良和精耕细作对微生物量、酶活性及组成和蚯蚓种群数量的影响,* 土壤肥力生物学, 第 17 卷, 第 3 期, 185-190;
[8]. Gebhardt R. M., Daniel C. T., Schweizer E., Allmaras R. (1985) - *保护性耕作.* 科学, 第 230 卷, 第 4726 期, 625-630;
[9]. 张鹤丰, 叶兴南, 成天涛, 等. (2008) - *中国地区农作物秸秆燃烧排放大气污染物模拟及 GIS 分析* [C], 中国化学会第 26 届学术年会环境化学分会, 7 月, 天津, 中国.
[10]. 高焕文, 李问盈, 李洪文. (2003) - *中国特色保护性耕作技术,* 农业工程学报, 第 19 卷, 第 3 期, 1-4;
[11]. 杜建涛, 何文清, Vinay Nangia, 等. (2008) - *北方旱区保护性耕作对农田土壤水分的影响,* 农业工程学报, 第 24 卷, 第 11 期, 25-29;
[12]. Ketcheson J. W. (1980) - *精耕细作和单一作物种植对安大略省南部地区土壤质量的长期影响,* 加拿大土壤杂志, 第 60 卷, 第 3 期, 403-410;
[13]. Ketema H., Yimer F. (2014) - *埃塞俄比亚南部农林业和玉米保护性耕作下土壤性质的变化,* 土壤耕作研究, 第 141 卷, 25 – 31;
[14]. Lal R., Kimble J.M. (1997) - *保护性耕作下碳封存,* 农业生态系统养分循环, 第 49 卷, 第 1-3 期, 243 – 253;
[15]. 王丽学, 姜熙, 等. (2014) - *保护性耕作对农田土壤水蚀及土壤紧实度的影响,* 灌溉排水学报, 第 33 卷, 第 2 期, 83-85;
[16]. López-Garrido R., Madejón E., Moreno F., and Murillo J. M. (2014) - *地中海条件下保护性耕作对碳动态的影响,* 土壤圈, 第 24 卷, 第 1 期, 65 – 75;
[17]. Page K., Dang Y., Dalal R. (2013) - *聚焦于半干旱粮食种植系统的统保护性耕作对包括土传病害的土壤质量的影响,* 澳大利亚植物病理学, 第 42 卷, 第 3 期, 363 – 377;
[18]. 刁培松, 杜瑞成, 李复辉, 等. (2013) – *小麦深松免耕施肥播种机的研制,* 农机化研究, 第 11 期, 103-106;
[19]. Plaza C, Courtier-Murias D, 等. (2013) - *保护性耕作体系下土壤有机质物理、化学、生化稳定机制：副产品微生物*

central role for microbes and microbial by-products in C sequestration, Soil Biology & Biochemistry, vol. 57, pp. 124-134;
[20]. Saini G. R., Grant W. J., (1980) - *Long-term effects of intensive cultivation on soil quality in the potato-growing areas of New Brunswick (Canada) and Maine (U.S.A.),* Canadian journal of soil science, vol. 60, pp. 421-428;
[21] Shenzhong Tian, Zengjia Li, et al. (2008) - *Effects of conservation tillage on different soil nutrient forms*, Journal of Qingdao Agricultural University (Natural Science), vol. 25, no.3, pp. 171-176;
[22]. Van Wie J. B., Adama J.C., Ullman J.L. (2013) - *Conservation tillage in dryland agriculture impacts watershed hydrology,* Journal of Hydrology, vol.483, pp.26-38;
[23] Yan Wang, Xiaobin Wang, et al. (2008) - *Conservation tillage and its effect on soil organic carbon,* Chinese Journal of Eco-Agriculture, vol.16,no.3, 766-771;
[24]. Yilai Lou, Minggang Xu, et al. (2012) - *Stratification of soil organic C, N and C: N ratio as affected by conservation tillage in two maize fields of China*, Catena, vol. 95, pp. 124–130.
[25]. Yun Wang, Zengjia Li, et al. (2007) - *Effects of conservation tillage on soil microbial biomass and activity,* Acta Ecologica Sinica, vol. 27, no. 8, pp. 3384-3390;
[26]. Zidong Yang, Ningning Liu, Duayang Geng, et al. (2013) - *Design and Experiment on Type 2BYM-12 Folding and Dynamic Anti-blocking No-till Planter,* Transactions of the CSAM, vol. 44, supplement 1, pp. 46-50.

碳吸收的核心作用, 土壤生物与生物化学, 第 57 卷, 124-134;
[20]. Saini G. R., Grant W. J. (1980) - *精耕细作在新不伦瑞克省（加拿大）和缅因州（美国）马铃薯种植区土壤质量的长期影响,* 加拿大土壤杂志, 第 60 卷, 421-428;
[21]. 田慎重, 李增嘉, 等. (2008) - *保护性耕作对农田土壤不同养分形态的影响,* 青岛农业大学学报(自然科学版), 第 25 卷, 第 3 期, 171-176;
[22] Van Wie J. B., Adama J.C., Ullman J.L. (2013) - *旱作农业区保护性耕作对流域水文的影响,* 水文学报, 第 483 卷, 26-38;
[23]. 王 燕, 王小彬, 等. (2008) - *保护性耕作及其对土壤有机碳的影响,* 中国生态农业学报, 第 16 卷, 第 3 期, 766-771;

[24]. Yilai Lou, Minggang Xu, 等. (2012) - *在中国两个保护性耕作玉米地分层土壤有机碳, N 和 C:N 比,* 连锁; 土壤科学-水文学-地貌学杂志, 第 95 卷, 124 – 130;
[25]. 王芸, 李增嘉, 等. (2007) - *保护性耕作对土壤微生物量及活性的影响,* 生态学报, 第 27 卷, 第 8 期, 3384-3390;
[26]. 杨自栋, 刘宁宁, 耿端阳, 等. (2013) - *2BYM-12 型折叠式动力防堵免耕播种机设计与试验,* 农业机械学报, 第 44 卷, 增刊 1, 46-50.

DESIGN OF AN INTELLIGENT MONITORING SYSTEM FOR A PESTICIDE SPRAYING MACHINE BASED ON ZIGBEE TECHNOLOGY
/
基于 ZIGBEE 技术的农药喷施机智能监控系统设计

Lect. Master. Zou Zhiyong[1)], Prof. Ph.D. Xu Lijia[*1)], Prof. Master. Kang Zhiliang[1)], Ph.D. Nocklos Tenret [2)]
[1)] College of Mechanical and Electronic Engineering, Sichuan Agricultural University, Sichuan / P.R. China;
[2)] University of Bayreuth, 95440, Bayreuth / Germany
Tel: (+86) 0835-2882035; Email: lijiaxu13@163.com

Abstract: *Implementing intelligent control in pesticide spraying machines is a key technology in improving spray efficiency, decreasing pesticide pollution, and lowering production cost. This paper presents an intelligent monitoring system for pesticide spraying machines. This system focuses on the ZigBee technology and integrates sensors, motors, a Wi-Fi camera, and a 32-bit embedded controller. This intelligent monitoring system consists of a monitoring node of a rotary pesticide selection unit, monitoring node of a real-time preparation unit, monitoring node of a nozzle unit, monitoring node of an intelligent mobile platform, a Wi-Fi camera image collecting module, and a PDA remote controller. Test results show that the average packet drop ratio of the ZigBee network is 0.21%, and the success ratio of sending 10,000 commands through the responder communication strategy of the ZigBee network is 100%. This intelligent monitoring system can be remotely controlled from a distance of up to 110 m.* The spraying efficiency is 2–3 times greater than of manual spraying. *The wireless remote operation is also convenient for pesticide preparation and operator safety.*

Keywords: *Pesticide Spraying Machine; ZigBee; PDA; Embedded Controller; Sensor*

INTRODUCTION

Given the excessive use of pesticides, the additive effect of toxicity residues in the environment and food is an increasingly serious problem that has exceeded the natural degrading capacity of the environment. Thus, it has caused underground water and surface water pollution, as well as toxin accumulation in foods [11]. Therefore, intelligent pesticide application technology developed on the basis of agricultural mechanical equipment is an efficient way to promote the health and sustainable development of agriculture, as well as lower the harmful effects of pesticides on the environment and human body [8].

Researchers have proposed many methods in terms of pesticide spraying technologies in recent years [1], [2], [5]. Spraying technologies presented in literature [3], [6], [7], [9] mainly realize variable application control. Spraying machines are usually costly, whereas some application technologies are in high demand in the landform. This paper presents a pesticide application technology based on ZigBee technology to realize its operation in a diversified environment, decrease waste and excessive use of pesticides, prevent operators from directly contacting with pesticides, and improve the spraying efficiency of pesticides. ZigBee technology is a short-distance wireless network communication technology with low energy consumption, cost, and complexity [10]. It is applicable to multipoint control

摘要: *对农药喷施机实施智能控制是提高喷施效率、减少农药污染、降低生产成本的关键技术。该文以 ZigBee 技术为核心，结合传感器、电机、Wi-Fi 摄像头、32 位嵌入式控制器等对农药喷施机设计了智能监控系统。该监控系统由旋转式选药装置监控节点、实时配药装置监控节点、喷头装置监控节点、智能移动平台监控节点、Wi-Fi 摄像头图像采集模块和 PDA 遥控器组成。试验测试结果表明，ZigBee 网络平均丢包率为 0.21%，通过应答式通信策略 ZigBee 网络发送 1 万个指令的成功率达 100%。该智能监控系统的遥控距离可达 110m，*喷施效率是人工的 2～3 陪，*无线遥控操作保障了配药作业的便捷和作业人员的安全。*

关键词: *农药喷施机; ZigBee; PDA; 嵌入式控制器; 传感器*

引言

农药的过量使用，在环境和食物中残留毒性的积累效应已日益成为严重问题，超过了环境对农药的自然消解能力，造成了地下水以及地表水污染，形成了食物中有害毒素的积累[11]。因此，为促进农业的健康和可持续发展，减少农药对环境和人体的危害，发展基于农业机械装备的智能施药技术是一种有效途径[8]。

近年来，针对农药喷施技术研究人员提出了很多方法[1]、[2]、[5]，文献[3]、[6]、[7]、[9]提出的喷施技术主要实现变量施药控制，其中，有些喷施设备成本高，有些喷施技术对地形要求较高。为了实现多种环境作业、减少农药的浪费和过量使用，避免作业人员与农药直接接触，提高农药喷施效率本文提出一种以 ZigBee 技术为核心的施药技术。ZigBee 技术是一种低能耗、低成本、低复杂度的短距离无线网络通信技术[10]，适合多点控制应用系统，农药喷施机通常是由多个装置组成，因此，采用 ZigBee 技术为核心结合 PDA（Personal Digital Assistant）等技

application systems. A pesticide spraying machine consists of multiple units. Therefore, an intelligent monitoring system for such a machine is developed by employing ZigBee technology combined with a personal digital assistant (PDA) to realize intelligent control of pesticide selection, pesticide preparation, multi-mode spraying, and nozzle.

MATERIAL AND METHOD

The Structure and Principle of the Pesticide Spraying Machine

This pesticide spraying machine consists of a rotary pesticide selection unit, real-time preparation unit, nozzle unit, and intelligent mobile platform. Figure 1 shows pesticide spraying machine [4].

The rotary pesticide selection unit mainly consists of a solution tank, laser photoelectric sensor, solenoid valve, and stepper motor. The operator selects the exact type of pesticide according to the images sent to the PDA remote controller. It then controls the rotation of the solution tank and makes it rise to a corresponding height to draw the pesticide. The solution tank is divided into eight sections with the same volume for holding eight types of pesticides. The corresponding solenoid valve hole is mounted at the bottom of each section for the operator to select appropriate pesticides according to the state of crop disease.

The real-time preparation unit mainly consists of a solution preparation tank, solution temporary storage tank, water storage tank, and level switch. When the level switch in the solution temporary storage tank detects that the level of the solution is lower than the set value, it immediately starts to prepare the solution for the next round of spraying. The real-time preparation unit can realize real-time rapid preparation.

The nozzle unit mainly consists of a lifting rod, stepper motor, water pump, and nozzle, which adjust the nozzle height by driving the lifting rod with the stepper motor.

The intelligent mobile platform employs Beijing Borch Company's Traveler No. 4 whole landform mobile platform, which is applicable for traveling on sand, soil, and grass. It can also run in diversified environments such as fruit gardens, vegetable bases, and greenhouses.

术开发出农药喷施机智能监控系统，旨在实现选药智能控制、实时配药智能控制、多模式喷施智能控制和喷头智能控制。

材料与方法

农药喷施机的结构与原理

该农药喷施机由旋转式选药装置、实时配药装置、喷头装置、智能移动平台等组成，农药喷施机如图 1 所示[4]。

旋转式选药装置主要由溶液箱、激光光电传感器、电磁阀、步进电机构成，作业人员依据传至 PDA 遥控器的图像选择出正确的农药类型，继而控制溶液箱旋转并上升至相应的高度，以便进行农药的抽取。其中，溶液箱被分割成 8 个相同容积的区域，用于盛放 8 种类型的农药， 8 个区域的低部均安装有对应的电磁阀孔，以便工作人员依据农作物病况选择合适的农药类型。

实时配药装置主要由喷施液配制箱、喷施液暂存箱、蓄水箱和液位开关等组成。当喷施液暂存箱内的液位开关检测到喷施液的液位低于设定值时，随即启动下一轮喷施液的配制，实时配药装置可达到实时快速配制目的。

喷头装置主要由升降杆、步进电机、水泵、喷头组成，通过步进电机驱动升降杆实现喷头高度调节。

智能移动平台，选用北京博创公司旅行家 4 号全地形移动平台，能适应沙石、泥土、草地行走，可在果园、蔬菜基地、农作物、大棚等多种环境中作业。

Fig. 1 - The pesticide spraying machine

Design of an Intelligent Monitoring System

By monitoring the working state of a pesticide spraying machine with sensors and cameras, this monitoring system coordinates the rotary pesticide selection unit, real-time preparation unit, and nozzle unit to enable the pesticide spraying machine to spray in three modes: automatic fixed spot spraying mode, automatic travel spraying mode, and manual mode. The design project of the intelligent monitoring system is shown in Figure 2. This plan consists of two major parts of the spraying machine monitor and PDA remote controller. The spraying machine monitor is designed on the basis of ZigBee and consists of a monitoring node of the rotary pesticide selection unit, monitoring node of real-time preparation unit, monitoring node of nozzle unit, monitoring node of intelligent mobile platform, and a Wi-Fi camera image collecting module. The PDA controller communicates with the Wi-Fi camera image collecting module through Wi-Fi and communicates with the ZigBee monitoring node through the ZigBee network. The Wi-Fi camera collects images with the CS-R5110 module, whose main performance parameters are as follows: 1280 × 760 pixels; 8-direction pan/tilt/zoom (PTZ) that can rotate in 335° horizontally and 120° vertically; built-in Wi-Fi communication chips; wireless communication distance of up to 120 m; and fully meets the spraying machine's demands of image collection. The 4 monitoring nodes and PDA remote controller are powered by 12 V, 5 AH storage batteries. A 5 V and 3.3 V DC is provided after the power is regulated by LM2596-5 and LM1117-3.3 regulating chips. The intelligent mobile platform is powered by 48 V, 20 AH storage batteries.

智能监控系统设计

通过传感器、摄像头监测农药喷施机的工作状态，该智能监控系统控制旋转式选药装置、实时配药装置和喷头装置协调工作，使得农药喷施机可以实现三种喷施作业模式，即定点喷施自动模式、边走边喷自动模式和手动模式。智能监控系统设计方案如图 2 所示，此方案由农药喷施机监控器和 PDA 遥控器两大部分组成。农药喷施机监控器以 ZigBee 技术为核心进行设计，由选药装置监控节点、实时配药装置监控节点、喷头装置监控节点、移动平台监控节点和 Wi-Fi 摄像头图像采集模块共同构成。PDA 遥控器与 Wi-Fi 摄像头图像采集模块通过 Wi-Fi 实现相互通信，与 ZigBee 监控节点通过 ZigBee 网络实现相互通信。Wi-Fi 摄像头图像采集模块采用 CS-R5110 模块，其主要性能参数是，支持 1280*760 像素，自带 8 方位云台支持水平 335°，上下 120°范围转动，内置 Wi-Fi 通信芯片且无线通信距离达 120m，完全满足农药喷施机作业图像采集需求。4 个监控节点和 PAD 遥控器都采用 12V5AH 蓄电池提供电能，经 LM2596-5、LM1117-3.3 调压芯片调整提供 5V 和 3.3V 直流供电电压。智能移动平台采用 48V20AH 蓄电池提供电能。

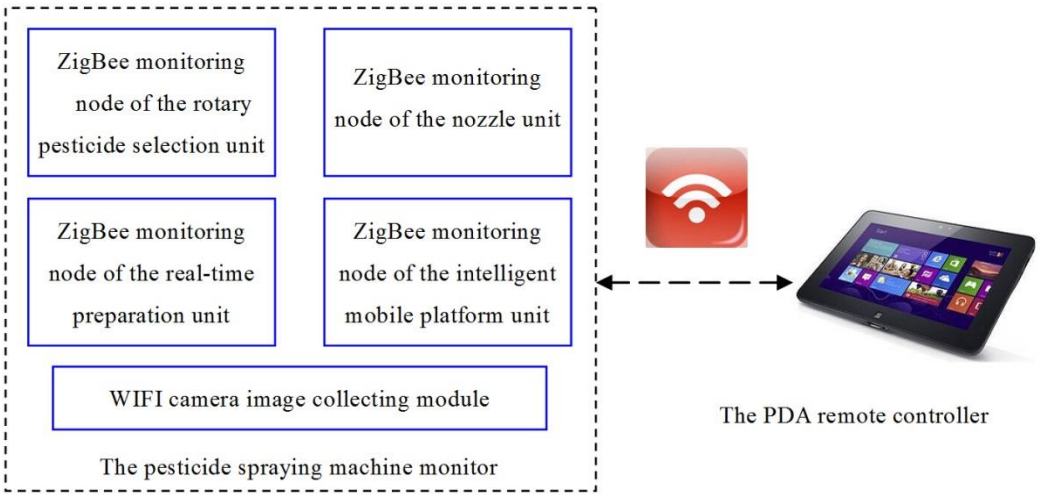

Fig. 2 - Design project of the intelligent monitoring system

Design of the pesticide spraying machine monitor

All the monitoring nodes of the rotary pesticide selection unit, real-time preparation unit, nozzle unit, and mobile platform are designed with the CC2530 wireless single chip microcomputer (SCM) as the core. The CC2530 wireless SCM is a type of system-on-chip developed by TI, a US company. By integrating the RF transceiver with leading performance and industrial standard enhanced 8051 CPU, this chip has excellent sensitivity, anti-interference capacity and strong GPIO

农药喷施机监控器设计

选药装置监控节点、实时配药装置监控节点、喷头装置监控节点和移动平台监控节点都以CC2530无线单片机为核心进行设计。CC2530无线单片机是由美国TI 公司研制出的一种片上系统，它结合了性能领先的RF收发器和业界标准的增强型8051 CPU，具有出色的灵敏度和抗干扰能力，同时还具有强大的GPIO接口，遵循ZigBee协议。3

interface, and it follows ZigBee protocol. The three monitoring nodes are designed by employing the minimum applied system circuit proposed by TI and integrating the GPIO interface circuit. The secondary application development is performed for monitoring the node program on the basis of TI's Z-Stack-CC2530 protocol stack.

Monitoring node of the rotary pesticide selection unit

The stepper motor drives the solution tank of the rotary pesticide selection unit to rotate and select the pesticide type to be sprayed. The stepper motor then uses the 57BYGH module. The P1.0 to P1.2 ports of the CC2530 wireless SCM are connected to the pulse port CLK, direction port DIR, and enabling port EN of the 57BYGH module, respectively. The CC2530 wireless SCM control rotation of the solution tank is in accordance with the commands sent by the PDA controller. The emission heads of 8 laser photoelectric sensors are installed at the bottom of the solution tank, and each head corresponds to a section of the tank. The P0.0 to P0.7 ports of the CC2530 wireless SCM drive the eight relay switches, and their output ports control the corresponding emission head to emit laser. The laser photoelectric sensor uses M12NPN geminate transistors such that the laser beam is concentrated and has intensive energy that largely decreases the false ratio. The external interrupt input port INT1 of the CC2530 wireless SCM connects the output port NO of the receiver of the laser photoelectric sensor. When the receiver receives laser signals, the output low level of the NO port triggers external interruption of the CC2530 wireless SCM, so that pesticide selection control is realized. The steps of the pesticide selection control are as follows:

(1) The CC2530 wireless SCM drives the corresponding emitter to emit laser on the basis of the commands of the PDA remote controller. The solution tank stops rotating when the receiver receives laser signals. At this point, the solenoid valve installed at the bottom of the areas that correspond to the solution tank is aligned with the pesticide drawing tube of the real-time preparation unit to realize positioning for pesticide selection.

(2) With the stepper motor, the CC2530 wireless SCM drives the solution tank to move up or down to an appropriate height. The pesticide drawing tube of the preparation unit is then inserted into the solution of the corresponding section of the solution tank through a solenoid valve hole to draw the pesticide for preparation.

Monitoring node of a real-time pesticide preparation unit

The OKD-HZ21WA Hall flow meter sensor module is used and installed in the water drawing tube. The preparation unit consists of a preparation tank and temporary storage tank. A mixer, temperature sensor, and heater are installed in the preparation tank. The preparation unit works as follows:

(1) The amounts of water and pesticide are controlled. The water in the water storage tank and the pesticide in the solution tank are drawn through the mini pump, flow meter sensor module, and under the control of the solenoid valve as per the required amount into the

个监控节点采用TI公司推荐的最小应用系统电路，并结合GPIO接口电路设计而成，监控节点程序在TI公司Z-Stack-CC2530协议栈的基础上进行二次应用开发。

旋转式选药装置监控节点

旋转式选药装置的溶液箱由步进电机驱动其旋转，用于选择待喷施的农药类型。其中，步进电机选用57BYGH模块。CC2530无线单片机的P1.0-P1.2端口分别接57BYGH模块的脉冲端口CLK、方向端口DIR和使能端口EN。CC2530无线单片机根据PDA遥控器发送的指令，用于控制溶液箱的转动。8个激光光电传感器的发射头安装在溶液箱的底部，每个发射头对应溶液箱的一个分割区域。CC2530无线单片机的P0.0-P0.7端口驱动8个继电器开关，8个继电器开关的输出端口控制相应发射头发出激光。激光光电传感器选用M12NPN对管，激光发射光束集中且能量强，可以极大地降低误报率。CC2530无线单片机的外部中断输入端口INT1连接激光光电传感器的接收头的输出端口NO，当接收头接收到激光信号时，NO端口输出的低电平触发CC2530无线单片机的外部中断，从而实现了选药控制。选药控制的步骤为：

（1）根据PDA遥控器的指令，CC2530无线单片机驱动相应的发射头发出激光，接收头接收到激光信号时，溶液箱停止转动，此时，安装在溶液箱对应区域低部的电磁阀对准了实时配药装置的取药管，实现选药定位；

（2）CC2530无线单片机通过步进电机驱动溶液箱升降至合适的高度，配药装置的取药管通过电磁阀孔插入溶液箱相应区域的药液里，进行农药的抽取以便配药所用。

实时配药装置监控节点

流量计传感器模块选用OKD-HZ21WA霍尔流量计传感器模块，安装在抽水管中。配药装置由配制箱和暂存箱组成，配制箱内安装有搅拌器、温度传感器和加热器。配药装置的监控步骤为：

（1）水量和农药量的控制。通过微型水泵、流量计传感器模块和电磁阀控制，将蓄水箱的水和溶液箱内的药液按所需量抽入喷施液配制箱内。CC2530无线单片机的

solution preparation tank. The P1.2 port of the CC2530 SCM drives the relay switch to the output power to control the mini pump. The external interruption counter port is connected to the pulse signal output port of the OKD-HZ21WA module, so the metered water is drawn by indirectly measuring the water drawing amount through pulse counting. The P1.0 port of the CC2530 wireless SCM controls the pesticide drawing solenoid valve and realizes quantitative pesticide drawing each time together with eight solenoid valve holes at the bottom of the solution tank.

(2) Pesticide preparation and temperature in the preparation tank are controlled. When the required amounts of water and pesticide are drawn into the preparation tank of the pesticide preparation unit, the CC2530 wireless SCM controls the actions of the mixer through the P1.3 port. The CC2530 wireless SCM also monitors the temperature of the mixture in the preparation tank to thoroughly blend the pesticide solution. The DS18B20 digital temperature sensor is used for the temperature sensor. The CC2530 wireless SCM is also connected with the DQ port of DS18B20 through its P1.4 port to directly read the temperature data measured by DS18B20. The CC2530 SCM also controls the heater mounted at the bottom of the preparation tank through the P1.5 port to heat up the mixture in the preparation tank to the required temperature.

(3) The spraying of the temporary storage tank is controlled. Two level switches are installed in the temporary storage tank to detect the solution height in the tank. The MJ-0825PX mini switches are used for level switches. P2.0 and P2.1 ports of the CC2530 wireless SCM are connected to the two level switches to detect the solution level in the temporary storage tank. When the upper limit level switch in the temporary storage tank detects that the solution level exceeds the upper limit, the CC2530 wireless SCM closes it by controlling the solenoid valve between the preparation tank and the temporary storage tank through the P2.2 port. When the lower limit level switch in the temporary storage tank detects that the solution level is below the lower limit, the CC2530 wireless SCM opens it by controlling the solenoid valve to place the mixed solution into the temporary storage tank. Thus, the nozzle unit can spray in real time and start to prepare the solution for the next round.

Monitoring node of the nozzle unit

The nozzle unit of the pesticide spraying machine can spray in all directions. The nozzle height can be adjusted in real time according to the height of the crops to be sprayed. The CC2530 SCM drives the lifting rod through the stepper motor to adjust the nozzle on such rod to an appropriate height according to the wireless control command sent by the PDA remote controller. The P1.0 to P1.2 and P2.0 to P2.5 ports of the CC2530 wireless SCM are then connected to the stepper motor driver. The spraying angle of the nozzle is controlled by four telescopic rods connected to the nozzle. The four rods are divided into two groups that are time-sharing controlled by two motors. The CC2530 wireless SCM controls the four telescopic rods through the driving motor to realize clockwise and counterclockwise flexible spraying.

P1.2端口驱动继电器开关，继电器开关输出端口控制微型水泵的电源，CC2530无线单片机的外部中断计数端口接OKD-HZ21WA模块的脉冲信号输出端口，通过脉冲计数间接测得抽水的流量实现按量抽水的功能。CC2530无线单片机的P1.0端口控制取药电磁阀，并结合溶液箱低部的8个电磁阀孔控制，实现每次定量取用农药。

（2）配制箱内的配药和温度控制。当所需的水量和农药量抽入配药装置的配制箱内后，CC2530无线单片机通过其P1.3端口控制搅拌器的动作。为了喷施药液的充分混合，CC2530无线单片机还进行了配制箱内混合液的温度监控。温度传感器选用DS18B20数字温度传感器。CC2530无线单片机通过其P1.4端口与DS18B20的DQ端口相连接，从而直接读取DS18B20测量的温度数据。CC2530无线单片机通过其P1.5端口控制安装在配制箱底部的加热器工作，使得配制箱内的混合液温度达到所需温度。

（3）暂存箱的喷施控制。暂存箱内安装有2个液位开关用于检测箱内的喷施液高度。液位开关选用MJ-0825PX微型开关，CC2530无线单片机的P2.0、P2.1端口与2个液位开关相连接，用于采集暂存箱内喷施液的液位高度。当暂存箱内的上限液位开关检测到喷施液的液位高于上限值时，CC2530无线单片机通过其P2.2端口控制配制箱和暂存箱之间的电磁阀，使之关闭；当暂存箱内的下限液位开关检测到喷施液的液位小于下限值时，CC2530无线单片机控制配制箱和暂存箱之间的电磁阀，使之开启，从而将配制好的喷施液从配制箱放入暂存箱内，以供喷头装置实时喷施，并同时启动下一轮喷施液的配制。

喷头装置监控节点

农药喷施机的喷头装置可以实现全方向的喷施动作，喷头的高度可以依据所需喷施农作物的高度实时调节。根据PDA遥控器发送的无线控制指令，CC2530无线单片机通过步进电机驱动升降杆动作，使得安装在升降杆上的喷头调整至合适的高度。其中，CC2530无线单片机的P1.0-P1.2、P2.0-P2.5端口与步进电机的驱动器相连接。喷头的喷施角度由4个连接在喷头上的伸缩杆进行控制，伸缩杆分成2组由2个电机进行分时控制。CC2530无线单片机通过驱动电机控制4个伸缩杆从而实现顺时针和逆时针灵活喷施。

Monitoring node of the intelligent mobile platform

The Traveler No. 4 whole landform mobile platform of Borch Company is employed. It is a powerful whole landform mobile platform with an open system, flexible expansion, excellent cross-country capacity, and all-weather operation capacity. It can travel on sand, soil, and grass, and it has a loading capacity of up to 60 kg. This mobile platform reserves the RS232 communication interface. The RXD and TXD ports of the CC2530 wireless SCM are connected to the RS232 communication port of the Traveler No. 4 whole landform mobile platform and control the proceedings of such platform by writing commands.

Design of the PDA remote controller

The PDA controller uses ARM11 core architecture 32-bit S3C6410 embedded controller and is designed with an LCD touch screen. This controller has strong data processing capacity, low energy consumption, a user-friendly interface, and simple operation.

Design of the PDA remote controller circuit

The PDA remote controller adopts the design concept of the core board with the base board added to improve the electromagnetic compatibility of the circuit design and maintenance convenience. Its structure is shown in Figure 3. The core board consists of a S3C6410 embedded controller, a 256 MB SDRAM with two pieces of K4X1G163PC-FGC6 memory, and a 4 GB NAND Flash with two pieces of K9GAG08U0E-S memory. The base board mainly consists of a power supply module, USB interface, JTAG interface, LCD interface, and URAT interface. The UART interface of the S3C6410 embedded controller is linked to the serial port of the ZigBee coordinator node to achieve communication between the ZigBee control nodes. The IIC interface of the S3C6410 embedded controller is linked to the Wi-Fi communication module to realize communication with the image collecting module of the Wi-Fi camera. The PDA remote controller employs an AT070TN83V 7” LCD touch screen for visual display to facilitate manipulation by touch.

Design of the PDA controller program

The PDA remote controller uses Microsoft Platform Builder and is customized by the WinCE6.0 graphical embedded operation system. The SQLite embedded database is transplanted in WinCE6.0 to store prompt data of the expert system. SQLite is small, open source, simple to operate, and requires only a small memory. The SQLite database is realized by adding two database files, namely, sqlite.lib and sqlite.dll, to the application project and calling its API function to read and write in the database. An application program for the monitoring system of the pesticide spraying machine is developed on the WinCE6.0 embedded operation system. Its program flow is shown in Figure 4.

Figure 5 shows the monitoring interface of the application program of the monitoring system for a pesticide spraying machine. This interface consists of pesticide selection control, mode selection, travel route control, camera control, nozzle unit control, and residual amount and temperature display modules.

智能移动平台监控节点

选用博创公司旅行家 4 号全地形移动平台，它是一款功能强大、系统开放、扩展灵活、具有出众越野能力和全天候工作能力的全地形移动平台，能适应沙石、泥土、草地行走，具有 60kg 负载工作能力。该移动平台预留 RS232 通信接口，CC2530 无线单片机的 RXD、TXD 端口与旅行家 4 号全地形移动平台的 RS232 通信接口相连，通过写入指令控制旅行家 4 号全地形移动平台行进。

PDA 遥控器设计

PDA 遥控器采用 ARM11 内核架构的 32 位 S3C6410 嵌入式控制器，并结合液晶触摸屏进行设计，具有数据处理能力强、功耗低、界面友好和操控简单的优点。

PDA 遥控器的电路设计

通为提高电路设计的电磁兼容性和维护的方便性，PDA 遥控器采用核心板加底板的设计思路，其结构如图 3 所示。核心板由 S3C6410 嵌入式控制器、两片 K4X1G163PC-FGC6 存储器接成 256MB 容量的 SDRAM、两片 K9GAG08U0E-S 存储器接成 4GB 容量的 NAND Flash 共同组成；底板主要由电源模块、USB 接口、JTAG 接口、LCD 接口、URAT 接口组成。S3C6410 嵌入式控制器的 UART 接口与 ZigBee 协调器节点的串口相连，实现与 ZigBee 控制节点之间的相互通信。S3C6410 嵌入式控制器的 IIC 接口与 Wi-Fi 通信模块相连，实现与 Wi-Fi 摄像头图像采集模块相互通信。为了直观显示和方便操控，PDA 遥控器选用 AT070TN83V 七寸液晶触摸屏，以便实现实时显示和触摸操控。

PDA 遥控器的程序设计

PDA 遥控器采用微软在 WinCE6.0 上移植 SQlite 嵌入式数据库存储专家系统提示数据。Platform Builder 软件，自行定制出 WinCE6.0 图形化的嵌入式操作系统，SQlite 具有体积小、开源、运行内存所需存储量小、操作方便等优点，SQlite 数据库的实现方式是将 sqlite.lib 和 sqlite.dll 两个库文件加入应用程序工程，调用其 API 函数即可读写数据库。在 WinCE6.0 嵌入式操作系统上开发出农药喷施机监控系统应用程序，其程序流程如图 4 所示。

农药喷施机监控系统应用程序的监控界面如图 5 所示，由选药控制模块、模式选择模块、行走路线控制模块、摄像头控制模块、喷头装置控制模块和剩余量及温度显示模块组成。

Figure 5 shows that this monitoring system provides all-around monitoring functions by determining the human–machine monitoring interface. The functions of each monitoring module are described as follows:

(1) The pesticide selection control module consists of a crop variety selection button, expert system prompt box, drop-down pesticide, or nutrient solution selection list, preparation proportion setting box, and pesticide or nutrient selection indicator light. Before the pesticide spraying machine works, operators determine the variety of pesticide or nutrient solutions and proportion them on the basis of the spraying object, expert system prompt box, and their own experiences.

(2) The mode selection module consists of six buttons for fixed distance automatic mode, travel spraying automatic mode, manual mode, cleaning, reset, and stop preparing. The real-time preparation unit is cleaned automatically by clicking the washing button. All units of the pesticide spraying machine are reset by clicking the reset button. The pesticide spraying machine performs spraying in accordance with the pre-set program by clicking the fixed distance automatic mode button or travel spraying automatic mode. The operator controls the pesticide spraying machine by itself by clicking the manual mode button. The pesticide solution preparation tank stops preparing the pesticide by clicking the stop preparing button. The solution temporary storage tank then sprays all the solution inside.

(3) The travel route control module consists of five buttons, namely, forward, backward, turn left, turn right, and stop. The operator can control the travel route of the intelligent mobile platform according to the monitoring video transmitted by the image collecting module of the Wi-Fi camera under the manual mode.

(4) The nozzle unit control module consists of four buttons, namely, ascending, descending, clockwise, and counterclockwise. The operator can adjust the nozzle height using the ascending and descending buttons under the manual mode.

(5) The camera control module adjusts the camera angle using four buttons, namely, upward, downward, leftward, and rightward. The camera shooting and video monitoring are controlled by the shooting and video buttons.

(6) The residual amount and temperature display module displays the residual amount of the solution, residual water amount, and temperature in the preparation tank.

由图 5 所提供的人机监控界面可知，该监控系统提供了全面的监控功能。各个监控模块的功能分别描述如下：

（1）选药控制模块由作物种类选择按钮，专家系统提示框，农药或营养液选择下拉菜单，配制比设置框和农药或营养液选择指示灯共同组成。农药喷施机作业前，作业人员根据喷施对象、专家系统提示框的帮助信息和自身经验，确定农药或营养液种类以及配比。

（2）模式选择模块由定点距离自动模式、边走边喷自动模式、手动模式、清洗、复位和停止配药 6 个按钮组成。点击清洗按钮，自动完成实时配药装置的清洗。点击复位按钮则农药喷施机所有装置全部复位。点击定点距离自动模式按钮或边走边喷自动模式，农药喷施机按照事先设置好的程序执行喷施工作。点击手动模式按钮，作业人员自行控制农药喷施机作业。点击停止配药按钮，则农药喷施液配制箱停止配药，喷施液暂存箱将其内部的喷施液全部喷施完毕。

（3）行走路线控制模块由前进、后退、左转、右转和停止 5 个按钮组成，在手动模式下作业人员可根据 Wi-Fi 摄像头图像采集模块传输回来的监控视频，对智能移动平台的行进路线进行控制。

（4）喷头装置控制模块由上升、下降、顺时针、逆时针 4 个按钮组成。在手动模式下作业人员通过上升、下降按钮调节喷头装置的高度。

（5）摄像头控制模块由上调、下调、左调、右调 4 个按钮调节摄像头角度，拍照按钮和视频按钮控制摄像头拍照和视频监视。

（6）剩余量及温度显示模块显示溶液的剩余量、水量剩余量和配制箱内的温度。

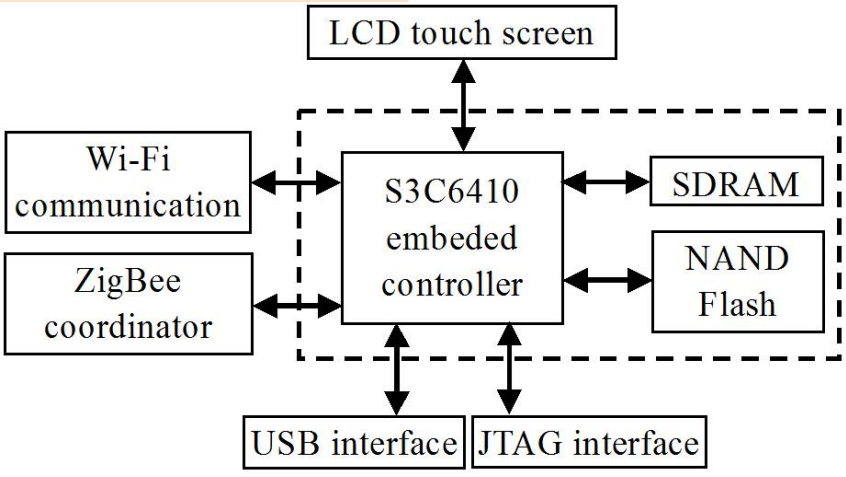

Fig. 3 - Hardware structure of the PDA remote controller

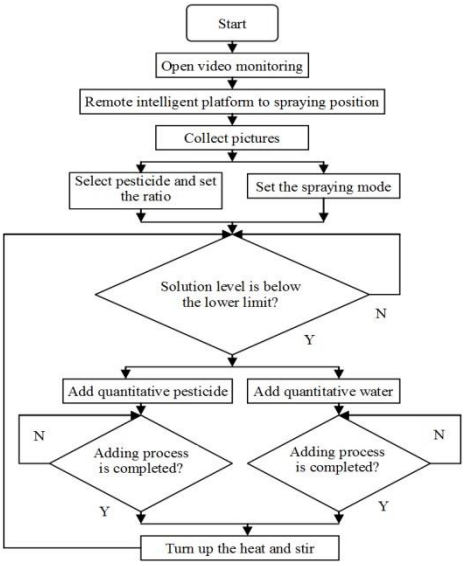

Fig. 4 - Program flowchart of the intelligent monitoring system

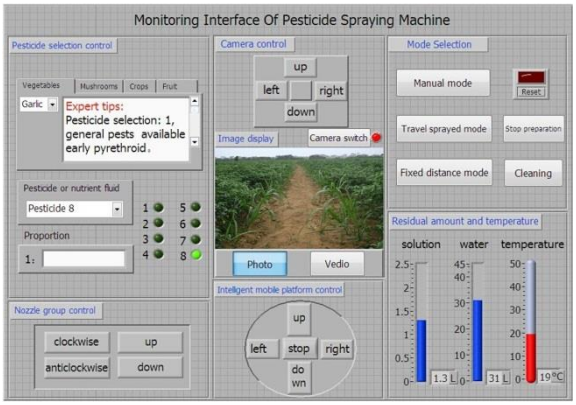

Fig. 5- Monitoring interface

RESULTS

The test was performed in June when weeds were flourishing. The test site was the test park of a farm. An intelligent monitoring system was set up based on the structure shown in Figure 2. This system comprises four ZigBee monitoring nodes, a PDA remote controller, and a Wi-Fi camera module. The test mainly includes a packet drop ratio of the ZigBee network and performance test of a PDA controller.

Test of the packet drop ratio of the ZigBee network

Given the test of the packet drop ratio of ZigBee network, command data packets are sent through the PDA remote controller. The data packets received by the ZigBee monitoring node are then counted to determine the data transfer stability of ZigBee network. The test results are shown in Table 1.

The data in Table 1 show that the maximum packet drop ratio of a single node is 0.24%, whereas the average packet drop ratio of the entire ZigBee network is 0.21%. These results show that the wireless transfer of data is highly stable. Each control command is responsively sent to further improve the reliability of data wireless transfer. The ZigBee monitoring node sent responsive signals upon receiving the control command from the PDA remote controller. If the PDA remote controller does not receive the responsive signals, it resends the control command. Through tests of 10,000 wireless control commands sent by the PDA remote controller with this method, the success rate of command sending is determined to be up to 100%.

Performance test of the PDA remote controller

The response time and remote control distance of the monitoring nodes of the pesticide selection unit, real-time preparation unit, nozzle unit, and intelligent mobile platform are measured by sending control commands through the PDA remote controller in the performance test of the PDA remote controller. The test results are shown in Table 2. The data show that the response time of each monitoring node is fast, the PDA remote control can completely control each monitoring node in real time, and the effective control distance is up to 110 m.

结果

试验时间选在杂草生长茂盛的6月份，试验地点选在农场试验园区。按照前述的图2所示结构构建起智能监控系统。该系统包括4个ZigBee监控节点、1个PDA遥控器、1个Wi-Fi摄像头模块，测试试验主要包括ZigBee网络的丢包率和PDA遥控器的性能测试。

ZigBee网络丢包率测试

ZigBee 网络传输丢包率测试，通过 PDA 遥控器发送控制指令数据包，对 ZigBee 监控节点接收的数据包进行统计，得出 ZigBee 网络数据传输稳定性的结论。测试结果如表 1 所示。

从表 1 数据可知，单个节点最大丢包率为 0.24%，整个 ZigBee 网络的平均丢包率为 0.21%，这表明数据的无线传输稳定性高。为进一步提高数据无线传输的可靠性，每条控制指令采用应答式发送。ZigBee 监控节点收到来自 PDA 遥控器的控制指令后发出应答信号，若 PDA 遥控器未收到应答信号，将重新发送控制指令。采用此种方式对 1 万个 PDA 遥控器发送的无线控制指令进行测试，指令发送成功率达 100%。

PDA 遥控器的性能测试

PDA 遥控器的性能测试，就是通过 PDA 遥控器发送控制指令，测试选药装置监控节点、实时配药装置监控节点、喷头装置监控节点、智能移动平台监控节点的响应时间和遥控距离，测试结果如表 2 所示。从表 2 中数据可知，各个监控节点的响应时间快，PDA 遥控器完全可以实时控制各个监控节点，其有效遥控距离可达 110m。

Spraying efficiencies test

Sichuan Province of China belongs to the basin and hilly area. For the pesticide spraying operation, there is no intelligent mechanical equipment suitable for the ground walking, using artificial piggyback operation completed. Spraying efficiencies of the machine, obtained through calculating practical spraying area within a unit of time, are shown in Table 3. According to the data, the spraying efficiency of the spraying machine in time unit is 2–3 times bigger than that in artificial spraying.

喷施效率测试

中国四川省属于盆地、丘陵地区，当前农药喷施作业无适合地面行走的智能机械设备，采用人工背负式操作完成。喷施机的喷施效率见表 3。其中，喷施效率通过对喷施机单位时间内实际喷施面积的测量得出。从表 3 的数据可知，该喷施机单位小时的喷施效率是人工喷施效率的 2～3 倍。

Table 1

Packet drop ratio of the ZigBee network

ZigBee monitoring node	Sent data packets	Received data packets	Packet drop ratio / %
Pesticide selection unit	2880	2874	0.21
Real-time preparation unit	2880	2875	0.17
Nozzle unit	2880	2873	0.24
Average	2880	2874	0.21

Table 2

Performance test of the PDA remote controller

Remote control distance / m	Pesticide selection response time / ms	Real-time preparation response time / ms	Nozzle response time / ms	Spraying response time / ms	Intelligent mobile platform response time / ms
1	15	18	16	15	23
20	18	20	17	17	25
50	22	22	21	23	28
80	24	25	23	25	31
100	27	29	28	26	36
110	29	32	30	30	45
120	380	No response	860	710	No response

Table 3

Spraying efficiencies

Working environment	Lawn	Greenhouses	Orchard
Artificial piggyback operation / $m^2.h^{-1}$	1917	1203	1003
Machine operation / $m^2.h^{-1}$	6018	3527	3012

CONCLUSIONS

An intelligent monitoring system is developed to improve the safety and intelligence of pesticide spraying machines. Focusing on the mechanical structure of the pesticide spraying machine, the ZigBee technology-based design project is proposed. The monitoring node of the rotary pesticide selection unit, monitoring node of the real-time preparation unit, monitoring node of the nozzle unit, Wi-Fi camera image collecting module, monitoring node of the intelligent mobile platform, and PDA controller are also designed.

The graphics-embedded operating system of WinCE6.0 is designed on the PDA remote controller and transplanted with the embedded SQLite database to achieve strong data processing and management capacity. This system employs an LCD touch screen with a friendly human–machine interface that is easy to use and publicize. A dialogue box-based monitoring system program is developed to increase pesticide spraying

结论

为提高农药喷施机作业的安全性及智能化水平开发出智能监控系统，针对农药喷施机的机械结构，提出基于 ZigBee 技术为核心的设计方案，设计出旋转式选药装置监控节点、实时配药装置监控节点、喷头装置监控节点、智能移动平台监控节点、Wi-Fi 摄像头图像采集模块和 PDA 遥控器。

在 PDA 遥控器上设计出 WinCE6.0 图形化的嵌入式操作系统并移植了嵌入式 SQlite 数据库，实现强大的数据处理与管理能力。系统采用液晶触摸屏操控，人机界面友好，使用简单，易于推广。为提高农药喷施效率，开发出基于对话框的监控系统程序，可实现三种喷施作业模式即定点

efficiency. This program has three spraying modes, namely, fixed spot spraying automatic mode, travel spraying automatic mode, and manual mode. The spraying efficiency is 2–3 times bigger than of manual spraying.

The system wiring is decreased and the machine can be flexibly used with ZigBee technology. The ZigBee network transfers data stably. The average packet drop ratio of the entire ZigBee network is 0.21%, and the effective remote-controlled distance is up to 110 m.

ACKNOWLEDGEMENT

The paper was supported by the project (No. 12ZA277) of Natural Science Foundation of Sichuan Education Department in China.

REFERENCES

[1]. Changyuan Z, Chunjiang Z, Xiu W. (2014) - *Nozzle test system for droplet deposition characteristics of orchard air-assisted sprayer and its application*, International Journal of Agricultural and Biological Engineering, vol. 7, no. 2, pp.122-129;

[2]. Faiçal B S, Costa F G, Pessin G. (2014) - *The use of unmanned aerial vehicles and wireless sensor networks for spraying pesticides*, Journal of Systems Architecture, vol. 60, no. 4, pp. 393-404;

[3]. Lixia W, Shuhui Z, Chenglin M. (2010) - *Design of variable spraying system based on ARM*, Transactions of the Chinese Society of Agricultural Engineering, vol. 26, no. 4, pp.113-118;

[4]. Lijia X, Chunseng R, Wenjuan W, et al. (2012) - *Development on small pesticide spraying machine with real-time mixing and remote-control spraying*, Transactions of the Chinese Society of Agricultural Engineering, vol. 28, no. 10, pp. 13–19;

[5]. Mamidi, V R, Ghanshyam, C, ManojKumar P. (2013) - *Electrostatic hand pressure knapsack spray system with enhanced performance for small scale farms*, Journal of Electrostatics, vol. 71, no. 4, pp. 785-790;

[6]. Shuren C, Dongfu Y, Xinhua W, et al. (2011) - *Design and simulation of variable weed spraying controller based on adaptive neural fuzzy inference system*, Journal of Drainage and Irrigation Machinery Engineering, vol. 29, no. 3, pp.272-276;

[7]. Wei D, Huang Y, Chunjiang Z, et al. (2013) - *Spatial distribution visualization of PWM continuous variable-rate spray*, International Journal of Agricultural and Biological Engineering, vol. 6, no. 4, pp.1-8;

[8]. Ximin F, Xiaolan L, Weimin D, et al. (2009) - *Present state and technical requirement about orchard plant protection machinery in China*, Chinese Agricultural Mechanization, no. 6, pp.10-13;

[9]. Xinghua W, Bing J, Hongwei S, et al. (2012) - *Design and test of variable rate application controller of intermittent spray based on PWM*, Transactions of the Chinese Society of Agricultural Machinery, vol. 43, no. 12, pp.87-89;

[10]. Yick J, Mukherjee B, Ghosal D. (2008) - *Wireless sensor network survey*, Computer Networks, vol.52, no.12, pp.2292–2330;

[11]. Zetian F, Lijun Q, Junhong W. (2007) - *Developmental tendency and strategies of precision pesticide application techniques*, Transactions of the Chinese Society for Agricultural Machinery, vol. 38, no. 1, pp.189-192.

喷施自动模式、边走边喷自动模式、手动模式，喷施效率是人工的 2～3 陪。

采用 ZigBee 技术减少了系统布线，使用灵活。ZigBee 网络数据传输稳定，平均丢包率为 0.21%，有效遥控距离达 110m。

致谢

本文受到四川省教育厅自然科学基金项目资助（项目号：No. 12ZA277）。

参考文献

[1]. Changyuan Z, Chunjiang Z, Xiu W. (2014) - *果园风送喷雾机的喷头雾滴沉积特性测试与应用*, 国际农业与生物工程学报, 第 7 卷, 第 2 期, 122-129;

[2]. Faiçal B S, Costa F G, Pessin G. (2014) - *基于无线传感器网络和无人机的喷雾杀虫*, 系统结构, 第 60 卷, 第 4 期, 393-404;

[3]. 王利霞, 张书慧, 马成林. (2010) - *基于 ARM 的变量喷药控制系统设计*, 农业工程学报, 第 26 卷, 第 4 期, 113-118;

[4]. 许丽佳, 冉春森, 王文娟, 等. (2012) - *小型无线遥控和实时配药喷施机的研制*, 农业工程学报, 第 28 卷, 第 10 期, 13–19;

[5]. Mamidi, V R, Ghanshyam, C, ManojKumar P. (2013) - *静电手压背负式喷雾提高小农场喷施性能*, 静电学报, 第 71 卷, 第 4 期, 785-790;

[6]. 陈树人, 尹东富, 魏新华, 等. (2011) - *变量喷药自适应神经模糊控制器设计与仿真*, 排灌机械工程学报, 第 29 卷, 第 3 期, 272-276;

[7]. Wei D, Huang Y, Chunjiang Z, et al. (2013) - *基于可视化空间分布的 PWM 连续变量喷雾*, 国际农业与生物工程学报, 第 6 卷, 第 4 期, 1-8;

[8]. 傅锡敏, 吕晓兰, 丁为民, 等. (2009) - *我国果园植保机械现状与技术需求*, 中国农机化, 第 6 期, 10-13;

[9]. 魏新华, 蒋杉, 孙宏伟, 等. (2012) - *PWM 间歇喷雾式变量喷施控制器设计与测试*, 农业机械学报, 第 43 卷, 第 12 期, 87-89;

[10]. Yick J, Mukherjee B, Ghosal D. (2008) - *无线传感器网络综述*, 计算机网络, 第 52 卷, 第 12 期, 2292–2330;

[11]. 傅泽田, 祁力钧, 王俊红. (2007) - *精准施药技术研究进展与对策*, 农业机械学报, 第 38 卷, 第 1 期, 189-192.

THE USE OF DIMENSIONAL ANALYSIS IN STUDYING THE SPRAYING PROCESS THROUGH NOZZLES AT PHYTOSANITARY TREATMENT MACHINES
/
PREZENTAREA METODEI ANALIZEI DIMENSIONALE ÎN STUDIUL PROCESULUI DE PULVERIZARE PRIN DUZE LA MAŞINILE DE APLICAT TRATAMENTE FITOSANITARE

Ph.D. Stud. Eng. Dumitraşcu A[1)]**., Ph.D. Eng. Manea D.**[1)]**,**
Univ. Em. Prof. Ph.D. Eng. Căsăndroiu T.[2)]
[1)] National Institute of Research-Development for Machines and Installations designed to Agriculture and Food Industry - INMA, Bucharest
[2)] University POLITEHNICA of Bucharest, Faculty of Biotechnical Systems Engineering / Romania
E-mail: a.dumi@yahoo.com

Abstract: *The quality of phytosanitary treatments performed in crops is largely determined by how substances are sprayed on the plant, by the droplets size, the coverage of the plant and the reduction of the phenomenon of drift. The main elements responsible for the quality of working process of phytosanitary treatment machines are the nozzles, which are the main elements of any sprayers. This explains the great variety of spraying systems. In this paper are detailed some theoretical issues regarding the spraying process through nozzles as the basis for experiments to be carried out using the machine for high precision application of phytosanitary treatments in orchards, MSL. Analysis and modeling of this process is achieved using as main working instrument the dimensional analysis theory.*

Keywords: *spraying process, nozzles, droplets, dimensional analysis*

INTRODUCTION

The gas-liquid two-phase fluid flow is widely found in nature such as, for example, in raindrops fall. In practical applications, an important type of such process is the flow of a two-phase fluid with an initial impulse, which leads to liquid cleavage in droplets.

This spraying process often takes place by passing the liquid through a diffuser - a nozzle. Spraying is the process that leads to the conversion of liquid flow in droplets by passing liquid under pressure through a nozzle. The forces of surface tension of the liquid, which provide it homogeneousness, are canceled by internal and external factors.

Figure 1 schematically illustrates the structure of a liquid spray jet.

Rezumat: *Calitatea tratamentelor fitosanitare efectuate în culturile agricole este determinată în mare măsură de modul cum sunt pulverizate substanţele fitosanitare pe plantă, mărimea picăturilor, gradul de acoperire a plantei şi reducerea fenomenului de derivă. Principalele elemente responsabile de calitatea procesului de lucru al maşinilor de aplicat tratamente fitosanitare sunt duzele, care se constituie ca elemente principale ale oricărei maşini de stropit. Acest fapt explică şi marea diversitate de sisteme de pulverizare. În această lucrare sunt aprofundate unele aspecte teoretice privind procesul de pulverizare prin duze, ca bază pentru experimentările ce vor fi efectuate folosind Maşina pentru aplicarea cu precizie ridicată a tratamentelor fitosanitare în plantaţiile pomicole, MSL. Analiza şi modelarea acestui proces se fac utilizând ca instrument principal de lucru teoria analizei dimensionale.*

Cuvinte cheie: *proces de pulverizare, duze, picături, analiză dimensională*

INTRODUCERE

Curgerea fluidelor bifazice lichid-gaz este întâlnită pe scară largă în natură, ca, de exemplu, în căderea picăturilor de ploaie. În aplicaţiile practice, un tip important de astfel de proces este curgerea unui flux bifazic având un impuls iniţial, care conduce la scindarea lichidului în picături mici.

Acest proces de pulverizare are loc adesea prin trecerea lichidului printr-un ajutaj divergent - o duză. Pulverizarea este procesul care conduce la conversia vânei de lichid în picături, prin trecerea lichidului sub presiune printr-o duză. Forţele de tensiune superficială a lichidului, care îi conferă omogenitatea, sunt anulate de factori interni şi externi.

Figura 1 ilustrează schematic structura unui jet de lichid pulverizat.

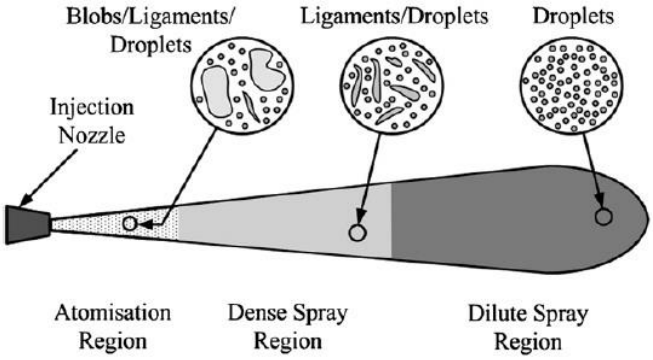

Fig. 1 – The structure of a liquid spray jet [3]

In the initial zone, liquid fraction is dominant, the liquid being decomposed into bubbles and ligaments (liquid non-spherical particles). In the intermediate, dense spraying zone, liquid fraction has a smaller, but significant share.

În zona iniţială, fracţiunea lichidă e dominantă, lichidul fiind descompus în bule şi ligamente (particule de lichid non-sferice). În zona intermediară, de pulverizare densă, fracţiunea lichidă are o pondere mai mică, dar semnificativă.

Here a secondary fragmentation takes place and droplet/droplet interactions, such as collision and coalescence, occur. In the diluted spraying zone spherical well formed droplets, strongly interacting with turbulent air jet are prevailing. In general, the spraying depends on the injection pressure through nozzle, the flow of fluid, the geometric characteristics of the nozzle, the viscosity and density of the liquid.

Fragmentation or hydraulic spraying is accomplished by forcing the passing of liquid through calibrated orifices, called nozzles. In the case of phytosanitary treatment machines fragmentation is achieved by means of:

- hydraulic spraying nozzles with projected jet (either flat or conical directly projected jet, or jet making an impact with a lamination surface, which changes the direction of the jet, i.e. nozzles with indirectly projected jet);
- swirling nozzles, also called tangential nozzles (with helical deflector or swirling pad), where fluid is inducted into a circular motion in a room placed before the calibrated orifice;
- twinjet hydraulic nozzles where jets hit each other, thus achieving dispersion.

Some of the most utilized nozzles (at vineyards and orchards spraying machines) are those tangential with helical deflector and conical jet. The deflector imparts a swirling motion to the liquid. The resulting turbulence splits the jet into droplets that form a cone, when leaving the calibrated orifice. The swirling chamber may be with constant volume or adjustable volume. The swirling chamber volume adjustment is done by shifting the deflector.

Depending on the average droplet size and the amount of liquid applied per unit of surface area, most authors use a classification system of the types of treatment shown in table 1.

Aici are loc o fragmentare secundară şi apar interacţiuni picătură/picătură, cum ar fi coliziunile şi coalescenţa. În zona de pulverizare diluată predomină picăturile sferice, bine formate, care interacţionează puternic cu jetul turbulent de aer. În general, pulverizarea depinde de presiunea de injecţie prin duză, de debitul de lichid, de caracteristicile geometrice ale duzei, de vâscozitatea şi densitatea lichidului.

Fragmentaţia sau pulverizarea hidraulică se realizează prin trecerea forţată a lichidelor de stropit prin orificii calibrate, denumite duze. În cazul maşinilor de aplicat tratamente fitosanitare fragmentaţia se realizează:

- prin duze de pulverizare hidraulică cu jet proiectat (fie jet plat sau conic direct proiectat, fie jet care face un impact cu o suprafaţă de laminare, care schimbă direcţia jetului, adică duze cu jet indirect proiectat);
- prin duze de turbionare, denumite şi duze tangenţiale (cu deflector elicoidal sau pastilă de turbionare), unde lichidului i se imprimă o mişcare circulară într-o cameră plasată înaintea orificiului calibrat;
- prin duze hidraulice cu două jeturi care se lovesc între ele, realizându-se astfel dispersia.

Unele dintre cele mai utilizate duze (la maşinile de stropit în vii şi livezi) sunt cele tangenţiale cu deflector elicoidal şi jet conic. Deflectorul imprimă o mişcare turbionară lichidului. Turbulenţa rezultantă scindează jetul în picături, care se constituie într-un con, când ies din orificiul calibrat. Camera de turbionare poate fi cu volum constant sau cu volum reglabil. Reglarea volumului camerei de turbionare se face prin deplasarea deflectorului.

În funcţie de dimensiunea medie a picăturilor şi de cantitatea de lichid aplicată pe unitatea de suprafaţă, majoritatea autorilor folosesc un sistem de clasificare al tipurilor de tratament prezentat în tabelul 1.

Table 1 [7]

The classification of phytosanitary treatments

The diameter of sprayed liquid droplets [µm]	The assignment to grades of fineness	The treatments classification depending on particle fineness	The dose of applied liquid [l/ha]	The treatment classification depending on the volume of applied liquid
0-5	aerosols	atomization	< 0,5	UULV - Ultra Ultra Low Volume
5-50	mist	atomization	0,5-5,0	ULV - Ultra Low Volume
50-100	very fine	spraying	5-50	LV - Low Volume
100-200	fine	aspersion	50-150	MV - Medium Volume
200-300	medium	aspersion	150-600	HV - High Volume
300-1000	coarse	aspersion	>600-2500	VHV - Very High Volume

The quantitative distribution of the pulverized liquid is influenced by a number of factors such as the working pressure of the sprayer, the initial speed of the atomized jet, the flow rate of the sprayer, the spraying system used [5].

The diversification of spraying types and of phytosanitary application systems aims to improve the effectiveness of treatment.

METHODOLOGY

Up to now it was not possible to establish the complex spray laws. Although the phenomenon of fluid decomposition was the subject of a series of theoretical and experimental research in the last 100 years, however a general theory, on which is possible to determine a priori the degree of pulverization for different types of nozzles, features of the liquid and working conditions has not yet developed.

Applying mathematical analysis confines generally to the formulation the problem, i.e. the establishment of

Repartiţia cantitativă a volumului de lichid pulverizat este influenţată de o serie de factori cum ar fi presiunea de lucru a pulverizatorului, viteza iniţială a jetului de lichid pulverizat, debitul pulverizatorului, sistemul de pulverizare folosit [5].

Diversificarea tipurilor de pulverizare şi a sistemelor de aplicare a tratamentelor fitosanitare are ca scop îmbunătăţirea eficacităţii tratamentului.

METODOLOGIE

Până în prezent nu a fost posibilă stabilirea legilor pulverizării complexe. Deşi fenomenul descompunerii vânei de lichid a constituit obiectul unei serii de cercetări teoretice şi experimentale în ultimii 100 de ani, totuşi nu s-a elaborat încă o teorie generală, pe baza căreia să fie posibilă determinarea apriorică a gradului de pulverizare pentru diferite tipuri de duze, caracteristici ale lichidului şi condiţii de lucru.

Aplicarea analizei matematice se mărgineşte, în general, la formularea problemei, adică la stabilirea

differential equations and contour conditions.

Solving these equations is possible only in a few special cases and with a whole range of simplifying assumptions. A complete analytical solution to the problem of droplet sizes present considerable difficulties for two reasons:

a. There are not accurately known the wavelength and the intensity of oscillations that exist in jet and which depend on the initial conditions of flow through nozzle, the nozzle design, the machining and surface condition, etc.

b. The droplets obtained are the result of a complex process of sprinkling the droplets formed in the substitution area [2].

For the reasons given above, the possibility of a complete analytical solving of the problem is excluded. Therefore, studying the spraying is done experimentally, and the results, based on the similarity theory, are generalized to similar dynamic systems.

For establishing physical relations, the relationship between the values used for the description of physical phenomena, the dimensional analysis may be used. This method is based on the fundamental theorem of dimensional analysis, Π theorem, of Vaschy-Buckingham. According to this theorem, the physical processes or physicochemical processes can be described by functions of independent similarity criteria that can be formed of controlling process variables. It is considered that those criteria are independent which can not be expressed through arithmetic combinations of other criteria.

Thus, if a process is determined by n dimensional variables:

$X_1, X_2, X_3 ... X_n$

it can be expressed by means of a general form criteria function:

$f(\Pi_1, \Pi_2, \Pi_3 ... \Pi_{n-m}) = 0$

The Π theorem reads as follows: *the number of independent criteria from the criteria function is the difference* n-r, *where* n *is the number of dimensional variables and* r *is the rank of the dimensional matrix, which is equal to the number of fundamental values depending on which may be expressed the analyzed variables* [6].

In the case of the spraying process through nozzles, dimensional analysis takes into account the following function of m = 7 variables:

ecuaţiilor diferenţiale şi a condiţiilor de contur.

Rezolvarea acestor ecuaţii este posibilă numai în câteva cazuri speciale şi cu o serie întreagă de ipoteze simplificatoare. O soluţie analitică completă a problemei referitoare la dimensiunile picăturilor prezintă greutăţi considerabile din două motive:

a. Nu se cunoaşte cu precizie lungimea undelor şi intensitatea oscilaţiilor care există în jet şi care depind de condiţiile iniţiale ale scurgerii jetului prin duză, de construcţia duzei, de prelucrarea şi starea suprafeţelor, etc.

b. Picăturile ce se obţin sunt rezultatul unui proces complex de granulare a picăturilor formate în spaţiul de schimb [2].

Din motivele arătate mai sus, posibilitatea unei rezolvări analitice complete a problemei este exclusă. De aceea, studierea pulverizării se face pe cale experimentală, iar rezultatele obţinute, în baza teoriei similitudinii, sunt generalizate pentru sisteme dinamic asemenea.

Pentru stabilirea relaţiilor fizice, a legăturii care există între mărimile utilizate la descrierea fenomenelor fizice, poate fi utilizată analiza dimensională. Această metodă se bazează pe teorema fundamentală a analizei dimensionale, teorema Π, a lui Vaschy-Buckingham. Conform acestei teoreme, procesele fizice sau procesele fizico-chimice pot fi descrise prin funcţii ale criteriilor de similitudine independente ce se pot forma cu variabilele care controlează procesul. Se consideră că sunt independente acele criterii care nu pot fi exprimate prin combinaţii aritmetice ale altor criterii.

Astfel dacă un proces este determinat de n variabile dimensionale:

$X_1, X_2, X_3 ... X_n$

acesta poate fi exprimat printr-o funcţie criterială de forma generală:

$f(\Pi_1, \Pi_2, \Pi_3 ... \Pi_{n-m}) = 0$

Teorema Π are următorul enunţ: *numărul de criterii independente din funcţia criteriala este dat de diferenţa* n-r, *unde* n *este numărul variabilelor dimensionale iar* r *este rangul matricei dimensionale, care este egal cu numărul mărimilor fundamentale în funcţie de care se pot exprima variabilele luate în analiză* [6].

În cazul procesului de pulverizare prin duze, analiza dimensională ia în considerare următoarea funcţie de m = 7 variabile:

$$f(D, v, \rho_l, d, \eta_l, \sigma, \rho_g) = 0 \quad (1)$$

where:

D – nozzle diameter, v – the relative velocity of the liquid to the surrounding gas, ρ_l – the liquid density, d – the droplet diameter, η_l – the dynamic viscosity of the liquid, σ – the surface tension of the liquid, ρ_g – the gas density

D, v, ρ_l are fundamental values.

Dimensionless complexes (independent criteria) are:

unde:

D – diametrul duzei, v – viteza relativă a lichidului faţă de gazul înconjurător, ρ_l – densitatea lichidului, d – diametrul picăturii, η_l – vâscozitatea dinamică a lichidului, σ – tensiunea superficială a lichidului, ρ_g – densitatea gazului

D, v, ρ_l sunt mărimile fundamentale.

Complexii adimensionali (criteriile independente) sunt:

$$\Pi_1 = \frac{d}{D}; \Pi_2 = \frac{\eta_l}{D^{x_1} v^{x_2} \rho_l^{x_3}}; \Pi_3 = \frac{\sigma}{D^{x_1'} v^{x_2'} \rho_l^{x_3'}}; \Pi_4 = \frac{\rho_g}{\rho_l} \quad (2)$$

The dimensional matrix of variables for d = 3 fundamental values, L (length), M (mass), T(time), is:

Matricea dimensională a variabilelor pentru d = 3 mărimi fundamentale, L (lungime), M (masă), T(timp), este:

$$\begin{array}{c|ccccccc} & D & v & \rho_l & d & \eta_l & \sigma & \rho_g \\ L & 1 & 1 & -3 & 1 & -1 & 0 & -3 \\ M & 0 & 0 & 1 & 0 & 1 & 1 & 1 \\ T & 0 & -1 & 0 & 0 & -1 & -2 & 0 \end{array} \quad (3)$$

The dimensional linear system of equations, expressing the condition of homogeneity, for the dimensionless complex Π_2 , is:

Sistemul de ecuaţii dimensionale liniare care exprimă condiţia de omogenitate, pentru complexul adimensional Π_2 , este:

$$\begin{aligned} &(L)\ x_1 + x_2 - 3x_3 = -1 \\ &(M)\ x_3 = 1 \\ &(T)\ x_2 = 1 \end{aligned} \quad (4)$$

The solutions obtained are $x_1 = 1$; $x_2 = 1$; $x_3 = 1$ and results:

Se obţin soluţiile $x_1 = 1$; $x_2 = 1$; $x_3 = 1$ şi rezultă:

$$\Pi_2 = \frac{\eta_l}{Dv\rho_l} \quad (5)$$

The dimensional linear system of equations, expressing the condition of homogeneity, for the dimensionless complex Π_3 , is:

Sistemul de ecuaţii dimensionale liniare care exprimă condiţia de omogenitate, pentru complexul adimensional Π_3 este:

$$\begin{aligned} &(L)\ x_1' + x_2' - 3x_3' = -1 \\ &(M)\ x_3' = 1 \\ &(T)\ -x_2' = -1 \end{aligned} \quad (6)$$

The solutions obtained are $x_1' = 1$; $x_2' = 2$; $x_3' = 1$ and results:

Se obţin soluţiile $x_1' = 1$; $x_2' = 2$; $x_3' = 1$ şi rezultă:

$$\Pi_3 = \frac{\sigma}{Dv^2\rho_l} \quad (7)$$

so that: $\varphi_1(\Pi_1,\Pi_2,\Pi_3,\Pi_4) = 0$ or $\Pi_1 = \varphi_1(\Pi_2,\Pi_3,\Pi_4)$, i.e:

astfel încât: $\varphi_1(\Pi_1,\Pi_2,\Pi_3,\Pi_4) = 0$ sau $\Pi_1 = \varphi_1(\Pi_2,\Pi_3,\Pi_4)$, adică:

$$\frac{d}{D} = \varphi_2\left(\frac{\eta_l}{Dv\rho_l} \cdot \frac{\sigma}{Dv^2\rho_l} \cdot \frac{\rho_g}{\rho_l}\right) \quad (8)$$

The dimensionless complex Π_1 can be put in the form of:

Complexul adimensional Π_1 poate fi pus sub forma:

$$\Pi_1 = k\Pi_2^a\Pi_3^b\Pi_4^c \quad (9)$$

Combinations between dimensionless complexes are made, so that appears a physical value, easy to vary in a single complex, i.e. *v*, the relative velocity of the liquid to the surrounding gas. So, dimensionless complexes are combined Π_2 şi Π_3 , to remove *v*, and result the new complexes Π_2' şi Π_3':

Se fac combinaţii între complexii adimensionali, astfel încât să apară o mărime fizică uşor de variat într-un singur complex, în cazul în speţă *v*, viteza relativă a lichidului faţă de gazul înconjurător. Astfel, se combină complexii adimensionali Π_2 şi Π_3 , pentru a elimina *v*, şi apar noii complexi Π_2' şi Π_3':

$$\Pi_2' = \frac{\Pi_2^2}{\Pi_3} = \frac{\eta_l^2}{D^2v^2\rho_l^2} \cdot \frac{Dv^2\rho_l}{\sigma} = \frac{\eta_l^2}{D\rho_l\sigma} \quad (10)$$

$$\Pi_3' = \frac{\Pi_3}{\Pi_4} \cdot \frac{\sigma}{Dv^2\rho_l} \cdot \frac{\rho_l}{\rho_g} = \frac{\sigma}{Dv^2\rho_g} \quad (11)$$

The relation (9) becomes:

Relaţia (9) devine:

$$\Pi_1 = k_1\Pi'^a_2\Pi'^b_3\Pi^c_4 \quad (12)$$

but

dar

$$\Pi_4 = \frac{\rho_a}{\rho_l} = const. \Rightarrow k_1\left(\frac{\rho_a}{\rho_l}\right)^c = k \quad (13)$$

and results:

şi rezultă:

$$\frac{d}{D} = k\left(\frac{\eta_l^2}{D\rho_l\sigma}\right)^a \cdot \left(\frac{\sigma}{Dv^2\rho_g}\right)^b \Rightarrow d = k\left(\frac{\eta_l^2}{D\rho_l\sigma}\right)^a \cdot \left(\frac{\sigma}{Dv^2\rho_g}\right)^b D \quad (14)$$

The scientific literature [4] indicates the following formulas for the size of the average diameter, *d*, of the spraying droplets, obtained by generalizing the results of

În literatura ştiinţifică [4] se indică următoarele formule pentru mărimea diametrului mediu, *d,* al picăturilor de lichid pulverizat, obţinute prin generalizarea rezultatelor

experimental measurements, where fluids were water and air.

- for the domain $\eta_l^{\,2}$: $\rho_l \sigma D < 0{,}0333$

$$d = D\left(\frac{\sigma}{\rho_g v^2 D}\right)^{0,52}\left[1{,}24 + 0{,}0128 \cdot \left(\ln\frac{\eta_l^2}{\rho_l \sigma D} + 12\right)\right] \quad (15)$$

- for the domain $\eta_l^{\,2}$: $\rho_l \sigma D > 0{,}0333$

$$d = D\left(\frac{\sigma}{\rho_g v^2 D}\right)^{0,52}\left(2{,}25 + 0{,}24 \cdot \ln\frac{\eta_l^2}{\rho_l \sigma D}\right) \quad (16)$$

The experiments to be performed, in 2015, with the Machine for the application with high accuracy of phytosanitary treatments in orchards, MSL (Figure 2) will determine the coefficients k, a, b, which intervene in relation (14), for different phytosanitary substances, varying the velocity of the liquid and the diameter of the nozzles.

unor măsurători experimentale, unde fluidele au fost apa şi aerul.

- pentru domeniul $\eta_l^{\,2}$: $\rho_l \sigma D < 0{,}0333$

- pentru domeniul $\eta_l^{\,2}$: $\rho_l \sigma D > 0{,}0333$

În experimentările ce urmează a fi efectuate, în anul 2015, cu Maşina pentru aplicarea cu precizie ridicată a tratamentelor fitosanitare în plantaţiile pomicole, MSL (Figura 2) se vor stabili coeficienţii k, a, b, care intervin în relaţia (14), pentru diverse substanţe fitosanitare, variind viteza lichidului şi diametrul duzelor.

Fig. 2 – The machine for high accuracy application of phytosanitary treatments in orchards MSL [8]
1 - the frame with rolling system; 2 - the spraying device; 3 - the liquid installation; 4 - the angular gear; 5 - the detection system of the presence / absence of the tree canopy; 6 - the automatic control system

The ultrasonic sensors detect the existence of vegetal mass. The information is transmitted to a programmable logic controller PLC that controls the feeding power-on/off of the spraying device by means of electrovalves. In the absence of vegetal mass the flow of solution is stopped. Depending on the distance that exists between the sensors and the spraying ramp and the speed of the unit equipment, the PLC applies a correction for opening the electrovalves, at the moment when ramp passes the objective to be sprayed [1].

For the determination of droplet diameter will be applied the LDPS (Laser Diffraction Particle Sizing) method, based on laser technology and electronic data processing. Laser diffraction technique is based on the principle that particles passing through a laser beam scatter light at an angle that is directly related to their size. As the particle size decreases, the spreading angle increases logarithmically. The intensity of the the dispersion is also dependent on the particle size and decreases proportionally to the cross-sectional area of the particle. Therefore, large particles disperse light at small angles, with high intensity, while small particles disperse light at greater angles, but at a lower intensity [9].

Following the experiments will be obtained the shape of equation (14), which describes the variation of droplets diameter. Equation (14) will replace equations (15) and (16), limited by the fact that only water was considered as pulverized fluid and obtained by technical means inferior to modern ones.

Senzorii cu ultrasunete sesizează existenţa masei vegetale. Informaţia este transmisă unui automat programabil PLC care comandă pornirea sau întreruperea alimentării dispozitivului de pulverizare, prin intermediul unor electrovalve. În cazul lipsei de masă vegetală fluxul de soluţie este oprit. În funcţie de distanţa existentă între senzori şi rampa de stropit, cât şi de viteza de înaintare a agregatului echipamentului, PLC-ul aplică o corecţie de timp pentru deschiderea electrovalvelor, în momentul când rampa trece prin dreptul obiectivului ce trebuie stropit [1].

Pentru determinarea diametrului picăturilor se va folosi metoda LDPS (Laser Diffraction Particle Sizing), bazată pe tehnica laserului şi a prelucrării electronice a datelor. Difracţia cu laser se bazează pe principiul că particulele care trec printr-un fascicul laser împrăştie lumina la un unghi direct proporţional cu mărimea lor. Pe măsură ce dimensiunea particulelor scade, unghiul de împrăştiere creşte logaritmic. Intensitatea dispersiei este dependentă şi de mărimea particulelor şi se diminuează proporţional cu suprafaţa secţiunii transversale a particulei. Prin urmare, particulele mari dispersează lumina la unghiuri mici, cu intensitate mare, în timp ce particulele mici dispersează lumina la unghiuri mai mari, dar cu o intensitate redusă [9].

În urma experimentărilor se va obţine forma ecuaţiei (14), care descrie variaţia diametrului picăturilor. Ecuaţia (14) va înlocui ecuaţiile (15) şi (16), obţinute cu mijloace tehnice inferioare celor actuale, în condiţiile limitării dictate de faptul că nu s-a luat în considerare decât apa, ca fluid pulverizat.

CONCLUSIONS

Due to the multiple interactions between droplets and turbulent gas phase, spraying is an extremely complex phenomenon. To describe it, quasi-empirical methods were used until the recent development of digital technology (the exponential growth of computer performance). Technological advances allow a deeper understanding of this phenomenon and, what is relevant, to the development of practical applications. In particular, it is important to know which type of nozzle is suitable for a certain type of spraying and how its performance is affected by liquid properties and operating conditions. Numerical simulation through CFD algorithms (Computational Fluid Dynamics, a branch of fluid mechanics that uses numerical methods and algorithms to analyze and solve problems involving the flow of fluids) allows the study of the process, of the state variables at all spatial and temporal coordinates.

The study results carried out on an experimental basis spray will be presented as generalized. This way of working will allow the setting of very important relations between the average diameter of the droplets, geometric characteristics of the nozzles and physical parameters of the fluid the nozzles spray, relationships that can be the starting point for the the optimal sizing of the nozzles.

ACKNOWLEDGMENT

This paper has been financially supported within the project entitled ***"Horizon 2020 - Doctoral and Postdoctoral Studies: Promoting the National Interest through Excellence, Competitiveness and Responsibility in the Field of Romanian Fundamental and Applied Scientific Research",*** contract number POSDRU/159/1.5/S/140106. This project is co-financed by European Social Fund through Sectoral Operational Programme for Human Resources Development 2007-2013. **Investing in people!**

REFERENCES

[1] Bolintineanu Gh., Vlăduţ V., Voicea I., Matache M., Savin L., Langenakens J. (2010) **-** *Integration of centralized monitoring and warning system on technical equipment for phytosanitary treatments in the concept of precision agriculture*, INMATEH, Vol. 31, Nr.2, p. 55 - 63;
[2] Dukowicz J.K., (2006) - *A particle-fluid numerical model for liquid sprays*, Journal of Computational Physics, Vol. 35, p. 229 - 253;
[3] Jiang X., Siamas G.A., Jagus K., Karayiannis T.G., (2010) - *Physical modeling and advanced simulation of two-phase fluid flow spraying processes*, Progress in Energy and Combustion Science, Vol. 36, p. 131 - 167;
[4] O'Rourke P.J., Bracco F.V., (1980), *Modeling the interaction between droplets and comparison with experiments*, Proceedings of the Institution of Mechanical Engineers, No. 9, p. 101-116;
[5] Popescu M., Gângu V., Cojocaru I., Brătucu Gh., Aurel M. (2007) - *Research on optimization work quality indices of field crops sprayers*, INMATEH, Vol. 21, Nr.3, p. 63 - 69;
[6] Staicu C. I., (1976) - *General dimensional analysis*, Editura Tehnică, Bucureşti, 1976;
[7] Stahli W. (2003) - *Machines for applying phytosanitary treatments and foliar fertilization of crops*, Editura AGROPRINT, Timişoara;
[8] *** (2011) *Machine for the high precision application of phytosanitary treatments in orchards MSL, Memorandum for presentation*, Nepublicat;
[9]***http://malvern.bsky/laser_diffraction/particle_sizing.htm

CONCLUZII

Datorită interacţiunilor multiple între picături şi faza gazoasă turbulentă, fenomenul pulverizării este deosebit de complex. Pentru a-l descrie s-a apelat, până la dezvoltarea recentă a tehnologiei digitale (creşterea exponenţială a performanţelor calculatoarelor), la metode cvasi-empirice. Avansul tehnologic permite o înţelegere mai profundă a acestui fenomen şi, ceea ce este relevant, la perfecţionarea aplicaţiilor practice. În particular, este foarte important să se ştie care este tipul de duză indicat pentru un anume tip de pulverizare şi cum sunt influenţate performanţele acestuia de proprietăţile lichidului şi de condiţiile de operare. Simularea numerică prin algoritmii CFD (Computational Fluid Dynamics, ramură a mecanicii fluidelor ce utilizează metode numerice şi algoritmi pentru analiza şi rezolvarea problemelor implicate de curgerea fluidelor) permite studierea procesului, a variabilelor de stare în orice coordonate spaţiale şi temporale.

Rezultatele studiului pulverizării efectuat pe bază experimentală vor fi prezentate sub formă generalizată. Acest mod de lucru va permite stabilirea unor relaţii deosebit de importante, între diametrul mediu al picăturilor, caracteristicile geometrice ale duzelor şi parametrii fizici ai fluidului pulverizat, relaţii care pot constitui punctul de plecare pentru dimensionarea optimă a duzelor.

ACKNOWLEDGMENT

Lucrarea a beneficiat de suport financiar prin proiectul cu titlul ***"Studii doctorale şi postdoctorale Orizont 2020: promovarea interesului naţional prin excelenţă, competitivitate şi responsabilitate în cercetarea ştiinţifică fundamentală şi aplicată românească",*** număr de identificare contract POSDRU/159/1.5/S/140106**.** Proiectul este cofinanţat din Fondul Social European prin Programul Operaţional Sectorial Dezvoltarea Resurselor Umane 2007-2013. **Investeşte în oameni!**

BIBLIOGRAFIE

[1] Bolintineanu Gh., Vlăduţ V., Voicea I., Matache M., Savin L., Langenakens J. (2010) **-** *Integrarea unui sistem centralizat de monitorizare şi avertizare pe echipamentele tehnice destinate tratamentelor fito-sanitare in conceptul de agricultura de precizie*, INMATEH, Vol. 31, Nr.2, p. 55 - 63;
[2] Dukowicz J.K., (2006) - *Un model numeric particulă-fluid pentru spray-uri lichide*, Journal of Computational Physics, Vol. 35, p. 229 - 253;
[3] Jiang X., Siamas G.A., Jagus K., Karayiannis T.G., (2010) - *Modelarea fizică şi simularea avansată pentru curgerea fluidelor bifazice în procesele de pulverizare*, Progress in Energy and Combustion Science, Vol. 36, p. 131 - 167;
[4] O'Rourke P.J., Bracco F.V., (1980), *Modelarea interacţiunii dintre picături şi comparaţia cu experimentele*, Proceedings of the Institution of Mechanical Engineers, No. 9, p. 101-116;
[5] Popescu M., Gângu V., Cojocaru I., Brătucu Gh., Aurel M. (2007) - *Cercetări privind optimizarea indicilor calitativi de lucru ai maşinilor de stropit culturile de câmp*, INMATEH, Vol. 21, Nr.3, p. 63 - 69;
[6] Staicu C. I., (1976) - *Analiza dimensională generală*, Editura Tehnică, Bucureşti, 1976;
[7] Stahli W. (2003) - *Maşini pentru aplicarea tratamentelor fitosanitare şi fertilizarea foliară a culturilor*, Editura AGROPRINT, Timişoara;
[8] *** (2011) *Maşina pentru aplicarea cu precizie ridicată a tratamentelor fitosanitare în plantaţiile pomicole MSL, Memoriu de prezentare*, Nepublicat;
[9] *** http://malvern.bsky/laser_diffraction/particle_sizing.htm

A NEW METHOD FOR TREE SPECIES ARRANGEMENT IN FARMLAND SHELTERBELTS AND SAND PREVENTION ANALYSIS
/
农田防护林配置及防治风沙效应的新型方法分析

Ph.D. Stud. Deng Jifeng[1,2)], Prof. Ph.D. Ding Guodong[*1,2)], Ph.D. Gao Guanglei[1,2)], Ph.D. Stud. Gao Lin[3)]
[1)] Yanchi Research Station, School of Soil & Water Conservation, Beijing Forestry University, Beijing / P.R. China;
[2)] Key Laboratory of Soil and Water Conservation and Desertification Combating, Ministry of Education, Beijing Forestry University, Beijing / P.R. China
[3)] Faculty of Forestry and Environmental Management, University of New Brunswick, Frederiction / Canada
Tel: +8618504508251; E-mail: dengjifeng1984@gmail.com

Abstract: *Farmland shelterbelts can yield maximum ecological benefits with the smallest occupied area of forests and result in sustainable use of farmland resources. Rapid and efficient planning of farmland shelterbelts at various scales is becoming an urgent task in ecological landscape design. Until now, the problems in studies on farmland shelterbelts combined with wind erosion models are associated with conflicts between scientific and practical requirements. Based on previous research results, a case study was conducted in Yanchi County in north-western China. The primary objectives of this study were to use a new method for the arrangement of tree species and to investigate the effects of sand prevention. In addition, changes in the trends of the input parameters under multiple wind erosion events were analyzed and tested. The results indicated that under a single arrangement of tree species, better shelter protection was provided within the shrub shelterbelt or outside the arbor shelterbelt forest. Under a different arrangement of tree species, shrubs arranged with arbor belts gave little protection on the leeward side. Arbor trees arranged with shrub belts could effectively prevent sand from the windward side, while low trees in the upwind direction provided limited protection. Cumulative percentiles of sand displacement showed that under different arrangements of tree species, the sand prevention benefit was better than that of a single tree species. In addition, the experimental error was less than 3.00% and there was close correlation between percentiles of sand displacement under multiple wind erosion events, indicating a preferable simulation effect.*

Keywords: *farmland shelterbelt, exponential model, summation curve method, wind erosion*

摘要：*农田防护林占森林面积最小却能发挥最大的生态效益，体现在对农田资源的可持续利用方面。如何在不同尺度上快速而又有效地规划农田防护林是生态景观设计急需解决的命题。目前为止，对于农田防护林结合现有风蚀模型的研究存在科学性与实用性需求之间的矛盾。本文在前人研究的基础上，以中国西北地区盐池县为例，主要研究目的在于应用新型方法对防护林各树种配置的治沙效应进行分析。另外，分析并检验了连续风蚀作用下的参数输入变化。结果表明：单一树种下，灌木林林内防护效应明显，乔木林林外防护效应显著；不同树种配置下，灌木搭配乔木树种，在林带背风处，有效防护范围较小。乔木搭配灌木树种在迎风处能有效的阻止风沙，但是低矮的乔木树种对上风向的风沙防护效果有限。风沙量累积百分数移动距离表明不同树种配置下的防治风沙效果要好于单一树种。另外，实验误差小于 3.00%，并且多次风蚀作用下，各风沙量百分数移动距离相关性较强，模型模拟效果较好。*

关键词: *农田防护林；指数模型；累积曲线方法；风蚀*

INTRODUCTION

Shelterbelts are artificial barriers used to reduce wind velocity. In history they have been used to protect homes and enhance the agricultural landscape [1]. As an important type of shelterbelts, farmland shelterbelts can increase animal and plant species and enhance the ecological function of agricultural systems. Furthermore, it can protect soils from erosion forms, and boosts crop yields [5, 15]. Therefore, the construction of farmland shelterbelts plays a significant role in achieving sustainable development. So far, researches related to the farmland shelterbelt have paid more attention to the structure and protective effects of shelterbelts combined with the existing wind erosion models at a small scale.

Studies on the structure of farmland shelterbelt systems focused mainly on forest structural characteristics and their relationship with meteorological variables. In recent years, various methods and studies showed that establishing multi-band arbor trees and

引言

防护林作为人工屏障用途在于减缓风速，以往防护林用于保护村庄和改善农田景观[1]。作为防护林系统中的重要类型，农田防护林可以增加动植物种类，并改善农田系统的生态功能。而且保护土壤免受各侵蚀影响和增加农作物产量[5,15]。因此，农田防护林建设对实现可持续发展具有重要意义。目前，对农田防护林的研究，主要针对在小尺度下防护林的结构配置和结合现有的风蚀模型验证其防护效果两方面。

对防护林结构配置的研究多集中在对林带结构特征及其与环境因子之间的相互关系方面。近些年，多种方法、研

mesh shrub tree forests within or along the edge of farmlands can provide multiple functions including ecological benefits.

Wind erosion models include theoretical and empirical models. A theoretical model is based on the fluid mechanics principle, with a strong scientific nature founded on the laws of physical movement of sand and provides a superior explanation. The disadvantage and difficulty in developing physical-based models of sand displacement results from the high degree of complexity and randomness, which is a characteristic feature of the mechanical processes of erosion and sediment transport. Hence, the goal of a complete and applicable theoretical model seems unreachable under the given circumstances. Empirical models include the Wind Erosion Equation (WEQ) and the Revised Wind Erosion Equation (RWEQ) models. Different from the theoretical models, empirical models are able to quantify the external factors with minimum assumptions and simple calculations, and provide a wider scope of application. However, with these models, the transport mass must increase without limits for average soil erosion to remain constant for large farm fields; this does not agree with the theory that wind has a limited capacity to transport sand material. This may be true for large farm fields, i.e., there is an increase in transport mass due to the dust carried in suspension, but this portion is relatively small compared with the proportion being transported in suspension, saltation, and creep. While the wind may pick up the surface fine material, the total transport cannot increase without limit [4, 12]. Therefore, empirical models are fundamentally flawed.

At present, scientists and policy makers plan and design farmland shelterbelt forest systems at large scales, i.e., soil erosion control and desertification prevention, from a protection function perspective. Consequently, the rationality of shelterbelt patterns at the landscape scale is key for shelterbelt construction and management. However, the data required for these methods are not easy to obtain, and the methods themselves are difficult to operate, leading to the failure of farmland shelterbelt establishment. Therefore, forestry planners need a reasonable, simple, and easy to operate sand control method for the large-scale construction of farmland shelterbelt forests. New methods should overcome the parameter uncertainties and computational complexities in theoretical models as well as the physical defects in empirical models [2]. Meanwhile, a physically-based wind erosion model coupled with empirical functions and methods needs to be developed.

The objective of this study was to use the existing typical farmland shelterbelts as examples to apply a new method to quantitatively analyze the effects of sand prevention and dynamics of sand movement under different arrangements of tree species. In addition, changes in the trends of the input parameters under multiple wind erosion events were analyzed to test their stability and applicability. Our results will provide useful information for supporting the management of farmland shelterbelt forest systems.

MATERIAL AND METHOD

Experimental site

The experimental site was located at the Ningxia Yanchi Research Station of the State Forestry Administration (between 37°04´N and 38°10´N, and 106°300´E and 107°410´E, with an altitude of 1,354 m above sea level) covering an area of approximately 6,700 km^2. The annual precipitation averages 287 mm

究表明，在农田中或沿农田边缘营造的带状乔木和网状灌木林分可以提供包括景观生态效益的多种功效功能。

风蚀模型分为理论模型和经验模型。理论模型基于流体力学原理，建立在风沙物理学运动定律上面，具有较强的科学性，并拥有合理解释。而发展基于风沙物理学运动的理论模型缺点和难点在于具有高度的复杂性和不确定性，这是实际的侵蚀过程和风沙流运动机理内部特性所决定的。因此，发展完整且可实际应用的理论模型在给定条件下几乎是不可能的。经验模型包括 Wind Erosion Equation（WEQ）和 Revised Wind Erosion Equation （RWEQ）模型。不同于理论模型，经验模型能够量化外界因子以最少的假定条件和简单计算，提供了较广的适用范围。然而，这些模型都假定在平均土壤侵蚀作用下，侵蚀量会一直增加且没有限制，以确保较大农田范围内侵蚀量为常量。这有悖于理论叙述中的风对风沙的作用能力是有限的。在较大农田范围内，这也许是对的，如粉尘被风吹蚀产生悬移使得总风沙量不断被增加。但是悬移颗粒量比例相较于总体的悬移、跃移和蠕移颗粒量比例较小，风力作用下细小颗粒量可以被吹蚀，但是总体风沙颗粒量不会无限制增加[4,12]。因此经验模型存在基础性缺陷。

当前，科研工作者和政策制定者们对农田防护林系统的规划设计，主要在大尺度下从防护功能角度入手，例如，土壤侵蚀控制和风沙防治。所以，追求景观尺度下合理的防护林样式结构是防护林建设管理的主要目标。然而，这些方法所需数据在实际过程中不易获取，且方法本身操作难度较大，导致防护林体系出现建设失败问题。因此，对于林业规划者来说，大规模营造农田防护林需要合理、简单并易操作的风沙防治模型。新方法既要克服理论模型中的参数不确定性、计算的复杂性也要克服经验模型中存在的物理学缺陷[2]。同时需要发展基于风沙物理学模型，并嵌套经验模型的功能与方法。

本文以现有典型农田防护林为研究对象，应用新方法，量化分析了不同树种配置的防护林防沙效应和风沙移动动态过程。另外，分析了多次风蚀作用下的参数输入的变化来检验模型的稳定性和实用性。本文研究结论可以为农田防护林配置管理提供支持和依据。

材料与方法

研究区概况

实验地点位于中国国家林业局宁夏盐池研究站（北纬37°04´~38°10´°、东经 106°300´~107°410´，海拔为1354m），占地面积约为 6,700km^2。年均降水量 287mm

(1950~2010). Mean annual potential evaporation is 1273 mm. Mean annual temperature is approximately 8.1 °C. The prevailing wind is mainly from the northwest, and wind speed averages 3.0 m/s. The landscape is a typical transitional zone; the terrain changes from the Loess to the Ordos plateau. The soils are primarily dark loessial soil, eolian sandy soil, and sierozem soil. The vegetation type varies from dry steppe to desert grassland species [6]. The farmland shelterbelt system in the Yanchi semi-arid area is mainly distributed in the flat drought farmland and wind erosion plough land.

Tree species selection

A survey on the structure of the farmland shelterbelt was conducted in 2009 [14] and 2012. The results of this investigation are as follows:

Shrub shelter forest: This is 17-year pure, band shelter forest of *Hedysarum scoparium*. The shelterbelt length and width is 150 m and 40 m, respectively. The average tree height is 2.8 m, and average tree crown width is 1.5 m×2.0 m; *Salix psammophila* is a pure, band shelter forest. The direction of the forest belt runs from northeast to southwest. The length and width of the shelterbelt is 200 and 10 m, respectively, with an average tree height of 2.8 m.

Arbor shelter forest: This is a 30-year pure band shelter forest of *Populus bolleana* Lauche; the forest belt direction runs from northeast to southwest; the shelterbelt is 200 m long and 50 m wide with a plant spacing of 4.0 m×4.0 m. The average tree height is 12 m, average diameter at breast height is 0.22 m, average tree crown width is 7.5 m×8.0 m, and average under branch height is 2.5 m. The porosity is 60%; The *Pinus sylvestris* var. *mongolica* stand is at the initial stage of growth. This is a 7-year, mesh shelterbelt forest, with a northeast to southwest direction. The shelterbelt length is 70 m, with a width of 50 m, and a plant spacing of 1.2 m×1.5 m. The average tree height is 2.8 m, average diameter at breast height is 0.27 m, and canopy density is 40%.

Dry farming farmland surrounds the shelterbelt forests. Except for the *Populus bolleana* Lauche forest, the porosity of the tree belts range from 20% to 40%. The survival rate of the shelter forest is determined by the width of the shelterbelt [13] considering the semi-arid and arid climate and the restrictions of land utilization and water resources. Therefore, this article only focuses on the width of the shelter forest (at this time, the protective direction is perpendicular to the wind direction) when determining its influence on wind erosion. In addition, it was assumed that the shelterbelt was complete without any damage and there were no dead trees in the forest. In order to simplify the calculation process, an arrangement of two tree species was considered, and a maximum protective width of 100 m was used.

Model description

The simulation functions used to characterize the non-uniform displacement of eroded particles were the rational function, simplified Gaussian function and exponential function. Among these three models, the rational function model is limited by mathematical calculations, and the Gaussian function can only simulate the unidirectional distance. For this study, we adopted the exponential model due to its advantages of applicability and reliability in data simulation.

The exponential model has been described by Lobb et al. [10]. The exponential model used to simulate the non-uniform displacement of eroded particles under multiple wind erosions is:

（1950~2010），年均蒸发量 1273mm，年均气温约为 8.1°C。主风向为西北风，平均风速为 3.0m/s。地貌景观属于交替区域，地貌从黄土高原变化至鄂尔多斯平原。土壤类型为黑垆土、风沙土和灰钙土。植被类型从干草原变化至荒漠植被[6]。盐池县沙区农田防护林主要分布在农田集中的平缓干旱沙滩地和风蚀滩地。

防护林树种选择

农田防护林林分结构调查时间为 2009 年[14]和 2012 年，调查结果如下：

灌木防护林：花棒 17 年生纯林，带状防护林，长 150m，宽 40m，平均树高为 2.8m，平均冠幅为 1.5m×2.0m；沙柳纯林，带状防护林，林带呈东北-西南走向，带长 200m，带宽 10m，平均树高为 2.8m。

乔木防护林：新疆杨 30 年生带状纯林，林带呈东北-西南走向，带长 200m，带宽 50m，株行距为 4.0m×4.0m，平均树高为 12m，平均胸径为 0.22m，平均冠幅为 7.5m×8.0m，平均枝下高为 2.5m。林带疏透度为 60%；樟子松林分处于生长初期，为 7 年生网状防护林，林带呈东西—南北走向，带长 70m，带宽 50m，株行距为 1.2m×1.5m，平均树高为 2.8m，平均胸径为 0.27m，郁闭度为 40%。

各防护林带周围为平坦开阔的沙质旱作农田。除新疆杨林外，其它防护林疏透度在 20%到 40%。防护林带宽度是决定防护林存活率的重要决定因素[13]。考虑到在半干旱、干旱地区气候条件和受制于土地利用率、水资源限制，因此，本文只针对防护林宽度（此时防护林方向与风向成垂直方向）对风蚀作用的影响分析，并假定防护林带无破损、树木无死亡情况出现，为了简化计算过程，对 2 种树种进行配置组合，最大防护距离为 100m。

模型描述

模拟功能可以模拟可蚀性颗粒的不均匀分布状态，有：有理函数模型、简化的高斯模型和指数模型。在这三种模型，有理函数模型在数理学计算上存在局限性。高斯模型只能模拟风沙流在单一水平下的移动距离。本文采用指数模型，优点是在数据模拟、预测拥有更好的适用性和可靠性。

本文采用 Lobb[10]对指数模型的描述，可模拟连续风蚀下可蚀性颗粒的的不均匀移动距离分布，公式为：

$$\frac{C^{S*}_{(x)}}{C_u} = 1 - D^*_W e^{-\frac{x}{D_W}}, [\%] \quad (1)$$

where: C_u is the total amount of sand, x is the sand displacement distance (m), $C^{S*}_{(x)}$ is the amount of sand at x after wind erosion, and D^*_W is the ratio of the windblown depth and eroded soil depth, with a value of 1. D_W is the wind erosion model coefficient (defined as an average sand displacement distance (m)).

This model assumes that the extent of sand translocation is infinite (the series of distributions is summed to generate a summation curve, c_s); this extent is described experimentally as the extreme point at which applied eroded particles can be measured above background levels. The data generated by the exponential model can be used with the summation curve method to quantify the sand prevention effect.

Summation Curve Method: The methods used to calculate the summation curve are described by Lobb and Kachanoski [8, 9, 11]. In this paper, the summation curve method was improved for application to wind erosion studies. Eroded particles under wind erosion events were measured using established methods, i.e., the estimated eroded particle distribution for a series of sequential hypothetical sand sources with a length exceeding the maximum distance to which particles were transported was used to generate a summation curve to calculate the mean eroded particle movement in the windblown direction (Fig.1a). Using the summation curve method, the mean eroded particle distance per unit width and the average eroded depth (D_W) was calculated using the following equation (2):

式中，C_u 为风沙总量，x 为风沙移动距离（m），$C^{S*}_{(x)}$为风蚀后在 x 距离处的风沙量，D^*_W 为吹蚀深度与可蚀性土壤层深度比，值为 1；D_W 为风蚀模型系数（定义为风沙平均移动距离（m））。

指数模型假定风沙移动量是趋于无限的（累积比例量为 c_s），并描述在风力作用下所有被吹蚀的颗粒移动距离大于起始位置处。将指数方程产生的模拟数据代入到累积曲线方法中，可以对防沙效果进行定量分析。

累积曲线方法：累积曲线方法由 Lobb 和 Kachanoski[8,9,11]提出，本文中，累积曲线方法被改进以应用至风蚀研究中。在风蚀作用下，采用累积量计算方法，例如，在风蚀方向下，假设一系列相同的风沙源被吹蚀，直到可蚀性颗粒移动至最大距离，此时对风蚀方向下的可蚀性颗粒量累积加和计算，得到累积曲线（图 1a）。因此，D_W 代表颗粒物在平均风蚀宽度和深度下的平均移动距离，计算公式（2）：

$$D_W = \int_0^\infty (1 - c_s) dx, [\text{m}] \quad (2)$$

The summation curve was used to quantify the dispersion of the eroded particles. Three steps were used in this process. First, the areas above and below the summation curve, delineated by x=0, were used to calculate u_{S1}:

累计曲线方法可以用于量化可蚀性风沙颗粒分布过程，分为三步计算过程：第一步从 x=0 处计算风沙颗粒分布过程，得到 u_{S1}：

$$u_{S1} = \sqrt{\frac{(\int_{-\infty}^{0} c_s x^2 dx + \int_0^\infty (1-c_s) x^2 dx - \int_{-\infty}^{0} (c_s x dx)^2 + \int_0^\infty (1-c_s) x dx)^2) / C}{C}}, [\text{m}] \quad (3)$$

Second, the areas above and below the summation curve, delineated by $x=D_W$, were used to calculate u_{S2} (Fig.1b):

第二步，当风蚀颗粒移动至平均移动距离（$x=D_W$），u_{S2} 计算公式为（图 1b）：

$$u_{S2} = \int_{D_W}^\infty (1 - c_s) dx, [\text{m}] \quad (4)$$

Third, the cumulative percentiles of the eroded particles amount were calculated. D_{W50}, D_{W75}, D_{W90} and D_{W95} correspond to the 50th, 75th, 90th, and 95th cumulative percentiles of the amount of eroded particle displacements respectively (Fig. 1b).

To characterize the general form of the distribution of eroded particles, u_{S1} and u_{S2} were expressed as relative measures of D_W, $u^*_{S1,2}$ (%):

第三步，风沙量累积百分数计算，D_{W50}，D_{W75}，D_{W90} 和 D_{W95} 分别代表累积百分数 50%，75%，90%和 95%的风沙量移动距离（图 1b）。

区分对颗粒物一般性分布过程的描述，可将计算出的 u_{S1} 和 u_{S2} 与实际输出值 D_W 比较，得到计算误差 $u^*_{S1,2}$，（%），公式为：

$$u^*_{S1,2} = 100 \times \frac{u_{S1,2}}{D_W}, [\%] \quad (5)$$

The first and second steps still take the general form of the distribution of the amount of sand particles based on the empirical results. Consequently, for the actual calculations, u^*_{s1} and u^*_{s2} should equal 100% of D_W and 50% of D_W.
D_W can also be converted directly to mass, D_M (kg/m), which is the eroded particle mass per unit width:

第一种和第二种计算方式仍采用基于经验模型结果的风沙颗粒一般性分布描述。所以，在实际计算中，u^*_{s1} 和 u^*_{s2} 应该分别接近于 100% 的 D_W 值和 50 %的 D_W 值。

D_W 也可以转换为风沙侵蚀量 D_M（kg/m），为风蚀作用宽度侵蚀量：

$$D_M = s\rho D_W \text{, [kg/m]} \quad (6)$$

where: ρ is bulk density (kg/m^3). s is wind erosion width (m).

式中 ρ 为容重（kg/m^3）。s 是风蚀作用宽度（m）。

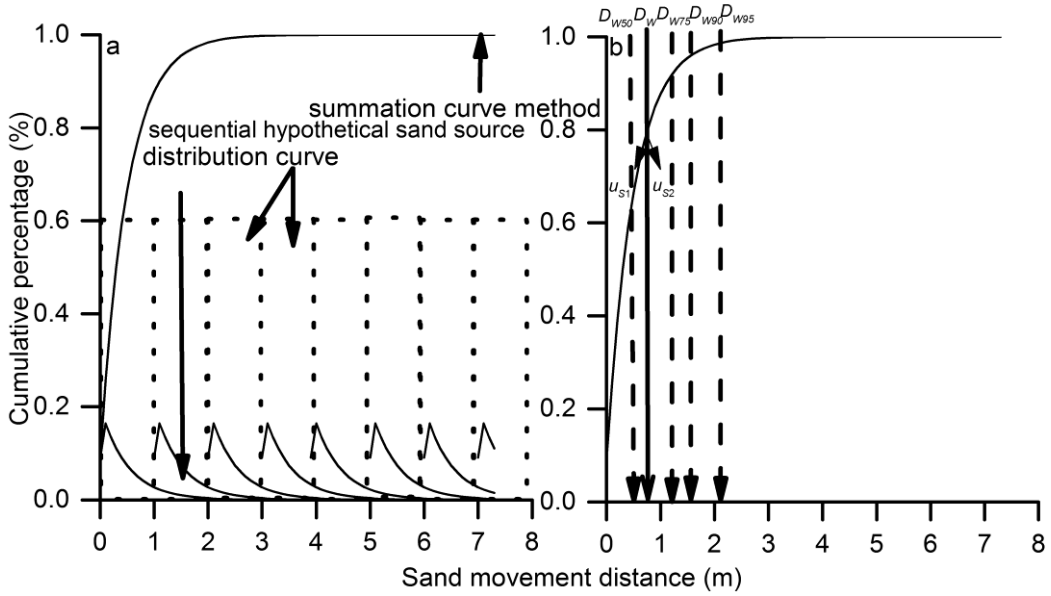

Fig.1 - Summation Curve Method. a) Sand source: sand before wind erosion is indicated by the dotted line (L_P= 1.00 m); sand after wind erosion is indicated by the distribution line below; the summation curve represents the accumulation of sand (D_W= 0.50 m; top line above). b) Dispersion is indicated by D_{W50}, D_{W75}, D_{W90}, and D_{W95}, i.e., the cumulative percentile of the particles along the path of 50%, 75%, 90%, and 95% displacement, respectively. Arrows represent sand movement to a distance of D_W where u_{s2} was calculated

The magnitude of the undulations on the summation curve, ε (m), was calculated over a distance equal to L_P (m), beyond the distance to which the eroded particles were observed, L_S (m). The coefficient of the experimental error and translocation variability (ε^*) was estimated as:

累计曲线方法计算会产生波动，波动距离 ε 是在风沙颗粒移动距离等于或超过 L_P 处并在 L_S（m）处计算、观测得到的，实验误差及变异程度 ε^*表示为公式：

$$\varepsilon^* = \left(\frac{\int_{L_S}^{L_S+L_P} |1-c_s|\,dx}{D_W + L_P}\right) \times 100 \text{, [\%]} \quad (7)$$

where:
L_P is sand source (m), L_S is maximum sampling distance (m).

Theoretically, the summation curve should increase steadily from x = 0 to its maximum at L_S+L_P and then decrease steadily to a value of zero. However, the summation curves generated from experimental data are not smooth; rather, they undulate (Fig. 2a). These undulations are a result of experimental errors. Therefore, experimental errors exist. ε^* is a measure of the inherent variability in translocation (Fig. 2b). Hence, ε^* is referred to as the experimental error.

式中

L_P为风沙源距离（m），L_S为最大风沙采样距离（m）。

理论上，累积曲线从 x=0 处上升，直到移动至最大距离 L_S+L_P，然后平稳下降至 0。然而，源于实验数据计算得到的曲线方程并非是一条平滑的直线，相反，会产生波动（图 2a）。这些波动是由于实验内部误差造成的，因此，实验误差一直存在，由于 ε 为实验内部系统性存在结果（图 2b）。所以 ε^*可认定为是实验误差。

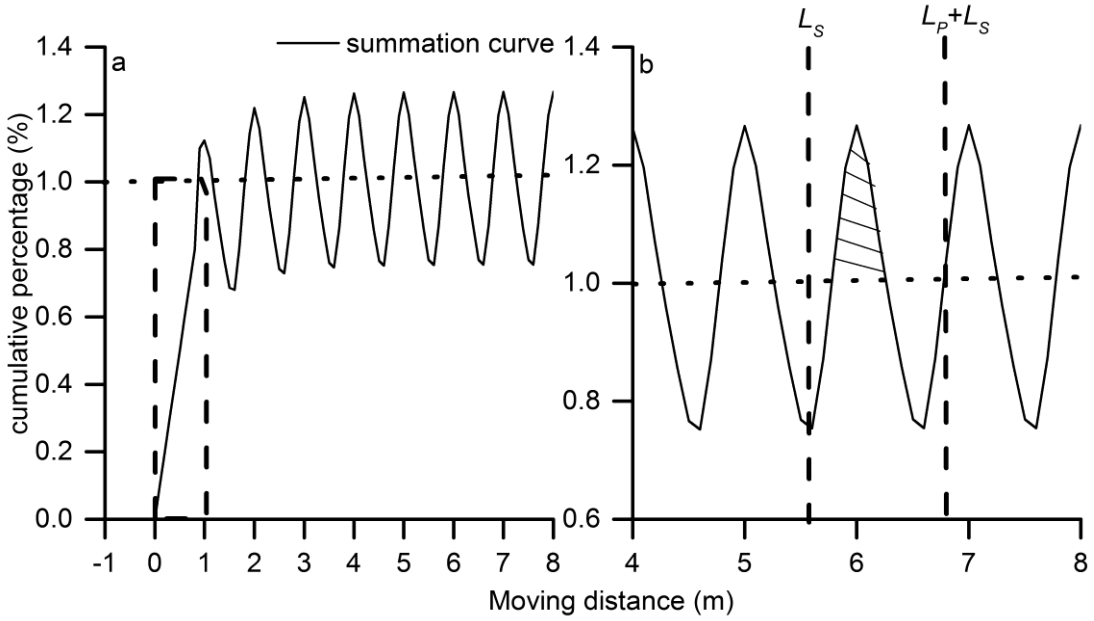

Fig.2 - Experimental error demonstration: a) Sand source: sand before wind erosion is indicated by the dotted line (L_P=1.00 m, D_W=0.50 m); b) ε for the summation curve method, represented by the hatched area (L_P= 1.00 m, L_S= 5.70 m)

D_W was calculated under different tree species arrangements using the following:

不同树种配置下的D_W计算公式见：

$$D_W = \frac{D_{W-\text{tree species A}} + D_{W-\text{tree species B}}}{n}, \text{[m]} \quad (8)$$

where:

$D_{W\text{-tree species A, B}}$ is the average sand displacement distance (m) of the shelter tree species A and B. The value of D_W was determined as the mean of $D_{W\text{-tree species A}}$ and $D_{W\text{-tree species B}}$.

式中

$D_{W\text{-tree species A, B}}$ 是防护林树种 A 和 B 的林内风沙平均移动距离（m）。总 D_W 的计算为防护林树种 A 和 B 的风沙移动距离的平均值。

RESULTS

Outside forest sand source parameter input selection

In this study, it was assumed that all sand particles originated from outside the forest (bare sandy land, no shelter forest) and were distributed within the farmland shelterbelts. Therefore, we defined the outside forest farmland as sand sources and the shelter belts as storage sinks. This paper focuses on sand with a moving distance less than or equal to 100 m; therefore, the sand source parameter input should ensure that the average sand moving distance is greater than 50 m (the boundary between tree species A and B), and that the largest moving distance exceeds 100 m from the outer boundary. Here, the diameter of the outside forest sand source was set as 100 m, the sampling point interval was 1 m, the sand bulk density was 1100 kg/m^3 and the wind erosion depth was 0.0010 m. The distribution pattern of the eroded particles was simulated by applying the exponential model, and then the D_W value was obtained using the summation curve method. The optimal parameter was selected when D_W was 60 m, 50% of the accumulated amount of sand concentrated around a distance of 50 m, and the largest moving distance exceeded 100 m (Fig. 3).

结果

林外风沙源参数输入选择

本文假定所有风沙颗粒来自于林外（裸沙地，无防护林），并最终分布在农田防护林内。因此，林外裸沙地设定为源，防护林林内为汇。本研究只考虑 100m 范围内的风沙移动走向。因此，在林外风沙源参数输入上，应确保风沙源风沙移动平均距离大于 50m（树种 A 和 B 的配置边界），外边界最大移动距超过源内 100m。在本文中，设定林外风沙源直径距离为 100m，采样点为 1m，风沙容重为 1100kg/m^3。土壤层吹蚀深度为 0.0010m。指数方程提供风沙分布模拟值，代入到累计曲线方法中，得到各参数 D_W 输出值。图 3 为参数筛选后得到最佳参数输入值，当 D_W 为 60m 时，50%的累积风沙量集中在 50m 处，最大移动距离超过 100m（图 3）。

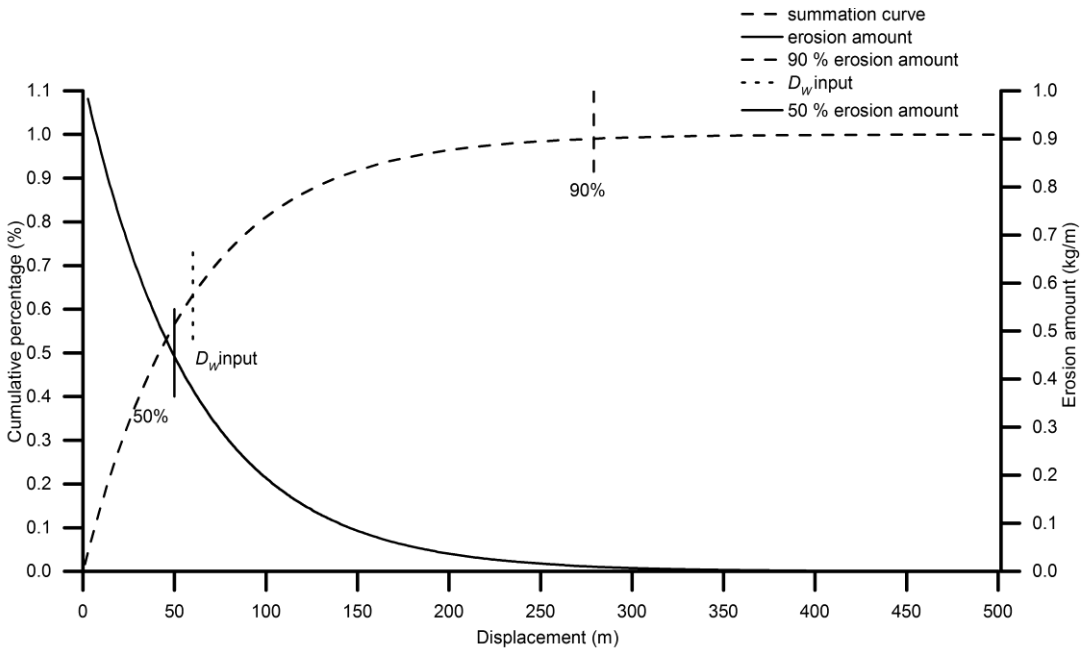

Fig.3 - Estimation of the wind erosion rate based on the summation curve method associated with 50 % and 90 % of total sand moving distance when D_W equaled 60 m

Effects of different arrangements of shelterbelt tree species

Previous studies indicated that the ventilation coefficients of *Hedysarum scoparium*, *Salix psammophila,* and *Pinus sylvestris* var. *mongolica* shelter forests belonged to a tight structure with ventilation coefficients of 0.2. In contrast, the *Populus bolleana* Lauche shelter forest had a loose structure with a ventilation coefficient of 0.3 [7]. The effective sand prevention distances (outside forest) were 0.5 H for *Hedysarum scoparium*, 1 H for *Salix psammophila*, 4 H for *Populus bolleana* Lauche, and 2 H for *Pinus sylvestris* var. *mongolica*. The effective sand prevention distances (inside forest) were 4 H, 2 H, 0.5 H, and 1 H for *Hedysarum scoparium*, *Salix psammophila*, *Populus bolleana* Lauche, and *Pinus sylvestris* var. *mongolica*, respectively [14].

Thus, the value of the sand moving distance within the *Populus bolleana* Lauche shelter forest was set at 6 m. The D_W values of *Hedysarum scoparium*, *Salix psammophila,* and *Pinus sylvestris* var. *mongolica* were set at 2 m, 4 m, and 8 m, respectively, according to different ventilation coefficients, and L_P was 1 m, and the sand sampling point was 0.1 m.

Under the single arrangement of tree species, the shrub shelter forest could not prevent sand movement outside the forest belt, but effectively prevented sand movement within the forest belt (table 1). The arbor forest effectively prevented wind erosion outside the forest. However, such a prevention effect was not obvious inside the forest.

The results of different tree species arrangements indicated that when the shrub tree species was arranged with the arbor tree species, there were vast quantities of sand accumulation on the lee side of the shelterbelt. Although the sand prevention effect was better than a single tree species, the effect was insignificant. An arbor forest with shrub tree species can effectively prevent most of the sand on the windward side, but was

不同防护林树种配置效应

以往研究表明，花棒、沙柳和樟子松林为紧密结构，对应通风系数为 0.2，新疆杨为疏散结构，对应的通风系数为 0.3[7]。各树种的林外的阻沙效应为 0.5H（花棒）、1 H（沙柳）、4H（新疆杨）和 2H（樟子松）；林内的阻沙效应分别为 4H（花棒）、2H（沙柳）、0.5H（新疆杨）和 1H（樟子松）[14]。

因此，本文设定新疆杨林的林内风沙移动距离为 6m。根据通风系数的比例计算得出花棒、沙柳和樟子松的 D_W 值输入分别为 2m，4m 和 8m。本文中 L_P 设置为 1m，风沙采样点设置为 0.1m。

单一树种下，灌木林未能有效阻止外部的风沙源，但是能有效的阻止林内风沙的移动。乔木林可以有效的阻止林外风沙侵蚀。然而，林内阻沙效应并不明显（表 1）。

不同树种配置结果表明，灌木搭配乔木树种，在防护林带背风处，风沙大量堆积，虽然比单一树种配置要好，但是防风蚀效果不显著。乔木搭配灌木树种在迎风处能有效的阻止绝大部分的风沙，但是计算误差较高。然而，低矮的乔木林搭配灌木树种，如樟子松不能对外部的风沙源形

associated with a higher calculation error. However, short arbor trees with shrub tree species such as *Pinus sylvestris* var. *mongolica* could not provide effective protection to external sand sources.

The numerical procedures used to calculate eroded particle displacement resulted in errors. Under a single tree species arrangement, the *Pinus sylvestris* var. *mongolica* shelter forest showed the highest error of 1.40%. Under a different tree species arrangement, the *Populus bolleana* Lauche shelter forest was associated with the highest error of 2.97%. The main reason for these errors is that sand loss was calculated using the exponential model. In this research, the calculation error was controlled within 3.00% under conditions where was assumed that experimental errors were negligible and the results were satisfactory.

For the hypothetical data, u^*_{S1} and u^*_{S2} were lower than the average D_W. This is due to the fact that these measures relate to the general form of the distribution of eroded particles. As the form of the distribution approached that of a step, u^*_{S1} approached a value of 100 % and u^*_{S2} approached a value of 50 %, which agree with the previous equations mentioned above.

成有效的防护。

累积曲线方法能够计算得到风沙吹蚀分布中产生的实验误差。单一树种配置下，樟子松防护林的计算误差最高，为 1.40%。不同树种配置下，新疆杨与各树种防护林配置下的计算误差最高，为 2.97%。造成误差的主要原因是，指数方程计算下产生的风沙损失量。本研究中，计算误差被控制在 3.00%以内，认为实验误差可以忽略，计算结果较为满意。

对于模拟数据输出值，u^*_{S1} 和 u^*_{S2} 要小于 D_W，这是由于其计算方式仍然采用一般性风蚀颗粒的分布描述。作为其分布描述步骤，u^*_{S1} 更接近实际值的 100%和 u^*_{S2} 接近实际值的 50%，这与之前的模型计算公式描述结果一致。

Table 1

D_W input, values of D_W calculated using the summation curve method associated with experimental errors

Tree species arrangement	D_W input	D_W output	u^*_{S1}	u^*_{S2}	ε
	[m]	[m]	[%]	[%]	[%]
H*	2.00	1.99	79.86	50.54	0.95
S*	4.00	3.99	65.89	45.08	0.91
B*	6.00	5.99	84.67	36.78	1.26
P*	8.00	7.99	77.13	37.08	1.40
HS	-	2.41	83.03	44.07	0.67
HP	-	3.02	78.99	42.89	0.69
HB	-	2.05	98.23	50.46	0.92
SH	-	2.42	97.22	49.27	0.65
SP	-	5.72	87.53	40.85	1.22
SB	-	4.61	97.66	39.67	1.03
B,HSP	-	1.12	98.32	49.69	2.97
PH	-	6.12	78.94	40.81	1.32
PS	-	6.15	87.70	41.01	1.33
PB	-	6.19	92.45	40.71	1.34

* H represents *Hedysarum scoparium*, S represents *Salix psammophila*, B represents *Populus bolleana* Lauche, P represents *Pinus sylvestris var. Mongolica*

Amount of eroded particle dispersion (50%, 75%, 90%, and 95%) expressed as percentiles of cumulative translocation can provide useful information for understanding wind erosion and the dynamics of sand movement.

Figure 4 shows that greater sediment deposition occurred on the lee side of the arbor trees, and the potential of wind erosion was higher than with shrub tree species. Complete shelter belts (tall trees), such as *Populus bolleana* Lauche, had the greatest sand prevention effect, while incomplete shelter belts (short trees), such as *Pinus sylvestris* var. *Mongolica,* did not exhibit a clear sand prevention effect. In general, the combination of different tree species showed a better sand prevention effect than a single shelter forest.

风沙量百分数移动分布（50%、75%、90%和 95%）能为更好理解风蚀作用和风沙移动的动态过程提供有效信息。

图 4 表明，乔木林在背风处严重积沙，并且其潜在风蚀率要高于灌木树种。完整的防护林带（高大的乔木树种），如新疆杨防护林对于风沙防治效应效果最为明显。但是不完整的防护林带（低矮的乔木树种），如樟子松防护林，防治风沙效果并不明显。总体来说，不同树种组合下的防治风沙效果要好于单一树种下的防护林配置。

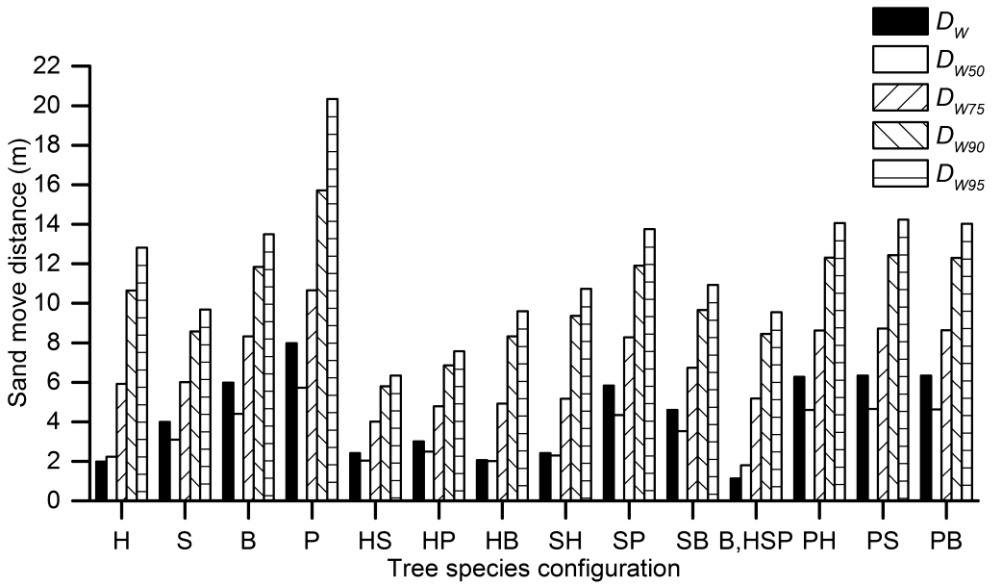

Fig.4 - Bars of different shelter tree species combinations indicated by D_{W50}, D_{W75}, D_{W90}, and D_{W95} represent the 50, 75, 90, and 95% cumulative percentiles, respectively, of the amounts of sand along the path of displacement

Sand loss

Sand loss was estimated using the exponential model. In general, small amounts of sand loss are associated with a low experimental error in the summation curve method. Figure 5 shows that there was a positive correlation between sand loss and the D_W input. Sand loss with *Pinus sylvestris* var. *mongolica* was 3 times that of a single tree species and 6 times that of different tree species arrangements. But this difference was considered insignificant. In theory, only when the D_W value exceeds the maximum distance (L_S) will calculation results generate significant error [3]. Therefore, L_S should be set as far as possible. In addition, for accurate measurement of sand displacement, L_P should be set as short as possible, at least 1 m, and the sand sampling interval should be set to least 0.1 m to filter out this undulation (error). Consequently, a smoother summation curve will be generated, which can provide better results.

风沙损失量

指数方程用来估算风沙损失量。一般而言，较小的损失量带入到累计曲线方法中产生误差也较小。图 5 看出，D_W 输入值与损失量成一定程度的正相关。樟子松树种配置上风沙的损失量分别是单树种损失量的 3 倍和不同树种配置损失量的 6 倍。但是差异并不显著。理论上，只有当 D_W 值超过最大的距离 L_S 时，计算结果会造成较大误差[3]。因此 L_S 值应尽量设置较远。另外，为准确计算风沙移动距离，L_P 应设置较小，至少为 1m，并且风沙采样点设置至少为 0.1m，这样可以过滤掉波动带来的实验误差。因此，计算得到的累计曲线会更加平滑，可提供较为理想的实验结果。

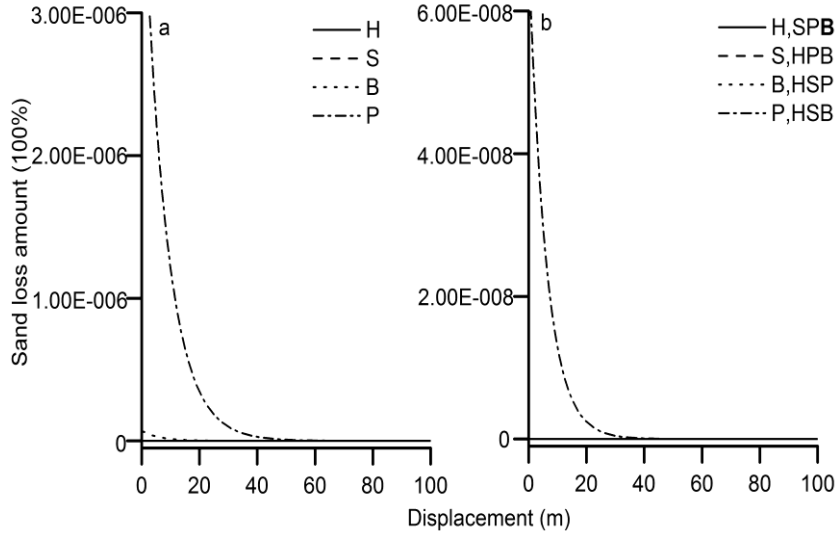

Fig.5 - Sand losses of different shelter tree species
a) Sand loss of a single tree shelterbelt.
b) Sand loss of a different arrangement of trees species

Multiple wind erosion process analysis

Wind erosion can significantly affect the underlying surface. For the purpose of long-term planning of sand prevention, it is essential to analyze these effects under multiple wind erosion events. As discussed above, the exponential function can simulate the distribution of eroded particles under a continuous wind erosion process, and the summation curve method can determine the dynamics of sand movement. Therefore, the data generated by the exponential model can be understood as the process of sand movement under continuous wind erosion events or multiple years of wind erosion. In this paper, *Pinus sylvestris* var. *mongolica* and *Hedysarum scoparium* trees were selected to demonstrate the process of sand movement under 5 continuous wind erosion events. Figure 6 shows that under a constant D_W parameter input, the output values were stable; a small amount of sand loss did not affect the simulation results. Linear regression analysis indicated that there was strong correlation between sand movements under multiple wind erosion events, whereas R^2 decreased with an increase in the cumulative percentage. Theoretically, during multiple wind erosion events, the cumulative percentage of the sand moving distance should show a decreasing trend due to the shelter forest controlling the wind effect. In general, the summation curve is stable and accurate, and can be used as a mid- or long-term protective model.

连续风蚀过程分析

风蚀作用能显著影响下垫面，作为长期防治风沙的重要手段，分析多次风蚀作用对于下垫面的影响效果是十分必要的。以上研究表明，由于指数方程可以模拟可蚀性颗粒在连续多次的风蚀下的分布过程，累计曲线模型可计算可蚀性颗粒动态运动分布过程。因此，指数方程计算的连续风蚀过程下的可蚀性颗粒运动过程也可以理解为连续或连年的风蚀过程下的可蚀性颗粒分布过程。本文中，以花棒和樟子松分析为例，在连续 5 次风蚀作用下，分析可蚀性颗粒的移动过程。图 6 表明，在相同的 D_W 参数输入下，指数方程计算参数输出稳定，少量风沙损失量并未影响模拟效果。线性回归分析结果表明，多次风蚀作用下的风沙移动数据相关程度较强，R^2 随移动距离百分比增大而减小。理论上，受制于防护林防风效果，风沙量移动百分比移动距离应呈减小趋势。总体上，累积曲线模型计算方法稳定程度较高，较为精确，可作为防护林中长期的防护模型。

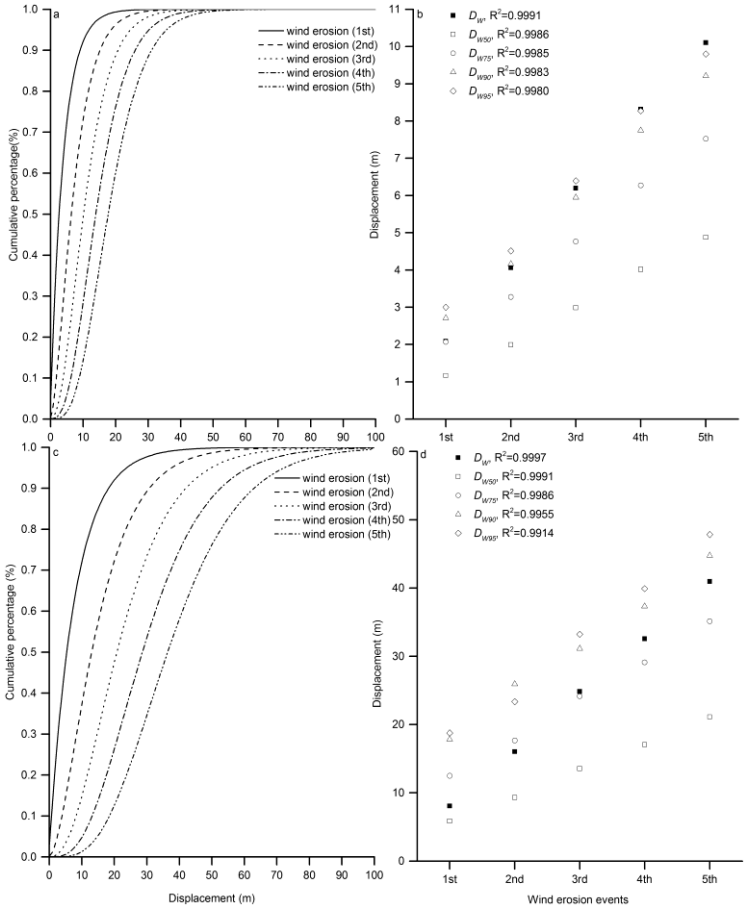

Fig.6 - Analysis of multiple wind erosion events. (a, b) Sand source (inside forest) changing trend (using *Hedysarum scoparium* as an example) and linear relationship of the D_{W50}, D_{W75}, D_{W90}, and D_{W95} values. (c, d) Sand source (inside forest) changing trend (using *Pinus sylvestris* var. *mongolica* as an example) and linear relationship of the D_{W50}, D_{W75}, D_{W90}, and D_{W95} values

CONCLUSIONS

The ultimate goal of wind erosion research is to establish erosion models that can predict particle erosion losses at different temporal and spatial scales. In general, the scientific and practical explorations of wind erosion studies are rather limited; therefore, it is a necessary to rebuild the theoretical based method for a wider application.

Based on former studies, this paper proposed a new method of analysing the effects of sand prevention in a shelterbelt forest. Because it is difficult to obtain accurate data, this paper used general conclusions from previous studies as estimates. The results indicated that experimental errors were well controlled and the conclusions drawn from the final analysis indicate that this method can provide direction and idea for shelterbelt management.

Compared with the empirical model, the summation curve method accounts for the fundamental theories of physical principles of blown sand and sedimentation processes. In addition, the theoretical model is more complicated than the summation curve due to the numerical calculations. Thus, the summation curve is the best method.

In the actual calculation and application, the summation curve method has two advantages. The first is that the input parameters are simple; the second is that this method can be used at different scales. Therefore, the summation curve can be applied to a wider scope when assessing farmland protection forest.

Considerable work needs to be conducted in future research. In this study, the assessment method was based on a single direction (width of the belts). However, different areas vary with respect to the topography, land use, degree of wind erosion and other factors, and these factors interact with each other. Therefore, it is necessary to establish a classification standard in future studies.

An additional decision factor in the design of optimal farmland shelterbelt systems involves the water requirements of the tree species because water is a limited resource and may be the main factor that prevents long-term maintenance of farmland shelterbelt systems in arid or semi-arid regions. Further studies are required to determine the water consumption of shelter forest tree species and the local water resources to explore the best afforestation density and shelterbelt forest structure.

ACKNOWLEDGEMENT

This work was supported by the National Basic Research Program of P. R. China (2013CB429906); National "Twelfth Five-Year" Plan for Science & Technology Support (2012BAD16B02);The Commonweal Project of State Forestry Administration of P. R. China (201304325)

REFERENCES

[1]. Brandle J.N., Hodges L., Zhou X.H., (2004) – *Windbreaks in North American agricultural systems*, Agroforestry Systems, vol.61, no.1/3, pp.65-78;

[2]. Cleugh H.A., (1998) – *Effects of windbreaks on airflow, microclimates and crop yields*, Agroforestry Systems, vol.41, no.1, pp.55-84;

[3]. Dale A., Passi G.R., (2012) – *Modeling dust emission caused by wind erosion*, Journal of Geophysical Research: Atmospheres, vol.93, no.11, pp.14233-14242;

讨论与结论

风蚀研究最终目标是建立能够预测不同时间尺度和不同地表类型的风蚀模型。一般而言，过去对风蚀研究的探索兼顾科学性和实用性较少。因此，重新构建具有理论基础与更广泛适用性的风蚀模型势在必行。

本文在现有防护林研究基础上，加入了新的研究方法，分析了防护林防治风沙效果。因为计算所需要的精确数据获取难度大，故本文采用前人研究中的一般结论进行估算。研究结果表明，实验误差被较好的控制，并且最终分析得到的结论可以为防护林建设管理提供新的研究方向和思路。

对比经验模型，累积曲线方法采用了风沙吹蚀沉降的基础物理学理论。另外，理论模型较累积曲线方法在数理计算上要更加复杂。因此累计曲线方法要优于以上模型。

实际计算、应用上，累积曲线方法具有两方面优势，一是输入参数简单；二是可以应用至各个尺度。因此，累积曲线方法可以应用至更大范围内的农田防护林评估。

下一步需要进行的工作是，本文只考虑单一方向的风蚀效应（防护林带的宽度）。然而，不同地区的地形、土地利用、风蚀率和其他相关因子也不尽相同，并且这些因子相互作用影响。因此未来的工作需要将这些因子进行分类研究。

另外，需要考虑的因素是在设计最优化合理的农田防护林时将农田防护林树种的水分利用情况考虑进来，因为在干旱和半干旱地区，受制于水资源限制，水分是阻碍农田防护林系统长期维持的主要因素。未来工作也需要结合防护林各树种蒸腾耗水规律和当地水资源条件，研究探讨最佳防护林造林密度和结构。

致谢

国家重点基础研究发展计划项目（2013CB429906）、“十二五”国家科技支撑计划项目（2012BAD16B02）、国家林业局公益性行业科研专项（201304325）。

参考文献

[1]. Brandle J.N., Hodges L., Zhou X.H. (2004) –*北美农田系统的防风林带研究*, 农田森林系统, 第 61 卷, 第 1/3 期, 65-78;

[2]. Cleugh H.A. (1998) – *防风林带对气流、微气候和农作物产量的影响*, 农田森林系统, 第 41 卷, 第 1 期, 55-84;

[3]. Dale A., Passi G.R. (2012) – *风蚀作用下的粉尘释放模型*, 地球物理学研究, 第 93 卷, 第 11 期, 14233-14242;

[4]. Fryrear D.W., Bilbro J.D., Saleh A., Schomberg H.,

[4]. Fryrear D.W., Bilbro J.D., Saleh A., Schomberg H., Stout J.E., Zobeck T.M., (2000) – *RWEQ: Improved wind erosion technology*, Journal of Soil and Water Conservation, vol.55, no.2, pp.183-189;
[5]. Fukuda Y., Moller H., Burns B., (2011) – *Effects of organic farming, fencing and vegetation origin on spiders and beetles within shelterbelts on dairy farms*, New Zealand Journal of Agricultural Research, vol.54, no.3, pp.155-176;
[6]. Guanglei Gao, Guodong Ding, Yuanyuan Zhao, Wei Feng, Yanfeng Bao, Ziwei Liu., (2014) – *Effects of Biological Soil Crusts on Soil Particle Size Characteristics in Mu Us Sandland*, Transactions of the Chinese Society for Agricultural Machinery, vol.45, no.1, pp.115-120;
[7]. Juan E.P., Daniel E.B., Ted M.Z., (2010) – *Comparison of different mass transport calculation methods for wind erosion quantification purposes*, Earth Surface Processes and Landforms, vol.35, no.13, pp.1548-1555;
[8]. Lobb D.A., Kachanoski R.G., Miller M.H., (1995) – *Tillage Translocation and Tillage Erosion on Shoulder Slope Landscape Positions Measured Using Cs-137 as a Tracer*, Canadian Journal of Soil Science, vol.75, no.2, pp.211-218;
[9]. Lobb D.A., Kachanoski R.G., (1999) – *Modelling tillage erosion in the topographically complex landscapes of southwestern Ontario, Canada*, Soil and Tillage Research, vol.51, no.3-4, pp.261-277;
[10]. Lobb D.A., Kachanoski R.G., (1995) – *Modelling tillage translocation using step, linear-plateau and exponential functions*, Soil and Tillage Research, vol.51, no.3-4, pp.317-330;
[11]. Lobb D.A., Quine T.A., Govers G., Heckrath G.J., (2001) – *Comparison of methods used to calculate tillage translocation using plot-tracers*, Journal of Soil and Water Conservation, vol.56, no.4, pp.321-328;
[12]. Mao Y., Wilson J.D, Kort J., (2013) – *Effects of a shelterbelt on road dust dispersion*, Atmosphere Environment, vol.79, pp.590-598;
[13]. Mohammed A.E., Stigter C.J., Adam H.S., (1996) – *On shelterbelt design for combating sand invasion*, Agriculture Ecosystems & Environment, vol.57, no.2-3, pp.81-90;
[14]. Qiang Cui, Jiarong Gao, Mingyue He, Zheguang Zhao, Jinrui Zhang., (2009) – *Effects of farm land shelterbelts in controlling wind and sand in sandy land of Yanch*i, Journal of Ecology and Rural Enviroment, vol.25, no.3, pp.25-29;
[15]. Wiseman G., Kort J., Walker D., (2009) – *Quantification of shelterbelt characteristics using high-resolution imagery*, Agriculture Ecosystems and Environment, vol.131, no.1/3, pp.111-117.

Stout J.E., Zobeck T.M. (2000) – *RWEQ: 风蚀模型的改进*, 水土保持学报, 第 55 卷, 第 2 期, 183-189;
[5]. Fukuda Y., Moller H., Burns B. (2011) –*乳牛场防护林内的有机耕作、围犁和基于蜘蛛和甲壳虫的植被覆盖的效果研究*, 新西兰农业研究, 第 54 卷, 第 3 期, 155-176;
[6]. 高广磊, 丁国栋, 赵媛媛, 冯 薇, 包岩峰, 刘紫薇. (2014) – *生物结皮发育对毛乌素沙地土壤粒度特征的影响*, 农业机械学报, 第 45 卷, 第 1 期, 115-120;
[7]. Juan E.P., Daniel E.B., Ted M.Z. (2010) – *量化分析风蚀为目的，对比不同风蚀颗粒吹蚀的计算方法*, 地貌变化与地理地形, 第 35 卷, 第 13 期, 1548-1555;
[8]. Lobb D.A., Kachanoski R.G., Miller M.H. (1995) – *利用 Cs-137 为示踪物测量肩坡地形下的耕作过程和耕作侵蚀率*, 加拿大土壤科学, 第 75 卷, 第 2 期, 211-218;
[9]. Lobb D.A., Kachanoski R.G. (1999) – *加拿大安大略省南部复杂地形地貌下的耕作侵蚀模型*, 土壤和耕作研究, 第 51 卷, 第 3-4 期, 261-277;
[10]. Lobb D.A., Kachanoski R.G. (1995) –*耕作过程模型分析，以逐步回归、线性回归和幂指数函数为例*, 土壤和耕作研究, 第 51 卷, 第 3-4 期, 317-330;
[11]. Lobb D.A., Quine T.A., Govers G., Heckrath G.J. (2001) – *利用大田示踪物对比不同耕作过程的研究方法*, 水土保持学报, 第 56 卷, 第 4 期, 321-328;
[12]. Mao Y., Wilson J.D, Kort J. (2013) –*公路防护林对粉尘的作用影响*, 大气环境, 第 79 卷, 第 4 期, 590-598;
[13]. Mohammed A.E., Stigter C.J., Adam H.S. (1996) – *以阻碍风沙为目的的防护林设计方法*, 农业生态系统与环境, 第 57 卷, 第 2-3 期, 81-90;
[14]. 崔 强, 高甲荣, 何明月, 赵哲光, 张金瑞. (2009) – *宁夏盐池沙地农田防护林的防风阻沙效益*, 生态与农村环境学报, 第 25 卷, 第 3 期, 25-29;
[15]. Wiseman G., Kort J., Walker D. (2009) – *利用高分辨率影像对防护林特性进行量化分析*, 农业生态系统与环境, 第 131 卷, 第 1/3 期, 111-117.

INFLUENCE OF PRE-SOWING ELECTROMAGNETIC TREATMENTS AND DURATION OF STORAGE ON GERMINATION ENERGY AND LABORATORY GERMINATION OF SEEDS FROM BULGARIAN TOMATO VARIETIES

ВЛИЯНИЕ НА ПРЕДСЕИТБЕНИТЕ ЕЛЕКТРОМАГНИТНИ ОБРАБОТКИ И СРОКА НА СЪХРАНЕНИЕ ВЪРХУ КЪЛНЯЕМАТА ЕНЕРГИЯ И ЛАБОРАТОРНАТА КЪЛНЯЕМОСТ НА СЕМЕНА ОТ БЪЛГАРСКИ СОРТОВЕ ДОМАТИ

Assoc. Prof. PhD Ganeva D.[1)], Assoc. Prof. PhD Eng. Sirakov K.[2)], Prof. PhD Eng. Mihov M.[1)], PhD Stud. Eng. Zahariev S.[2)], Prof. PhD Eng. Ivan Palov[2)]

[1)]Maritsa Vegetable Crops Research Institute, Plovdiv / Bulgaria; [2)]Angel Kanchev University of Ruse / Bulgaria

Tel: +359 32 952296; E-mail: dganeva@abv.bg

Abstract: The study has found a continuing beneficial impact of electromagnetic treatments on seeds of Bulgarian tomato varieties: *Milyana, Plovdivska karotina, Vodoley F_1, IZK Alya and Ideal* after 365 days storage to sowing at a voltage between the electrodes U=12 kV and duration of impact τ=35 s. The germinating energy and laboratory germination increase compared to that of control seeds of 1.25 to 15%.

Keywords: pre-sowing electromagnetic treatments, tomato seeds, germination energy, laboratory seed germination

INTRODUCTION

Tomato is a traditional vegetable crop for the territory of Bulgaria. There is a close relation between high and qualitative yields and sowing qualities of the seeds [3]. The germination energy and germination are ones of the most important features of the seeds. The low germination energy is a reason for slower initial rate of root and hypocotyl growth for tomato seed germination as well as later for germination in field conditions. The sowing rate is determined depending on the seed germination [7]. Alternative, ecological pure methods and technologies for stimulation of the sowing properties of the seeds by their treatment in electric [12], magnetic [1.9] and electromagnetic [11] fields are being searched. Positive effect of the laboratory (5...12%) and field germination (16...20%) of cabbage seeds after electromagnetic treatment [2] has already been recorded.

A peculiarity of the Bulgarian tomato seeds variety after electromagnetic pre-sowing has been established and it depends on the duration of the electromagnetic impact and duration of storage prior to planting [4]. The longer the duration of seed stays (12 days) from treatment to sowing and the higher value of applied voltage of treatment (12 kV) is, a stimulating effect on the seed quality in the studied tomato varieties has been found.

The favourable pre-sowing electromagnetic impact on the tomato seeds from variety *Milyana* is retained after stay prior to sowing of 365 days. It is of interest whether the impact of the pre-sowing electromagnetic treatments would be retained after longer stay in seeds from other tomato varieties [4].

The purpose of the study is to establish the effect of pre-sowing electromagnetic treatment and duration of storage on the sowing qualities of the seeds from Bulgarian tomato varieties.

Резюме: Констатирано е продължаващо благотворно въздействие на предсеитбените електромагнитни обработки върху семена от български сортове домати: Миляна, Пловдивска каротина, Водолей F_1, ИЗК Аля и Идеал след 365 денонощен престой до засяването им при третиране с напрежение между електродите U=12 kV и продължителност на въздействието τ=35 s. Установено е увеличаване на кълняемата енергия и на лабораторната кълняемост спрямо контролните семена от 1,25 до 15%.

Ключови думи: предсеитбена електромагнитна обработка, семена домати, кълняема енергия, кълняемост.

УВОД

Доматите са традиционна зеленчукова култура за нашата страна. Получаването на високи и качествени добиви е в тясна връзка с посевните свойства на семената [4]. Кълняемата енергия и кълняемостта са едни от най-важните характеристики на семената. Ниската кълняема енергия е причина за по-бавния първоначален темп на развитие на корена и хипокотила при покълване на семената от домати и по-късно при поникване в полски условия. В зависимост от кълняемостта на семената се определя сеитбената норма [5]. Търсят се алтернативни, екологично чисти методи и технологии за стимулиране посевните качества на семената чрез обработката им в електрически [13], магнитни [10,12] и електромагнитни [8] полета. Отчетен е положителен ефект на лабораторната (5...12%) и полска кълняемост (16...20%) на семена от зеле след електромагнитна обработка [1].

След проведени лабораторни изследвания на предсеитбени електромагнитни обработки на семена от български сортове домати е констатирана сортова особеност, която зависи от продължителността на предсеитбеното електромагнитно въздействие и срока на съхранение до засяването [2]. Установено е, че по-голямата продължителност на престой (12 денонощия) от обработката до сеитбата и по-голямата стойност на използваното напрежение на обработка (12 kV) оказват стимулиращо въздействие върху качеството на семената при проучваните сортове домати.

Благотворното предсеитбено електромагнитно въздействие върху семена от домати сорт *Миляна* се запазва и след престой до засяването в продължение на 365 дни. Интерес представлява и дали въздействието на предсеитбените електромагнитни обработки ще се съхрани и след по-продължителен престой и при семената от други сортове домати [2].

Целта на изследването е да се установи влиянието на предсеитбените електромагнитни обработки и срока на съхранение върху посевните качества на семена от български сортове домати.

MATERIAL AND METHOD

The object of the study are the seed qualities from the accepted Bulgarian tomato varieties *Milyana*, *Plovdivska karotina*, *Vodoley F$_1$*, *IZK Alya* and *Ideal*, described in our previous investigation [4]. The seeds have been subject to electromagnetic treatment and have then stayed for 365 day prior to sowing.

As in other similar studies [5,13] the pre-sowing electromagnetic treatments were performed in the AC corona discharge field between the electrodes (blade-plate). The adopted controlled factors of impact for this study were also the voltage between the electrodes U (kV) and the duration of treatment τ (s). The experiment planning matrix [10] with two controlled factors on two levels (type 2^2) of pre-sowing treatment is presented in Table 1.

ОБЕКТ И МЕТОДИКА НА ИЗСЛЕДВАНЕТО

След 365 денонощия престой от предсеитбената електромагнитна обработка до засяването, обект на изследването са качества на семена от признати и внедрени в производството български сортове домати: *Миляна, Пловдивска каротина, Водолей F$_1$, ИЗК Аля и Идеал,* описани в предходно наше изследване [2].

Съгласно други подобни изследвания [3,9] предсеитбените електромагнитни обработки са извършвани в полето на променливотоков коронен разряд, създаван между електроди острие-плоскост. Възприетите и при това изследване управляеми фактори на въздействие са напрежението между електродите U (kV) и продължителността на въздействие τ (s). Матрицата на планиране на пълния факторен експеримент [7] с два управляеми фактора на две нива (ПФЕ от типа 2^2) на предсеитбените обработки е представена в табл.1.

Table 1

Experiment planning matrix

Treatments	Voltage, U		Duration of impact, τ	
	level	kV	level	s
1	+1	12	+1	35
2	-1	6	+1	35
3	+1	12	-1	5
4	-1	6	-1	5
Control	untreated seeds			

After treatment the seeds were kept in packing paper in a dry and dark storeroom. After 365-day storage i.e., on February the 7th 2014 the seeds from each variant of impact were set in 4 replications with 20 seeds in each replication according to the adapted methods by ISTA [6], for germination in Petri dishes in thermostat at temperature of 25^{o}C and relative humidity of 95%. Untreated seeds for the relevant varieties were used as a control.

The following sowing qualities of the seeds were studied: *germination energy – g.e.* (%) and *laboratory germination – g.* (%) being read on 5-th and 14-th day, respectively after seed set for germination. For greater comparability the data from each variant of treatment is presented as percentage in relation to that of the control (%/c).

The obtained data was processed statistically by variation [8] and regression analysis [10].

RESULTS

The results for germination energy and laboratory germination of the seeds untreated in the electromagnetic field are given in Table 2.

След обработките семената са съхранявани в семехранилище, на тъмно и сухо, в хартиени пликчета. На 365-я ден от обработката, т.е. на 07.02.2014 г., семената от всеки вариант на въздействие са заложени в 4 повторения по 20 броя, по адаптирана методика на ISTA [11], за покълване в петриеви блюда в термостат при температура 25^{o}C и относителна влажност 95%. За контрола са използвани необработени семена от съответните сортове.

Изследвани са посевните качества на семената: *кълняема енергия – к.е.* (%) и лабораторна *кълняемост – к.* (%), които са отчетени съответно на 5-я и 14-я ден от залагането на семената за покълване. За по-голяма сравняемост данните за всеки вариант на обработка са приведени в процент, спрямо тези на контролата (%/к).

Получените данни са обработени статистически чрез вариационен [6] и регресионен анализ [7].

РЕЗУЛТАТИ И ОБСЪЖДАНЕ

Резултатите, получени за кълняемата енергия и лабораторната кълняемост на необработените семена от проучваните сортове, са представени в табл. 2.

Table 2

Propagating seed quality of untreated seeds

Sowing qualities		Variety				
		Milyana	*Plovdivska karotina*	*Vodoley F$_1$*	*IZK Alya*	*Ideal*
Germination energy, %	$\bar{X}$ ± sd	81,25	88,75	83,75	32,50	90,00
	± sd	± 3,75	± 4,27	± 3,75	± 3,22	±3,74
	CV%	9,23	9,62	8,96	19,86	7,86
Germination, %	$\bar{X}$	87,50	92,50	90,00	76,25	93,75
	± sd	± 4,79	± 3,23	± 3,54	± 4,27	± 2,39
	CV%	10,94	6,98	7,86	11,20	5,11

In further studies these results are accepted for 100% and the data from the other crops is reduced to them.

The variety *IZK Alya* demonstrates the lowest percentage of germination energy and laboratory germination in comparison to the remaining studied varieties. This is cherry type tomato variety which seeds are the smallest amongst the studied seeds, with the lowest absolute weight being probably a reason for lower sowing qualities of the seeds compared to the other varieties included in the study. In 2013 it was established that the germination energy and the laboratory germination of the seeds from variety *IZK Alya* are 33.75% and 91.25%, respectively [4]. The sowing qualities of the control seeds are *g.e.*=32.5% and *g.*=76.5% after stay of 365 days. These values are lower than those obtained in 2013 that are 33.75% and 91.25%, respectively. The laboratory germination and germination energy decrease with increase of the seed age that is both species and variety peculiarity.

The analysis of data given in Table 2 shows that in comparison with 2013, a decrease of *g.e.* in the control seeds of the other tomato varieties in 2014 is observed but it is within the range of (5…10)%, but of *g.* – (2…12)%.

При по-нататъшните изследвания тези резултати са приети за 100% и спрямо тях са приведени данните от другите наблюдения.

Сортът *ИЗК Аля,* спрямо останалите проучвани сортове, показва най-нисък процент на кълняема енергия и лабораторна кълняемост. Това е единственият сорт в проучването от типа ”чери”, чиито семена са най-дребни, с най-ниска абсолютна маса и поради тази причина посевни качества на семената по-ниски. Както и в [2], така и след 365 дни престой контролните семена на сорт *ИЗК Аля* имат: *к.е.*=32,5% и *к.*=76,5%. Тези стойности са по-ниски от получените през 2013 г., които са съответно 33,75% и 91,25%. С увеличаване на възрастта на семената постепенно се понижава лабораторната кълняемост и кълняемата енергия, което е както видова, така и сортова особеност.

Анализът на данните от табл. 2 показва, че в сравнение с 2013 г., през 2014 г. при контролните семена и на другите сортове домати има намаление на *к.е.,* но то е в рамките на (5…10)%, а за *к.* – (2…12)%.

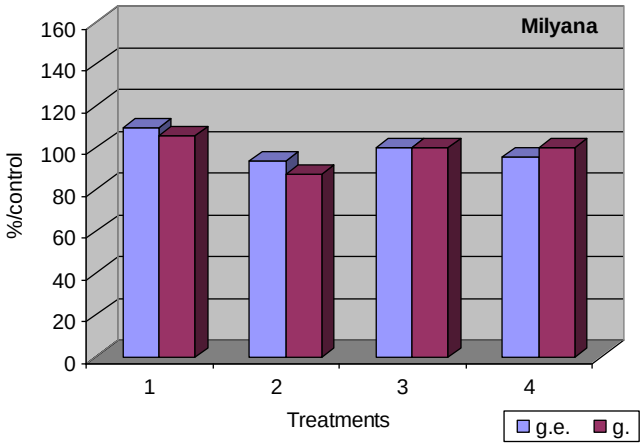

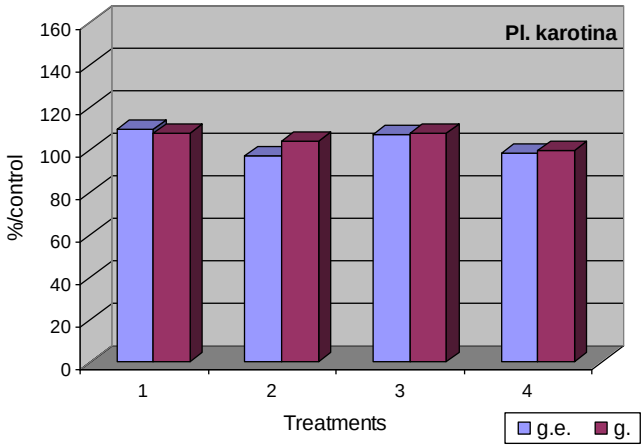

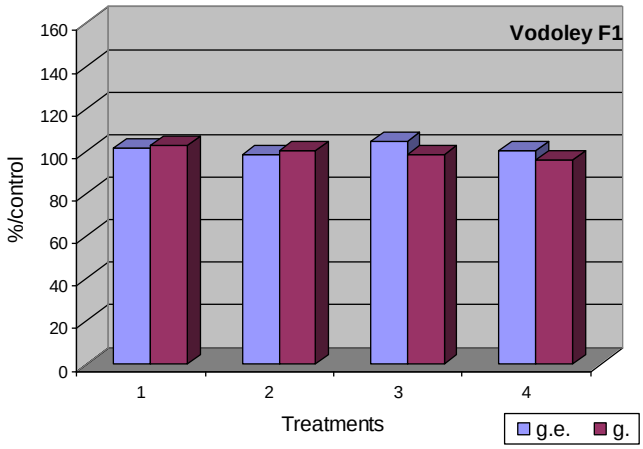

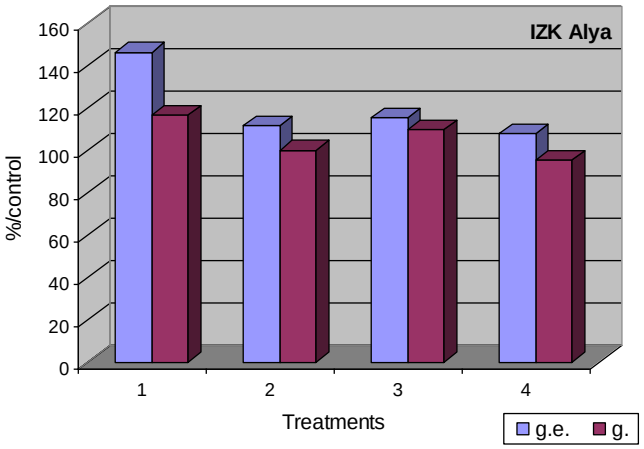

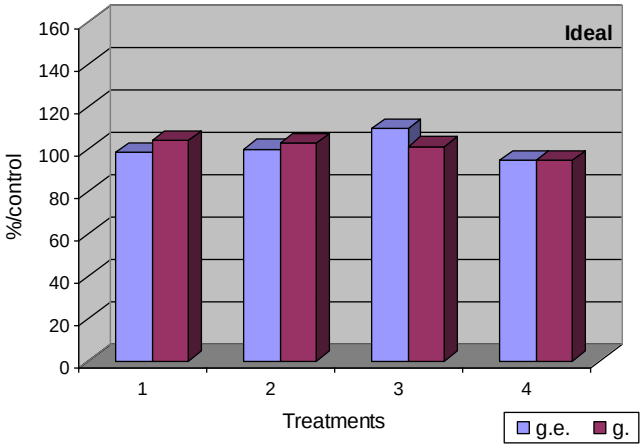

Fig. 1 – Germination energy and seed laboratory germination of electromagnetic treated seeds after 365 days length of storage

The results from the study for germination energy and laboratory germination of the seeds from all varieties treated in electromagnetic field according to the variants in Table 1 and stay 365 days prior to sowing in 2014 are presented in Figure 1. The results were given as percentage in relation to the ones from the control (%/c). The analysis demonstrates that for varieties *Milyana, Plovdiska karotina* and I*ZK Alya* a dominant positive impact on *g.e.* and *g.* after treatment of the seeds by variant 1 (U=12 kV, τ=35 s) is obtained. This effect is kept for 365 days after electromagnetic treatment as for *Milyana g.e.*=109.23%/c and *g.*=105.71%/c and for variety *Plovdivska karotina g.e.*=109.86%/c and *g.*=108.11%/c.

The established low natural (for seed from the control) *g.e.* and *g.* in variety *IZK Alya* have the highest impact from the electromagnetic treatments among the mentioned two varieties. The values of the two studied parameters, obtained after treatment of the seeds from this variety by variant 1 and stay for a period of 365 days prior to sowing are *g.e.*=146.15%/c and *g.*=116.39%/c. This is significantly more than the observed parameters of the above mentioned varieties *Milyana* and *Plovdivska karotina.*

The seeds form variety *Vodoley* F_1 show a slight increase of the two observed parameters after treatment by variant 1. After stay for a year the values are g.e.=101.49%/c and *g.*=102.78%/c.

It was established that after treatment of the seeds from variety *Ideal* by variant 1 and stay of 365 days prior to sowing, the germination energy is slightly depressed. It is 98.61%/c towards the control. The peculiarity for this variety is that the read laboratory germination is *g.*=104.00%/c.

The above could be explained with variety peculiarity of the individual seeds when the other factors of influence and conditions are identical.

Figure 1 also shows that after seed treatment with the parameters of the other variant there is a depression of the germination energy and laboratory germination in different degrees, for different variants of treatment, in different tomato varieties. An exception was established in variant of treatment 3 (U=12 kV and τ=5 s) where the seeds of variety *Ideal* demonstrated the highest value of their response after pre-sowing treatment. Germination

На фиг.1 са представени резултатите от изследване на кълняемата енергия и лабораторната кълняемост на семената от всички сортове, обработени в електромагнитно поле, съгласно вариантите от табл. 1 и престояли 365 дни до засяването им през 2014 г. Резултатите са приведени в % спрямо контролата (%/к). Анализът показва, че за сортове: *Миляна, Пловдивска каротина и ИЗК Аля* се получава доминиращо положително въздействие върху *к.е.* и *к.* след обработката на семената по вариант 1 (U=12 kV, τ=35 s). Това въздействие се е запазило 365 денонощия след електромагнитната обработка, като за *Миляна к.е.*=109,23%/к и *к.*=105,71%/к, а за сорт *Пловдивска каротина к.е.*=109,86%/к и *к.*=108,11%/к.

Спрямо споменатите два сорта установените ниски естествени (за контролните семена) *к.е.* и *к.* за сорт *ИЗК Аля* са повлияни най-силно от електромагнитното въздействие. След обработката на семената на този сорт по вариант 1 и престой от 365 денонощия до засяването им, стойностите на двата регистрирани параметъра са *к.е.*=46,15%/к и *к.*=116,39%/к. Това е значително повече от наблюдаваните параметри на описаните по-горе сортове *Миляна* и *Пловдивска каротина.*

След обработката по вариант 1 семената на сорт *Водолей* F_1 имат, макар и незначително, повишаване на двата наблюдавани параметъра. След престой от една година *к.е.*=101,49%/к, а *к.*=102,78%/к.

За семената от сорт *Идеал* е констатирано, че след обработката им по вариант 1 и престой до засяването 365 денонощия кълняемата енергия е незначително потисната. Спрямо контролата тя е *к.е.*=98,61%/к. Особеното при този сорт е, че отчетената лабораторна кълняемост е *к.*=104,00%/к.

При други еднакви фактори на въздействие и условия, описаното по-горе може да се обясни със сортовата особеност на отделните семена.

От фиг. 1 може да се констатира също, че след обработката на семената с параметрите на другите варианти се получава потискане на кълняемата енергия и лабораторната кълняемост, което е в различни степени за различните варианти на обработка и за отделните сортове домати. Но и тук има изключения. При вариант на обработка 3 (U=12

energy for this variety is *g.e.*=109.72%/c and *g.*=101.33%/c. The similar situation was observed in variety *Plovdivska karotina*. The values read for the seeds of this variety, treated by variant 3 are *g.e.*=107.04%/c and *g.*=108.11%/c.

The established repression of the germination energy or laboratory germination of the seeds can be due to the combination of the factors levels, prolonged stay of the seeds within 365 days and their variety peculiarity.

The analysis of the statements made in [4, 5, 13] show a regularity of the impact of the pre-sowing treatment. It could be concluded that after pre-sowing electromagnetic treatment in values of the controlled factors by variant 1 (U=12 kV and τ=35 s) and longer stay of the seeds (12 or 365 days), dominating positive responses were obtained followed by increases in the germination energy and laboratory germination of the seeds.

According to the data from Table 1 the experiment that was conducted is with two controlled factors of influence: the applied voltage between the electrodes U (kV), accepted as coded quantity x_1 and duration of the impact, τ (s) – x_2. This gives a possibility to calculate the equations of regression of the studied parameters germination energy and laboratory germination being given in %/c. All equations are from the following type [10]:

kV и τ=5 s) семената на сорт *Идеал* са показали най-високи стойности на реакцията си от предсеитбената обработка. При тях *к.е.*=109,72%/к, а *к.*=101,33%/к. Подобно е положението и при сорт *Пловдивска каротина*. За неговите семена, обработени по вариант 3, са отчетени *к.е.*=107,04%/к и *к.*=108,11%/к.

Констатираното потискане на кълняемата енергия, или лабораторната кълняемост на семената може да се отдаде на съчетанието на нивата на факторите, продължителния престой на семената от 365 денонощия и тяхната сортова особеност.

Анализът на изложенията, направени в [2, 3, 9] показва закономерност на въздействието на предсеитбените обработки. Последното се заключава в това, че след предсеитбена електромагнитна обработка при стойности на управляемите фактори по вариант 1 (U=12 kV и τ=35 s) и по-продължителен престой на семената (12 или 365 денонощия) се получават доминиращи положителни реакции, а с това и повишение на кълняемата енергия и лабораторната кълняемост на семената.

Съгласно табл. 1 провежданият експеримент е с два управляеми фактора на въздействие: приложеното напрежение между електродите U (kV), възприет като кодирана величина x_1 и продължителност на въздействието, τ (s) – x_2. Това дава възможност да се пресметнат уравненията на регресия на изследваните параметри кълняема енергия и лабораторна кълняемост, които са представени в %/к. Всички уравнения са от типа [7]:

$$\hat{Y} = b_0 + b_1 x_1 + b_2 x_2 + b_1 b_2 x_1 x_2 \quad (1)$$

According to the established values (in %/c) of the particular observed parameters, the following equations of regression are obtained:

Според установените средни стойности (в %/к) на отделните наблюдавани параметри, са получени следните уравнения на регресия:

for variety *Milyana*:

за сорт *Миляна:*

- germination energy

$$\hat{Y}_{g.e.\ Milyana} = 99{,}615 + 5{,}000 x_1 + 1{,}925 x_2 - 2{,}690 x_1 x_2 \quad (2)$$

- laboratory germination

$$\hat{Y}_{g.\ Milyana} = 98{,}320 + 4{,}535 x_1 - 1{,}680 x_2 + 4{,}535 x_1 x_2 \quad (3)$$

for variety *Plovdivska karotina*:

за сорт *Пловдивска каротина:*

- germination energy

$$\hat{Y}_{\text{g.e. } Pl.karotina} = 103{,}167 + 5{,}282 x_1 + 0{,}352 x_2 + 1{,}058 x_1 x_2 \quad (4)$$

- laboratory germination

$$\hat{Y}_{\text{g. } Pl.karotina} = 105{,}067 + 3{,}042 x_1 - 1{,}012 x_2 - 1{,}012 x_1 x_2 \quad (5)$$

for variety *Vodoley F_1*:

за сорт *Водолей F_1:*

- germination energy

$$\hat{Y}_{\text{g.e. } Vodoley} = 101{,}120 - 1{,}865 x_1 - 1{,}120 x_2 - 0{,}375 x_1 x_2 \quad (6)$$

- laboratory germination

$$\hat{Y}_{\text{g. } Vodoley} = 99{,}305 + 1{,}390 x_1 + 2{,}085 x_2 \quad (7)$$

for variety *IZK Alya*:

за сорт *ИЗК Аля:*

- germination energy

$$\hat{Y}_{g.e.\ IZK\,Alya} = 120{,}015 + 10{,}615\,\overset{\circ}{x}_1 + 8{,}655\,\overset{\circ}{x}_2 + 6{,}730\,\overset{\circ}{x}_1\,\overset{\circ}{x}_2 \quad (8)$$

- laboratory germination

$$\hat{Y}_{g.\ IZK\,Alya} = 120{,}325 + 7{,}785\,\overset{\circ}{x}_1 + 2{,}870\,\overset{\circ}{x}_2 + 0{,}410\,\overset{\circ}{x}_1\,\overset{\circ}{x}_2 \quad (9)$$

for variety *Ideal*: за сорт *Идеал:*

- germination energy

$$\hat{Y}_{g.e.\ Ideal} = 100{,}692 + 3{,}472\,\overset{\circ}{x}_1 - 1{,}387\,\overset{\circ}{x}_2 - 4{,}167\,\overset{\circ}{x}_1\,\overset{\circ}{x}_2 \quad (10)$$

- laboratory germination

$$\hat{Y}_{g.\ Ideal} = 100{,}667 + 1{,}997\,\overset{\circ}{x}_1 + 2{,}6670\,\overset{\circ}{x}_2 - 1{,}332\,\overset{\circ}{x}_1\,\overset{\circ}{x}_2 \quad (11)$$

The examination that was performed demonstrates that all equations are adequate since the calculated criteria of Fisher are smaller than their critical values and the coefficients of the regression equations are significant according to the criterion of Student [10].

The analysis of the equations (2)…(11) shows that the size of the coefficients in front of the coded factor $\overset{\circ}{x}_1$ are significantly higher compared to the other in the particular equations. This is an indication that the degree of influence of the factor voltage U of treatment of seeds is greater compared to that of the duration of impact τ. This is confirmed by the higher values of germination energy and laboratory germination of the seeds treated in U=12 kV that have been reached.

The values of the coefficients $\overset{\circ}{x}_1$ for variety *IZK Alya* are the greatest compared to the other equations – for example for *g.e.* (8) the value is 10,615. In this case it was found that the germination energy is the highest - 146,15%/c. (Figure 1). The coefficient in front of factor $\overset{\circ}{x}_1$ in the equation (9) for laboratory germination is 7,785, i.e. the effect of voltage on this parameter is slighter than that for the germination energy. It was established that for the laboratory germination of the seeds from variety *IZK Alya* is 116,39%/c in variant 1 (U=12 kV and τ=35 s) i.e. it is lower than the germination energy reached by the seeds (Figure 1). The values of the coefficient in front of $\overset{\circ}{x}_1$ in (9) however are the highest compared to the coefficients in the equations for laboratory germination of the rest of varieties.

The coefficients in front of the coded factor $\overset{\circ}{x}_1$ (voltage U) are the smallest in the equations (7) and (11) -1,390 and 1,997 for germination of the varieties *Vodoley F1* and *Ideal.* According to the data obtained and Figure 1 was established that the laboratory germination of the mentioned varieties, for example in variant 1 is102,78%/g and 104,00%/g, respectively. These values correlate with the size of the coefficients in front factor $\overset{\circ}{x}_1$.

The impact of the factor duration of treatment τ, with coded kind $\overset{\circ}{x}_2$, on the germination energy and laboratory germination is smaller compared to that of the factor voltage U. The last fact is proven by the values in front of the coefficients $\overset{\circ}{x}_2$ in the equations (2)…(11). The coefficient in front $\overset{\circ}{x}_2$ are with negative value (-1,680 and

Направената проверка показва, че всички уравнения са адекватни, тъй като изчислените критерии на Фишер са по-малки от критичните им стойности, а коефициентите на регресионните уравнения са значими, съгласно критерия на Стюдънт [7].

Анализът на уравнения (2)…(11) показва, че големината на коефициентите пред кодирания фактор $\overset{\circ}{x}_1$ са значително по-големи от другите в отделните уравнения. Това означава, че степента на влияние на фактора напрежение U на обработка на семената е по-голяма от тази на продължителността на въздействието τ. Това се потвърждава от достигнатите по-големи стойности на кълняемата енергия и лабораторна кълняемост на семената, когато те са обработени при U=12 kV.

За сорт *ИЗК Аля* стойностите на коефициентите $\overset{\circ}{x}_1$ са най-големи в сравнение с другите уравнения – напр. за *к.е.* (8) той е 10,615. От фиг. 1 може да се констатира, че там кълняемата енергия е най-висока – 146,15%/к. Коефициентът пред фактора $\overset{\circ}{x}_1$ в уравнение (9) за лабораторната кълняемост е 7,785, т.е. влиянието на напрежението върху този параметър е по-слабо от това при кълняемата енергия. За вариант 1 (U=12 kV и τ=35 s) и от фиг. 1 може да се констатира, че лабораторната кълняемост на семената от сорт *ИЗК Аля е* 116,39%/к, т.е по-малка от достигната от семената кълняема енергия. Стойността на коефициента пред $\overset{\circ}{x}_1$ в (9) обаче е най-голяма в сравнение с коефициентите в уравненията за лабораторна кълняемост на останалите сортове.

Най-малките коефициенти пред кодирания фактор $\overset{\circ}{x}_1$ (напрежението U) са в уравнения (7) и (11) -1,390 и 1,997 за кълняемост на сортовете *Водолей F1 и Идеал.* Съгласно получените данни и фиг. 1 лабораторната кълняемост на споменатите сортове, напр. за вариант 1 е съответно 102,78%/к и 104,00%/к. Тези стойности корелират с големините на коефициентите пред фактора $\overset{\circ}{x}_1$.

Влиянието на фактора продължителност на обработката τ, с кодиран вид $\overset{\circ}{x}_2$, върху кълняемата енергия и лабораторната кълняемост, е по-малко от това на фактора напрежение U. Последното се доказва от стойностите пред коефициентите $\overset{\circ}{x}_2$ в уравнения (2)…(11). Само в уравнения (3) и (5) за сортовете *Миляна* и *Пловдивска каротина*

-1,012, respectively) in equations (3) and (5) only for varieties *Milyana* and *Plovdivska karotina*. The analysis of the equations demonstrates that these coefficients are the smallest compared to similar ones. This could be explained with variety peculiarity of the seeds from varieties *Milyana* and *Plovdivska karotina*.

The interaction between the factors voltage U and duration of treatment τ could be found and analyzed from the values in front the coefficients x_1 and x_2. The results obtained for germination energy and laboratory germination of the tomato seeds from the mentioned varieties after stay of 365 days from treatment to sowing, correlate with those in variety *Milyana* [4], whose seeds have stayed for 12 days from treatment to sowing in laboratory conditions. The treatment with parameters of variant 1 (U=12 kV and τ=35 s) could be recommended as the most efficient for stimulation of the germination energy and laboratory germination of tomato seeds.

CONCLUSIONS

The study found an extended favourable impact of the pre-sowing electromagnetic treatment (in specified values for the controlled factors) on the seeds from Bulgarian tomato varieties *Milyana*, *Plovdivska karotina*, *IZK Alya F1* and *Ideal* after 365 days of stay to sowing.

An increase of the germination energy *(g.e.)* and laboratory germination *(g.)* of the seeds towards the control (untreated) seeds was established after pre-sowing electromagnetic treatment in the corona discharge field with parameter of the controlled factors: voltage between the electrodes U=12 kV and duration of the impact τ=35 s and after one year stay of the seeds to their sowing. The increase is as follows: for variety *Milyana* – *g.e.*=109,23%/c and *g.*=105,71%/c, for variety *Plovdivska karotina* – *g.e.*=109,86%/c, *g.*=108,11%/c, for variety *Ideal* – *g.e.*=98,61%/c, *g.*=104,00%/c and for variety *Vodoley F1* – *g.e.*=101,49%/c, *g.*=102,78%/c.

It was established that in low values of the controlled factors of electromagnetic treatment: voltage between the electrodes U=6 kV and period of impact τ=5 s and after one year stay of the seeds to their sowing, a depression of the observed laboratory parameters is observed in which the germination energy and laboratory germination reach 95%/c.

It was found that in the calculated equations, the coefficient of regression in front of the coded value $\overset{\circ}{x}_1$ of the controlled factor of impact voltage U are with higher values compared to these in front of the coded value of the factor duration of treatment $\overset{\circ}{x}_2$, that demonstrates the greater influence of the voltage on the effect of the pre-sowing treatment.

Electromagnetic treatment with parameters: voltage U=12 kV and duration of the treatment τ=35 s could be recommended as the most efficient for stimulation of the germination energy and the germination of the seeds from Bulgarian tomato varieties.

коефициентите пред $\overset{\circ}{x}_2$ са с отрицателна стойност (съответно -1,680 и -1,012). Анализът на уравненията показва, че тези коефициенти са най-малките в сравнение с другите подобни. Описаното може да се обясни със сортовата особеност на семената от сортове *Миляна* и *Пловдивска каротина*.

Взаимодействието между факторите напрежение U и продължителност на обработка τ може да се констатира и анализира от стойностите пред коефициентите x_1 и x_2. Получените резултати за кълняема енергия и лабораторна кълняемост на семената от домати на споменатите сортове, след престой от обработка до засяването им 365 денонощия напълно корелират с тези при сорт *Миляна* [2], чиито семена са престояли 12 денонощия от обработката до засяването в лабораторни условия. При това обработката с параметрите на вариант 1 (U=12 kV и τ=35 s) може да се препоръча като най-ефективна за стимулиране на кълняемата енергия и лабораторна кълняемост на семената от домати.

ИЗВОДИ

След 365 денонощия престой до засяването е констатирано продължаващо благотворно въздействие на предсеитбените електромагнитни обработки (при определени стойности на управляемите фактори) върху семена от български сортове домати: *Миляна, Пловдивска каротина, ИЗК Аля, Водолей F1 и Идеал.*

След предсеитбени електромагнитни обработки в полето на коронен разряд с параметри на управляемите фактори: напрежение между електродите U=12 kV и продължителност на въздействието τ=35 s, и след едногодишен престой на семената до засяването им е установено увеличаване на кълняемата енергия *(к.е.)* и на лабораторната кълняемост *(к.)* спрямо контролните семена както следва: за сорт *Миляна – к.е.*=109,23%/к и *к.*=105,71%/к, за *сорт Пловдивска каротина - к.е.*=109,86%/к и *к.*=108,11%/к, за сорт *Идеал – к.е.*=98,61%/к и *к.*=104,00%/к и за сорт *Водолей F1 – к.е.*=101,49%/к и *к.*=102,78%/к.

Установено е, че при ниските стойности на управляемите фактори на електромагнитна обработка: напрежение между електродите U=6 kV и продължителност на въздействието τ=5 s, и след едногодишен престой на семената до засяването им се получава потискане на наблюдаваните лабораторни параметри, при което кълняемата енергия и лабораторната кълняемост достигат до 95%/к.

Констатирано е, че в пресметнатите уравнения, коефициентите на регресия пред кодираната стойност $\overset{\circ}{x}_1$ на управляемия фактор на въздействие напрежение U са с по-големи стойности от тези пред кодираната стойност на фактора продължителност на обработката $\overset{\circ}{x}_2$, което показва по-голямото влияние на напрежението върху ефекта от предсеитбената обработка.

Електромагнитна обработка с параметри: напрежение U=12 kV и продължителност на обработката τ=35 s може да се препоръча като най-ефективна за стимулиране на кълняемата енергия и кълняемостта на семената на българските сортове домати.

REFERENCES

[1]. Aladjadjiyan A. (2007) – *The use of physical methods for plant growing stimulation in Bulgaria.* Journal of Central European Agriculture, 8 (3): 369-380;

[2]. Antonova G., Decheva S., Mihov M., Sirakov K., Zahariev S., Palov I. (2013) – *Study on the effect of pre-sowing electromagnetic treatment on germination of head cabbage seeds*, Agricultural Engineering, Vol.50, Issue 1, pg.22-26;

[3]. Danailov Zh. (2012) – *Breeding and seed production of tomato (Solanum lycopersicum* L*.). History, methods, achievements, trends. Academic* Publishing House "Prof. M. Drinov", Sofia;

[4]. Ganeva D., Mihov M., Palov I., Sirakov K., Zahariev S. (2013) – *Results of laboratory tests after pre-sowing electromagnetic treatment of seeds of Bulgarian tomato varieties,* Agricultural Engineering, Vol. 50, Issue 3, pg.13-21;

[5]. Ganeva D., Sirakov K., Mihov M., Palov I., Zahariev S. (2014) – *Study on the effect of pre-sowing electromagnetic treatment of tomato seeds on germination in laboratory and field conditions,* Agricultural Engineering, Volume 51, Issue 2, pg.13-18;

[6]. International Seed Testing Association (ISTA). (2004) – *International rules for seed testing*. Bassersdorf, Switzerland;

[7]. Kartalov P., Petrov H., Doykova M., Boshnakov P. (1990) – *Vegetable growing and seed production*. Zemizdat, Sofia;

[8]. Lakin G. (1990) – *Biometry*. Publishing House "Graduated school", Moscow;

[9]. Martinez E., Carbonell M., Florez M. (2004) – *Influence of 125 and 250 mT stationary magnetic field on the rate of germination of barley seeds (Hordeum vulgare* L*.).* Proceedings of the Union of scientist "Energy Efficiency and Agricultural Engineering*"*, Ruse, Bulgaria, 3-5 June 2004, pg. 131-136;

[10]. Mitkov A., Kardashevski S. (1977) – *Statistical methods in Agricultural technique*, Zemizdat, Sofia;

[11]. Palov I., Stoilova A., Radevska M., Sirakov K. (2008) – *Results from research of pre-sowing electromagnetic treatment of seeds from Bulgarian cotton varieties.* Agricultural Engineering, Vol. 46, Issue 5, pg.12-19;

[12]. Pozeliene A., Lynikiene S. (2009) – *The treatment of rape (Brassica napus L.) seeds with the help of electrical field*. Agronomy Research, 7 (1): 39-46;

[13]. Sirakov K., Ganeva D., Mihov M., Martev K., Zahariev S. Palov I. (2014) – *Study of the influence of electromagnetic treatment and storage period on propagating seed quality of tomato Milyana variety*, Agricultural Engineering, Vol. 51, Issue 3-4, pg. 21-26.

ЛИТЕРАТУРА

[1]. Антонова, Г., С. Дечева, М. Михов, К. Сираков, Св. Захариев, Ив. Палов (2013) – *Проучване на ефекта от предсеитбена електромагнитна обработка върху кълняемостта на семена от главесто зеле*. Селскостопанска техника, 50 (1): 22-26;

[2]. Ганева, Д., М. Михов, Ив. Палов, К. Сираков, Св. Захариев (2013) – *Резултати от лабораторни изследвания след предсеитбена електромагнитна обработка на семена български сортове домати.* Селскостопанска техника, 50 (3): 13-21;

[3]. Ганева, Д., К. Сираков, М. Михов, Ив. Палов, Св. Захариев (2014) – *Анализ на посевните качества на семена от домати след електромагнитна обработка при изследвания в лабораторни и полски условия.* Селскостопанска техника, 51 (2): 13-18;

[4]. Данаилов, Ж. (2012) – *Селекция и семепроизводство на домати (Solanum lycopersicum* L*.). История, методи, постижения, тенденции*. Академично издателство "Проф. М. Дринов", София, 265;

[5]. Карталов, П., Х. Петров, М. Дойкова, П. Бошнаков (1990) – *Зеленчукопроизводство със семепроизводство*. Земиздат, София, 295;

[6]. Лакин, Г. (1990) – *Биометрия*. Высшая школа, Москва, 352;

[7]. Митков, А., С. Кардашевски (1977) – *Статистически методи в селскостопанската техника*. Земиздат, София, 501;

[8]. Палов, Ив., А. Стоилова, М. Радевска, К. Сираков (2008) – *Резултати от изследвания на предсеитбена електромагнитна обработка на семена от нови български сортове памук.* Селскостопанска техника, 46 (5): 12-19;

[9]. Сираков, К., Д. Ганева, М. Михов, К. Мартев, Св. Захариев, Ив. Палов (2014) – *Изследване влиянието на предсеитбената електромагнитна обработка и срока на съхранение върху посевните качества на семена от домати сорт Миляна.* Селскостопанска техника, 51 (3-4): 21-26;

[10]. Аладжаджиян. А. (2007) - *Използване на физични методи за стимулиране на растежа на растенията в България.* Списание на Централното Европейско селско-стопанство, 8 (3): 369-380;

[11]. Международна асоциация за тестиране на семена (ИСТА) (2004) - Международни нормативи за тестиране на семена, Басерсдорф, Швейцаря.

[12]. Мартинез., Е., М. Карбонел и М. Флорез (2004) - *Влияние на стационарно магнитно поле от 125 и 250 mT върху степента на поникване на ечемични семена (Hordeum vulgare L.).* Сборник трудове от Съюз на учените „Енергийна ефективност и аграрно инженерство", Русе, България, 3-5 юни, 2004, 131-136

[13]. Позелене, А. С. Линикиене (2009) - Третиране на семена от рапица *(Brassica napus* L*.)* с помоща на електрично поле. Аграрна наука, 7 (1): 39-46.

UTILIZATION OF LABVIEW PROGRAM FOR ACQUIRING AND PROCESSING THE VIBRATIONS OF AN OSCILLATING CONE-SHAPED SIEVE WITH VERTICAL AXLE USED FOR CLEANING THE AGRICULTURAL CROPS SEEDS

/

UTILIZAREA PROGRAMULUI LABVIEW PENTRU ACHIZIŢIA ŞI PRELUCRAREA VIBRAŢIILOR UNEI SITE CONICE OSCILANTE CU AX VERTICAL

PhD. Eng. Stoica D.[1)], Prof. PhD. Eng. Voicu Gh.[1)], Lect. PhD. Eng. Covaliu C.[1)], PhD. Eng. Vlăduţ V.[2)]
[1)]University POLITEHNICA of Bucharest / Romania [2)]INMA Bucharest / Romania
Tel: 0724917143; E-mail: dorelstc@yahoo.com

Abstract: *There were performed experimental researches on vibration of a conical sieve with vertical axle equiangularly suspended by three thin elastic cables both at upper and lower part. The sieve driving was made by a driving mechanism with oscillating slide way through a connecting arm rigidly fixed at conical sieve edge and spherically articulated at the mechanism rod. The paper presents the components of acquisition program and describes the vibrations parameters for several geometrical and functional variants of driving mechanism. Results presented and utilization method of LabView program can be a model for the researchers studying vibrations of equipment working surfaces from agriculture and food industry.*

Keywords: *cone-shaped sieve, oscillating movement, Labview program*

INTRODUCTION

Driving sieves used for cleaning the agricultural crop seeds can be performed with different mechanisms, of rod-handle type, eccentric, or vibrating motors with balance weight type.

Therefore, the separating surface vibrating movement is transmitted to particles of material, which gives a certain state of sieving process, able to achieve the passage of small particles through sieve holes.

A sieve with an external conical separating surface, suspended in three equidistant points both at upper and bottom part, with elastic metallic cables, was used for cleaning the rape seeds of big foreign bodies.

The sieve driving mechanism was designed so that it mainly ensures a circular alternative movement with a certain amplitude, measured at the edge of the sieve, from one hand, and from the other- the neutral oscillation position in which the connecting of the length is fixed to operating mechanism (of swinging saw type).

The driving mechanism is made of an electric engine of alternative current of 710 W and a driving system of worm type-spiral wheel with oscillating slideway(3, 3^{I}, 6, 8 fig.1), with acting button placed eccentrically on spiral wheel of mechanism transmission, [1, 2].

The lift of oscillating slideway of driving system is of 16 mm, the slideway arm 3^{I} being articulated by a spherical joint to arm 7 fixed with sieve 1, placed in radial direction to cone base cercle. The experimental stand is endowed with a system of regulating the oscillating movement parameters, namely the oscillation frequency, F and oscillation amplitude, A_i.

The oscillation frequency can be modified from electric engine by varying the electric current parameters, and oscillation amplitude can be modified by changing the arrangement position of driving mechanism comparing to sieve radial arm, articulated between them by spherical articulation 6, (fig.1).

Rezumat: *Au fost realizate cercetări experimentale privind vibraţia unei site conice cu ax vertical suspendată echiunghiular a trei cabluri elastice subţiri atât de la partea de sus cât şi la partea de jos. Acţionarea sitei s-a făcut cu un mecansim de acţionare cu culisă oscilantă printr-un braţ de legătură fixat rigid de marginea sitei conice şi articulat sferic la biela mecanismului. În lucrare se prezintă componentele programului de achiziţie şi se descriu parametrii vibraţiilor pentru mai multe variante geometrico-funcţionale ale mecanismului de acţionare. Rezultatele prezentate şi modul de utilizare a programului Labview pot fi luate ca model de alţi cercetători ai vibraţiilor suprafeţelor de lucru ale utilajelor din agricultură şi industria alimentară.*

Cuvinte cheie: *sită conică, mişcare oscilantă, programul Labview*

INTRODUCERE

Acţionarea sitelor utilizate la curăţirea seminţelor culturilor agricole se poate realiza cu mecanisme din cele mai diverse, de tip bielă-manivelă, de tip excentric, motoare vibratoare cu contragreutăţi, etc.

Astfel mişcarea vibratorie a suprafeţelor de separare se transmite particulelor de material, ceea ce imprimă o anumită stare de cernere materialului capabilă să realizeze trecerea particulelor mici prin orificiile sitei.

O sită cu suprafaţă de separare conică exterioară, suspendată în trei puncte echidistante, atât la partea de sus, cât şi la partea de jos, cu cabluri metalice elastice flexibile, a fost utilizată la curăţirea seminţelor de rapiţă de corpuri străine mari.

Mecanismul de acţionare al sitei a fost astfel conceput încât să asigure în principal o mişcare circulară alternativă cu o anumită amplitudine, măsurată la marginea sitei conice, de o parte şi de cealaltă a poziţiei neutre de oscilaţie în care este fixat un braţ de legătură de lungime d, la mecanismul de acţionare (de tip ferăstrău pendular).

Mecanismul de acţionare este compus dintr-un motor electric de curent alternativ cu puterea de 710 W şi un sistem de acţionare de tip melc roată melcată cu culisă oscilantă, (3, 3^{I}, 6, 8 fig.1) cu butonul de acţionare dispus excentric pe roata melcată a transmisiei mecanismului, [1, 2].

Cursa culisei oscilante a sistemului de acţionare este de 16 mm, braţul culisei 3^{I} fiind articulat printr-o articulaţie sferică la braţul 7 rigidizat cu sita 1 dispus pe direcţie radială la cercul de bază al conului. Standul experimental este prevăzut cu posibilitatea reglării parametrilor mişcării oscilante, şi anume a frecvenţei de oscilaţie, F şi a amplitudinii oscilaţiei, A_i.

Frecvenţa de oscilaţie se poate modifica de la motorul electric prin variaţia parametrilor curentului electric, iar amplitudinea oscilaţiei se poate modifica prin schimbarea poziţiei de dispunere a mecanismului de acţionare în raport cu braţul radial al sitei, articulate între ele prin articulaţia sferică 6, (fig.1).

MATERIAL AND METHOD

Sieve movement is limited by metallic cables elasticity, which do not seem to be extendible, but due to their very small displacements, the movement can be considered mostly oscillating around sieve central axle.

Therefore, for experimental researches of vibrations and process have been used oscillating frequencies of 250, 520, 790 osc/min and amplitudes (3.58; 3.74; 3.91; 4.10 mm), by modifying the distance *d* at values 480, 460, 440 and 420 mm.

By eccentric tangential layout of arm joint of driving mechanism to cone-shaped sieve, it performs approx. circular oscillations, related to cone vertical axle.

MATERIAL ŞI METODĂ

Deplasarea sitei este restricţionată de elasticitatea cablurilor metalice, care par inextensibile, dar datorită deplasărilor foarte mici ale acestora mişcarea poate fi considerată preponderent oscilantă în jurul axei centrale a sitei.

Pentru cercetările experimentale de vibraţii şi de proces au fost utilizate frecvenţe de oscilaţie de 250, 520, 790 osc/min şi amplitudinile (3,58; 3,74; 3,91; 4,10 mm), prin modificarea distanţei *d* la valorile 480, 460, 440 şi 420 mm.

Prin dispunerea excentrică, tangenţială a articulaţiei braţului mecanismului de acţionare la sita conică, aceasta realizează oscilaţii aproximativ circulare faţă de axa verticală a conului.

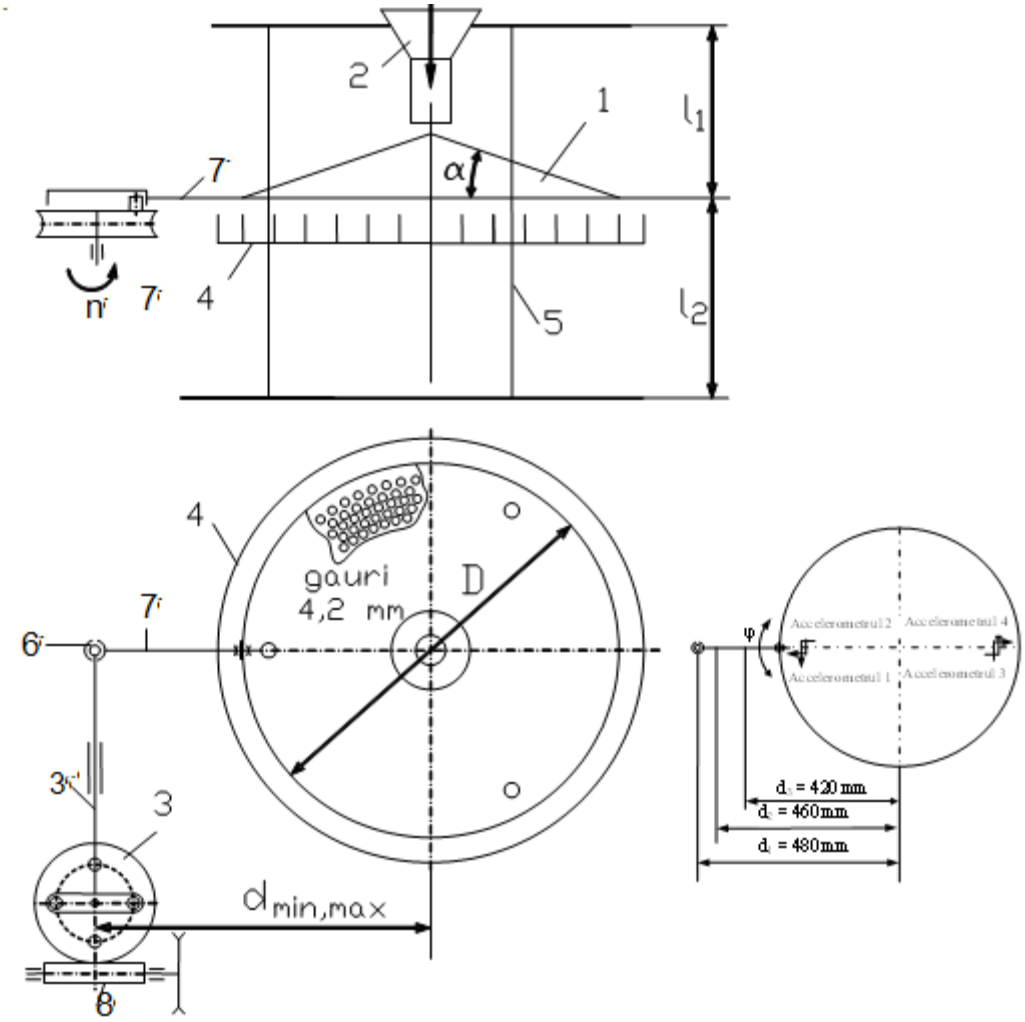

Fig. 1 – Scheme of experimental stand with suspended conical sieve [6]

1. conical sieve with circular holes; 2.supplying hopper; 3.driving mechanism with spiral wheel and oscillating slideway; 3'.arm of oscillating slideway; 4.collecting box of separated material; 5.metalic suspension cables; 6.spherical joint; 7.radial connecting arm to sieve driving mechanism, 8.worm pinion

For performing the experimental vibrations determinations, a measuring chain comprising the following devices, was used:

1) National Instruments data acquisition system with the following characteristics:
- 24 –bit resolution
- sampling rate of 50 kS/s,
- 4 simultaneous analogous input channels, dynamic domain 102 dB, input domain +/- 5 V
- USB 2.0 interface for computer connecting

2) four accelerometers Brüel & Kjær 4508B with magnetic fixing system and by metallic clamp, each with magnetic connecting fixing cable;

Pentru efectuarea determinărilor de vibraţii experimentale s-a utilizat un lanţ de măsură compus din următoarele dispozitive:

1) placă de achiziţie de date Naţional Instruments având următoarele caracteristici:
- rezoluţie de 24 biţi
- rată de eşantionare de 50 kS/s,
- 4 canale simultane de input analog, domeniu dinamic 102 dB, domeniu de input +/- 5 V
- interfaţă USB 2.0 pentru conectare la calculator

2) patru accelerometre Brüel & Kjær 4508B cu sistem de fixare magnetic şi prin clemă metalică, fiecare cu cablu de conectare, de fixare magnetic;

3) computer with Labview data acquisition and processing;

For performing the measurements, the 4 accelerometers used were placed two by two, diametrically opposed to sieve centre, able to determine the vibrations both on tangential direction and radial direction.(fig.1)

Mounting scheme corresponds to specialty literature indications related to acquisition of vibration signals of circular oscillating surfaces. [4, 5].

Accelerometers 2 and 4 have the possibility to determine the parameters of vibrations comparing to radial direction from cone base (sieve), while the accelerometers 1 and 3 can determine vibration parameters according to tangential direction.

In figure 2 is shown the block scheme of measuring chain used for determining variations of accelerations and speed measured by the 4 accelerometers, respectively the signal spectra.

3) calculator cu soft de achiziţie şi prelucrare de date Labview;

Pentru realizarea măsurătorilor cele 4 accelerometre folosite au fost amplasate două câte două diametral opus faţă de centrul sitei având posibilitatea determinării vibraţiilor atât pe direcţie tangenţială, cât şi pe direcţie radială, (fig.1).

Schema de montare corespunde cu indicaţiile din literatura privind achiziţia semnalelor de vibraţii ale suprafeţelor cu mişcare oscilantă circulară, [4, 5].

Accelerometrele 2 şi 4 au posibilitatea determinării parametrilor vibraţiilor după direcţia radială la baza conului (sitei), în timp ce accelerometrele 1 şi 3 au posibilitatea determinării parametrilor vibraţiei după direcţie tangenţială.

În figura 2 este prezentată schema bloc a lanţului de măsură utilizat pentru determinarea variaţiilor acceleraţiilor şi vitezelor măsurate de cele patru accelerometre, respectiv spectrele de semnal.

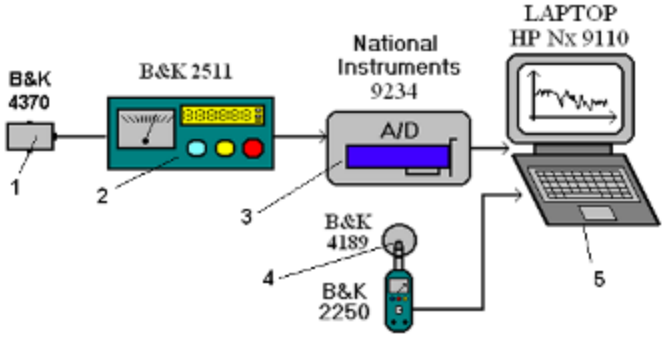

Fig. 2 – Block scheme of measuring chain used to experimental determinations [6]

It comprises the vibration transducers (1), located two by two diametrically opposed, on the separating surface of sieve with oscillating movement, the signal amplifier (2), National Instruments acquisition system (3), for acquiring the vibration signals from the 4 transducers and laptop (5), for processing the data acquired.

In order to trace the acquired signals, a printer which may be connected to laptop (5), can be also used.

Processing the experimental data was achieved with Labview program. Signals acquired were processed and transformed into acceleration units (m/s^2), for being integrated in order to obtain the speed values of sieve points on the sieve where transducers were placed.

In fig. 3 is shown the structure of LabView written program for processing the signals acquired by the four accelerometers.

Block “Read From Measurament File” (fig.3) represents the data acquisition board, the signal registered by the four accelerometers being cached by it.

Blocks "Simulate Signal" are introduced for generating four steady signals (one for each accelerometer), necessary to correct the errors introduced by accelerometers: when nothing is measured, accelerometers still indicate a constant small acceleration but other than zero (noted with a_0)

As a result, for each signal measured, a constant signal equal to „$-a_0$”, is generated, which is added to measured signal, for restoring zero value.

After registering the signal in data acquisition board and corrected in "Simulate Signal" blocks, it was multiplied by 9.81 - gravity acceleration.

Multiplication by 9.81 is performed because the signal acquired is measured in g units (gravity acceleration), and

Aceasta cuprinde traductoarele de vibraţii (1), amplasate două câte două diametral opus, pe suprafaţa de separare a sitei cu mişcare oscilantă, amplificatorul de semnal (2), placa de achiziţie de date Naţional Instruments (3), pentru achiziţia semnalelor de vibraţii de la cele patru traductoare, şi calculatorul laptop (5), pentru prelucrarea datelor achiziţionate.

În vederea trasării semnalelor achiziţionate se poate utiliza şi o imprimantă ce poate fi conectată la calculatorul laptop (5).

Prelucrarea datelor experimentale s-a realizat cu programul Labview. Semnalele achiziţionate au fost prelucrate şi transformate în unităţi de acceleraţie (m/s^2), care apoi au fost integrate în vederea obţinerii valorilor vitezelor punctelor de pe sită în care au fost amplasate traductoarele.

În fig. 3 este prezentată structura programului scris sub LabView pentru prelucrarea semnalelor achiziţionate de către cele patru accelerometre.

Blocul “Read From Measurament File” (fig.3) reprezintă placa de achiziţie de date, semnalul înregistrat de cele patru accelerometre fiind captat de acesta.

Blocurile "Simulate Signal" sunt introduse pentru a genera patru semnale constante (câte unul pentru fiecare accelerometru), necesare pentru a corecta erorile pe care le introduc accelerometrele: când nu se măsoară nimic, accelerometrele indică totuşi o acceleraţie constantă, mică, dar diferită de 0 (notată a_0).

Drept urmare, pentru fiecare semnal măsurat, se generează un semnal constant, egal cu „$-a_0$”, care se adună la semnalul măsurat, pentru a restabili valoarea zero.

După ce semnalul a fost înregistrat în placa de achiziţie de date şi corectat în blocurile "Simulate Signal" s-a multiplicat cu 9,81, acceleraţia gravitaţională.

Înmulţirea cu 9,81 este efectuată pentru că semnalul achiziţionat este măsurat în unităţi de g (acceleraţia

in subsequent processing, it should be expressed in S.I. (m/s^2) units, [7].

FFT (Fast Fourier Transform) function from program structure calculates and displays the signal spectrum.

For each of four accelerometers a FFT block is used, so four signals.

Frequencies and amplitudes of harmonic components (of Acosωt or Asinωt type which the periodic signal is made of) are obtained by means of spectra.

These frequencies and amplitudes give information on oscillating (vibrating) system movement, in this case on suspended conical oscillating sieve movement.

gravitaţională), iar în prelucrările ulterioare este nevoie ca el să fie exprimat în unităţi S.I. (m/s^2), [7].

Funcţia FFT (Fast Fourier Transform) din structura de program calculează şi afişează spectrul semnalului.

Pentru fiecare din cele patru accelerometre se utilizează câte un bloc FFT, deci patru semnale.

Frecvenţele şi amplitudinile componentelor armonice (de tip Acosωt sau Asinωt din care se compune semnalul periodic) se obţine cu ajutorul spectrelor.

Aceste frecvenţe şi amplitudini dau informaţii despre mişcarea sistemului oscilant (vibrator), în cazul de faţă despre mişcarea sitei conice oscilante suspendate.

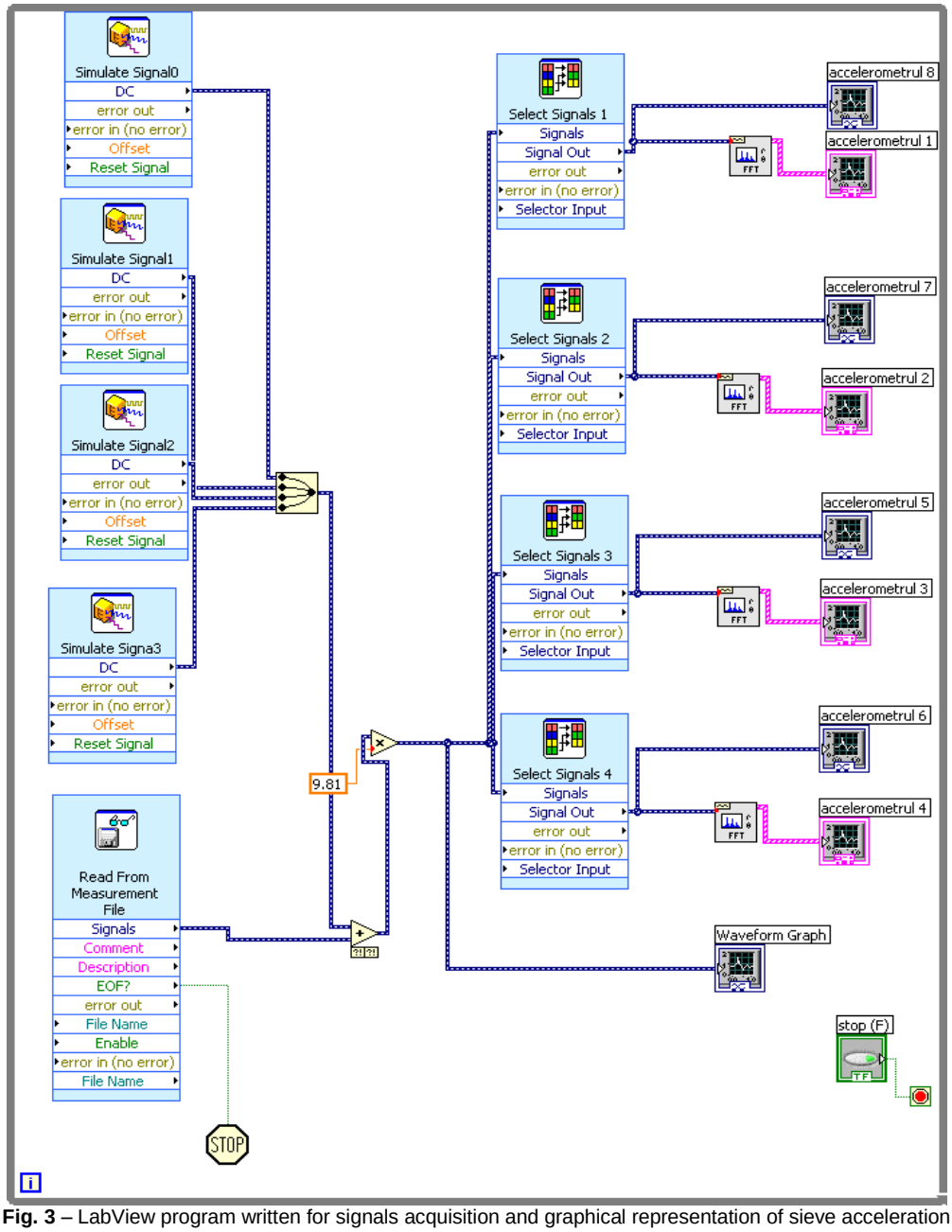

Fig. 3 – LabView program written for signals acquisition and graphical representation of sieve acceleration

Data measured are generally affected by different types of errors, determined by causes such as: apparatus calibration (sensors, acquisition board etc); numerical processing methods (numerical integral, decimal number truncating etc).

Such errors determine periodical phenomena that lead to measured periodical signals, but which are displaced comparing to zero line (fig.4.a), or even non periodical signals (fig.5.a). Therefore, appears the necessity of

Datele măsurate sunt în general afectate de diferitele tipuri de erori, datorate unor cauze precum: etalonarea aparatelor (senzori, placă de achiziţie etc); metode de prelucrare numerică (integrală numerică, trunchiere a numerelor cu zecimale etc).

Astfel de erori fac ca fenomene periodice să conducă la semnale măsurate periodice, dar deplasate faţă de linia de zero (fig.4.a), sau chiar neperiodice (fig.5.a). Drept urmare, apare necesitatea corectării valorilor măsurate,

correcting the measured values, by repositioning comparing to zero line (fig. 4.b) or by tilting the middle line (fig.5.b).

Correction of „0" degree, aims to place again the measured data related to zero line.

Data measured are replaced by data corrected:

prin repoziţionarea faţă de linia zero (fig. 4.b) sau prin înclinarea liniei de mijloc (fig.5.b).

Corecţia de gradul „0", vizează repoziţionarea datelor măsurate în raport cu linia de zero.

Datele măsurate sunt înlocuite cu cele corectate:

$$y_{mas} \leftarrow y_{cor} = y_{mas} - a \tag{1}$$

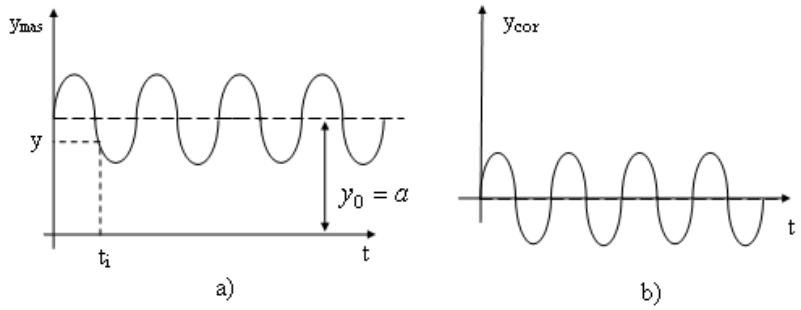

Fig. 4 –Example regarding the correction of „0" degree [2, 3]

Value of correction parameter is determined from the condition of minimizing the average square meter error [5]:

Valoarea parametrului de corecţie *a* se determină din condiţia de minimizare a erorii pătratice medii [5]:

$$\varepsilon(a) = \sum_{i=1}^{n} (y_i - a)^2 \tag{2}$$

This condition is equal to derivative annulation

Această condiţie echivalează cu anularea derivatei

$$\frac{d\varepsilon}{da} = 0 \tag{3}$$

From where, the correction parameter results

De unde rezultă parametrul de corecţie

$$a = \frac{\sum_{i=1}^{n} y_i}{n} \tag{4}$$

Correction of „1"degree

Correction of „1" degree aims to „make the horizontal the middle line. Data measured are replaced by the corrected ones:

Corecţia de gradul „1"

Corecţia de gradul „1" vizează „orizontalizarea" liniei de mijloc. Datele măsurate sunt înlocuite cu cele corectate:

$$y_{mas} \leftarrow y_{cor} = y_{mas} - at - b \tag{5}$$

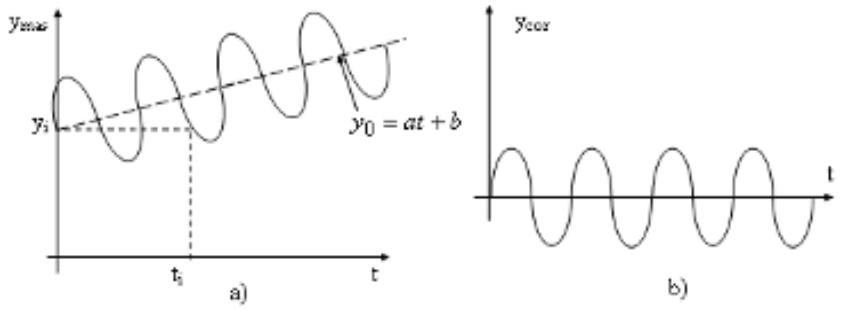

Fig. 5 – Example regarding correction of „1"degree

Values of correction parameters *a* and *b* are determined from condition of minimizing the average square meter error

Valorile parametrilor de corecţie *a* şi *b* se determină din condiţia de minimizare a erorii pătratice medii

$$\varepsilon(a,b) = \sum_{i=1}^{n} (y_i - at_i - b)^2 \tag{6}$$

This condition is equivalent to annulations of partial derivatives

Această condiţie echivalează cu anularea derivatelor parţiale

$$\frac{\partial \varepsilon}{\partial a} = 0 \; ; \; \frac{\partial \varepsilon}{\partial b} = 0 \tag{7}$$

The correction parameters are obtained

Se obţin parametrii de corecţie

$$a = \frac{\sum_{i=1}^{n} t_i \sum_{i=1}^{n} y_i - n \sum_{i=1}^{n} t_i y_i}{\left[\left(\sum_{i=1}^{n} t_i \right)^2 - n \sum_{i=1}^{n} t_i^2 \right]} \; , \; b = \frac{\sum_{i=1}^{n} t_i \sum_{i=1}^{n} t_i y_i - \sum_{i=1}^{n} t_i^2 \sum_{i=1}^{n} y_i}{\left[\left(\sum_{i=1}^{n} t_i \right)^2 - n \sum_{i=1}^{n} t_i^2 \right]} \tag{8}$$

In fig 6, are presented the signals and spectra appropriate to four accelerometers mounted on cone-shaped sieve surface

În fig 6, sunt prezentate semnalele şi spectrele de vibraţii corespunzătoare celor patru accelerometre montate pe suprafaţa sitei conice

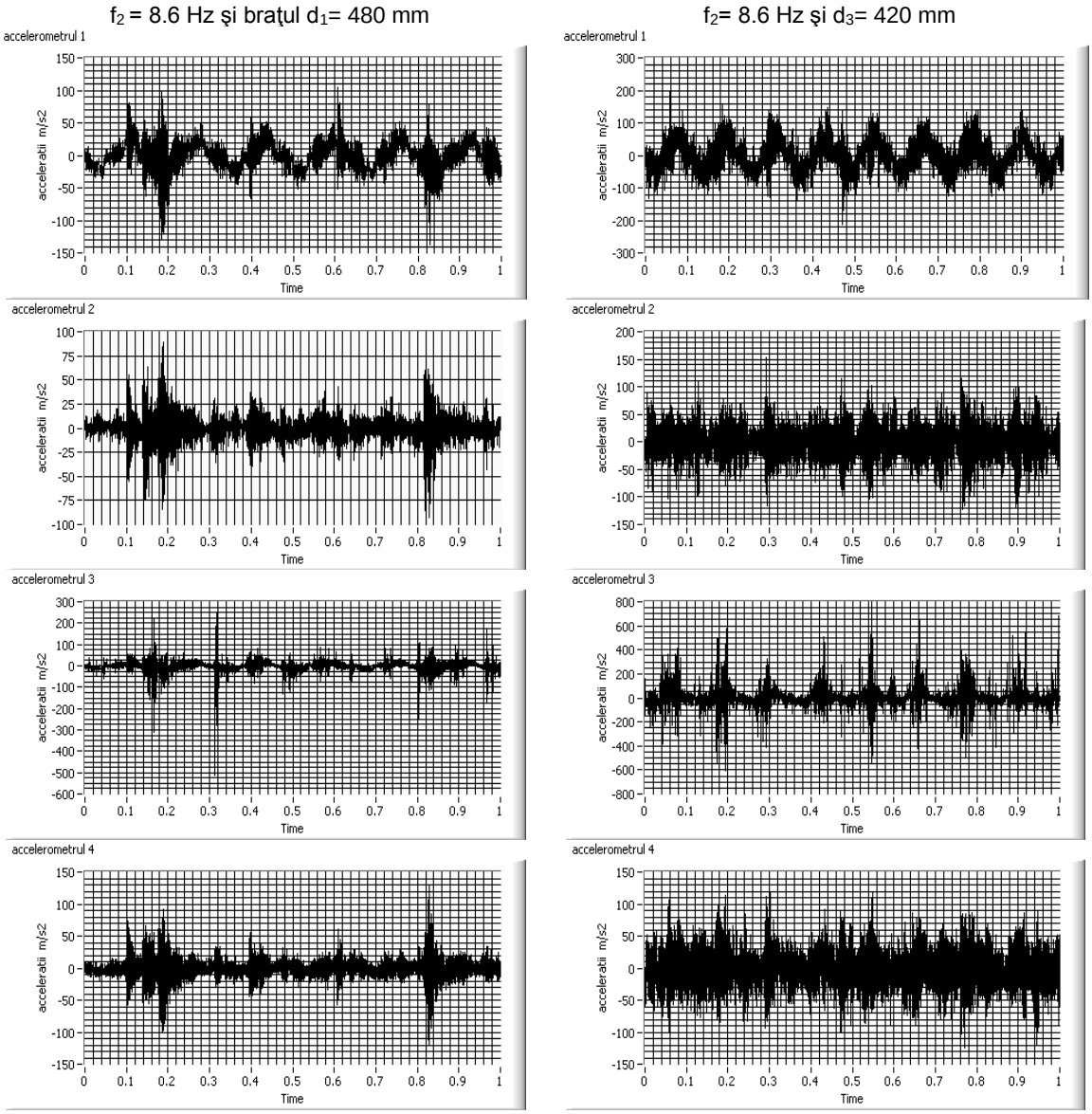

Fig. 6 - Vibration spectra corresponding to four accelerometers for 8.6 frequency and two length of sieve arm

Application example

By means of acquisition system achieved and Labview written program, vibration signals were acquired at the four accelerometers, placed on sieve separation surface.

Exemplu de aplicaţie

Cu ajutorul sistemului de achiziţie realizat şi a programului realizat în Labview, au fost achiziţionate semnale de vibraţii, la cele patru accelerometre, poziţionate pe suprafaţa de

Two accelerometers acquire the signal on arm direction, and the other two on a direction perpendicular to arm connected to driving mechanism rod.

Determinations for no-load run have been performed for oscillation frequency of f_2=8.6 Hz, for three different lengths of sieve arm, while the determinations for load run have been made with rape seeds for three oscillating frequencies (f_1 = 4.1 Hz, f_2 = 8.6 Hz, f_3 = 13.1 Hz) and three different lengths of sieve arm (d_1 = 480 mm, d_2 = 460 mm, d_3 = 420 mm).

Based on analysis of acceleration signal acquired and shown in fig 6, the oscillation sinusoidal variation for the four accelerometers is found out. The variation can be very well noticed at accelerometer 1 mounted near the sieve arm, which gets the signal on tangential direction (perpendicular on oscillating average position direction of sieve arm).

For no-load running, the amplitude of signal acquired at the oscillating frequency of f_2=8.6 Hz, is inversely proportional, as value, to length of sieve arm d. Thus, at accelerometer 1, the oscillation acceleration reaches maximum values, of 100 m/s^2, the general oscillation being of sinusoidal type with minimum disturbances related to elastic suspension system and sieve own vibration.

The bigger the arm's length is, the smaller will be the sieve acceleration size, reaching values under 50 m/s^2 at an arm's length of 480 mm, but with more profound disturbing vibrations superposed on the general oscillation.

At accelerometer 3, which acquires the signal always on tangential direction (perpendicular to sieve arm) placed at a bigger distance comparing to operating point, the general oscillation, even though of sinusoidal type, is not anymore so evident as at accelerometer 1, being much more flatten, but also in this very case, the oscillation acceleration size decreases with sieve's arm length increment from average values of approx.100 m/s^2 to values under 50 m/s^2, for an arm's length of 420 mm.

It has been also found out the existence of oscillations determined by other factors than the oscillation printed on driving mechanism.

At accelerometers 2 and 4 acquiring the signal on radial direction (namely, in parallel with sieve's arm) placed at about the same distance from the operating point, the general sinusoidal oscillations are not so visible as at accelerometers 1 and 3, and disturbing vibrations are stronger.

But, it has been noticed the same tendency of reducing the sieve oscillation acceleration size along with arm's length increasing, namely diminishing the sieve movement amplitude.

CONCLUSIONS

For the sieve presented, with suspension wires length of 240 mm on top and 180 mm under the sieving surface, with sieve diameter of 410 mm and a tilting cone generator to horizontal surface of 8^o, the acceleration of sieve had values of $\pm 150 m/s^2$ for the arm connected to the driving mechanism of d=480 mm. When the arm's length d decreases, the sieve accelerations are modified, reaching values of $\pm 300 m/s^2$ on tangential direction and $\pm 200 m/s^2$ on radial direction, which demonstrates a better movement on tangential direction and a quicker falling of seeds.

The oscillating movement of separating surfaces is characterized by its basic parameters: oscillations frequency and amplitude; at the same time, other parameters related to the process and material features have to be taken into account: sieves tilting angle,

separare a sitei. Două accelerometre achiziţionează semnalul pe direcţia braţului, iar celelalte două, pe o direcţie perpendiculară pe braţul de legătură cu tija mecanismul de acţionare.

Determinările la mersul în gol au fost efectuate numai pentru frecvenţa de oscilaţie f_2=8,6 Hz, la trei lungimi diferite ale braţului sitei, în timp ce determinările la mersul în sarcină au fost efectuate cu seminţe de rapiţă pentru trei frecvenţe de oscilaţie (f_1 = 4,1 Hz, f_2 = 8,6 Hz, f_3 = 13,1 Hz) şi trei lungimi diferite ale braţului sitei (d_1 = 480 mm, d_2 = 460 mm, d_3 = 420 mm).

Pe baza analizei semnalelor de acceleraţie achiziţionate şi prezentate în fig 6, se constată variaţia sinusoidală a oscilaţiilor pentru cele patru accelerometre. Aceasta este profund vizibilă la accelerometrul 1 montat în apropierea braţului sitei care achiziţionează semnal pe direcţie tangenţială (perpendiculară pe direcţia poziţiei medii de oscilaţie a braţului sitei).

Pentru mersul în gol, amplitudinea semnalului achiziţionat, la frecvenţa de oscilaţie f_2=8,6 Hz, este invers proporţională, ca valoare, cu lungimea braţului sitei d. Astfel la accelerometrul 1, mărimea acceleraţiei oscilaţiei atinge valori maxime, de ordinul a 100 m/s^2, oscilaţia generală fiind de tip sinusoidal cu perturbaţii minore legate de sistemul elastic de suspendare şi vibraţia proprie a sitei.

Cu cât lungimea braţului creşte, cu atât mărimea acceleraţiei sitei scade, până la valori sub 50 m/s^2 la o lungime a braţului de 480 mm, dar cu mai profunde vibraţii perturbatoare suprapuse peste oscilaţia generală.

La accelerometrul 3, care achiziţionează semnalul tot de pe direcţia tangenţială (perpendiculară pe braţul sitei) aflat însă la o distanţă mai mare faţă de punctul de acţionare, oscilaţia generală, deşi este evident de tip sinusoidal, nu mai este la fel de pronunţată ca la accelerometrul 1, fiind mult mai aplatizată, dar şi în acest caz, mărimea acceleraţiei oscilaţiei, descreşte cu creşterea lungimii braţului sitei, de la valori medii de circa 100 m/s^2 la valori sub 50 m/s^2, pentru o lungime a braţului de 420 mm.

Se constată, de asemenea, existenţa oscilaţiilor perturbatoare cauzate de alţi factori decât oscilaţia imprimată de mecanismul de acţionare.

La accelerometrele 2 şi 4 care achiziţionează semnal pe direcţie radială (adică paralel cu braţul sitei) aflate, aproximativ la aceeaşi distanţă faţă de punctul de acţionare, oscilaţiile sinusoidale generale nu mai sunt aşa de vizibile, ca la accelerometrele 1 şi 3, iar vibraţiile perturbatoare sunt mult mai pronunţate.

Se constată, însă, aceeaşi tendinţă de scădere, a mărimea acceleraţiei oscilaţiei sitei, cu creşterea lungimii braţului, adică cu scăderea amplitudinii deplasărilor sitei.

CONCLUZII

Pentru sita prezentată, cu lungimi ale firelor de suspendare de 240 mm deasupra şi 180 mm sub suprafaţa de cernere, cu diametrul sitei de 410 mm şi o înclinarea a generatoarei conului faţă de suprafaţa orizontală de 8^o, acceleraţia sitei a avut valori de $\pm 150 m/s^2$ pentru un braţ de legătură cu mecanismul de acţionare de d=480 mm. În situaţia în care lungimea braţului d scade, acceleraţiile sitei se modifică la valori de $\pm 300 m/s^2$ pe direcţie tangenţială şi la valori de $\pm 200 m/s^2$ pe direcţie radială, ceea ce arată o mişcare mai bună pe direcţie tangenţială şi o cădere mai rapidă a seminţelor.

Mişcarea oscilatorie a suprafeţelor de separare este caracterizată prin parametri săi de bază: frecvenţa oscilaţiilor şi amplitudinea oscilaţiei; trebuie avuţi în vedere şi alţi parametri care ţin atât de proces, cât şi de caracteristicile materialului ce trebuie prelucrat : unghiul

friction coefficients, optimum sieving speed and limit speed imposed by passing through sieves, particles interactions with sieving surfaces, processing power consumption, dimensions and shape of separating holes.

In order to avoid the inefficient sieving areas, restrictions related to sieve binding or a symmetrical driving system, should be introduced. There is also the possibility of operating by means of a generator of vibrations with non-balanced masses, which should be placed on symmetry axle of sieve.

REFERENCES

[1]. Bratu P., (2000) – *Vibrations of elastic systems*, Technical Publishing House, Bucharest;
[2]. Ion C., Crăifăleanu A., (2002) – *Dynamics and analytical mechanics syntheses*, Matrix-Rom Publishing, Bucharest;
[3]. Magheţi I., Voiculescu L., (2000) – *Elements of applied mechanics*, Printech Publishing, Bucharest;
[4]. Munteanu M., (1969) – *Some problems related to vibrating mono-mass sieves dynamics, driven by eccentric flywheel,* Machinery manufacturing, vol. 21 (1);
[5]. Segărceanu M., Căsăndroiu T. (1968) - *Contributions to seeds movement on plane sieves surface*, Studies and researches of agricultural mechanics Journal, vol II (4);
[6]. Stoica D., (2011) - *Contributions to vibrating phenomena study regarding the equipment of processing agricultural products*, Ph.D. Thesis, U.P.B.;
[7]. Voinea R., Voiculescu D., (1979) – *Mechanical vibrations,* I.P. Bucharest.

de înclinare a sitelor, coeficienţii de frecare, viteza optimă de cernere şi viteze limită impuse de trecerea prin site, interacţiunile dintre particule, interacţiunile cu suprafeţele de cernere, consumul energetic la prelucrare, dimensiunile şi forma orificiilor de separare.

Pentru a evita zonele cu cernere ineficientă, ar trebui, cumva introduse restricţii în ceea ce priveşte legarea sitei sau o acţionare simetrică. Există, de asemenea, posibilitatea acţionării cu ajutorul unui generator de vibraţii cu mase neechilibrate care să fie plasat pe axa de simetrie a sitei.

BIBLIOGRAFIE

[1]. Bratu P., (2000) – *Vibraţiile sistemelor elastice*, Editura Tehnică, Bucureşti;
[2]. Ion C., Crăifăleanu A., (2002) – *Sinteze de dinamică şi mecanică analitică*, Editura Matrix-Rom, Bucureşti;
[3]. Magheţi I., Voiculescu L. (2000) – *Elemente de mecanică aplicată,* Editura Printech, Bucureşti;
[4]. Munteanu M., (1969) - *Unele probleme ale dinamicii sitelor vibratoare monomasice acţionate prin volant excentric*, Construcţia de maşini, vol. 21 (1);
[5]. Segărceanu M., Căsăndroiu T., (1968) – *Contribuţii la studiul mişcării seminţelor pe suprafaţa sitelor plane*, Revista - Studii şi cercetări de mecanică agricolă, vol.II(4);
[6]. Stoica D., (2011) - *Contribuţii la studiul fenomenelor vibratorii privind utilajele din domeniul prelucrării produselor agricole*, Teza de doctorat, U.P.B.;
[7]. Voinea R., Voiculescu D., (1979) - *Vibraţii mecanice*; I.P. Bucureşti.

THEORETICAL RESEARCH ON DETERMINING THE VIBRATIONS ISOLATION DEGREE OF A VIBRATING SEPARATOR
/
CERCETĂRI TEORETICE PRIVIND DETERMINAREA GRADULUI DE IZOLARE A VIBRAȚIILOR PENTRU UN SEPARATOR VIBRATOR

Ph.D.Stud. Eng. Ivancu B.[1)], Prof. PhD. Eng. Voicu Gh.[2)], PhD. Eng. Brăcăcescu C.[1)], PhD.Stud. Eng. Persu C.[1)], PhD.Stud. Eng. Zaica Al.[1)]
[1)] INMA Bucharest / Romania; [2)] University Politehnica of Bucharest
Tel: 0758331415; E-mail: ivancu_bogdan@yahoo.com

Abstract: *Mechanical vibrations occur in any system where there are motors for driving mechanisms or inertial elements elastically supported. The presence of mechanical vibrations is generally harmful because of their effects. Depending on the complexity of the machine, characterized by the distribution of weight and flexible system configuration, the parameters of vibration isolation can be determined only on the basis of a model able to reproduce the dynamic behavior of the machine. This paper presents the scheme for calculating the parameters of vibration isolation from a vibrating separator equipped with metal elastic elements.*

Keywords: *degree of isolation, vibration, calculation scheme, elastic element, vibrating separator*

INTRODUCTION

The vibrations analysis of mechanical systems is necessary to determine the causes of their occurrence, the ways to reduce the absorbed energy, or to control the vibration and reduce noise. The failure or breakage phenomena of elastic systems made from different materials are very complex and differ fundamentally from static cases to variable cases. Fatigue is strongly localized and occurs in areas of high stress and strain of various parts or structures.

In order to model and analyze properly a problem of fatigue, it should, previously, determine the sequences of variable stress that can produce - or not - damage to the structure. The protection against vibration increases the lifetime of vibrating equipment thus ensuring reduced costs for maintenance and repairs. A vibrating system consists of the actual structure to which distributed masses (according to a certain law) and / or concentrated masses, are attached. Any structure is capable, under the action of causes with dynamic character (time-varying), to perform relative movement around an equilibrium position. This phenomenon is due to the fact that the structure possesses inertial properties (concentrated and distributed masses) and elastic elements (defined by flexibility or stiffness). Using on larger scale of the equipment with vibratory motion in the milling industry is due to significant increase in productivity of sorting and separation process of impurities from the cereal seeds mass, from this category being part the vibrating separator for removing stones from cereal seeds mass (Figure 1).

The stone separator SP-00 is used to separate impurities from cereal seed mass, that combines the principle of separation based on the difference in specific weight (through the movement of vibration of sieve) and separation by their aerodynamic properties (through the action of air currents).

Rezumat: *Vibrațiile mecanice se produc în orice sistem acolo unde există motoare pentru acționarea mecanismelor sau elemente inerțiale sprijinite elastic. Prezența vibrațiilor mecanice este, în general, dăunătoare ca urmare a efectelor lor. Funcție de complexitatea mașinii, caracterizată de repartiția masei și de configurația sistemului elastic, parametrii de izolare a vibrațiilor pot fi determinați numai pe baza unui model capabil să reproducă comportarea dinamică a mașinii. În acest articol se prezintă schema de calcul a parametrilor de izolare a vibrațiilor de la un separator vibrator prevăzut cu elemente elastice metalice.*

Cuvinte cheie: *grad de izolare, vibrații, schemă de calcul, elemente elastice, separator vibrator*

INTRODUCERE

Analiza vibrațiilor sistemelor mecanice este necesară pentru a cunoaște cauzele producerii lor, modalitățile de a le diminua energia absorbită, sau pentru controlul vibrațiilor și reducerea zgomotului produs. Fenomenele de cedare sau rupere a sistemelor elastice, realizate din diferite materiale, sunt foarte complexe și diferă fundamental pentru cazul solicitărilor statice față de cele variabile. Oboseala este puternic localizată și se produce în zonele cu tensiuni și deformații mari ale diferitelor piese sau structuri.

Pentru a modela și analiza corect o problemă de oboseală, trebuie, în prealabil, determinate secvențele solicitărilor variabile care pot produce – sau nu – deteriorarea structurii prin oboseală. Protecția împotriva vibrațiilor mărește durata de viață pentru echipamentele vibratoare asigurând astfel reducerea costurilor pentru întreținere și reparații. Un sistem vibrant este constituit din structura propriu-zisă la care se atașează mase distribuite (după o anumită lege) și/sau mase concentrate. Orice structură este capabilă, sub acțiunea unor cauze cu caracter dinamic (variabile în timp), să efectueze mișcări relative în jurul unei poziții de echilibru. Acest fenomen se datorează faptului că structura posedă proprietăți inerțiale (mase concentrate și distribuite) și elastice (definite prin flexibilitate sau rigiditate). Utilizarea pe scară tot mai largă a echipamentelor cu acțiune vibratoare în domeniul morăritului se datorează creșterii semnificative a productivității proceselor de sortare și separare a impurităților din masa de semințe de cereale, din această categorie făcând parte și separatoarele vibratoare pentru eliminarea pietrelor din masa de cereale (Figura 1).

Separatorul de pietre SP–00 este utilizat la separarea impurităților din masa de cereale ce combină principiul de separare pe baza diferenței de greutate specifică (prin mișcarea de vibrație a sitei) și separarea după proprietățile aerodinamice ale acestora (prin acțiunea curenților de aer).

Fig. 1 – The stone separator SP-00

MATERIAL AND METHOD

Based on the analysis of structural and functional structure of the vibrating separator shown in Figure 1, it is therefore necessary to study the dynamic model of calculation. The vibrating separator, is modeled in Figure 2 to meet simultaneously, the technical performance (including the vibration parameters of work), and vibration isolation parameters of parts which need to be protected.

MATERIAL ŞI METODĂ

Pe baza analizei structurii constructive și funcționale a separatorului vibrator din Figura 1, rezultă necesitatea studierii modelului dinamic de calcul. Separatorul vibrator este modelat în Figura 2 pentru a satisface simultan, atât performanțele tehnice (inclusiv parametrii vibrațiilor de lucru), cât și parametrii izolării vibrațiilor părților ce trebuie protejate.

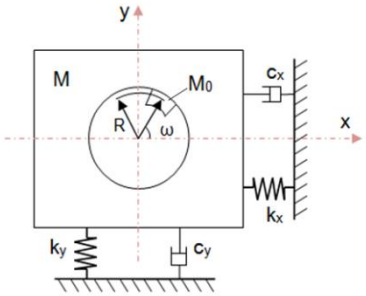

Fig. 2 – Dynamic model of vibratory separator [4]

Given the system in Figure 2, the differential equations of motion are [4]:

Dat fiind sistemul din figura 2, ecuațiile diferențiale ale mișcării sunt [4]:

$$\begin{cases} \dfrac{d^2x}{dt^2} + 2\cdot\eta_x\dfrac{dx}{dt} + p_x^2 x = \dfrac{M_0\cdot R\cdot\omega^2}{M+M_0}\cos\omega t \\ \dfrac{d^2y}{dt^2} + 2\cdot\eta_y\dfrac{dy}{dt} + p_y^2 y = \dfrac{M_0\cdot R\cdot\omega^2}{M+M_0}\sin\omega t \end{cases} \quad (1)$$

where, the damping factors have the expressions:

unde, factorii de amortizare au expresiile [4]:

$$\eta_x = \frac{c_x}{2(M+M_0)}; \eta_y = \frac{c_y}{2(M+M_0)} \quad (2)$$

and the system's own pulsations have the expressions:

iar pulsațiile proprii ale sistemului au expresiile [4]:

$$p_x = \sqrt{\frac{k_x}{M+M_0}}; p_y = \sqrt{\frac{k_y}{M+M_0}} \quad (3)$$

Because own vibration is damped down rather quickly in the transitional regime, in this case, it presents practical interest only the operating stationary regime (forced vibration). The solutions of equations (1) corresponding to stationary regime (forced vibration) have the form [4]:

Deoarece vibrația proprie se amortizează destul de rapid în cadrul regimului tranzitoriu, în cazul de față, prezintă interes practic numai regimul staționar de funcționare (vibrația forțată). Soluțiile ecuațiilor (1) corespunzătoare regimului staționar (vibrația forțată) au forma [4]:

$$\begin{cases} x = A_x\cdot\cos(\omega t - \varphi_x) \\ y = A_y\cdot\sin(\omega t - \varphi_y) \end{cases} \quad (4)$$

where the amplitudes of motion are:

unde amplitudinile mișcării sunt [4]:

$$\begin{cases} A_x = \dfrac{M_0 \cdot R}{M + M_0} A_{0x} \\ A_y = \dfrac{M_0 \cdot R}{M + M_0} A_{0y} \end{cases} \quad (5)$$

(A_{0x} and A_{0y} being the amplification factors and φ_x and φ_y the initial stages).

Vibrating separators work in stationary regime in post resonance ($\omega >> p$) passing under stationary regime through resonance (resonance pulsations are determined with relations (3)). Under the functioning conditions in post resonance regime (when damping system can be neglected), the amplitudes of motion are given by the relation [4]:

(A_{0x} și A_{0y} fiind factorii de amplificare, iar φ_x și φ_y fazele inițiale)

Separatoarele vibratoare, funcționează în regim staționar în postrezonanţă ($\omega >> p$) trecând, în cadrul regimului tranzitoriu, prin rezonanță (pulsațiile de rezonanță se determină cu relațiile (3)). În condițiile funcționării în regim de postrezonanţă (când amortizările în sistem se pot neglija), amplitudinile mișcării sunt date de relația [4]:

$$A_x = A_y = A = \frac{M_0 \cdot R}{M + M_0} \quad (6)$$

In the case of functioning regime in post resonance, the effect of damping being insignificant, in order to obtain vibrations of the sieve casing as circular trajectory, the elastic constants of the elastic system, by the two directions, should to be equal. So, in this case the value of k_y adopted equal to that of the k_x is given by [4]:

În cazul regimului de funcționare în postrezonanţă efectul amortizării fiind nesemnificativ, pentru a obține vibrații ale carcasei sitei după traiectorii circulare, trebuie ca constantele elastice ale sistemului elastic, după cele două direcții să fie egale. Deci în acest caz valoarea lui k_y adoptată egală cu cea a lui k_x este dată de relația [4]:

$$k_y = p_y^2 (M + M_0) \quad (7)$$

The parameters that determine the performance of vibration isolation are the transmissibility T and the degree of isolation of vibrations I. The two parameters are complementary, and the relation is: [1]

Parametrii care stabilesc performanțele de izolare a vibrațiilor sunt transmisibilitatea T a vibrațiilor și gradul de izolare I. Cei doi parametrii sunt complementari, iar relația de legătură este de forma: [1]

$$I = (1 - T) \cdot 100 \ [\%] \quad (8)$$

For a vibratory separator leaning against metal elastic elements, with small viscous damping, modeled as a system with one degree of freedom in vertical translation, the T parameter has the form: [1]

Pentru un separator vibrator rezemat pe elemente elastice metalice, cu amortizare vâscoasă mică, modelată ca un sistem cu un grad de libertate la translație verticală, parametrul T este de forma: [1]

$$T = \frac{F_{Tr}}{F_0} = \left[\frac{1 + (2 \cdot \zeta \cdot \Omega)^2}{(1 - \Omega^2)^2 + (2 \cdot \zeta \cdot \Omega)^2}\right]^{1/2} \quad (9)$$

where: F_{Tr} is the force transmitted through the elastic element of k constant and through viscous damping element; F_0 is the amplitude of the disturbing force; Ω is the report of pulsations, defined by the relation $\Omega = \omega / p$; ζ is a fraction of critical damping.

The variation of parameters T and I is given by the report of pulsations Ω and ζ parameter shown in Figure 3.

unde: F_{Tr} este forța transmisă prin elementul elastic de constantă k și prin elementul de amortizare vâscoasă; F_0 este amplitudinea forței perturbatoare; Ω este raportul pulsațiilor, definit de relația $\Omega = \omega/p$; ζ este fracțiunea din amortizarea critică.

Variația parametrilor T și I este dată funcție de raportul pulsațiilor Ω și de parametrul ζ în Figura 3.

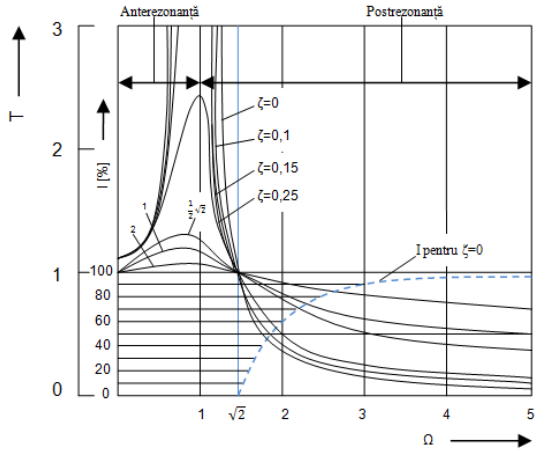

Fig. 3 – The variation of transmissibility T and degree of isolation I function of report of pulsation $\Omega = \omega / p$ and fraction of critical damping ζ / *Variația transmisibilității T și a gradului de izolare I funcție de raportul pulsațiilor $\Omega = \omega/p$ și a fracțiunii din amortizarea critică ζ [1]*

For design calculations, it is more convenient to use the static arrow due to the action of weight *m g*.

Thus, the own pulsation of the system can be expressed as [1]:

Pentru calculele de proiectare, este mai comod să se folosească săgeata statică datorită acțiunii greutății *m·g*. Astfel, pulsația proprie a sistemului poate fi exprimată sub forma [1]:

$$p = \sqrt{\frac{k \cdot g}{m \cdot g}} = \sqrt{\frac{g}{\frac{m \cdot g}{k}}} = \sqrt{\frac{g}{\delta_{st}}} \quad (10)$$

With the nomogram in Figure 4 can be determined the degree of isolation according to the static arrow and vibration frequency (the frequency of the disturbing force). In the nomogram field are plotted two types of oblique lines, the first line (dashed line) represents natural frequency of the system and the rest of lines (solid lines) represent the degree of vibration isolation.

Cu ajutorul nomogramei din Figura 4 se poate determina gradul de izolare, funcție de săgeata statică și frecvența vibrațiilor (frecvența forței perturbatoare). În câmpul nomogramei sunt trasate două categorii de linii oblice, prima linie oblică (linia întreruptă) reprezintă frecvența proprie a sistemului, iar restul liniilor (liniile continue) reprezintă gradul de izolare a vibrațiilor.

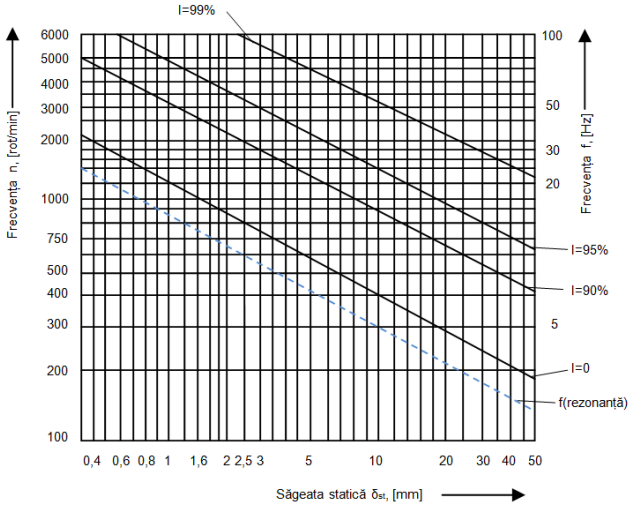

Fig. 4 – Nomogram for calculating the degree of isolation [1]

RESULTS

Based on the calculation scheme previously presented, we presented a calculation example for determining the degree of vibration isolation for a vibrating separator, in our case, SP-00. Because the determination of elastic constant of the entire system is more difficult to perform, in this example, we will determine the calculation of constant elasticity of elastic system of springs and used it in calculation example.

First of all it must be determined the spring constant of the coil springs system. According to STAS 12243/2-86, the coil spring, used in the construction of the vibrating separator SP-00, has the following dimensions:

- the spiral diameter d = 7 mm;
- the outer diameter of the winding, D = 50 mm;
- number of turns, n = 9.5.

Using relation (2) is determined the spring constant of a coil spring:

RESULTATE

Pe baza schemei de calcul prezentată anterior, am prezentat un exemplu de calcul pentru determinarea gradului de izolare al vibrațiilor pentru un separator vibrator, în cazul nostru, SP–00. Pentru că determinarea constantei elastice a întregului sistemului este mai dificil de efectuat, în acest exemplu de calcul vom determina constanta de elasticitate a sistemului elastic de arcuri și o vom folosi in exemplul de calcul.

Mai întâi, trebuie determinată constanta de elasticitate a sistemului de arcuri elicoidale. Conform STAS 12243/2 – 86, arcul elicoidal, folosit în construcția separatorului vibrator SP – 00, prezintă următoarele dimensiuni:

- diametrul spirei, d = 7 mm;
- diametrul exterior de înfășurare, D = 50 mm;
- numărul de spire, n = 9,5.

Cu ajutorul relației (2) se stabilește constanta elastică unui arc elicoidal:

$$k_1 = \frac{G \cdot d^4}{8 \cdot n \cdot D^2} = \frac{8100 \cdot 7^4}{8 \cdot 9{,}5 \cdot 50^2} = 2{,}05 \text{ [kgf/mm]} \quad (11)$$

$\rightarrow k = 4 \cdot k_1 = 8{,}2$ [kgf/mm] (elastic constant of coil springs system)

According to [3], the determined circular trajectory amplitude is $A_x = A_y = A = 2{,}5$ [mm], and frequency $\upsilon = 960$ [osc./min], $\rightarrow$ in accordance with (6), M_0 = 14 [kg], where the eccentricity R = 120 [mm].

$\rightarrow k = 4 \cdot k_1 = 8{,}2$ [kgf/mm] (constanta elastică a sistemului de arcuri elicoidale)

Conform [3], amplitudinea traiectoriei circulare determinată este $A_x = A_y = A = 2{,}5$ [mm], și frecvența $\upsilon = 960$ [oscil/min], $\rightarrow$ conform (6), M_0 = 14 [kg], unde excentricitatea R = 120 [mm].

The pulsation of oscillation, ω is: $\upsilon = 960$ [osc./min] $\rightarrow \omega = 960 \cdot 2 \cdot \pi = 100{,}53$ [s^{-1}]

The mass of the vibrating part of the separator (without the material load from the sieve, negligible compared to the mass vibrating system) is about 250 [kg], and the mass of generators vibration, M_0 = 14 [kg].

With the relation (7) $\rightarrow p = \sqrt{\frac{k}{M + M_0}} = 17{,}66$ [s^{-1}] $\rightarrow$ in accordance with (10), $\delta_{st} = \frac{g}{p^2} = 31{,}45$ [mm]

Using the static arrow of the coil spring, 31.45 [mm] and the frequency of oscillation of the stone separator, 960 [rot/min], the degree of isolation I of the generated vibrations can be identified in the nomograph of Figure 4.

Pulsaţia oscilaţiei, ω este: $\upsilon = 960$ [oscil/min] $\rightarrow \omega = 960 \cdot 2 \cdot \pi = 100{,}53$ [s^{-1}]

Masa părţii vibratoare a separatorului (fără încărcătura de material de pe sită, neglijabilă în raport cu masa sistemului vibrator) este de 250 [kg], iar masa generatoarelor de vibraţii, M_0 = 14 [kg].

Cu ajutorul relaţiei (7) $\rightarrow p = \sqrt{\frac{k}{M + M_0}} = 17{,}66$ [s^{-1}] $\rightarrow$ conform (10), $\delta_{st} = \frac{g}{p^2} = 31{,}45$ [mm]

Cu ajutorul săgeţii statice a arcului elicoidal, 31,45 [mm] şi a frecvenţei de oscilaţie a separatorului de pietre, 960 [rot/min], se poate identifica pe nomograma din figura 4, gradul de izolare I al vibraţiilor generate.

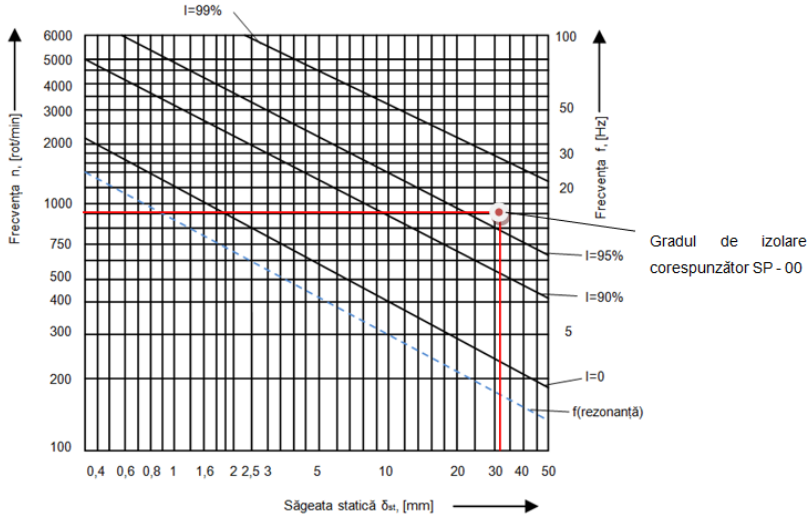

Fig. 5 – The degree of isolation for the vibrating separator, SP-00

It results in a degree of isolation I = 95÷99%, as shown in Figure 5. With the relations (7) and (8) is calculated exactly which is the value of the degree of isolation for the vibrating separator SP - 00. First, we calculate the vibration transmissibility *T*, noting that the percentage of critical damping, *ζ*, is *0* for a transmissibility of *T < 1* (as shown in Figure 3), and *Ω = ω/p=5.69*:

Rezultă un grad de izolare I = 95 ÷ 99 %, aşa cum este arătat în figura 5. Prin intermediul relaţiilor (7) şi (8) se calculează cu exactitate care este valoarea gradului de izolare pentru separatorul vibrator SP – 00. Mai întâi se calculează transmisibilitatea *T* a vibraţiilor, cu menţiunea că, fracţiunea din amortizarea critică, *ζ*, este *0* pentru o transmisibilitate *T < 1*(aşa cum reiese din Figura 3), iar raportul *Ω = ω/p=5,69*:

$$T = \left[\frac{1 + (2 \cdot 0 \cdot 5{,}69)^2}{(1 - 5{,}69)^2 + (2 \cdot 0 \cdot 5{,}69)^2}\right]^{1/2} = 0{,}032 \qquad (12)$$

According to (8), it results a degree of isolation:

Rezultă, conform (8) un grad de izolare

$$I = (1 - 0{,}032) \cdot 100 = 96{,}8 \ [\%] \qquad (13)$$

CONCLUSIONS

For most of the vibrating separators, the dynamic and reliability parameters are determined by the presence in the structure of the machine, of the vibratory elements.

To calculate the parameters for the isolation of vibrations, it must, first, to establish the equations of motion of the elastic system and the systems own pulsations that can be determined on the basis of a dynamic model of the vibrating separator.

CONCLUZII

Pentru cea mai mare parte a separatoarelor vibratoare, parametrii dinamici şi de fiabilitate sunt determinaţi de prezenţa, în structura maşinii, a elementelor vibratile.

Pentru a calcula parametrii de izolare a vibraţiilor, trebuie, mai întâi, stabilite ecuaţiile mişcării sistemului elastic şi pulsaţiile proprii ale sistemului, care pot fi determinate pe baza unui model dinamic al separatorului vibrator.

Based on the calculation of parameters of vibration isolation, the degree of isolation on the nomogram of a vibrating separator, and the resonant zone that should be avoided, are identified.

In order to have small force F_{Tr} transmitted, it is necessary that the report $\Omega = \omega / p$ should be as high as possible. Therefore, its own pulsation p shall be as small as possible, which can be achieved by using springs with a low spring constant.

Given the fact that in this article we performed a calculation example only for the elastic coil springs system, it is therefore necessary, to have in the future, experimental results on the determination of elastic constants of the whole system.

REFERENCES

[1]. Bratu P. (1990) – *Elastic systems of suspension for machinery and equipment*, Technical Publishing, Bucharest;
[2]. Brăcăcescu C., Sorică C., Manea D., Yao Guanxin, Constantin G.A., (2014) – *Theoretical contributions to the drive of cereal cleaning technical equipment endowed with non-balanced vibration generating systems*, INMATEH – Agricultural Engineering, Vol. 42, No.1/2014;
[3]. Brăcăcescu C., Matache M., Mihai M, Bunduchi G., Popescu S., (2011) – *Experimental researches regarding the optimization of working process of technical equipment driven by electrical motovibrators*, INMATEH – Agricultural Engineering, Vol. 33, No.1/2011;
[4]. Ene G., Marin C., (2009) – *Calculation and construction of vibrating machines*, Printech Publishing, Bucharest;
[5]. Munteanu M. (1986) – *Introduction to dynamics of vibrating machinery*, Academy Publishing, Bucharest;
[6]. Orasanu N., Voicu Gh., (2009) – *Some considerations on the study of plan sifter motion used for grain milling separation*, Bulgarian National Multidisciplinary Scientific Network of the Professional society for Research work, vol. 2, ISSN 1313-7735;
[7]. Voicu Gh., Plosceanu B., Voicu P., (2006) – *Aspects of the operation of the counter-vibration generating unit for separation with sieves used in the milling industry*, Scientific papers "Fast development of research results in mechanization technologies and construction of equipment for agriculture and food industry - Directions and examples of action", INMATEH Session, Bucharest, pp. 127-134, ISSN 1583-1019;
[8]. http://ro.scribd.com/doc/51584660/Vibratii-Mecanice.

Pe baza calculului parametrilor de izolare a vibrațiilor, se identifică pe nomogramă gradul de izolare al unui separator vibrator, precum și zona de rezonanță care trebuie evitată.

Pentru a avea forța transmisă F_{Tr} mică, este necesar ca raportul $\Omega = \omega/p$ să fie cât mai mare posibil. Pentru aceasta, pulsația proprie p trebuie să fie cât mai mică, ceea ce se poate realiza prin utilizarea unor arcuri cu o constantă elastică mică.

Dat fiind faptul că în acest articol am efectuat un exemplu de calcul doar pentru sistemul elastic de arcuri elicoidale, rezultă necesitatea unor rezultate experimentale viitoare privind determinarea constantelor elastice și ale întregului sistem.

BIBLIOGRAFIE

[1]. Bratu P. (1990) – *Sisteme elastice de rezemare pentru mașini și utilaje*, Editura Tehnică, București;
[2]. Brăcăcescu C., Sorică C., Manea D., Yao Guanxin, Constantin G.A., (2014) – *Contribuții teoretice la acționarea echipamentelor tehnice de curățire a cerealelor cu sisteme generatoare de vibrații cu mase neechilibrate*, INMATEH – Agricultural Engineering, Vol. 42, Nr.1/2014;
[3]. Brăcăcescu C., Matache M., Mihai M, Bunduchi G., Popescu S., (2011) – *Cercetări experimentale privind optimizarea procesului de lucru al echipamentelor tehnice de separare acționate cu motovibratoare electrice*, INMATEH – Agricultural Engineering, Vol. 33, Nr.1/2011;
[4]. Ene G., Marin C., (2009) – *Calculul și construcția mașinilor vibratoare*, Editura Printech, București;
[5]. Munteanu M. (1986) – *Introducere în dinamica mașinilor vibratoare*, Editura Academiei, București;
[6]. Orasanu N., Voicu Gh., (2009) – Cateva *consideratii asura studiului miscarii unei site plane folosita pentru separarea cerealelor in morarit*, Bulgarian National Multidisciplinary Scientific Network of the Professional society for Research work, vol. 2, ISSN 1313-7735;
[7]. Voicu Gh., Plosceanu B., Voicu P., (2006) – *Aspecte cu privire la acţionarea cu generatoare de vibraţii cu contragreutăţi a blocurilor de separare cu site utilizate în industria morăritului*, Lucrări ştiinţifice "Valorificarea rapidă a rezultatelor cercetărilor în domeniul tehnologiilor de mecanizare şi al construcţiei de echipamente pentru agricultură şi industria alimentară – Direcţii şi exemple de acţiune", Sesiunea INMATEH, Bucureşti, pag. 127-134, ISSN 1583-1019;
[8]. http://ro.scribd.com/doc/51584660/Vibratii-Mecanice.

EXPLAINING THE PHENOMENON OF SEPARATION INTO FRACTIONS OF A MIXTURE OF PARTICULATE MATTER BY APPLYING THE PRINCIPLE OF MINIMUM ENERGY
/
EXPLICAREA FENOMENULUI DE SEPARARE ÎN FRACŢII A UNUI AMESTEC DE PARTICULE MATERIALE ÎN BAZA APLICĂRII PRINCIPIULUI ENERGIEI MINIME

Prof.PhD.Eng. Paraschiv G., Prof.PhD.Eng. Manole C.
University POLITEHNICA of Bucharest, Faculty of Biotechnical Systems Engineering / Romania
Tel: 0727378361; E-mail: constantinmanole@ymail.com

***Abstract**: The paper explains, on the basis of the minimum power principle, the phenomenon of layering a mixture of material particles (especially seeds of cereals) maintained under an oscillating motion, with or without the action of an air stream. This phenomenon of separation into fractions is also generalized on a mass of particles with the same specific weight, but with different sizes, an untreated aspect, in this form, in the specific literature.*

***Keywords:** minimum energy principle, seed mixture, unstable technical system, unstable equilibrium, vibrating flat surface, equivalent pyramid, fluidized bed*

INTRODUCTION

The great majorities of agricultural products, but also those resulting from various industries, represent mixtures consisting of material particles with different physico-mechanical features [3, 6].

Their processing through different separation methods is made in order to bring them at the level of the conditions imposed by standards, the norms imposed in consumption or the requirements of prior processing and storage operations [4].

Filtering [1] is a process of separation in more fractions (three, four etc.) according to specific criteria (dimension, weight, color etc.), regarding components of the same nature of an agricultural products mixture found in the same state of granulation, fragments etc. (seeds, potato tubers, fruit etc.).

Filtering is made for obtaining uniform fractions as size, shape, weight etc., for the prior processes such as: sowing with machines provided with special distribution machinery, industrial processing, packaging etc., to be conducted easier, more accurately and with a greater performance, or for commercial purpose [2].

Filtering machines are built and work according to different principles, depending on the product to be filtered and the filtering criterion [5]. Thus, the majority of seeds can be filtered depending on their dimension by way of sifters or sorters.

Sifters with circular orifices filter the seeds according to width (the average size), those with elongated orifices filter the seeds according to thickness (the minimal size), and the alveolar sorters filter the seeds according to length (the maximum size).

Given the specific weight and the aerodynamic resistance, the seeds can be filtered by means of air stream (pneumatic filtering), water or some type of solutions (hydraulic filtering), or air vibrator masses.

The air vibrator mass is a part of a seed filtering machine depending on the specific mass, consisting of a sifter with vibratory motion, under which one or more fans creating an air stream passing through the sifter's orifices can be found, operating upon the seeds, without detaching them of the sifter's surface, though. The sifter is sloped both lengthwise and transversely. Due to the vibratory motion and the air stream's action, the seeds

***Rezumat**: În lucrare se explică, în baza principiului energiei minime, fenomenul de stratificare a unui amestec de particule materiale (în particular a seminţelor de cereale) supus unei mişcări de oscilaţie întreţinute, cu sau fără acţiunea unui curent de aer. Fenomenul de separare în fracţii se generalizează şi asupra unei mase de particule de aceeaşi greutate specifică dar de dimensiuni diferite, aspect netratat, sub această formă, în literatura de specialitate.*

***Cuvinte cheie**: principiul energiei minime, amestec de seminţe, sistem tehnic nestabilizat, echilibru instabil, suprafaţă plană vibratoare, piramidă echivalentă, strat fluidizat*

INTRODUCERE

Marea majoritate a produselor agricole, dar şi o parte din cele rezultate din diferite industrii sunt amestecuri formate din particule materiale cu proprietăţi fizico-mecanice diferite [3, 6].

Prelucrarea lor prin diferite metode de separare se face în scopul aducerii acestora la nivelul condiţiilor prescrise în standarde, în normele impuse de consum sau de cerinţele proceselor ulterioare de prelucrare şi depozitare [4].

Sortarea [1] este o operaţie de separare în mai multe fracţii (trei, patru etc.), după anumite criterii (dimensiuni, greutate, culoare etc.) a componentelor de aceeaşi natură ale unui amestec de produse agricole aflate în stare de granule, bucăţi etc. (seminţe, tubercule de cartofi, fructe ş.a.).

Sortarea se face în scopul obţinerii unor fracţii uniforme ca mărime, formă, greutate, culoare etc., pentru a putea fi efectuate mai uşor, mai precis şi cu mai mare randament, operaţiile ulterioare, precum: însămânţarea cu maşini prevăzute cu aparate de distribuţie speciale; prelucrarea industrială; împachetarea etc., sau în scopuri comerciale [2].

Maşinile de sortat sunt construite şi funcţionează după principii diverse, în funcţie de produsul ce se sortează şi de criteriul de sortare [5]. Astfel, majoritatea seminţelor pot fi sortate după dimensiuni cu ajutorul sitelor sau trioarelor.

Sitele cu orificii circulare sortează seminţele după lăţime (dimensiunea medie), cele cu orificii alungite sortează seminţele după grosime (dimensiunea minimă), iar trioarele cu alveole sortează seminţele după lungime (dimensiunea maximă).

După greutatea specifică şi rezistenţa aerodinamică, seminţele pot fi sortate cu ajutorul curentului de aer (sortare pneumatică), cu ajutorul apei sau al unor soluţii (sortare hidraulică) sau cu ajutorul meselor pneumovibratorii.

Masa pneumovibratoare este un subansamblu din cadrul maşinii de sortat seminte după greutatea specifică, format dintr-o sită cu mişcare vibratorie sub care se găsesc unul sau mai multe ventilatoare care creează un curent de aer ce trece prin orificiile sitei, acţionând asupra seminţelor, fără însă a le desprinde de suprafaţa acesteia. Sita este înclinată atât în plan longitudinal, cât şi în plan transversal. Datorită mişcării

filter according to the specific weight, being separately collected.

The Minimum Energy Principle

It is known that if within an elementary filtering system (screen, sifter etc.) there is a mixture of objects relatively uniform in dimensions but with different specific weights (such as pebbles, lead shots, corn grains), and subject to oscillatory motion, these will stratify in such a way that the objects with the bigger specific weight (the lead shots) will occupy the inferior part, and the other components will occupy the following positions, stratifying according to their specific weight, in downward direction [3].

This type of placing is based on the "minimum energy principle" of an unstable technical system, according to which the objects will stratify in such a way that the potential energy of the system to be minimal. By virtue of this principle, a solid object, found in unstable equilibrium, will seek to occupy a stable position, whereas a mixture of solid objects or immiscible liquids, subject to an oscillatory motion of a certain amplitude and frequency, will separate in fractions.

MATERIAL AND METHOD

The stratification phenomenon of the material particles (especially of seeds) is carried by applying a continuous oscillatory motion to the seeds mass. In some cases, the oscillatory motion of the surface with seeds is accompanied by the action of an air stream which crosses the material layer subject to filtering, in a downward or upward direction.

In the case of filtering systems without air stream, the seeds' stratification can take place in the following cases:

- the seeds have relatively uniform d1, d2, ..., di, ..., dn dimensions, but different specific weights (γ1, γ2, ..., γi, ..., γn);
- the seeds have irregular dimensions, but the same specific weight;
- the seeds have irregular dimensions and different specific weights, but their dimensions are inversely proportional with their specific weights (particles with small dimensions have bigger specific weights, and those with bigger dimensions have smaller specific weights). In the case of filtering systems with an air stream, the above cases are admissible only if also taking into account the direction of the air stream, whose direction is chosen suitably to the filtering process.

The following cases can thus be identified:

- the seeds have relatively uniform dimensions and different specific weights, and the air stream is directed upwards;
- the seeds have irregular dimensions and the same specific weight, and the air stream is directed downwards;
- the seeds have irregular dimensions and different specific weights (their dimensions are inversely proportional with their specific weights), and the air stream is directed downwards.

a) The case where di = k (constant), γi ≠ k

If the seeds have relatively uniform di dimensions and their specific weights are then different, when taking into account the mass of two seeds categories of a given volume, the seeds which have bigger specific weight will also have a bigger mass:

vibratorii şi acţiunii curentului de aer, seminţele se separă după greutatea specifică, fiind colectate separat.

Principiul energiei minime

Este cunoscut faptul că, dacă într-un sistem elementar de sortare (ciur, sită etc.) avem un amestec de corpuri de dimensiuni relativ uniforme, dar de greutăţi specifice diferite (de ex. pietricele, alice de plumb, boabe de porumb etc.) şi le supunem unei mişcări de oscilaţie, acestea se vor stratifica astfel încât corpurile cu greutatea specifică cea mai mare (alicele de plumb) vor ocupa partea inferioară, iar celelalte componente vor ocupa poziţiile următoare, stratificându-se după greutatea specifică, în sens descrescător al acesteia [3].

Acest mod de dispunere are la bază „principiul energiei minime" a unui sistem tehnic nestabilizat, conform căruia corpurile se vor stratifica astfel încât energia potenţială a sistemului să fie minimă. Astfel, un corp solid, aflat în echilibru instabil, va tinde să ocupe o poziţie stabilă, iar un amestec de corpuri solide sau lichide nemiscibile, supus unei mişcări oscilatorii de o anumită amplitudine şi frecvenţă, se va separa în fracţii.

MATERIAL ŞI METODĂ

Fenomenul de stratificare a particulelor materiale (în particular a seminţelor) se realizează prin imprimarea unei mişcări de oscilaţie întreţinută masei de seminţe. În unele cazuri, mişcarea de oscilaţie a planului pe care se află seminţele este însoţită de acţiunea unui curent de aer care străbate, în sens ascendent sau descendent, stratul de material supus sortării.

La sistemele de sortare fără prezenţa unui curent de aer, stratificarea seminţelor poate avea loc în următoarele cazuri:

- seminţele au dimensiuni d1, d2, ..., di, ..., dn relativ uniforme, dar greutăţi specifice (γ1, γ2, ..., γi, ..., γn) diferite;
- seminţele au dimensiuni neuniforme, dar aceeaşi greutate specifică;
- seminţele au dimensiuni neuniforme şi greutăţi specifice diferite, dar dimensiunile acestora sunt în raport invers proporţional cu greutăţile lor specifice (particulele de dimensiuni mici au greutăţi specifice mai mari, iar cele de dimensiuni mari au greutăţi specifice mai mici). La sistemele de sortare în prezenţa unui curent de aer, la fiecare din cazurile de mai sus se ţine seama de influenţa curentului de aer, al cărui sens se alege convenabil procesului de sortare.

Se disting, astfel, următoarele cazuri:

- seminţele au dimensiuni relativ uniforme şi greutăţi specifice diferite, iar curentul de aer are sens ascendent;
- seminţele au dimensiuni neuniforme şi aceeaşi greutate specifică, iar curentul de aer are sens descendent;
- seminţele au dimensiuni neuniforme şi greutăţi specifice diferite (dimensiunile lor sunt în raport invers proporţional faţă de greutăţile lor specifice, iar curentul de aer are sens descendent.

a**) Cazul di = k (constant), γi ≠ k**

Dacă seminţele au dimensiuni di relativ uniforme, iar greutăţile lor specifice sunt diferite atunci, dacă se consideră masa a două categorii de seminţe dintr-un volum dat, seminţele care au greutatea specifică mai mare vor avea şi masa mai mare:

$$m_1 = \frac{\gamma_1}{g}V; \quad m_2 = \frac{\gamma_2}{g}V; \quad \gamma_1 \geq \gamma_2; \quad m_1 \geq m_2 \tag{1}$$

The mass of seeds subject to filtering in an oscillatory motion stratifies based on the "minimum energy principle".

b) The case where di ≠ k; γi = k

We assume that for a given volume we have material particles of a certain dimension; for another volume, equal to the first volume, we have particles with another dimension. We want to illustrate that for equal volumes, the particles with smaller dimensions fill better the area where they can be found.

In order to simplify this, we will consider the particles have a spherical shape.

Let us consider R being the radius of a particle. In one unity of volume shaped as a square pyramid (fig. 1), with the base side being a multiple of R, an N number of spheres will be able to fill the volume.

Masa de seminţe supusă sortării, aflată în mişcare de oscilaţie, se stratifică pe baza *„principiului energiei minime*".

b) Cazul di ≠ k; γi = k

Să admitem că, într-un volum dat, avem particule materiale de o dimensiune oarecare; într-un alt volum, egal cu primul, avem particule de o altă dimensiune. Vrem să demonstrăm că, la volume egale, particulele de dimensiuni mai mici umplu mai bine spaţiul în care se află.

Pentru simplificare, să considerăm că particulele au forma sferică.

Fie R, raza unei particule. Într-o unitate de volum în formă de piramidă pătrată (fig.1), cu latura bazei multiplu de R, va intra un număr N de sfere.

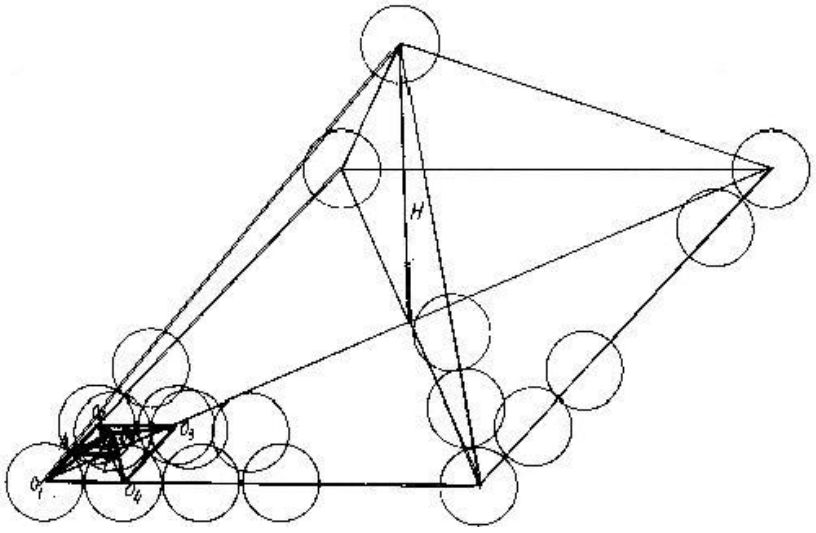

Fig. 1 - Particle pyramid

If on the square's base side of the pyramid we have "n" spheres, then the number of spheres from the inferior stratum will be n2. On the side of the second row we will have "n-1" spheres, and the number of spheres from this second row will be $(n-1)^2$ etc.

The total number of spheres from the entire pyramid will be:

Dacă pe latura pătratului de bază al piramidei avem „n" sfere, atunci numărul de sfere din stratul inferior va fi n2. Pe latura celui de-al doilea rând vom avea „n-1" sfere, iar numărul de sfere din acest al doilea rând va fi $(n-1)^2$ etc.

Numărul total de sfere din întreaga piramidă va fi:

$$N = n^2 + (n-1)^2 + (n-2)^2 + ... + 3^2 + 2^2 + 1^2 = \frac{n(n+1)(2n+1)}{6} \quad (2)$$

For *n* = 6 spherical particles with the *R* radius, it results *N* = 91, with their volume:

Pentru *n* = 6 particule sferice de rază *R*, rezultă *N* = 91, iar volumul lor:

$$V = N \cdot \frac{4\pi R^3}{3} = 91 \cdot \frac{4\pi R^3}{3} = 381.18R^3 \quad (3)$$

The height of the pyramid can be calculated based on the following relationship:

Înălţimea piramidei se poate calcula pe baza următoarei relaţii:

$$H = 2R + (n-1) \cdot h \quad (4)$$

where *h* is the distance, vertically measured, between the centers of the spheres displayed on two adjacent horizontal layers.

The height "*h*" can be determined if considering another pyramid, the latter having its peaks in the centers of 5 adjacent spheres (fig. 1). It results from the right triangles O_3IO_4, O_3IO_5 and AIO_5 that:

unde h este distanţa, măsurată pe verticală, dintre centrele sferelor dispuse în două straturi orizontale alăturate.

Înălţimea *„h"* se determină considerând o altă piramidă, aceasta din urmă având vârfurile în centrele a 5 sfere alăturate (fig.1). Din triunghiurile dreptunghice O_3IO_4, O_3IO_5 şi AIO_5, rezultă:

$$h = \overline{O_5 I} = \frac{R}{\sqrt{2}} = \frac{R\sqrt{2}}{2} \quad (5)$$

and the angle with the biggest slope of the lateral sides of the pyramid:

iar unghiul de cea mai mare pantă al laturilor laterale ale piramidei:

$$\alpha = \overset{\wedge}{IAO_5} = arctg\frac{R\sqrt{2}}{2R} = arctg\frac{\sqrt{2}}{2} = \frac{\pi}{4} \quad (6)$$

It results that:

Rezultă

$$H = 2R + (n-1)R\frac{\sqrt{2}}{2} = R\left[2 + (n-1)\frac{\sqrt{2}}{2}\right]$$

For n = 6, it results that:

Pentru n = 6, rezultă:

$$H = 2R + (6-1)R\frac{\sqrt{2}}{2} = 5.535R; \quad V = \frac{2}{9}\pi R^3 \cdot 6 \cdot (6+1)(2\cdot 6+1) = 381.18R^2 \quad (7)$$

We now assume we have a square pyramid, with the same base side and the same slope of the lateral sides, but consisting of spheres with the radius *r = R/2.*

In the pyramid formed of spheres with the radius *r* there will be *N1* spheres:

Să admitem acum o piramidă pătrată, cu aceeaşi latură a bazei şi aceeaşi înclinare a feţelor laterale, dar formată din sfere de rază *r = R/2.*

În piramida formată din sfere de rază *r,* vor fi *N1* sfere:

$$N_1 = (2n)^2 + (2n-1)^2 + (2n-2)^2 + ... + 3^2 + 2^2 + 1^2 = \frac{2n(2n+1)(4n+1)}{6} = \frac{n(2n+1)(4n+1)}{3}$$

For *n* = 6, it results that:

Pentru *n* = 6, rezultă:

$$N_1 = \frac{6(2\cdot 6+1)(4\cdot 6+1)}{3} = 2\cdot 13\cdot 25 = 650 \quad (8)$$

The volume of the spheres with the radius *r* will be:

Volumul sferelor de rază *r* va fi:

$$V = N \cdot \frac{4\pi R^3}{3} = N \cdot \frac{4\pi}{3} \cdot \left(\frac{D}{2}\right)^3 = 340.34R^3 \quad (9)$$

and the height of the pyramid consisting of these spheres will be:

iar înălţimea piramidei formată din aceste sfere:

$$H_1 = 2r + (2n-1)h_1 - R + (12-1)\frac{r\sqrt{2}}{2} = R\left(1 + \frac{11\sqrt{2}}{4}\right) = 4.889R \quad (10)$$

Let us consider V_R the volume of a square pyramid capturing all the balls of radius *R*:

Fie V_R volumul unei piramide pătrate în care intră toate bilele de rază *R:*

$$V = a^2 \cdot H = (6R)^2 \cdot 5.535R = 199.26R^3 \quad (11)$$

where *a* is the base side of the pyramid.

Similarly, the volume of the pyramid capturing all the balls of radius *r* will be:

unde a este latura bazei piramidei.

Analog, volumul piramidei în care vor intra toate bilele de rază *r* va fi:

$$V = a^2 \cdot H = (6R)^2 \cdot 4.889R = 176.004R^3 \quad (12)$$

Let us now consider *ε* the ratio of the two square pyramids capturing all the small balls, as well as all the larger balls:

Fie acum *ε* raportul celor două piramide pătrate în care intră toate bilele mici, respectiv toate bilele mari:

$$\varepsilon = \frac{V_1}{V_2} = \frac{177.004R}{199.26R} = 0.8833 = 88.33\% \quad (13)$$

It thus results that the balls of radius *r = R/2* fill in a smaller volume than the balls of radius *R*, from which it also results that the irregular particles shaped quasi-spherically, of the same specific weight, can stratify on an animated densimetric mass with an oscillatory

De aici rezultă că bilele de rază *r=R/2* ocupă un volum mai mic decât bilele de rază *R*, deci şi particulele neuniforme, de formă cvasi-sferică, de aceeaşi greutate specifică, se pot stratifica pe o masă densimetrică animată în mişcare de oscilaţie. Stratificarea se va face

motion. Stratification will be made reversely to their dimensions, with the smallest particles filling the inferior part of the seeds layer subject to filtering.

c) **The case where di ≠ k, ≠ k; di is inversely proportional to γi**

This case has an obvious explanation. Based on the phenomenon analyzed at b), here will also participate, accordingly, the specific weights of the particles.

d) **The case of an upward vertical air stream; di = k; γi ≠ k**

Having discussed case a) evidenced that the filtering of uniform dimensioned seeds and with different specific weights is possible even without the influence of an air stream.

In the case of a vertical air stream, this has a different effect on the seeds only if it acts upwards, compared to when it acts downwards.

It is important to determine the direction of the air stream favorable to filtering. In this sense, we will consider that upon a homogenous spherical material particle with the radius R and the density $\rho = \gamma/g$, an upwards vertical air stream will operate. Upon the particle (fig. 2), the dynamic pressure will operate, and subsequently the force:

în sens invers dimensiunilor lor, particulele cele mai mici ocupând partea inferioară a stratului de seminţe supus sortării.

c**) Cazul di ≠ k, γi ≠ k; di invers proporţional cu γi**

Acest caz este evident. În baza fenomenului analizat la punctul b) participă, în consens, şi greutăţile lor specifice.

d**) Cazul unui curent de aer vertical ascendent; di = k; γi ≠ k**

Punerea în discuţie a cazului a) a evidenţiat faptul că sortarea seminţelor de dimensiuni practic uniforme şi de greutăţi specifice diferite este posibilă chiar şi fără influenţa unui curent de aer.

În cazul existenţei unui curent de aer vertical, acesta are asupra seminţelor acţiune diferită în situaţia în care lucrează în sens ascendent, faţă de situaţia în care lucrează în sens descendent.

Este important să determinăm sensul curentului de aer favorabil sortării. Pentru aceasta, să considerăm că asupra unei particule materiale sferice omogene, de rază R şi densitate $\rho = \gamma/g$, acţionează un curent de aer vertical ascendent. Asupra particulei (fig. 2) acţionează presiunea dinamică, respectiv forţa.

$$p_{dm} = c \cdot \rho_a \cdot \frac{v_a^2}{2} \qquad \bar{F} = c \cdot \rho_a \cdot \frac{v_a^2}{2} \cdot \pi R \tag{14}$$

where c is a coefficient of aerodynamic resistance, ρ_a – air density and v_a – the speed of air.

unde c este un coeficient de rezistenţă aerodinamică, ρ_a – densitatea aerului, iar v_a – viteza aerului.

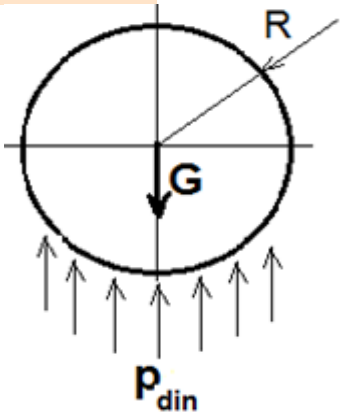

Fig. 2 - The action of the airflow vertical ascending

Reversely, upon the particles will operate the gravity force $G = mg$, where m is the mass of the particle. If the forces F and G virtually have equal values, when operating reversely, their resultant is zero, and the particle will receive a fluidized state, favorable to free movement under minimal impulses. Obviously, upon the particle with the density, $\gamma 1 > \gamma$, a $G1>G$ force will operate, and the fluidized action of the air stream is less definite. If the forces F and G work in the same direction, the fluidization of the fractions from the seeds layer subject to filtering is hampered, so the downwards direction of the air stream is not indicated.

CONCLUSIONS

The stratification phenomenon of the material particles is carried by applying a continuous oscillatory motion to the seeds mass. In some cases, the oscillatory motion of the surface with seeds is accompanied by the action of an air stream which crosses the material layer subject to filtering in a downward or upward direction.

Applying minimum energy principle, in the paper

În sens invers, asupra particulei acţionează forţa de greutate $G = mg$, unde m este masa particulei. Dacă forţele F şi G au valori practic egale, lucrând în sensuri contrarii rezultanta lor este nulă, iar particulei i se creează o stare o stare fluidizantă, favorabilă deplasării libere sub impulsuri minime. Evident, asupra unei particule de densitate $\gamma 1 > \gamma$, va acţiona o forţă $G1>G$, iar acţiunea fluidizantă a curentului de aer este mai puţin pronunţată. Dacă forţele F şi G lucrează în acelaşi sens, fluidizarea fracţiilor din stratul de seminţe supus sortării este îngreunată, deci sensul descendent al curentului de aer nu este indicat.

CONCLUZII

Fenomenul de stratificare a particulelor materiale se realizează prin imprimarea unei mişcări de oscilaţie întreţinută masei de seminţe. În unele cazuri, mişcarea de oscilaţie a planului pe care se află seminţele este însoţită de acţiunea unui curent de aer care străbate, în sens ascendent sau descendent, stratul de material supus sortării.

În cadrul lucrării s-a explicat, în baza principiului energiei minime, fenomenul de stratificare a unor

has been explained the stratification phenomenon of some material particles (especially of seeds) in the case where a fluidization of the fractions from the layer of seeds, subject to filtering, takes place or not.

REFERENCES

[1]. Anghel Ş., Manole C et al. (1972) - *Dictionary of Agricultural Mechanics,* Publisher: Ceres, Bucharest;
[2]. Balc G., Oltean O. (2002) - *The technique of preserving and primary processing of agricultural products,* Publisher: Alma-Mater, Cluj-Napoca.
[3]. Manole C. (1986) - *Seed sorting by specific weight*, PhD thesis, Polytechnic Institute of Bucharest;
[4]. Ristea M. (2014) – *Contribution to the Study of the Process of Aerodynamic Separation of Solid Particles Mixtures Applied in the Food Industry,* Doctoral Thesis, University "Vasile Alecsandri", Bacau, Faculty of Engineering;
[5]. Rus F. (2001) - *Separation operations in the food industry*, Publisher: Publisher: „Transilvania" University of Braşov;
[6]. Stoica D. et al (2011) - *Influence of oscillations amplitude of sieve on the screening process for a conical sieve with oscillatory circular motion,* Journal of Engineering Studies and Research, Bacău.

particule materiale (în particular a seminţelor) în situaţia în care are loc sau nu, fluidizarea fracţiilor din stratul de seminţe supus sortării, sortarea după greutatea specifică fiind un caz particular al stratificării particulelor.

BIBLIOGRAFIE

[1]. Anghel Ş., Manole C., ş.a., (1972) - *Dicţionar de mecanică agricolă*, Editura Ceres, Bucureşti;
[2]. Balc G., Oltean O. (2002) - *Tehnica păstrării şi procesării primare a produselor agricole*. Editura Alma-Mater, Cluj-Napoca.;
[3]. Manole C. (1986) - *Sortarea seminţelor după greutatea specifică*, Teză de doctorat, Institutul Politehnic Bucureşti;
[4]. Ristea M. (2014) - *Contribuţii la studiul procesului de separare aerodinamică a amestecurilor de particule solide, cu aplicaţie în industria alimentară*, Teză de doctorat, Univ. „Vasile Alecsandri", Bacău, Facultatea de inginerie;
[5]. Rus F., (2001) - *Operaţii de separare în industria alimentară,* Editura Univ. „Transilvania", Braşov;
[6]. Stoica D., ş.a., (2011) - *Influenţa amplitudinii oscilaţiilor sitei pentru investigarea procesului de separare pe o sită conică cu mişcare circulară oscilatorie*, Revista de cercetare si studii de inginerie, Bacău.

EXPERIMENTAL RESEARCHES UPON THE DOSING ACCURACY OF TECHNICAL DOSAGE EQUIPMENT DESTINED FOR AGRIFOOD PRODUCTS
/
CERCETĂRI EXPERIMENTALE PRIVIND ACURATETEA DOZARII PENTRU ECHIPAMENTUL TEHNIC DE DOZARE DESTINAT PRODUSELOR AGROALIMENTARE

Ph.D. Eng. Brăcăcescu C., Ph.D. Eng. Păun A., Eng. Milea D.,
Ph.D. Stud Eng. Ivancu B., Eng. Bunduchi G.
INMA Bucharest / Romania
Tel: 031.805.32.13; E-mail: carmenbraca@yahoo.com

Abstract: *The researches which results are herein presented, tackle the dosage process optimization in small and medium-sized enterprises.*

The dosing technical equipment DTE performs two main functions:
- automated setting of product flow rate for a programmed value and maintaining this value within certain pre-set limits, by respecting the regulations in force concerning the dosage precision imposed for this equipment type;
- automated control of quantities of products passing through the dosage equipment in a certain period of time.

In this paper, are presented this equipment experimental tests, the working qualitative indexes determined, by emphasizing the advantages of using this equipment type in small and medium-sized milling enterprises, in rural area.

Keywords: *dosage, agricultural products, milling units, automated control, PLC.*

INTRODUCTION

The field of systems and equipment for weighing, dosing and packaging agri food products is one of the fields with a high economic impact in Romania (especially in the last years), but also in the industrially developed countries.

Modern weighing and automated dosing devices represent ingenious technical solutions that comprise fields from both the mechanics and electronics, being characterized by a high precision and sensitivity according to several papers from the specialty literature. [1, 2, 3, 4, 8].

Usually, operations involving direct action on the processed material are exclusively done by mechanical mechanisms or components, but also the command and dosage adjustment operations are frequently done by mechanical systems, the electronic systems having a surveillance and fine adjustment role as described in the paper [5, 9].

Technological operations of weighing and dosing are not independent in the manufacturing process of products, but are integrated into various technological processes, so that the result of the operation does not emerge distinctively, but cumulated in the resulted final product, and as a result, the quality of the dosage/weighing directly influencing the quality of the final product. [6,7].

In the milling process in different points of the mill's technological flow, technical equipment used for weighing the grains that enter the processing and the finished products and by-products are provided.

Aligned with the most modern equipment in the field and encompassing innovative constructive solutions, the *Dosing Technical Equipment DTE* (fig. 1), developed at INMA Bucharest has a direct applicability in small and medium capacity milling units, and can be interleaved in their technological flow in several points of processing quantitative information, but also in combined fodder

Rezumat: *Cercetările ale căror rezultate sunt prezentate în acest articol au ca subiect optimizarea procesului de dozare în unităţile productive de mică şi medie capacitate.*

Echipamentul tehnic de dozare ETD realizează două funcţii principale:
- reglarea automată a debitului de produs la o valoare programată şi menţinerea acestei valori între anumite limite prescrise, cu respectarea normativelor referitoare la precizia de dozare pentru aceste tipuri de echipamente;
- gestionarea automată a cantităţilor de produse ce trec prin echipamentul de dozare într-un anumit timp.

În această lucrare sunt prezentate investigaţiile experimentale ale acestui echipament, indicii calitativi de lucru determinaţi cu evidenţierea avantajelor utilizării acestui tip de echipament tehnic în fluxul unităţilor de morărit săteşti de mică şi medie capacitate.

Cuvinte cheie: *dozare, produse agricole, unităţi de morărit, control automat, PLC*

INTRODUCERE

Domeniul sistemelor şi echipamentelor de cântărire, dozare şi ambalare pentru produsele agroalimentare este unul din domeniile de mare impact economic în România (mai ales în ultimii ani), dar şi în ţările dezvoltate din punct de vedere industrial.

Dispozitivele moderne de cântărire şi dozare automată sunt soluţii tehnice ingenioase ce cuprind domenii atât din mecanică cât şi din electronică fiind caracterizate printr-o precizie şi sensibilitate înaltă conform mai multor lucrări din literatura de specialitate [1, 2, 3, 4, 8].

De regulă, operaţiile ce presupun acţiunea directă asupra materialului prelucrat sunt efectuate în exclusivitate de mecanisme sau componente mecanice, însă şi operaţiile de comandă şi reglaj al dozării sunt efectuate de multe ori de sisteme mecanice, cele electronice având rolul de supraveghere şi reglaj fin după cum se arată în lucrarea [5, 9].

Operaţiile tehnologice de cântărire şi dozare nu sunt independente în procesul de fabricaţie al produselor, ci se integrează în procese tehnologice diverse, astfel încât rezultatul operaţiei nu apare distinct, ci cumulat în produsul final rezultat, iar ca urmare, calitatea dozării / cântăririi influenţând direct calitatea produsului final. [6, 7]

În cadrul procesului de măcinare în diferite puncte ale fluxului tehnologic din mori sunt prevăzute echipamente tehnice pentru cântărirea cerealelor ce intră în procesul de prelucrare, precum şi a produselor finite şi a subproduselor obţinute.

Aliniat celor mai moderne utilaje din domeniu şi înglobând soluţii constructive inovatoare, *Echipamentul tehnic de dozare ETD* (fig.1) conceput la INMA Bucureşti, are aplicativitate directă în cadrul unităţilor de morărit de mică şi medie capacitate putând fi intercalat în fluxul tehnologic al acestora în diverse puncte de prelucrare a informaţiei cantitative, cât şi în cadrul unor fabrici de

factories, where several dosing technical equipment can be connected and through a central computer, several recipes can be achieved.

MATERIAL AND METHOD

In a technological flow, the Dosing Technical Equipment DTE performs two main functions:
- automatic adjustment of the flow of product to a programmed value and maintaining that value within certain preset limits, in compliance with regulation on dosing precision for this type of equipment;
- automatic management of the quantities of products that pass through the dosing equipment in a certain time.

Fig. 1 – Dosing Technical Equipment - overview [...]
1 - bunker; 2 – dosing system; 3 – control panel

Mainly, the work process is carried out this way (fig.2):

- the dosed product flows through a pipe (pos. 2) provided at the end with a mobile flap actuated by using an electric command by an electric actuator (pos. 9);
- the product stream dimensioned by the flap falls from a certain height directed through a channel on an inclined plate (pos. 3);
- the inclined plate constitutes the end of a lever that transmits the impact force to a tensometric dose (pos. 7);
- the tensometric dose transforms de impact force into material flow, sending an impulse to the automation system;
- the electric impulse is processed and based on the programming, the automation system makes the comparison, recording and displaying of measured flow and managed values;
- the mobile flap, depending on the command it receives, increases or decreases the product flow in order to stabilize it.

nutreţuri combinate, în care caz se pot cupla mai multe echipamente tehnice de dozare şi prin intermediul unui calculator central se pot realiza diferite reţete.

MATERIAL ŞI METODĂ

În cadrul unui flux tehnologic, echipamentul tehnic de dozare ETD (fig.1) realizează două funcţii principale:
- reglarea automată a debitului de produs la o valoare programată şi menţinerea acestei valori între anumite limite prescrise, cu respectarea normativelor referitoare la precizia de dozare pentru aceste tipuri de echipamente;
- gestionarea automată a cantităţilor de produse ce trec prin echipamentul de dozare într-un anumit timp.

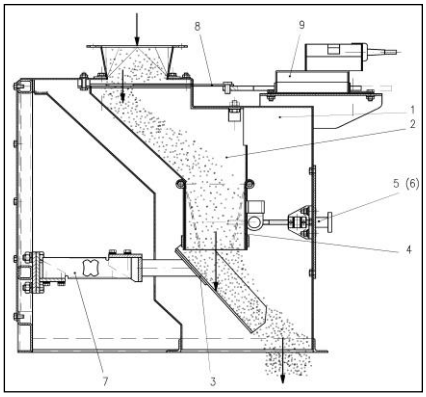

Fig. 2 – Technological scheme of DTE
1 - frame; 2 – guidance funnel; 3 – impact plan; 4 - mobile wall; 5(6) - actuating mechanism; 7 - tensometric dose; 8 - flap;
9 - electric actuator

În principal, procesul de lucru se desfăşoară astfel (fig. 2):

- produsul de dozat afluează printr-o pâlnie de dirijare (poz. 2) prevăzută la capăt cu o clapetă mobilă (poz. 8) acţionată prin comandă electrică de către un actuator electric (poz. 9);
- jetul de produs dimensionat de clapetă, cade de la o anumită înălţime dirijat printr-un canal pe o plan de impact (poz.3);
- planul de impact constituie capătul unei pârghii care transmite forţa de impact unei doze tensiometrice (poz. 7);
- doza tensiometrică transformă forţa de impact în debit de material, transmiţând un impuls instalaţiei de automatizare;
- în instalaţia de automatizare se prelucrează impulsul electric şi în funcţie de programare se efectuează compararea, înregistrarea şi afişare debitului măsurat şi a valorilor gestionate;
- clapeta mobilă, în funcţie de comanda ce o primeşte măreşte sau micşorează fluxul de produs pentru stabilizarea lui.

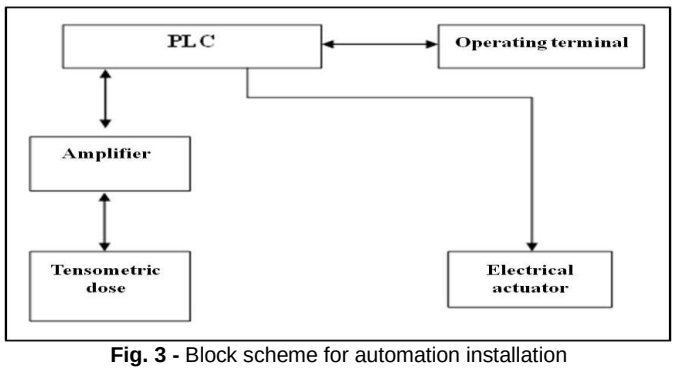

Fig. 3 - Block scheme for automation installation

The operating terminal (seen in fig.3 acts as graphical user interface. It communicates with the installation's PLC on a dedicated RS422 serial communication interface.

Using the settings, the working parameters for DTE are set (reference flow, weight counter) and product management data are viewed (total amount of material and measured current flow).

The analyzed dosing equipment constitutes an application of dynamics postulates. Thus, it is known that a particle's mass impulse "m" and speed "v" is:

Terminalul de operare (vezi fig.3) îndeplineşte funcţia de interfaţă grafică cu utilizatorul. Acesta comunică cu PLC-ul instalaţiei pe o interfaţă dedicată de comunicaţie serială RS422.

Prin setări se stabilesc parametrii de lucru ai ETD (debit de referinţă, contor de masă) şi se vizualizează datele de gestiune (cantitate totală de material şi debit curent măsurat).

Echipamentul tehnic de dozare supus analizei constituie o aplicaţie a unor postulate ale dinamicii. Astfel, se stie că impulsul unei particule de masă „m" şi viteză „v" este:

$$\vec{H} = m \bullet \vec{v} \tag{1}$$

and that the $\vec{H}$ vector is tied to the $\vec{P}$ vector of the resultant forces applied to the mobile point, through the equation:

şi că vectorul $\vec{H}$ este legat de vectorul $\vec{P}$ al rezultantei forţelor aplicate punctului mobil, prin ecuaţia:

$$\frac{\overrightarrow{dH}}{dt} = \vec{P} \tag{2}$$

Also, the impulse of a points system is written: $\vec{H} = \sum_i H_1 = \sum m_i \vec{v}_i$; this vector $\vec{H}$ can be regarded as the impulse of a fictive point with the mass M = $\sum_i m_i$, and the speed equal with the speed of the center of mass (weight). Thus, we have the impulse variation in the time interval (t_A, t_B):

De asemenea, impulsul unui sistem de puncte se scrie: $\vec{H} = \sum_i H_1 = \sum m_i \vec{v}_i$; acest vector $\vec{H}$ poate fi privit ca impulsul unui punct fictiv cu masa M = $\sum_i m_i$ şi viteza egală cu viteza centrului de masă (de greutate). Astfel, vom avea variaţia impulsului în intervalul de timp (t_A, t_B):

$$M_B \vec{v}_C(t_B) - M_A \vec{v}_C(t_A) = \vec{S} = \int_{t_A}^{t_B} \sum s_i dt \tag{3}$$

$$\sum m_{i_B} \bullet \vec{v}_C(t_B) - \sum m_{i_A} \bullet \vec{v}_C(t_A) = \vec{S} \tag{4}$$

It results that if the impulse is zero, the exterior forces will have a constant value and vice versa.

Therefore, we are constructively and functionally looking to achieve the solution $\vec{s} = 0$.

In order to achieve that, it was constructively imposed that H – vertical particle falling height H = constant, resulting that v = constant because $v = \sqrt{2gH}$ for any particle ($v_1 = const.$). It results:

Rezultă că dacă varianta de impuls este zero, forţele exterioare vor avea o valoare constantă şi invers.

Astfel, s-a căutat constructiv şi funcţional să se realizeze soluţia $\vec{s} = 0$.

Pentru aceasta, constructiv s-a impus H – înălţimea de cădere a particulelor pe verticală H=const. rezultând v=const. pentru că $v = \sqrt{2gH}$ pentru orice particulă ($v_1 = const.$).Rezultă:

$$\sum m_{i_B} \bullet (V_C)(t_B) - \sum m_{i_A} \bullet (V_C)(t_A) \tag{5}$$

$$V_C(t_A) = V_C(t_B) \tag{6}$$

$$\sum m_{i_B} - \sum m_{i_A} \tag{7}$$

It results that for this, $M_B = M_A$ therefore it is

Rezultă că pentru aceasta $M_B = M_A$ deci

ultimately constant with the flow.

Functionally, it was searched that the instant value taken by the tensometric dose and sent to the PLC, compared with a reference value – resulted from calibration and related adjustments – to be constant. If not, by comparing it to the reference value, actions will be taken through the electric actuator on the mobile flap to adjust the flow.

Taking into consideration that the equipment should only take the impulse and the material has to flow as smoothly as possible, an inclined plan was built to serve as an impact receptor (pos.3, fig. 2).

The inclination value $\sphericalangle\alpha$ has to be bigger than the fall limit $\sphericalangle$, the $\sphericalangle$ when the products start to roll $\alpha_{min} < \alpha$.

This value α_{min} is determined from the transport speed formula where the kinetic energy variation is equaled with the mechanical work of the forces acting on the material.

Therefore, we have the formula:

constanta debitului în ultimă instanţă.

Funcţional s-a căutat ca valoarea instantanee preluată de doza tensiometrică şi transmisă PLC-ului, unde, comparată cu o valoare de referinţă – rezultat al etalonării şi a reglajelor aferente –să fie constantă. Dacă nu, prin compararea faţă de valoarea de referinţă se va acţiona prin intermediul actuatorului electric asupra clapetei mobile de reglare a debitului.

Având în vedere că echipamentul de dozare trebuie să preia doar impulsul, iar materialul trebuie să se scurgă cât mai rapid, s-a construit un plan înclinat ca receptor de impact (poz.3, fig.2).

Valoarea $\sphericalangle\alpha$ de înclinare a planului trebuie să fie mai mare decât $\sphericalangle$ limită de cădere, $\sphericalangle$ la care produsele încep să se rostogolească $\alpha_{min} < \alpha$.

Această valoare α_{min} se determină din formula vitezei de transport unde variaţia energiei cinetice o egalăm cu lucrul mecanic al forţelor ce acţionează asupra meterialului.

Astfel avem formula:

$$\frac{G}{g} \bullet \frac{(v - v_0)^2}{2} = GH - G\cos\alpha \frac{h}{\sin\alpha} \bullet f \qquad (8)$$

where:

G = material weight, kgf.;
g = gravity acceleration, m/s^2;
v = transport speed, m/s;
h = falling height, m
α = falling angle, degrees;
f = $\tan\rho$ - friction coefficient, depending on the friction angle of the material on the inclined plan.

When $v_o = 0$ it results:

unde:

G = greutatea mat. în kgf.;
g = acceleraţia gravitaţională 9,81 m/s^2;
v = viteza de transport, în m/s;
h = înălţimea de cădere, în m
α = unghiul de cădere, în grade;
f = $\tan\rho$ - coeficient de frecare, în funcţie de unghiul de frecare al materialului pe planul înclinat.

Când $v_o = 0$ se obţine:

$$\frac{v^2}{2g} = h(1 - ftg\,\alpha) \qquad (9)$$

$$v = \sqrt{2gh(1 - ctg\,\alpha tg\rho)} \qquad (10)$$

at limit *v*=0 for *tg*α= *tg*ρ

RESULTS

The testing of the experimental model of DTE equipment was made at INMA, in laboratory and exploiting conditions, using its own experimental methods, carrying out the following activities: preliminary checks, initial technical expertise, experimenting operating without load, calibrating the weighing system, checking the functioning of the automation installation in simulated mode, experimenting operating under load.

For the experiments in working conditions were used agricultural products such wheat seeds and bran.

The dosing error (ε_d) was determined with the following relation [3]:

REZULTATE

Încercarea modelului experimental al echipamentului tehnic de dozare s–a realizat în cadrul INMA în condiţii de laborator şi de exploatare, utilizând o metodică de experimentare proprie fiind efectuate următoarele tipuri de activităţi: verificări preliminare, expertiza tehnică iniţială, experimentări de funcţionare în gol; calibrarea sistemului de cântărire, verificarea funcţionării instalaţiei de automatizare în regim simulat, experimentări de funcţionare în sarcină.

Pentru experimentări în condiţii de exploatare s-au folosit ca materie primă produse agricole precum seminţe de grâu şi tărâţă.

Eroarea de dozare (ε_d) s-a determinat cu relaţia [3]:

$$\varepsilon = \frac{|Qp - Q_C|}{Q_p} \bullet 100\ [\%] \qquad (11)$$

where: Qp - programmed flow, t/h;
Qc – calculated flow, t/h.

unde : Qp – debit programat, t/h;
Qc – debit calculate, t/h.

The calculation formula for Q_c is:

Formula de calcul pentru Q_c este:

$$Q_C = \frac{M_p}{T_p} \bullet 3600 \ [t/h] \quad (12)$$

where: M_p – sample weight, kg;
T_p - sample duration s.

unde : Mp – masa probei, kg;
Tp – durata probei, s.

Table 1

Results of test taken in operating conditions [1]

Sample	Programmed flow (Q_p) [t/h]	Sample duration (t_p) [s]	Sample weight (M_p) [kg]	Calculated flow (Q_c) [t/h]	Dosing error (ε_d) [%]
I	1	60	17,200	1,032	3,20
II		60	17,100	1,026	2,60
III		60	17,250	1,035	3,50
Average		60	17,183	1,031	3,10
I	2	60	34,300	2,058	2,90
II		60	34,400	2,064	3,20
III		60	32,900	1,974	1,30
Average		60	33,866	2,032	1,60
I	3	30	25,500	3,064	2,13
II		30	25,200	3,024	0,80
III		30	25,700	3,082	2,70
Average		30	25,466	3,056	1,86
I	4	30	34,300	4,116	2,90
II		30	34,100	4,092	2,30
III		30	33,900	4,068	1,70
Average		30	34,100	4,092	2,30
I	5	30	42,700	5,124	2,48
II		30	42,400	5,088	1,76
III		30	42,600	5,104	2,08
Average		30	42,566	5,108	2,16

Figure 4 shows the dosing error variation depending on the sample weight on sample duration of 30 seconds.

In figura 4 este arătată variaţia erorii de dozare în funcţie de masa probei la o durată de probei de 30 sw secunde.

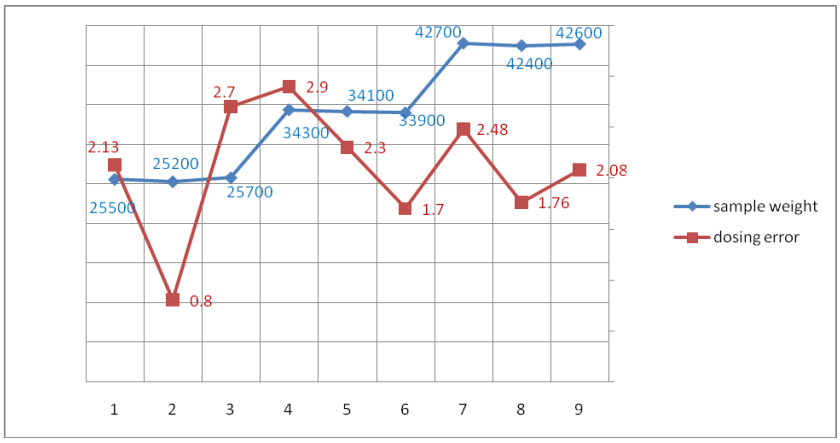

Fig. 4 - Variations of dosing error depending on the sample weight

CONCLUSIONS

Continuous flow dosage of finished agricultural products is a complex and important operation for the destination and future processing of those products. This operation is made using the Dosing Technical Equipment DTE integrated in different technological flows in small and medium capacity milling units and also in unit making concentrated fodder, in several points of processing the quantitative information, according to the programming of the electronic unit [1].

Through the constructive and functional solutions adopted following the experimental tests, it was found that the Dosing Technical Equipment DTE offers a series of advantages such as:

CONCLUZII

Dozarea în flux continuu a produselor agricole finite este o operaţie tehnologică complexă şi important pentru destinaţia ulterioară a acestor produse. Această operaţie se realizează utilizând echipamentul tehnic de dozare ce poate fi integrat în fluxul tehnologic al unităţilor de morărit de mică şi medie capacitate cât şi în cadrul unor fabrici de nutreţuri combinate în diverse puncte de prelucrare a informaţiei cantitative, în concordanţă cu unitatea electronică de programare [1].

Prin soluţiile constructive şi funcţionale adoptate în urma investigărilor experimentale s-a constatat că Echipamentul tehnic de dozare ETD prezintă următoarele avantaje:

- high dosing precision;
- adjusting the product flow to a programmed value;
- automated management of product quantities throughout the whole technological flow;
- easy maintenance and exploiting;
- visualizing the product feed through the transparent tube of the feeding funnel;
- hermetic connection to the piping of the technological installation where it is integrated;
- modern design;
- reduced specific material and energy consumption.

We can therefore conclude that the use of automated weighing and dosing technological operation bring a growth in the economical efficiency of the productive unit and have an immediate impact on the management of the processed product.

ACKNOWLEGEMENT

The experimental model of Dosing Technical Equipment DTE was achieved in the NUCLEU Program.

REFERENCES

[1]. Brăcăcescu C., Milea D., Păun A., Ganea I., Găgeanu I. (2013) – *Researches on automation of dosing and sacking process of finished agricultural products*, Annals of the University of Craiova – Agriculture Mountainology - Cadastre Vol. XLIII 2/2013, pg. 37-44;
[2]. Buium Gh. F. (1999) – *Researches on mechanisms in the structure of dosing systems*, Gh. Asachii" Technical University Publishing, Iaşi;
[3]. Merticaru V. (1997) – *Packing and packaging mechanisms, Documentary Information Office for the engineering industry*, Bucharest;
[4]. Ortega-Rivas Enrique, Juliano Pablo, Yan Hong (2005) – *Food Powders: Physical Properties, Processing, and Functionality,* 2005, XVI, pg. 272-287;
[5]. Ola D., Popescu S. (2006) – *Functional particularities of the gravimetric dosing systems used in agriculture and food industry,* Scientific Papers (INMATEH), vol.18 no.3/2006, pg. 261-268;
[6]. Păun A., Cojocaru I. (2007) – *Optimization of homogenization process in concentrated fodder installation-IONC*, Scientific Papers (INMATEH), vol.21 no.3/2007, pg. 21-29;
[7]. Popescu S. (2005) – *Influence of functional parameters of the gravimetric dosing process of granular agro-food material*, Buletin of The Transilvania University of Brasov, series A, vol II (47), pg. 169-176;
[8]. Rhodes M. (1998) – *Mixing and segregation*. In Introduction to Particle Technology, John Wiley & Sons, West Sussex, England, pg. 224–240;
[9]. Vetter G. (1998) – *The Dosing Handbook,* Vulkan-Verlag, Essen., Elsevier Science, pg. 670 -710

- precizie de dozare ridicată;
- reglarea debitului de produs la o valoare programată;
- gestionarea automată a cantităţilor de produs pe întregul parcurs al fluxului tehnologic;
- întreţinere şi exploatare facile;
- vizualizarea alimentării cu produs prin tubul transparent al pâlniei de alimentare;
- racordarea etanşă la tubulatura instalaţiei tehnologice în care se integrează;
- design modern;
- consumuri specifice de materiale şi energie reduse.

Putem concluziona deci, că utilizarea tehnologiilor de cântărire şi dozare automată aduc cu sine o creştere a eficienţei economice şi au un impact imediat asupra managementului produselor procesate.

MULŢUMIRI

Modelul experimental al Echipamentului tehnologic pentru cântărire şi gestionare automată ECGA a fost realizat în cadrul Programului NUCLEU.

BIBLIOGRAFIE

[1]. Brăcăcescu C., Milea D., Păun A., Ganea I., Găgeanu I (2013) – *Cercetări privind automatizarea dozării şi însăcuirii produselor agricole finite*, Analele Universităţii din Craiova, seria Agricultură – Montanologie – Cadastru Vol. XLIII 2/2013, p. 37-44;
[2]. Buium GH. F. (1999) – *Cercetări privind mecanismele din structura sistemelor de dozare*, Ed. Universităţii Tehnice "Gh. Asachii" Iaşi;
[3]. Merticaru V. (1997) – *Ambalaje şi mecanisme de ambalat*, Oficiul de Informare Documentară pentru Industria Constructoare de Maşini, Bucureşti;
[4] Ortega-Rivas Enrique, Juliano Pablo, Yan Hong (2005) – *Prafuri alimentare: Proprietati fizice, procesare si functionalitate*, 2005, XVI, pag. 272-287;
[5]. Ola D., Popescu S. (2006) – *Particularităţile funcţionale ale sistemelor de dozare gravimetrică utilizate în agricultură şi industria alimentară,* Lucrări Ştiinţifice (INMATEH),vol.18 nr.3/2006, pag. 261-268;
[6]. Păun A., Cojocaru I. (2007) - *Optimizarea procesului de omogenizare in instalatiile pentru obtinerea nutreturilor concentrate – IONC*, Lucrări Ştiinţifice (INMATEH), vol.21 nr.3/2007, pag. 21-29;
[7]. Popescu S. (2005) – *Influenta parametrilor functional ai procesului de dozare gravimetric a materialului agro-industrial granulat*, Buletinul Universitatii Transilvania Brasov, seria A, vol II (47), pag. 169-176;
[8]. Rhodes M. (1998) – *Amestecare si separare*. Introducere in tehnologia particulelor, John Wiley & Sons, West Sussex, Anglia, pag. 224–240;
[9]. Vetter G. (1998) – *Manualul dozării*, Elsevier Science, pag. 670 -710.

INVESTIGATION OF THE STABILITY OF THE TORSORIAL VIBRATIONS OF A SCREW CONVEYER UNDER THE INFLUENCE OF PULSE FORCES
/
ДОСЛІДЖЕННЯ СТІЙКОСТІ КРУТИЛЬНИХ КОЛИВАНЬ ШНЕКА ПІД ДІЄЮ ІМПУЛЬСНИХ СИЛ

Prof. Ph.D. Eng. Hevko I.B., Lect. Ph.D. Eng. Dyachun A.Ye., Lect. Ph.D. Eng. Hud V.Z., Rohatynska L.R., Klendiy V.M.
Ternopil Ivan Pul'uj National Technical University, Ruska str., 56, Ternopil / Ukraine
E-mail: gevkoivan1@rambler.ru .

Abstract: *The aim of the research is to analyze the influence of pulse forces on non-linear torsorial vibrations of a screw conveyer.*

The methodology is based on the combination of the methods by Bubnov-Halorkin and Van der Pol. With the help of this methodology we have developed the so called equations of a standard form for the case of pulse forces action.

A mathematical model of the torsorial vibrations of a screw conveyer under the influence of pulse forces is presented. It has been determined, that there is a jump pattern of change of the amplitude-frequency characteristics of the torsorial vibrations of a screw conveyer. Resonance torsorial vibrations of a screw conveyer under the influence of pulse forces have been considered. Torsorial vibrations of a screw conveyer have been investigated in case, when the moment of resistance forces is proportional to the relative angular velocity, and the moment of pulse forces is approximated by a non-linear function. It has been determined, that in such a case the influence of pulse forces becomes apparent only in the change of frequency of the vibrations of a screw conveyer. The amplitude-frequency characteristics of the torsorial vibrations of a screw conveyer of different geometrics have been presented.

Keywords: *screw conveyer, torsional vibrations, pulse forces*

INTRODUCTION

Conveyer transport and technological mechanisms are widely used in different branches of industry, including mining industry, for the transportation of bulk and lump material. The efficiency of the operation of many bays, shops and the whole enterprises depends on their reliable functioning. Screw conveyers can be characterized by the simplicity of their design and, consequently, high reliability, easiness of operation and adjustment when used in automated systems and by being ecologically-friendly to the environment because of their hermeticity [2], [4], [5]. High speed screw conveyers are used for all-purpose loading and unloading complexes, which are designed to transport load on horizontal, declining and vertical routes. The existing methods are based on a number of theoretical and experimental investigations as well as on the analysis of the statistical data on the results of their exploitation. In order to provide the reliability and the quality of the technological processes performed by conveyer mechanisms, it is necessary to take into account the dynamic vibrations, caused by outside power factors and the peculiarities of the functioning of screw conveyers.

The fundamentals of the designing and the investigation of screw conveyers were layed by such scientists as A.M. Grigoryev [5], B.M. Gevko [2], R.M. Rohatynskyi [2], V.S. Loveikin [6], R.B. Gevko [4] and

Резюме: *Мета роботи – провести аналіз впливу імпульсних сил на нелінійні крутильні коливання шнека.*

Методика базується на поєднанні методів Бубнова-Гальоркіна та Ван-дер-Поля. Із її допомогою отримано так звані рівняння у стандартному вигляді для випадку дії імпульсних сил.

Представлено математичну модель крутильних коливань шнека у випадку дії імпульсних сил. Встановлено стрибкоподібний характер зміни амплітудно-частотних характеристик крутильних коливань шнека. Розглянуто резонансні крутильні коливання шнека під дією імпульсних сил. Досліджено крутильні коливання шнека за умови, що момент сил опору пропорційний відносній кутовій швидкості руху шнека, а момент імпульсних сил апроксимується нелінійною функцією. Встановлено, що в цьому випадку вплив імпульсних сил проявляється в зміні лише частоти коливань шнека. Представлено амплітудно-частотні характеристики крутильних коливань шнека за різних значень його геометричних параметрів.

Key words: *шнек, крутильні коливання, імпульсні сили*

ПЕРЕДМОВА

Шнекові транспортно-технологічні механізми широко використовують у різних галузях промисловості, в тому числі і у видобувній для транспортування сипких та кускових матеріалів. Від надійної їх роботи залежить ефективність діяльності багатьох дільниць, цехів і підприємств загалом. Шнекові транспортери характеризуються простотою конструкції та, відповідно, високою надійністю, простотою в користуванні та легкістю адаптування при використанні в автоматизованих системах, екологічністю використання внаслідок їх герметичності [2], [4], [5]. Для універсальних розвантажувально-завантажувальних комплексів, які призначені для транспортування вантажу, як по горизонтальних, похилих, так і вертикальних трасах, використовують швидкохідні шнекові конвеєри. Існуючі методи їх розрахунку ґрунтуються на ряді теоретичних та експериментальних досліджень а також аналізі статистичних даних за результатами їх експлуатації. Для забезпечення надійності та якості виконання технологічних процесів шнековими механізмами необхідно враховувати динамічні коливання, які зумовлені зовнішніми силовими факторами та особливостями роботи шнеків.

Основи проектування та дослідження гвинтових конвеєрів заклали такі вчені як А.М. Григорьев [5],

other. The development of the theory of vibrations was elaborated by V.S. Loveikin [6], L.Q. Chen [1] and other. In case of forced vibrations, in other words those vibrations, which are caused by the influence of periodical forces, the frequency of which is altering in time, the amplitude of vibrations and the dynamic stress essentially depend on the frequency of the forcing power. When the above mentioned frequencies are the same, or when the frequency of forcing power approximitates the frequency of natural oscillations in a screw conveyer and in case of low damping, resonance is developing [7,3], that is the amplitude of vibrations which is increasing rapidly. Such a rise in the amplitude causes an essential increase of a twist angle or deflection of a conveyer. With the increase of angle or linear deformations, the dynamic stress in the working bodies of screw conveyers increases as well. In this case, dynamic stress (resonance) depends both on inside factors (physical and mechanical parameters of a screw conveyer, its geometrics etc.) and on the outside ones. The outside factors include the angle speed of the rotation of a conveyer and the value of ouside disturbing forces for flexural [3] and torsorial vibrations [7].

MATERIAL AND METHOD

General results, presented in papers [7,3], are used for the investigation of the influence of pulse forces on the torsorial vibrations of a screw conveyer. A screw conveyer rotates about an axis, making torsorial and flexural vibrations. In many cases the last ones cause short-lasting periodical influence on torsorial vibrations. The question is about the contact of a screw and a casing, transportation of bulk loads of relatively large sizes and other. A mathematical model of the torsorial vibrations of a screw conveyer for the above mentioned influence of outside immediate forces is the following differential equation

Б.М. Гевко [2], Р.М. Рогатинський [2], В.С. Ловейкін [6], Р.Б. Гевко [4] та інші. Розвитку теорії коливань присвячені праці В.С. Ловейкіна [6], L.Q. Chen [1] та інших. У випадку вимушених коливань, тобто таких, що викликані впливом змінних у часі періодичних сил, точніше кажучи таких, частота котрих змінюється в часі, амплітуда коливань, а значить динамічні напруження, суттєво залежать від частоти вимушуючої сили. При співпаданні вказаних частот, або при наближенні частоти вимушуючої сили до частоти власних коливань шнека та слабкому демпфуванні розвивається резонанс [7, 3], тобто різко збільшується амплітуда коливань. Такий ріст амплітуди спричиняє значне зростання кута закручення чи прогину шнека. Із ростом кутових чи лінійних деформацій зростають динамічні напруження у шнекових робочих органах. При цьому динамічні напруження (резонансні) залежать як від внутрішніх чинників (фізико-механічних параметрів шнека, геометричних розмірів та 78бу.), так і від зовнішніх. До зовнішніх слід віднести кутову швидкість обертання шнека й величину зовнішніх 78 збурюючих сил для згинних [3] та крутильних коливань [7].

МАТЕРІАЛ І МЕТОДИКА

Викладені загальні результати у роботах [7, 3] використаємо для дослідження впливу імпульсних сил на крутильні коливання шнека. Шнек обертається навколо осі, здійснюючи крутильні та згинальні коливання. В багатьох випадках останні спричиняють короткотривалу періодичну дію на крутильні коливання. Мова йде про контакт шнеку із кожухом, переміщення сипких вантажів відносно великих розмірів та ін. Математичною моделлю крутильних коливань шнеку для вказаної дії зовнішніх миттєвих сил є диференціальне рівняння

$$I\frac{\partial^2\theta}{\partial t^2}-\frac{\partial}{\partial x}\left(GJ\frac{\partial\theta}{\partial x}\right)=Q\left(\theta,\frac{\partial\theta}{\partial t},\frac{\partial\theta}{\partial x},\right)+\sum_{i=1}^{n}Q_i\left(\theta,\frac{\partial\theta}{\partial x},\frac{\partial\theta}{\partial t}\right)\cdot\sum_{j=1}\delta\left(t-\left(t_i+j\tau\right)\right),, \quad (1)$$

where $\theta(x,t)$ - twist angle of a screw conveyer, I - linear moment of inertia of a screw conveyer about a strain-free axis, G - shear modulus of the material of a screw conveyer, J - equatorial moment of the cross-section of a screw conveyer, $\delta(...)$ - Dirac function, which acts periodically over a period of τ at time moments t_i , $Q_i\left(\theta,\frac{\partial\theta}{\partial x},\frac{\partial\theta}{\partial t}\right)$ - function, which characterizes the intensity of pulse forces action at the time moments mentioned.

If the properties of δ –function are used:

де $\theta(x,t)$ - кут закручення шнека, I - погонний момент інерції шнека відносно недеформованої осі, G - модуль зсуву матеріалу шнека, J - екваторіальний момент поперечного перерізу шнека, $\delta(...)$ - функція Дірака, яка діє періодично із періодом τ у моменти часу t_i , $Q_i\left(\theta,\frac{\partial\theta}{\partial x},\frac{\partial\theta}{\partial t}\right)$ - функція, яка характеризує інтенсивність дії імпульсних сил у вказані моменти часу.

Якщо використати властивості δ – функції:

$$f(t)\delta(t)=f(0)\delta(t),$$

$$\sum_j\delta(t-j\tau)=\frac{\upsilon}{\pi}\left[\frac{1}{2}+\sum_{j=1}\cos j\upsilon t\right]; \quad (2)$$

$$\int_{-\infty}^{t}\delta(t)\,dt=\begin{cases}1, npu & t>0,\\ 0, npu & t\le 0,\end{cases} \quad (3)$$

the system of differential equations (1) after the averaging is as follows:

то система диференціальних рівнянь (1) після усереднення набуває вигляду

$$\frac{da}{dt} = -\frac{\mu}{\omega_\theta}\left\{F^s_{k0}(a) + \frac{\upsilon}{2\pi}\sum_{i=1} F^s_{ik0}(0)\right\}, \qquad (4)$$
$$\frac{d\varphi}{dt} = -\frac{\mu}{a\omega_\theta}\left\{F^c_{k0}(a) + \frac{\upsilon}{2\pi}\sum_{j=1} F^c_{jk0}\right\},$$

where $\upsilon = \frac{2\pi}{\tau}$, ω_θ – frequency of the vibrations in a screw conveyer.

If it is technically considered, the fact that the above mentioned equations can be integrated, then the dynamic process of a screw conveyer can be shown as

де $\upsilon = \frac{2\pi}{\tau}$, ω_θ – частота власних коливань шнека.

Якщо формально вважати, що вказані рівняння вдається зінтегрувати, то динамічний процес шнеку представляється у вигляді

$$\theta(x,t) = a(t)\,X(x)\cos\left(\omega_\theta t + \varphi(t)\right), \qquad (5)$$

In (5) the amplitude of torsorial vibrations $a(t)$ and its phase $\psi = \omega_\theta t + \varphi(t)$ are determined by the system (4).

The indicated solution will be the first approximation to the task stated. In order to describe a jump pattern of change for the main parameters of the torsorial vibrations of a screw conveyer, it is necessary to find its first improved approximation. In order to find it, we assume, that the solution of the differential equations (4) is the functions $a = a(t)$ і $\psi = \psi(t)$. Then, the first "improved" approximation of the parameters a and ψ is represented as follows

У (5) амплітуда крутильних коливань $a(t)$ та її фаза $\psi = \omega_\theta t + \varphi(t)$ визначаються системою (4). Вказаний розв'язок буде першим наближенням поставленої задачі. Щоб описати стрибкоподібний характер зміни основних параметрів крутильних коливань шнеку, необхідно знайти його перше покращене наближення. Для його знаходження припускаємо, що розв'язком диференціальних рівнянь (4) є функції $a = a(t)$ і $\psi = \psi(t)$. Тоді перше "покращене" наближення параметрів a і ψ представляється у вигляді

$$a_{покр.} = a - \frac{\mu}{\omega_\theta}\left\{\frac{\upsilon}{\pi}\sum_{i=1}^{n} F^s_{i0}(a)\,\sigma(t,t_i) + \frac{\upsilon}{2\pi}\sum_{i=1}^{n}\sum_{n}\frac{-F^{ss}_{in}(a)\cos(n\psi) + F^{sc}_{in}(a)\sin(n\psi)}{n\omega_\theta} + \right.$$
$$+\frac{\upsilon}{2\pi}\sum_{i=1}^{n}\sum_{n}\left(\frac{F^{ss}_{in}(a)}{(n\omega_\theta)^2 - (k\upsilon)^2}\left(2n\omega_\theta \sin(n\psi)\cos k\upsilon(t-t_i) - -2k\upsilon\cos(n\psi)\sin k\upsilon(t-t_i)\right) + \right. \qquad (6)$$
$$+\frac{F^{ss}_{in}(a)}{(n\omega_\theta)^2 - (k\upsilon)^2}\left(-2n\omega_\theta\cos(n\psi)\cos k\upsilon(t-t_i) + +2k\upsilon\sin(n\psi)\sin k\upsilon(t-t_i)\right)) +$$
$$\left.\left. +\sum_{n}\frac{-F^{sc}_{n}(a)\cos(n\psi) + F^{sc}_{n}(a)\sin(n\psi)}{n\omega_\theta}\right\},$$

$$\psi_{покр.} = \omega t - \frac{\varepsilon}{a\omega_\theta}\left\{\frac{\upsilon}{\pi}\sum_{i=1}^{n} F^c_{ki0}(a)\,\sigma(t,t_i) + \frac{\upsilon}{2\pi}\sum_{i=1}^{n}\sum_{n}\frac{-F^{cc}_{in}(a)\cos(n\psi_k) + F^{cs}_{in}(a)\sin(n\psi_k)}{n\omega_\theta} + \right.$$
$$+\frac{\upsilon}{2\pi}\sum_{i=1}^{n}\sum_{n}\left(\frac{F^{cs}_{in}(a)}{(n\omega_\theta)^2 - (k\upsilon)^2}\left(2n\omega_\theta \sin(n\psi)\cos k\upsilon(t-t_i) - -2k\upsilon\cos(n\psi)\sin k\upsilon(t-t_i)\right) + \right.$$
$$+\frac{F^{cs}_{in}(a)}{(n\omega_\theta)^2 - (k\upsilon)^2}\left(2n\omega_\theta\cos(n\psi_k)\cos k\upsilon(t-t_i) + +2k\upsilon\sin(n\psi)\sin k\upsilon(t-t_i)\right)) +$$
$$\left.\left. +\sum_{n}\frac{-F^{ss}_{n}(a)\cos(n\psi_k) + F^{ss}_{n}(a)\sin(n\psi_k)}{n\omega_\theta}\right\},$$

where $\sigma(t,t_i)$ – periodical function, which is the sum of $\sum_j \frac{\sin j\upsilon(t-t_i)}{j}$

The above mentioned shows, that in non-resonance case, the pulse pattern of loading becomes apparent in the jump change of the amplitude $a_{покр}$ and phase $\psi_{покр}$ at the moment of pulse forces action. The value of the jumps is low because the intensity of pulse forces is low. Despite of this, during the use of screw machinery their action is increasing and in some time it can lead to major amplitudes of torsorial vibrations.

Resonance torsorial vibrations of a screw conveyer under the influence of pulse forces should be considered. Much more important case of torsorial vibrations is the one, where the frequency of natural oscillations is connected with the frequency of pulse disturbance by the correlation $\omega_\theta \approx \frac{q}{p}\upsilon$ (p,q – reciprocals); here $\upsilon = \frac{2\pi}{\tau}$.

The above mentioned substantiates the following differential equation for pulse forces action

де $\sigma(t,t_i)$ – періодична функція, яка є сумою ряду $\sum_j \frac{\sin j\upsilon(t-t_i)}{j}$.

Із вищезазначеного випливає, що в нерезонансному випадку імпульсний характер навантаження проявляється в стрибкоподібній зміні амплітуди $a_{покр}$ та фази $\psi_{покр}$ в момент дії імпульсних сил. Величини стрибків малі, через те, що інтенсивність імпульсних сил мала. Не дивлячись на це, їх дія за період експлуатації шнекових машин наростає і з часом може привести до значних амплітуд крутильних коливань.

Розглянемо резонансні крутильні коливання шнека під дією імпульсних сил. Набагато важливішим випадком крутильних коливань є випадок, коли частота власних коливань пов'язана із частотою імпульсного збурення співвідношенням $\omega_\theta \approx \frac{q}{p}\upsilon$ (p,q – взаємно прості числа); тут $\upsilon = \frac{2\pi}{\tau}$.

Зазначене дає підстави диференціальне рівняння за дії імпульсних сил записати у вигляді

$$\frac{d^2T}{dt^2} + \left(\frac{q}{p}\upsilon\right)^2 T = \mu(\bar{F}\left(T, \frac{dT}{dt}, \upsilon t\right) - \Delta T + \sum_{j=1}^{n} \bar{F}_j\left(T, \frac{dT}{dt}, \upsilon t\right) \cdot \sum_{i=1}^{m} \delta\left(t - (t_i + j\tau)\right)); \quad (7)$$

$$\omega_\theta^2 = \left(\frac{q}{p}\upsilon\right)^2 + \mu\Delta, \quad (8)$$

where $\mu\Delta$ – deregulation of frequencies $T(t) = a\cos\psi$. In this case, the usual differential equations relative to variables $a(t)$ and $\varphi(t)$ acquire the form of

де $\mu\Delta$ – розбалансування частот, $T(t) = a\cos\psi$.

В такому разі звичайні диференціальні рівняння відносно змінних $a(t)$ і $\varphi(t)$ набувають вигляду

$$\frac{da}{dt} = -\sin\psi \frac{p\mu}{q\upsilon}\left(\bar{F}\left(a\cos\psi, -a\upsilon\frac{q}{r}\sin\psi\right) - \Delta a \frac{q}{p}\upsilon\cos\psi_k + \sum_{i=1}^{n}\bar{F}_i\left(a\cos\psi, -a\upsilon\frac{q}{p}\sin\psi\right)\sum_j \delta\left(t - (t_i + j\tau)\right)\right) \quad (9)$$

$$\frac{d\varphi}{dt} = -\cos\psi \frac{p\varepsilon}{aq\upsilon}\left(\bar{F}\left(a\cos\psi, -a\upsilon\frac{q}{p}\sin\psi\right) - \Delta a \frac{q}{p}\upsilon\cos\psi + \sum_{i=1}^{n}\bar{F}_i\left(a\cos\psi, -a\upsilon\frac{q}{p}\sin\psi\right)\sum_{j=1} \delta\left(t - (t_i + j\tau)\right)\right).$$

Taking into consideration the assumption, that $Q(...)$ and $Q_j(...)$ - multinominals, the functions $\bar{F}(a\cos\psi, -a\omega_\theta\sin\psi)$ and $\bar{F}_i(a\cos\psi, -a\omega_\theta\sin\psi)$ are represented in the form of Fourier series. Using the information above and the properties of δ of Dirac function (2), (3), the system of the differential equations (9) after the approximation acquires the form of

Беручи до уваги припущення, що $Q(...)$ та $Q_j(...)$ – многочлени, функції $\bar{F}(a\cos\psi, -a\omega_\theta\sin\psi)$ і $\bar{F}_i(a\cos\psi, -a\omega_\theta\sin\psi)$ їх представляємо у вигляді сум Фур'є. Використовуючи вище наведене та властивості δ функції Дірака (2), (3), система диференціальних рівнянь (9) після усереднення набуває вигляду

$$\frac{da}{dt} = -\frac{\mu p}{2\pi q\upsilon}\sum_{i=1}^{n}(F_{i0}^{s}(a) + \sum_n (F_{in}^{sc}(a)\cos n(p\varphi + q\upsilon t_i) + F_{in}^{ss}(a)\sin n(p\varphi + q\upsilon t_i))) + F_0^s(a)).$$

Thus, in resonance case, in contrast to non-resonance, in the approximated equations the additional terms have appeared. But similarly to non-resonance case, the values $a_{покр}$ and $\psi_{покр}$ at the

Таким чином, у резонансному випадку, на відміну від нерезонансного, в усереднених рівняннях з'явились додаткові члени. Проте, аналогічно нерезонансному випадку, величини

moment of pulse forces action show a jump change.

The torsorial vibrations of a screw conveyer should be considered in case, when the moment of sustaining power is proportional to relative angular velocity of a screw conveyer $\frac{\partial\theta(x,t)}{\partial t}$, and the moment of pulse forces is approximated by the function $\lambda\theta(x,t)+\gamma\theta^3(x,t)$. The differential equation of the torsorial vibrations of a screw conveyer is as follows

$a_{покр}$ і $\psi_{покр}$ в момент дії імпульсних сил змінюються стрибкоподібно.

Розглянемо крутильні коливання шнека за умови, що момент сил опору пропорційні відносній кутовій швидкості руху шнеку $\frac{\partial\theta(x,t)}{\partial t}$, а момент імпульсних сил апроксимується функцією $\lambda\theta(x,t)+\gamma\theta^3(x,t)$. Диференціальне рівняння крутильних коливань шнеку в такому разі матиме вигляд

$$\frac{\partial^2\theta}{\partial t^2}-\frac{GJ_0}{I_0}\frac{\partial^2\theta}{\partial x^2}=\mu(\lambda\theta(x,t)+\gamma\theta^3(x,t)\times\sum_{j=1}^{n}\sum_{i=1}^{m}\delta\left(t-\left(t_i+j\tau\right)\right)-\beta\frac{\partial\theta}{\partial t}). \quad (10)$$

According to the method by Bubnov-Halorkin, the solution to the equation (10) is shown to be the same as in paper [7] in the form of $\theta(x,t)=X(x)T(t)$. After simple transformations, the differential equations are reduced to a simple form of differential equation

Відповідно до методу Бубнова-Гальоркіна розв'язок рівняння (10) представимо як і в роботі [7] у вигляді $\theta(x,t)=X(x)T(t)$. Після нескладних перетворень диференціальні рівняння зводяться до звичайного диференціального рівнянь вигляду

$$\frac{d^2T(t)}{dt^2}+\left(\frac{k\pi}{l}\right)^2\frac{GJ_0}{I_0}T(t)=\mu(\left(\lambda T+\gamma T^3\right)\times\sum_{i=1}^{2}\sum_{j}\delta\left(t-\left(t_i+j\tau\right)\right)-\beta\frac{dT}{dt}). \quad (11)$$

For non-resonance vibrations of a screw conveyer, the amplitude and the frequency of the vibrations according to the results given in paper [3] ($t_1=0$, $t_2=\frac{\pi}{2\upsilon}$.) are described with the help of the differential equations

Для нерезонансних коливань шнеку амплітуда та частота коливань шнеку відповідно до результатів роботи [3] ($t_1=0$, $t_2=\frac{\pi}{2\upsilon}$.) описуються диференціальними рівняннями

$$\frac{da}{dt}=-\mu\beta\frac{a}{2},$$

$$\frac{d\psi}{dt}=\omega_\theta-\frac{\mu}{\omega_\theta\pi}\left(\frac{\lambda\upsilon}{8}+\frac{3\gamma a^2\upsilon}{32}\right).$$

Having integrated the obtained system of differential equations, the first approximation of the solution to the equation of the torsorial vibrations of a screw conveyer is found

Зінтегрувавши отриману систему диференціальних рівнянь, знаходимо перше наближення розв'язку рівняння крутильних коливань шнека у вигляді

$$T(t)=a_0e^{-\frac{\beta}{2}t}\cos\left(\omega t+\theta_0-\frac{\lambda\upsilon t}{8\pi\omega}+\frac{3\gamma\upsilon a_0^2}{32\pi\beta\omega}e^{-\beta t}\right), \quad (12)$$

Where

a_0 and θ_0 are determined to be starting conditions.

Thus, the influence of pulse forces becomes apparent only in change of the frequency of the vibrations of a screw conveyer.

Resonance vibrations should be considered. Let's assume, that the frequency of natural oscillations of a screw conveyer is connected with the frequency of the pulse disturbance by the following correlation

де

a_0 і θ_0 визначаються початковими умовами.

Таким чином, вплив імпульсних сил проявляється в зміні лише частоти коливань шнека.

Розглянемо резонансні коливання. Нехай частота власних коливань шнека зв'язана із частотою імпульсного збурення співвідношенням

$$\omega\approx q\frac{\upsilon}{2}. \quad (13)$$

In this case, a first approximation of the solution of the differential equation (12) has the following form

В такому разі перше наближення розв'язку диференціального рівняння (12) матиме вигляд

$$T(t) = a(t)\cos\left(\frac{\upsilon}{2}qt + \varphi(t)\right),$$

.where functions $a(t)$ and $\varphi(t)$ are determined from the system of differential equations.

де функції $a(t)$ і $\varphi(t)$ визначаються із системи диференціальних рівнянь.

$$\frac{da}{dt} = -\mu\left(\frac{\beta a}{2} + \frac{a\left(2\lambda+\gamma a^2\right)}{4\pi q}\left(\sin 2\varphi + \sin\left(2\varphi + q\frac{\pi}{2}\right)\right) - -\frac{\gamma a^3}{8\pi q}\left(1+(-1)^q\right)\sin 4\theta\right);$$

$$\frac{d\varphi}{dt} = \frac{\omega_\theta{}^2 - \left(\frac{q\upsilon}{2}\right)^2}{\omega_\theta} - \mu\left(\frac{4\lambda+3\gamma a^2}{4\pi q} + \frac{\lambda+\gamma a^2}{2\pi q}\times\left(\cos 2\varphi + \cos\left(2\varphi + q\frac{\pi}{2}\right)\right) + \frac{\gamma a^2}{8\pi q}\left(1+(-1)^q\right)\cos 4\varphi\right). \qquad (14)$$

Figure 1 shows the amplitudes of the torsional vibrations of a screw conveyer when there is a transition through the resonance at different parameter values $\omega_\theta = \frac{k\pi}{l}\sqrt{\frac{GJ_0}{I_0}}$ at $l = 10м;\quad G = 80ГПа;$ $I_0 = 3,4675кгм$ **.**

На рис. 1 наведено амплітуди крутильних коливань шнека при переході через резонанс за різних значень параметра $\omega_\theta = \frac{k\pi}{l}\sqrt{\frac{GJ_0}{I_0}}$ при $l = 10м;\ G = 80ГПа;\ I_0 = 3,4675кгм$.

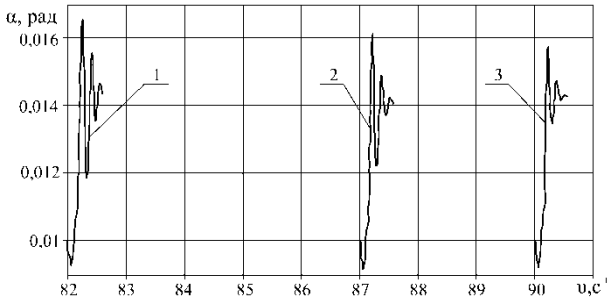

Fig. 1 – The amplitudes of resonance torsorial vibrations at different values of the parameter ω_θ at:

1 – $J_0 = 0,10248\times10^{-4}м^4$; 2 – $J_0 = 0,1147\times10^{-4}м^4$; 3 – $J_0 = 0,1215\times10^{-4}м^4$

RESULTS

In the above mentioned materials and methods for certain models of non-linear and periodical pulse forces, we have got differential equations of the change of amplitude and frequency characteristics of vibrations and on the basis of its numerical integration, graphical relations of the resonance amplitude of the torsorial vibrations of a screw conveyer at different values of its natural oscillations were developed. It is connected with the fact, that even relatively simple differential equations of standard form can be integrated only in some cases. Numerical integration of the equations of standard form provides relatively complete information about the dynamic process at specified fixed values of the parameters. However, it is not always possible to track how the change of starting conditions of the specified (and other) parameters can influence the dynamic process using the results of numerical integration. It can be stated based upon the stability of the process. The investigation of the stability of vibrations is as important as the task of finding a solution. That is why, we have to investigate the stability of the vibrations, which were considered, that is to say, permanent values of the amplitude of vibrations for resonance. In order to do this, it is necessary to put the right parts of the

РЕЗУЛЬТАТИ

У вказаних вище матеріалах і методиках для конкретних моделей нелінійних і періодичних імпульсних сил отримано диференціальні рівняння зміни амплітудно-частотних характеристик коливань та побудовано на основі чисельного його інтегрування графічні залежності резонансної амплітуди крутильних коливань шнеку за різних значень частоти його власних коливань. Це зв'язано з тим, що навіть отримані відносно прості, диференціальні рівняння у стандартному вигляді вдається зінтегрувати лише в окремих випадках. Чисельне ж інтегрування рівнянь у стандартному вигляді дає достаньо повну інформацію про динамічний процес за заданих фіксованих значень параметрів. Однак, прослідкувати як впливає зміна початкових значень наведених (та інших) параметрів на динамічний процес із результатів чисельного інтегрування не завжди вдається. Про наведене достатньо точно можна твердити виходячи із стійкості процесу. Дослідження стійкості коливань є не менш важливою задачею як знаходження розв'язку. Тому нижче дослідимо стійкість розглянутих коливань, точніше кажучи стаціонарних значень амплітуди коливань для резонансу. Для цього відповідно до, прирівняємо праві частини

correlations, which describe the resonance mode of the vibrations of a screw conveyer, to zero. We get a system of algebraic equations

співвідношень, які описують резонансний режим коливань шнека до нуля. Отримуємо систему алгебраїчних рівнянь

$$\frac{\beta a}{2}+\frac{a\left(2\lambda+\gamma a^2\right)}{4\pi q}\left(\sin 2\varphi+\sin\left(2\varphi+q\frac{\pi}{2}\right)\right)-\frac{\gamma a^3}{8\pi q}\left(1+(-1)^q\right)\sin 4\theta=0\,, \tag{15}$$

$$\frac{\omega_\theta{}^2-\left(\frac{q\upsilon}{2}\right)^2}{\omega_\theta}-\mu\left(\frac{4\lambda+3\gamma a^2}{4\pi q}+\frac{\lambda+\gamma a^2}{2\pi q}\left(\cos 2\varphi+\cos\left(2\varphi+q\frac{\pi}{2}\right)\right)+\frac{\gamma a^2}{8\pi q}\left(1+(-1)^q\right)\cos 4\varphi\right)=0$$

In this system of algebraic equations, parameter $\varphi(t)$ - the difference in phases is excluded. The correlation, which determines permanent values of the amplitude of the torsorial vibrations of a screw conveyer, is found for the case of the mathematical model (10)

Із отриманої системи алгебраїчних рівнянь виключаємо параметр $\varphi(t)$ - різницю фаз. Знаходимо співвідношення, яке визначає стаціонарні значення амплітуди крутильних коливань шнека для випадку математичної моделі (10)

$$\frac{4\pi^2\beta^2}{\left(2\lambda+\gamma a^2\right)^2}+\frac{\left(4\pi\left(2\omega_\theta-\upsilon\right)-\left(4\lambda+3\gamma a^2\right)\right)^2}{16\left(\lambda+\gamma a^2\right)^2}=2\ . \tag{16}$$

This relation shows, that the amplitude of permanent vibrations of a screw conveyer (16) is actual, if the conditions are met

Отримана залежність показує, що амплітуда стаціонарних коливань шнеку (16) буде дійсною, якщо виконуються умови

$$\begin{cases}\upsilon<4\omega_\theta-\dfrac{8\lambda}{\pi}-2\sqrt{17}\,|\beta|\\ \upsilon>4\omega_\theta-\dfrac{8\lambda}{\pi}+2\sqrt{17}\,|\beta|\end{cases}, \tag{17}$$

If we put $\beta=0$ in these relations, in case of resonance $\omega_\theta\approx\frac{\upsilon}{2}$ the invariant of motion can be found for a first approximation. I order to find it, we will limit to the values of first order of smallness.

Thus, at $q=1$ we get the correlation

Якщо в отримані залежності покласти $\beta=0$, то у випадку резонансу $\omega_\theta\approx\frac{\upsilon}{2}$ для першого наближення можна знайти інваріант руху. Для його знаходження будемо обмежуватись величинами першого порядку мализни.

Так, при $q=1$ отримуємо залежність

$$\left(2\omega_\theta-\upsilon\right)\frac{1}{2}a^2-\frac{2}{\pi}a^2-\frac{3\gamma a^4}{8\pi}-\frac{2\lambda a^2+\gamma a^4}{2\sqrt{2}\pi}\cos\left(2\theta+\frac{\pi}{4}\right)=c\,, \tag{18}$$

where c — is a constant, which is determined by starting conditions.

With the help of this correlation we can evaluate the value of the amplitude of resonance vibrations. For this reason, we transform the relation (18) to the form of

де c – стала, яка визначається початковими умовами.

Із вказаної залежності можна дати оцінку величини амплітуди резонансних коливань. Для цього залежність (18) трансформуємо до вигляду

$$\cos\left(2\theta+\frac{\pi}{4}\right)=\left(\left(2\omega_\theta-\upsilon\right)\frac{1}{2}a^2-\frac{2}{\pi}a^2-\frac{3\gamma a^4}{8\pi}-c\right)\frac{2\sqrt{2}\pi}{2\lambda a^2+\gamma a^4}\,. \tag{19}$$

Having marked $\Phi\left(a^2\right)$ in the right part, we develop graphical relations $\Phi\left(a^2\right)$ as the functions from a at different fixed values c. These graphical relations under the condition $-1\le\Phi\left(a^2\right)\le 1$ determine the domain of the stability of resonance vibrations. Figure 2-3 shows these domains.

Позначивши вираз у правій частині $\Phi\left(a^2\right)$, побудуємо графічні залежності $\Phi\left(a^2\right)$ як функції від a при різних фіксованих значеннях c. Такі графічні залежності при накладеній умові $-1\le\Phi\left(a^2\right)\le 1$ визначають область стійкості резонансних коливань. Вказані області показані на рис. 2 - 3.

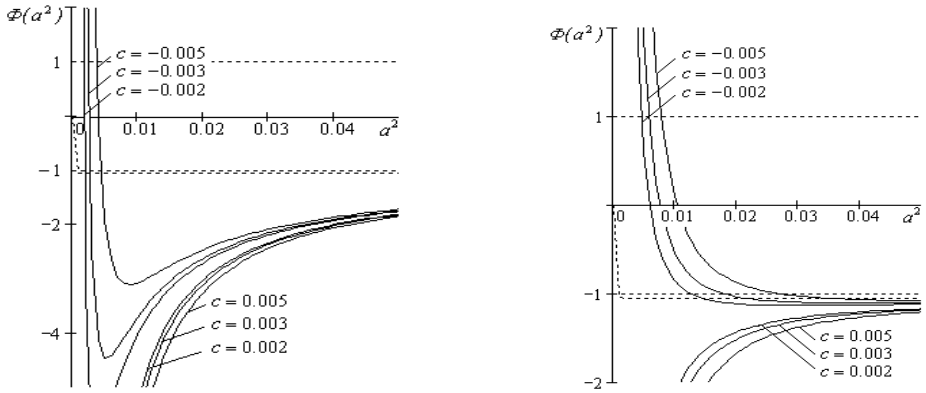

Fig. 2 – Domain of the stable values of the amplitude of the torsorial vibrations of a screw conveyer at different fixed c : a) $\gamma > 0$, $\upsilon = 2\omega_\theta + 1$, b) $\gamma > 0$, $\upsilon = 2\omega_\theta - 1$

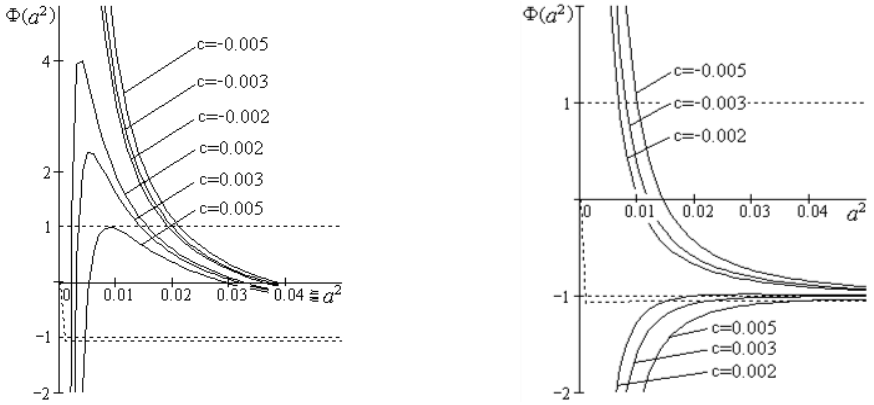

Fig. 3 - Domain of the stable values of the amplitude of the torsorial vibrations of a screw conveyer at different fixed c : a) $\gamma < 0$, $\upsilon = 2\omega_\theta + 1$, b) $\gamma < 0$, $\upsilon = 2\omega_\theta - 1$

The analysis of the graphical relations shows, that at different resonances under different conditions γ and υ, the amplitudes of the torsorial vibrations of a screw conveyer are limited. This limitedness of the amplitude of the vibrations in a system, which is described by the equation (10) in cases of the considered resonances, is the result of non-linearity of the system. This matches the known results concerning non-linear vibrations of a system. It is worth mentioning, that the action of pulse loading on a linear vibration system in resonance case leads to unlimited increase in the amplitude of vibrations.

Figure 4 shows graphical dependancies of the function $\Phi\left(a^2\right)$ - on the square of the amplitude at different values of deregulation of frequencies.

Із аналізу графічних залежностей випливає, що при резонансах за різних умов накладених γ і υ амплітуди крутильних коливань шнека будуть обмежені. Обмеженість амплітуд коливань системи, яка описується рівнянням (10) у випадку розглянутих резонансів, є наслідком нелінійності розглянутої системи. Це співпадає з відомими результатами, які стосуються нелінійних коливань систем. Слід зазначити, що дія навантаження імпульсного виду на лінійну коливну систему у резонансному випадку приводить до необмеженого росту амплітуди коливань.

Нижче на рис. 4 представлено графічні залежності функції $\Phi\left(a^2\right)$ - від квадрата амплітуди за різних значень величини розбалансування частот.

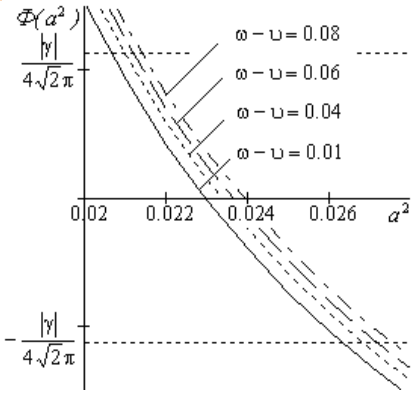

Fig. 4 – Domain of the stable values of the amplitude of the torsorial vibrations of a screw conveyer at different values of deregulation of frequencies $\omega_\theta = 79c^{-1}$, $c = -0.005$, $\gamma = 40$

The above mentioned dependancies in Figure 4 show, that the increase in the value of deregulation of frequencies shifts the domain of stable values of the amplitude of the vibrations of the flexible component of a drive to the right. In other words, the closer to the resonance, the less are the values of the amplitude of vibration, at which the dynamic process is stable. With an increase in the value of deregulation of frequencies from 0,01 c^{-1} to 0,08 c^{-1}, resonance values of the amplitude of vibrarions, at which the dynamic process is stable, increase up to 5%.

Figure 5 shows graphical dependancies of the influence of the value of non-linear restoring force (coefficient γ) on the domain of stable values for resonance amplitudes of the vibrations of a screw conveyer.

Із приведених на рис. 4 залежностей випливає, що зростання величини розбалансування частот зміщує область стійких значень амплітуди коливань гнучкого елемента привода вправо. Іншими словами, чим ближче до резонансу, тим меншими будуть значення амплітуди коливань, за яких динамічний процес стійкий. Так із зростанням величини розбалансування частот від 0,01 c^{-1} до 0,08 c^{-1} резонансні значення амплітуди коливань, за яких динамічний процес буде стійким, зростають на 5%.

На рис. 5 подані графічні залежності впливу величини нелінійної відновлювальної сили (коефіцієнта γ) на область стійких значень резонансних амплітуд коливань шнеку.

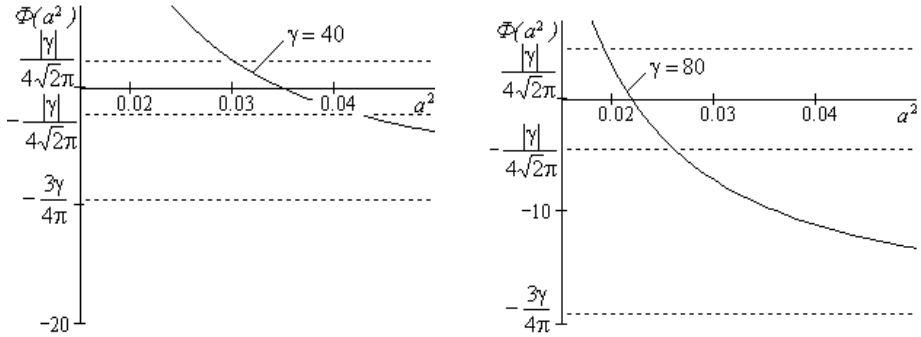

Fig. 5 – Область стійких значень амплітуди крутильних коливань шнека за різних значень коефіцієнта γ при $\omega_0 = 90$ c^{-1} $c = -0.005$

These dependancies show, that with an increase of the non-linearity of the system (for larger values of the coefficient γ), the domain of the values of the amplitude of the torsorial vibrations of a screw conveyer, at which the dynamic process is stable, narrows. At $\gamma = 80$, the domain of the values of the amplitude of the vibrations of a flexible component, at which the dynamic process is stable, is less from the domain of the values of the amplitude at $\gamma = 40$ for 42%.

Із наведених залежностей випливає, що із зростанням нелінійності системи (для більших значень коефіцієнта γ) область значень амплітуди крутильних коливань шнеку, за яких динамічний процес буде стійким звужується. При $\gamma = 80$ область значень амплітуди коливань гнучкого елемента, за яких динамічний процес буде стійким є меншою на 42% від області значень амплітуди при $\gamma = 40$.

CONCLUSION

The represented graphical dependancies and their comparison with the resonance curves in case of flexural vibrations [4] make possible to state, that resonance value of the amplitude of the vibrations of a screw conveyer takes a smaller value at larger frequencies. The obtained results give the possibility to avoid resonance torsorial vibrations of a screw conveyer in case of its exploitation under the influence of pulse forces due to the change of material transportation conditions. Based on the taken out equations, it is possible to develop the automated systems of management for the processes of material transportation using screw machinery.

ВИСНОВОК

Представлені графічні залежності та зіставлення їх із резонансними кривими для випадку згинних коливань [4] дозволяють стверджувати, що резонансне значення амплітуди коливань шнеку для більших частот приймає менше значення. Одержані результати досліджень надають можливість уникнути резонансних крутильних коливань шнека у випадку його експлуатації при дії імпульсних сил за рахунок зміни режимів транспортування матеріалів. На основі одержаних рівнянь можливе створення автоматизованих систем управління процесами транспортування матеріалів шнековими машинами.

REFERENCES

[1]. Chen L.Q., Wang B. and Ding H. (2009), *Nonlinear parametric vibration of axially moving beams: asymptotic analysis and differential quadrature verification*, Journal of Physics: Conference Series, Vol. 181, pg. 1-8;

БІБЛІОГРАФІЯ

[1]. Чен, LQ, Ван, Б. і Дін, Н. (2009) - нелінійних параметричних коливань осі рухомі пучки: асимптотический аналіз і диференціальна квадратурная перевірка ", журнал фізики: серії конференцій, Vol. 181, стор. 8 січня;

[2]. Gevko B.M. and Rogatynskiy R.M. (1989), *Screw feeding mechanisms of agricultural machines,* High school, Lviv, Ukraine;
[3]. Gevko I. (2012), *Mathematical model of nonlinear bending vibrations of auger*, Visnyk TNTU, no. 4 (68), pg. 141-154;
[4]. Gevko R.B., Vitrovyi, A.O. and Pik, A.I. (2012), *Raising of the technical level of flexible screw conveyors*, Aston, Ternopil, Ukraine;
[5]. Grigoryev A.M. (1972), *Screw conveyors*, Mashinostroyeniye, Moskow, Russia;
[6]. Loveykin V.S. and Nesterov, A.P. (2002), *Dynamic optimization of lifting machines*, LNU, Lugansk, Ukraine.
[7]. Rogatynskiy R., Gevko, I. and Dyachun, A. (2012), *Investigation of torsional vibrations of auger*, Nauchni trudove na Rusenskiya universytet, Vol. 51, pg. 42-46.

[2]. Гевко Б.М., Р. М. Рогатынский (1989) - *Винтовые подающие механизмы сельскохозяйственных машин*. – Львов: Вища школа – 176 с.
[3]. Гевко І. (2012) - *Математична модель нелінійних згинних коливань шнека*, Вісник ТНТУ. № 4 (68). 141-154.
[4]. Гевко Р. Б., А.О. Вітровий, А. І. Пік. (2012) - *Підвищення технічного рівня гнучких гвинтових конвеєрів: монографія*, Тернопіль: Астон, 204 с.
[5]. Григорьев А. М. (1972) - *Винтовые конвейеры* – Машиностроение, 184 с.
[6]. Ловейкин В. С. Нестеров А. П. (2002) - *Динамическая оптимизация подъемных машин* Луганськ: Вид-во ЛНУ, 387 с.
[7]. Рогатынский Р., Гевко И., А. Дячун, (2012) *Исследование крутных колебаний шнека,* Научни трудове на Русенския університет, Русе, Т.51. 42-46.

MODELLING OF THE VERTICAL SCREW CONVEYER LOADING
/
МОДЕЛЮВАННЯ ПРОЦЕСУ ЗАВАНТАЖЕННЯ ВЕРТИКАЛЬНОГО ГВИНТОВОГО КОНВЕЄРА

Lect. Ph.D. Eng. Lyashuk O.L., Lect. Ph.D. Eng. Rogatynsky O.R., Serilko D.L.
Ternopil Ivan Pul'uj National Technical University, Ruska str., 56, Ternopil, Ukraine
E-mail: Oleg-lashyk@rambler.ru

Abstract: *A mathematical model of the vertical screw conveyer loading has been proposed. Algorithm of solution of the differential equations with partial derivatives of the bulk-cargo medium movement in the screw channel has been developed. Taking advantage of the proposed model it makes possible to develop new designs of the screw conveyer intake devices and to interpret their efficient parameters.*

Key words: *mathematical model, screw conveyers, intake device, bulk-cargo*

INTRODUCTION

Nowadays screw conveyers are the major means of continuous transportation of agricultural bulk-cargo materials. A great number of screw carriers are used now for transporting of grain beside the screws, which are parts of complex agricultural machines [2,4,5,9]. They are of extremely simple design and are characterized by their small size and reliability in operation. But their disadvantage is that of decrease of efficiency under high frequency of the screw rotation caused by the increase of the centrifugal forces in the loading area, which results in the increase of the transporting process power-consumption by these devices.

Despite of great number of papers dealing with the studying of transporting materials by the screw mechanisms, there are only experimental investigations of different ways of loading, basing on which the recommendations on the choice of the loading devices are presented [1,6,7].

The objective of the work is to develop the mathematical model of the vertical screw conveyer loading, which can be used to obtain the picture of the stresses and speeds distribution in the screw channel and, consequently, the dependence of the screw conveyer efficiency on its geometric parameters, rate of angular motion, as well as physical-mechanical properties of the bulk-cargo.

MATERIAL AND METHOD

Screw conveyer, which is in the tank loaded with bulk-cargo, with given physical-mechanical properties is presented in Fig. 1.

To investigate the movement of bulk-cargo in the screw channel generally, the screw coordinates system, which is connected with the screw rigidly, is used.

But, to obtain even approximate solution of the movement equation in this system is difficult enough. That is why in order to simplify the given task, cylinder coordinates system is used instead of the screw one.

Резюме: *Запропонована математична модель процесу завантаження вертикального гвинтового конвеєра. Розроблений алгоритм розв'язку диференціальних рівнянь з частинними похідними руху сипкого середовища в гвинтовому каналі. Використання запропонованої моделі дає можливість розробляти нові конструкції забірних пристроїв гвинтових конвеєрів з обґрунтуванням їх раціональних параметрів.*

Ключові слова: *математична модель, гвинтовий конвеєр, забірний пристрій, сипкий матеріал*

ПЕРЕДМОВА

Гвинтові конвеєри в даний час є основними засобами безперервного переміщення сипких сільськогосподарських матеріалів. В світі використовується значна кількість шнекових транспортерів для транспортування зерна, не рахуючи шнеків, які є частинами складних сільськогосподарських машин [2,4,5,9]. Вони мають гранично просту конструкцію, відрізняються компактністю і надійні в експлуатації. Разом з тим, суттєвим недоліком гвинтових механізмів є зниження їх продуктивності при великих частотах обертання гвинта внаслідок збільшення відцентрових сил в зоні завантаження, що приводить до зростання енергоємності процесу транспортування даними пристроями.

Не дивлячись на значну кількість робіт, присвячених вивченню транспортування матеріалів шнековими механізмами, в даний час існують тільки експериментальні дослідження різних способів завантаження, виходячи з яких даються рекомендації по вибору завантажувальних пристроїв [1,6,7].

Метою роботи є розробка математичної моделі процесу завантаження вертикального гвинтового конвеєра, яку можна використати для отримання картин розподілу напружень і швидкостей в гвинтовому каналі шнека, а отже і залежності продуктивності гвинтового конвеєра від його геометричних параметрів, кутової швидкості, а також фізико-механічних властивостей сипкого матеріалу.

МАТЕРІАЛ І МЕТОДИКА

Розглянемо гвинтовий конвеєр, який знаходиться в бункері заповненому сипким матеріалом із заданими фізико-механічними властивостями (Рис.1).

Для дослідження руху сипкого матеріалу у гвинтовому каналі шнека в загальному випадку використовують гвинтову систему координат, яка жорстко зв'язана із шнеком.

Але отримати навіть наближений розв'язок рівняння руху в цій системі досить складно. Тому з метою спрощення поставленої задачі замість гвинтової, використовують циліндричну систему координат.

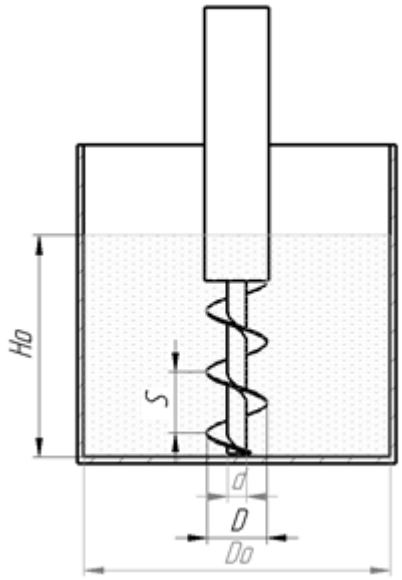

Fig.1 - Tank with screw conveyer

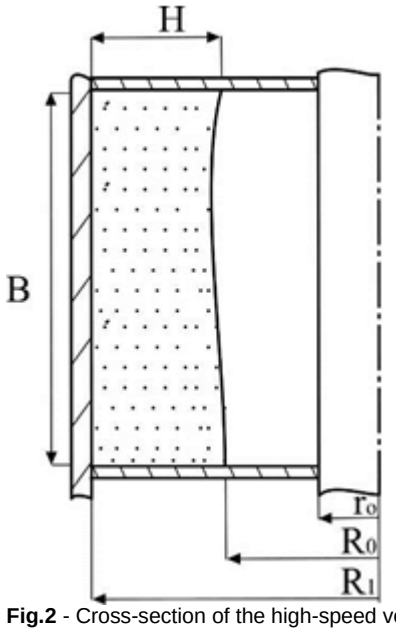

Fig.2 - Cross-section of the high-speed vertical screw conveyer screw channel

As we are analyzing high-speed vertical screw conveyer, the cross-section of the screw channel can be presented as in Fig.2, that is, bulk-cargo under the action of centrifugal forces moves in the channel of width $H = R_1 - R_0$ [8].

Here R_1 – screw radius, r_0 – screw shaft radius.

In this case the coefficient of loading will equal:

Оскільки ми розглядаємо швидкохідний вертикальний гвинтовий конвеєр, то переріз гвинтового каналу можна подати у вигляд (фіг 2), тобто сипкий матеріал під дією відцентрових сил рухається в каналі шириною $H = R_1 - R_0$ [8].

Де R_1 - радіус гвинта, r_0 - радіус вала гвинта.

В цьому випадку коефіцієнт заповнення буде рівний:

$$K_з = \frac{R_1^2 - R_0^2}{R_1^2 - r_0^2} \tag{1}$$

Hence $R_0 = \sqrt{R_1^2 - K_з\left(R_1^2 - r_0^2\right)}$.

If we assume, that coefficient of loading is $K_з = 0{,}8$, $r_0 = 0{,}3R_1$,we will obtain $R_0 \approx 0{,}5R_1$

Thus, further we will analyze the movement of the bulk-cargo in the “conventional” screw channel, the shaft radius of which equals R_0

Here friction force between the bulk-cargo and screw shaft is usually not available, as well as the shaft pressure on the screw surface.

As $H/B << 1$, $H = R_1 - R_0$, $B \approx 2R_1$, we can study the plane model of the bulk-cargo medium movement in the screw channel (Fig.3). In this case taking into account the fact, that bulk-cargo movement is of the layer-type , let us assume that $V_z = 0$, $\partial V_\varphi / \partial z = 0$.

The equation of movement will look like:

Звідки $R_0 = \sqrt{R_1^2 - K_з\left(R_1^2 - r_0^2\right)}$.

Якщо прийняти, що коефіцієнт заповнення $K_з = 0{,}8$, $r_0 = 0{,}3R_1$ то будемо мати $R_0 \approx 0{,}5R_1$.

Отже надалі будемо розглядати рух матеріалу в “умовному” каналі гвинта, радіус вала якого рівний R_0 .

При цьому звичайно відсутня сила тертя між матеріалом і валом шнека, а також тиск вала на поверхню шнека.

Оскільки $H/B << 1$, $H = R_1 - R_0$, $B \approx 2R_1$, то можна розглянути плоску модель руху сипкого середовища в гвинтовому каналі (фіг 3). В цьому випадку з врахуванням того, що рух матеріалу має характер шарів, приймемо що $V_z = 0$, $\partial V_\varphi / \partial z = 0$.

Рівняння руху матимуть вигляд:

$$\rho\left(V_r \frac{\partial V_r}{\partial r} + V_\varphi \frac{1}{r}\frac{\partial V_r}{\partial \varphi} - \frac{V_\varphi^2}{r}\right) = \frac{\partial \sigma_r}{\partial r} + \frac{1}{r}\frac{\partial \tau_{r\varphi}}{\partial \varphi} + \frac{\sigma_r - \sigma_\varphi}{r} + \rho F_r \tag{2}$$

$$\rho\left(V_r \frac{\partial V_\varphi}{\partial r} + V_\varphi \frac{1}{r}\frac{\partial V_\varphi}{\partial \varphi} - \frac{V_r V_\varphi}{r}\right) = \frac{\partial \tau_{r\varphi}}{\partial r} + \frac{1}{r}\frac{\partial \sigma_\varphi}{\partial \varphi} + \frac{2\tau_{r\varphi}}{r} + \rho F_\varphi , \tag{3}$$

$$\frac{\partial V_r}{\partial r} + \frac{V}{r} + \frac{1}{r}\frac{\partial V_\varphi}{\partial \varphi} = 0 . \tag{4}$$

where V_r V_φ – particle speed vector projection relatively on the radius-vector direction and on the perpendicular to it direction; F_φ, F_r – mass force projections on the same directions; σ_r , σ_φ , $\tau_{r\varphi}$,– components of the tensor stresses in the polar coordinates.

Equations 2, 3 are the equations of the total medium movement written as Eulerian variables, and equation 4 – continuity equation in the polar coordinates. Unlike the elastic medium, let us assume the rule of signs for stresses, according to which in the area the outside normal of which coincides with the positive direction of the coordinate axis, positive stress components have directions opposite to those of corresponding coordinate axes.

According to the investigations [6], the speed V_r^0 with which the bulk-cargo moves into the screw channel of the intake area of the screw, decreases from the maximum value to zero according to the linear law:

де V_r , V_φ - проекції вектора швидкості частинки відповідно на напрямок радіус-вектора та на перпендикулярний до нього напрямок; F_φ, F_r - проекції масових сил на тіж напрямки; σ_r , σ_φ , $\tau_{r\varphi}$, - компоненти тензора напружень в полярних координатах.

Рівняння 2, 3 є рівняннями руху суцільного середовища записаних у змінних Ейлера, а рівняння 4 – рівняння неперервності в полярних координатах. На відміну від пластичного середовища приймаємо правило знаків для напружень, згідно якого на площадці, зовнішня нормаль до якої співпадає з додатнім напрямком координатної осі, додатні компоненти напружень мають напрямки, протилежні напрямкам відповідних координатних осей.

Згідно досліджень [6]. швидкість V_r^0 з якою сипкий матеріал поступає в гвинтовий канал забірної частини шнека зменшується від максимального значення до нуля по лінійному закону:

$$V_r^0 = 2V_c\left(1-\frac{R_1}{L_0}\varphi\right) = 2V_c\left(1-\frac{\varphi}{\varphi_1}\right) \tag{5}$$

where V_c – average speed, with which the bulk-cargo moves from the tank to the screw channel.

де V_c – середня швидкість, з якою матеріал поступає з бункера у гвинтовий канал.

$$V_c = \frac{Q}{L_0 B}; \quad . \tag{6}$$

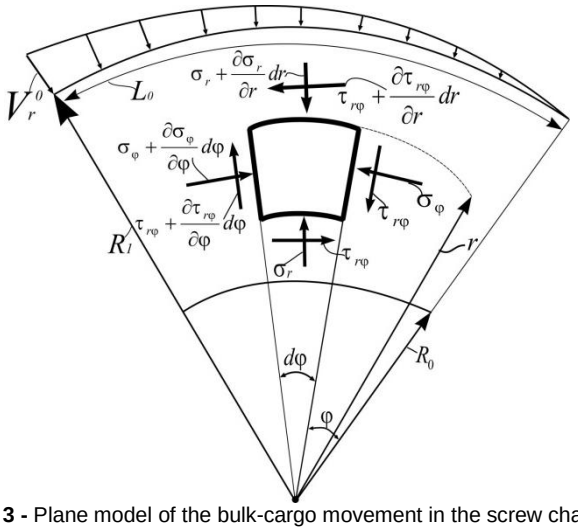

Fig. 3 - Plane model of the bulk-cargo movement in the screw channel

where Q – volumetric efficiency of the screw conveyer $м^3/с$. B – screw channel width $B = S \cdot \cos\alpha$; S – screw helix; α – screw line angle of elevation; L_0 – screw channel length in the intake area $\varphi_1 = L_0/R_1$

As in our case the channel height is greater enough than its length, we can assume, that radial speed decreases from the maximum value V_z^0 to zero along the radius according to the linear law:

де Q –об'ємна продуктивність гвинтового конвеєра $м^3/с$. B – ширина гвинтового каналу $B = S \cdot \cos\alpha$; S – крок гвинта; α – кут підйому гвинтової лінії; L_0 - довжина гвинтового каналу в забірній частині $\varphi_1 = L_0/R_1$.

Оскільки, в нашому випадку висота каналу набагато більша його довжини, то можна прийняти, що радіальна швидкість зменшується від максимального значення V_z^0 до нуля вздовж радіуса по лінійному закону:

$$\frac{\partial V_r}{\partial r} = C\,, \tag{7}$$

hence

звідки:

$$V_r = C(\varphi)r + C_0 \tag{8}$$

where $C = C(\varphi)$ – some function dependent on the coordinate φ (Fig. 3).

Let us write the boundary conditions:

де $C = C(\varphi)$ – деяка функція, яка залежить від координати φ (рис. 3).

Запишемо граничні умови:

$$V_r\big/_{r=R_0} = 0 \quad , \quad V_r\big/_{r=R_1} = -V_r^0 \quad . \tag{9}$$

Then from the equation (8), taking into account (9), we will obtain:

Тоді з рівняння (8), з врахуванням (9) отримаємо:

$$C(\varphi) = \frac{V_r^0}{R_1 - R_0} \, , \tag{10}$$

$$C_0(\varphi) = \frac{V_r^0}{R_1 - R_0} \cdot R_0 \, , \tag{11}$$

$$V_r = \frac{V_r^0 (r - R_0)}{R_0 - R_1} = \frac{2V_c (r - R_0)}{R_0 - R_1}\left(1 - \frac{\varphi}{\varphi_1}\right). \tag{12}$$

From the continuity equation (4) we will obtain:

З рівняння неперервності (4) отримаємо:

$$C(\varphi) + \frac{V_r}{r} + \frac{1}{2}\frac{\partial V_\varphi}{\partial \varphi} = 0 \tag{13}$$

or

або

$$\frac{\partial V_\varphi}{\partial \varphi} = V_r + C(\varphi) = \frac{2V_c (r - R_0)}{R_0 - R_1}\left(1 - \frac{\varphi}{\varphi_1}\right) + r2V_c\left(1 - \frac{\varphi}{\varphi_1}\right) = 2V_c\left(1 - \frac{\varphi}{\varphi_1}\right)\cdot\left(\frac{r - R_0}{R_0 - R_1} + r\right) \tag{14}$$

Having integrated this equation we will have

Інтегруючи це рівняння будемо мати:

$$V_\varphi = 2V_c\left(\frac{2r - R_0}{R_0 - R_1}\right)\left(\varphi - \frac{\varphi^2}{2\varphi_1}\right) + \psi(r), \tag{15}$$

where $\psi(r)$ – some function from r.

Then to find $\psi(r)$ let us assume, that relative rates of angular motion of the part of the bulk-cargo in the screw channel of the transporting area of the screw are distributed according to the law [3].

де $\psi(r)$ – деяка функція від r.

Для визначення $\psi(r)$ приймаємо, що відносні кутові швидкості частинки матеріалу в гвинтовому каналі транспортуючої частини шнека розподіляються по закону [3].

$$\omega = \omega_0 - \frac{CR_0}{r^2} \, , \tag{16}$$

where ω_0 – screw rate of angular motion, C – some constant, which depends on the physical-mechanical properties of the bulk-cargo and the screw parameters.

Then the volumetric efficiency of the screw conveyer will equal:

де ω_0 – кутова швидкість гвинта; C – деяка константа, яка залежить від фізико-механічних властивостей матеріалу, та параметрів гвинта.

Тоді об'ємна продуктивність гвинтового конвеєра буде рівна:

$$Q = B \times \int_{R_0}^{R_1} \frac{\omega r dr}{\cos\alpha_c} = \frac{B}{\cos\alpha_c}\left[0.5\omega_0\left(R_1^2 - R_0^2\right) - CR_0 \ln\frac{R_1}{R^0}\right] \tag{17}$$

where $B = S\cos\alpha_c$; taking into account that:

де $B = S\cos\alpha_c$; враховуючи, що:

$$Q = \frac{\pi\left[D_1^2 - D_0^2\right]}{4} \cdot n \cdot S \cdot K_n = \pi\left(R_1^2 - R_0^2\right)B \times n \cdot S \cdot K_n , \quad (18)$$

where $n = \omega/2\pi$ – frequency of revolving (rev/sec); K_i – screw conveyer efficiency coefficient.

де $n = \omega/2\pi$ – частота обертання об/с; K_i - коефіцієнт продуктивності гвинтового конвеєра.

$$C = \frac{\omega_0\left(R_1^2 - R_0^2\right)}{2R_0 \ln\frac{R_1}{R_0}}\left(1 - K_i\right) \quad (19)$$

Taking into account that at $\varphi = \varphi_1$ $V_\varphi = \left(\omega_0 - CR_0/r^2\right)r$, let us find function $\psi = \psi(r)$:

Враховуючи що при $\varphi = \varphi_1$, $V_\varphi = \left(\omega_0 - CR_0/r^2\right)r$ визначимо функцію $\psi = \psi(r)$:

$$V_{\varphi/\varphi=\varphi_1} = 2V_c\left(\frac{2r - R_0}{R_0 - R_1}\right)\left(\varphi_1 - \frac{\varphi_1^2}{2\varphi_1}\right) + \psi(r) = 2V_c\left(\frac{2r - R_0}{R_0 - R_1}\right)\left(\frac{2\varphi_1 - \varphi_1^2}{2\varphi_1}\right) + \psi(r) = 2V_c\left(\frac{2r - R_0}{R_0 - R_1}\right)\frac{\varphi_1}{2} + \psi(r), \quad (20)$$

$$\psi_r = \left(\omega_0 - \frac{CR_0}{r^2}\right)r - V_c\left(\frac{2r - R_0}{R_0 - R_1}\right)\varphi_1 , \quad (21)$$

$$V_\varphi = 2V_c\left(\frac{2r - R_0}{R_0 - R_1}\right)\left(\varphi_1 - \frac{\varphi_1^2}{2\varphi_1}\right) - V_c\left(\frac{2r - R_0}{R_0 - R_1}\right)\varphi_1 + \left(\omega_0 - \frac{CR_0}{r^2}\right)r = \left(\omega_0 - \frac{CR_0}{r^2}\right)r - \frac{V_c}{\varphi_1}\frac{\left(2r - R_0\right)}{R_0 - R_1}\left(\varphi_1 - \varphi\right)^2 . \quad (22)$$

As we are analyzing non-ramming screw, in the end of the intake area we can assume: at $\varphi_1 = \varphi$ $\frac{\partial \tau_{r\varphi}}{\partial \varphi} = 0$ $V_\varphi = \left(\omega_0 - \frac{CR_0}{r^2}\right)\cdot R_1$ $V_{r/\varphi=\varphi_1} = 0$. Besides let us assume that $\sigma_\varphi = k\sigma_r$, where k – lateral pressure coefficient. From the equation (12) we will obtain:

Оскільки ми розглядаємо безнапірний шнек, то в кінці забірної частини можна прийняти: при $\varphi_1 = \varphi$, $\frac{\partial \tau_{r\varphi}}{\partial \varphi} = 0$ $V_\varphi = \left(\omega_0 - \frac{CR_0}{r^2}\right)\cdot R_1$ $V_{r/\varphi=\varphi_1} = 0$

Також приймемо, що $\sigma_\varphi = k\sigma_r$, де k – коефіцієнт бокового тиску. З рівняння (12) отримаємо:

$$\frac{\partial V_r}{\partial \varphi} = \frac{2V_0\left(R_0 - r\right)}{\left(R_0 - R_1\right)\varphi_1} , \quad (23)$$

or

або

$$V_\varphi \cdot \frac{1}{r} \cdot \frac{\partial V_r}{\partial \varphi} = \left(\omega_0 - \frac{CR_0}{r^2}\right)\cdot \frac{2V_0\left(R_0 - r\right)}{\left(R_0 - R_1\right)\varphi_1} . \quad (24)$$

Then the equation (2) will look like:

Тоді рівняння (2) матиме вигляд:

$$\frac{\partial \sigma}{\partial r} + \frac{\sigma}{r} = \rho\left(\omega_0 - \frac{CR_0}{r^2}\right)^2 r - \rho\left(\omega_0 - \frac{CR_0}{r^2}\right)\frac{2V_C\left(R_1 - R_0\right)}{\left(R_1 - R_0\right)\varphi_1} . \quad (25)$$

where $\sigma = \sigma_r - \sigma_\varphi$

Let us find general solution of the equation (25) without the right part:

де $\sigma = \sigma_r - \sigma_\varphi$.

Знайдемо загальний розв'язок рівняння (25) без правої частини:

$$\frac{d\sigma}{dr} + \frac{\sigma}{r} = 0 , \quad (26)$$

$$\frac{d\sigma}{\sigma} = -\frac{dr}{r} , \quad (27)$$

$$\ln\sigma = -\ln r + \ln C , \quad (28)$$

$$\ln\sigma = \ln\frac{C}{r} , \ \sigma = \frac{C}{r} . \quad (29)$$

Let us change the integration constant *C* by the unknown function $u = u(r)$ and we will obtain

Замінимо сталу інтегрування С невідомою функцією. $u = u(r)$ і будемо мати:

$$\sigma = \frac{u}{r}. \tag{30}$$

then

тоді

$$\frac{d\sigma}{dr} = \frac{d}{dr}\left(u \cdot r^{-1}\right) = \frac{du}{dr} \cdot r^{-1} + u\left(-r^{-2}\right) = \frac{1}{r}\frac{du}{dr} - \frac{u}{r^2}, \tag{31}$$

Let us substitute (29) in (25).

Підставимо (29) в (25).

$$\frac{1}{r}\frac{du}{dr} - \frac{u}{r^2} + \frac{u}{r^2} = \rho\left(\omega_0 - \frac{CR_0}{r^2}\right)^2 r - \left(\omega_0 - \frac{CR_0}{r^2}\right)\frac{2V_C(r - R_0)}{(R_1 - R_0)\varphi_1}, \tag{32}$$

$$\frac{du}{dr} = \rho\left[\left(\omega_0 - \frac{B}{r^2}\right)^2 r^2 - \left(\omega_0 - \frac{B}{r^2}\right) \cdot A(r - R_0)\right]. \tag{33}$$

where $B = CR_0$, $A = \frac{2V_c}{(R_1 - R_0)\varphi_1}$.

Let us devide variables and integrate

де $B = CR_0$, $A = \frac{2V_c}{(R_1 - R_0)\varphi_1}$.

Розділимо змінні і проінтегруємо

$$\int du = \rho\int\left[\left(\omega_0 - \frac{B}{r^2}\right)^2 r - \left(\omega_0 - \frac{B}{r^2}\right) \cdot A(r - R_0)r\right]dr, \tag{34}$$

$$u = \rho\left[\int\left(\omega_0^2 - \frac{2B}{r^2} + \frac{B^2}{r^4}\right)r^2 dr - A\int\left(\omega_0 - \frac{B}{r^2}\right)r^2 dr \cdot + A\int\left(\omega_0 - \frac{B}{r^2}\right)rR_0 dr_1\right] + C_1 =$$

$$= \rho\left[\frac{(\omega_0^2 - A\omega_0)r^3}{3} + \frac{AR_0\omega_0 r^2}{2} + Br(A - 2\omega_0) + \frac{B^2}{r} - AR_0 B\ln r\right] + C_1, \tag{35}$$

$$\sigma = \frac{\rho}{r}\left[\frac{(\omega_0^2 - A\omega_0)r^3}{3} + \frac{AR_0\omega_0 r^2}{2} + Br(A - 2\omega_0) + \frac{B^2}{r} - AR_0 B\ln r\right] + \frac{C_1}{r}. \tag{36}$$

Integration constant C_1 can be found from the condition: $\sigma_{r=R_0} = 0$

Сталу інтегрування C_1 визначаємо з умови: $\sigma_{r=R_0} = 0$

$$C_1 = -\rho\left[\frac{(\omega_0^2 - A\omega_0^2)R_0^3}{3} + \frac{A\omega_0 R_0^3}{2} + BR_0(A - 2\omega_0) + \frac{B^2}{R_0} - AR_0 B\ln R_0\right]. \tag{37}$$

Finally we will obtain:

Остаточно отримаємо:

$$\sigma = \frac{\rho}{r}\left[\frac{(\omega_0^2 - A\omega_0)r^3}{3} + \frac{AR_0\omega_0 r^2}{2} + Br(A - 2\omega_0) + \frac{B^2}{r} - AR_0 B\ln r\right] -$$

$$-\frac{\rho}{r}\left[\frac{(\omega_0^2 - A\omega_0^2)R_0^3}{3} + \frac{A\omega_0 R_0^3}{2} + BR_0(A - 2\omega_0) + \frac{B^2}{R_0} - AR_0 B\ln R_0\right] \tag{38}$$

RESULTS

In Fig. 4 (a and b) diagrams of speeds distribution of the bulk-cargo parts in the transporting area of the screw channel with the following parameters are presented: screw diameter D=0.1 m, screw shaft diameter d=0.05m at different efficiency coefficients $K_{\Pi} = 0{,}7$ (Fig.4a) $K_{\Pi} = 0{,}8$ (Fig.4b).

РЕЗУЛЬТАТИ

На фіг. 4 (а і б) наведені епюри розподілу швидкостей частинок матеріалу в транспортуючій частині гвинтового каналу шнека з параметрами: діаметр гвинта D=0,1 м, діаметр вала гвинта d=0,05м, при різних коефіцієнтах продуктивності $K_{\Pi} = 0{,}7$ (фіг. 4а), $K_{\Pi} = 0{,}8$ (фіг. 4б).

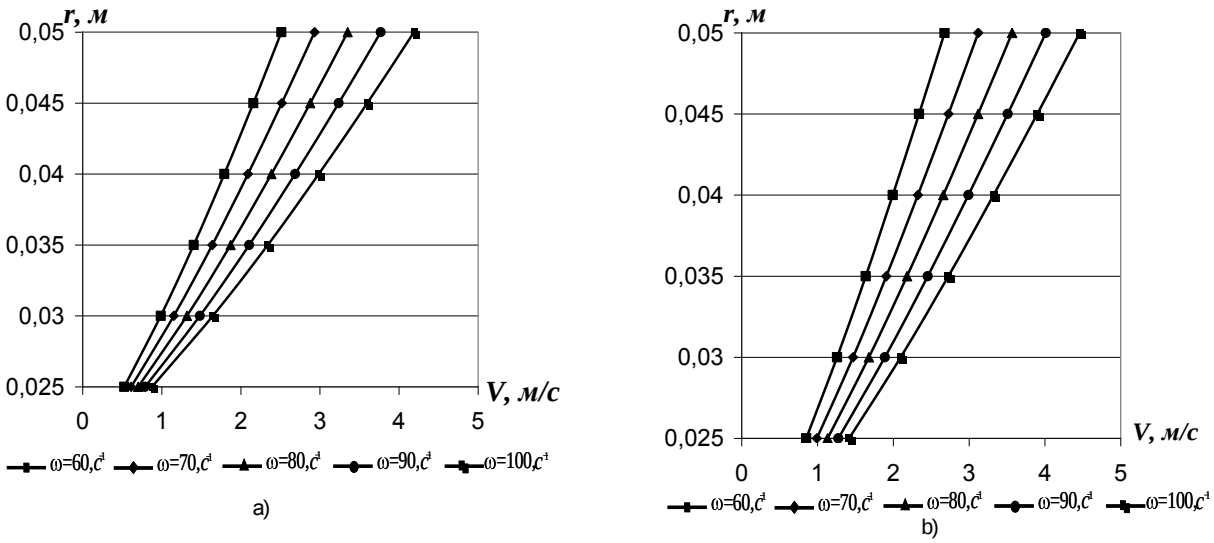

Fig. 4 - Diagrams of the speeds distribution of bulk-cargo parts in the transporting area of the screw channel at a) - $K_{П} = 0,7$; b)- $K_{П} = 0,8$

In Fig. 5 dependences of stresses σ_r in the end of the intake area of screw channel on the rate of the angular motion of the screw for different values of the efficiency coefficient $K_{П}$ are presented. The necessary value σ_r is likely to be equal to the lateral pressure of the bulk-cargo in the tank, which can be found analytically [10]. From the presented diagrams it is clear that in order to provide stable operation of the vertical screw conveyer it is necessary to provide sufficient pressure, which can be provided by increasing the tank sizes or using the forced feeding of the bulk-cargo in the intake area. Dependence of the efficiency coefficient k, on the screw rate of angular motion $K_{П}$ is presented in Fig.6 at $\sigma_r = 2000 Па$, which corresponds to the gravitation loading of the screw conveyer. As the efficiency of the high-speed screw conveyer is decreased with the increase of the screw rotation frequency, to provide the desired efficiency of this transporting means it is necessary to take advantage of special intake devices.

На фіг. 5. наведені залежності напружень σ_r в кінці забірної частини гвинтового каналу від кутової швидкості гвинта для різних значень коефіцієнта продуктивності $K_{П}$. Очевидно, що необхідна величина σ_r дорівнює боковому тиску сипкого матеріалу в бункері, який можна визначити аналітичним шляхом [10]. З наведених графіків видно, що для стабільної роботи вертикального гвинтового конвеєра необхідно створити значний тиск, який можна досягти збільшенням розмірів бункера, або застосовуючи примусову подачу сипкого матеріалу в забірну частину. Залежність коефіцієнту продуктивності $K_{П}$ від кутової швидкості гвинта ω наведена на фіг. 6 при $\sigma_r = 2000 Па$, що відповідає гравітаційному завантаженню шнекового транс-портера. Оскільки продуктивність швидкохідного гвинтового конвеєра зменшується із збільшенням частоти обертання гвинта, то для забезпечення необхідної продуктивності цього транспортного засобу необхідно використовувати спеціальні забірні пристрої.

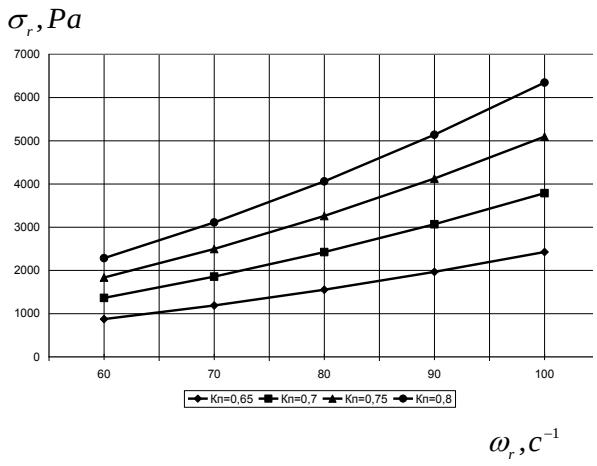

Fig. 5 - Dependence of stresses σ_r in the end of intake area of the screw channel on the screw rate of angular motion

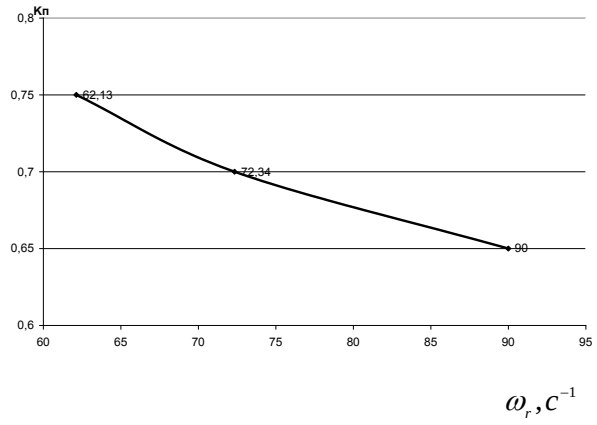

Fig. 6 - Dependence of efficiency coefficient of the screw conveyer $K_{П}$, on the screw rate of angular motion

CONCLUSIONS

Taking advantage of the obtained solution algorithm of differential equations, which describe the movement of bulk-cargo medium under certain boundary conditions, the picture of distribution speeds and stresses in the screw channel can be obtained. Achieving the proposed model makes possible to develop new designs of intake devices of screw conveyers and to interpret their efficient parameters.

REFERENCES

[1]. Adigamov K.A., Baibara S.N., Chernenko G.V. (2009) - *Critical frequency of the vertical screw rotation*. Digest of the East-Ukrainian National University named after Volodymyr Dal. – №2 (132), pg. 9-10;
[2]. Gevko B.M., Rogatynsky R.M. (1989) – *Screw feeding mechanisms of agricultural machines*. Higher school, pg.175., Lvov;
[3]. Generalov M.B. (1988) - *Movement of the bulk-cargo in the tank screw feeder*. Theoretical foundations of the chemical engineering. Vol. 22, №1, pg. 78-81;
[4]. Grigoryev A.M. (1972) – *Screw conveyers*. Mechanical engineering, pg. 286, Moscow;
[5]. Izrailevitch M.L. (2002) - *From the clamshell to conveyer: port trans-shipment complexes for bulk-cargo* Izrailevitch M.L. / PTO №2, pg. 9-10;
[6]. Fernandez J.W, Cleary P.W., Mcbride W., (2009), *Effect of screw design on hopper draw down to a horizontal screw feeder,* Seventh International Conference on CFD in the Minerals and Process Industries CSIRO, Melbourne, Australia 9-11 Decem;
[7]. Murashov M.V., Scherbakov A.S. (1978) - *The effect of the screw conveyer intake part design on its efficiency*, Peat extraction industry. №7. pg. 17-19;
[8]. Nilsson L.G. (1971) - *On the vertical serew conveyor for non- cohesive bulk materials*. Acta polytechnica Scandinavica. 4 Stokholm, pg. 96;
[9]. Rogatynsky R.M., Gevko B.M., Dyachun A.Y. (2014), *Scientific-applied foundations of creation of screw transporting-technological mechanisms,* TNTU named after Ivan Pul'uj.– 278 pg., Ternopil;
[10]. Serilko D.L. (2010) - *Determination of the bulk-cargo pressure in the screw conveyer intake part*, Digest of the Ternopil Ivan Pul'uj Technical University – pg. 97-102.

ВИСНОВОК

Використовуючи отриманий алгоритм розв'язку диференціальних рівнянь, які описують рух сипкого середовища, при відповідних граничних умовах можна отримати картину розподілу швидкостей та напружень у гвинтовому каналі шнека. Реалізація запропонованої моделі дає можливість розробляти нові конструкції забірних пристроїв гвинтових конвеєрів з обґрунтуванням їх раціональних параметрів

БІБЛІОГРАФІЯ

[1]. Адигамов К.А., Байбара С.Н., Черненко Г.В. (2009) - *Критическая частота вращения вертикального шнека*. Вісник Східноукраїнського національного університету імені Володимира Даля. – №2 (132) –С. 9-10;
[2]. Гевко Б.М., Рогатынский Р.М. (1989) - *Винтовые подающие механизмы сельскохозяйственных машин.* Выща школа, – 175 с., Львов;
[3]. Генералов М.Б. (1988) *Движение сыпучего материала в шнековом питателе бункера*. Теор. осню хим. технол. Т 22, №1, С. 78-81;
[4]. Григорьев А.М. (1972) - *Винтовые конвееры*. Машиностроение., - 286 с., Москва;
[5]. Израйлевич М. Л. (2002) - От грейфера к конвейеру: портовые перегрузочные комплексы для навалочных грузив / Израйлевич М. Л // ПТО №2. - С. 9-10;
[6]. Фернандес Дж W Клірі PW, Mcbride W. (2009), *Вплив гвинтової конструкції на бункер витяжки світанку горизонтальній шнекового живильника*, Сьома Міжнародна Конференція по ЦФО в мінералах і переробної промисловості CSIRO, Мельбурн, Австралія 9-11 груд;
[7]. Мурашов М. В., Щербаков А. С. (1978) - *Влияние конструкции заборной части шнека винтового конвейера на его производительность.* Торфяная промышленность. №7. С. 17 – 19;
[8]. Нільссон L. - G. (1971) - *На вертикальній гвинтовий конвеєр для неурядових зв'язкових сипучих матеріалів*. Acta політехніка Scandinavica. Він я 4 Стокгольм, - С. 96;
[9]. Рогатинський Р.М., Гевко І.Б., Дячун А.Є. (2014) - *Науково-прикладні основи створення гвинтових* транспортно-технологічних механізмів. – ТНТУ імені Івана Пулюя, – 278 с., Тернопіль;
[10]. Серілко Д. Л. (2010) - *Визначення тиску сипкого матеріалу в забірній частині гвинтового конвеєра* Вісник Тернопільського державного технічного університету імені Івана Пулюя. –С. 97 – 102.

FRUIT VOLUMETRIC DETERMINATION BASED ON MOIRÉ TECHNIQUES
/
RECONSTITUIÇÃO TOPOGRAFICA E VOLUMÉTRICA DE FRUTOS UTILIZANDO TÉCNICAS OPTICAS DE MOIRÉ

Ph.D. Stud. Eng. Marcos V. G. Silva[1)], Ph.D.Eng. Celina de Almeida, Ph.D.Eng. Antonio Carlos Loureiro Lino[2)], Prof. Ph.D. Eng. Inácio M. D. Fabbro[1)]
[1)]Faculty of Agricultural Engineering, UNICAMP, Campinas, SP / Brazil [2)] IAC, Jundiai, SP / Brazil
Tel: +55 19 3521-1059; E-mail: inacio@feagri.unicamp.br

Abstract: *Three-dimensional survey of irregular, as well as regular solids has recently received significant attention from the scientific community due to its wide range of applications, including topics in agricultural engineering as plant-machine mechanical relationship. The pertinent literature discloses several methods and techniques to carry out three-dimensional measurements associated to a wide variety of cases. Moiré techniques are included in a group of non-contact and non-destructive methods based on the Moiré phenomena which generate optical fringes onto the tested body surface. Moiré methods require simple and low cost experimental setup, yielding accurate results when compared to other measuring systems. This work was focused on the projection Moiré technique with phase shift, employing two types of optical grids named Ronchi and a sinusoidal one. Metrological errors of tested techniques as compared with the Moiré method have been determined as well. This work demonstrated the best performance of grid frequency variation through several experiments applied to irregular solids shape determination as fruits. Body volumes were compared with conventional techniques as water immersion; meanwhile linear measures were compared with reading caliper results. The application of free software such as ImageJ, RisingSun Moire, Scilab / SIP and routines was considered very useful to reach the final results.*

Keywords*: optical three - dimensional surveys, Moiré with phase shift techniques, volume determination and solid three-dimensional reconstruction*

INTRODUCTION

The Moiré optical techniques are of very broad application in agricultural fields, especially in agricultural engineering, as well as in the overall engineering fields. These applications include micro relief survey of the soil for tillage quality control, of fruit and vegetables, plant-machine mechanical relations, and mechanical behavior of vegetative materials. It worth emphasize the application of Moiré methods as photo-elastic technique, similarly as the classic photo-elasticity, as hologram, as speckle and others. The opportunity of generating scientific knowledge associated to the Moiré methods applied to agricultural engineering subjects has motivated this research work, attempting to the possibilities of generating Digital Elevation Models (DEM) of regular as well as irregular surfaces, generating the volume and the three-dimensional views of the body under study [5].

This research work emphasizes the optical grid frequency influence on the resulting DEM, discussing on the advantages and disadvantages of each tested grid frequency.

Phase shifting Moiré technique is considered a quite simple method, needing not moving equipment and being of low cost [10]. It also exhibits high precision and adaptable to objects of different sizes by just varying the

Resumo*: A medição de sólidos tridimensionais tem recebido uma grande atenção da comunidade científica, devido à sua ampla gama de aplicações. Porém existem diversos métodos e técnicas para se obter tais medições, este trabalho demonstra a técnica de moiré que é uma técnica sem contato e não destrutiva, com um rápido processo de digitalização cujos fenômenos de Franjas de Moiré são o resultado da subtração da projeção de grades sobre um certo objeto com relação as grades projetadas em um plano referencial. Possui medição precisa comparável com a de outros sistemas. Demonstra também a exatidão das técnicas de moiré, sendo dado maior enfoque na técnica de moiré de projeção com deslocamento de fase, e pela utilização de dois tipos de grades a de Ronchi e senoidal, onde são observados os possíveis erros. Neste trabalho foi comprovado o melhor desempenho dos tipos e variação da frequência de grades incluindo vários exemplos práticos da sua aplicação em sólidos irregulares (frutos), determinação volumétrica de sólidos irregulares. Emprego de "softwares" gratuitos o qual também foi uma preocupação para disseminação da técnica, tais como ImageJ, RisingSun Moiré, SCILAB/SIP e rotinas.*

Palavras-chave: *técnicas perfilometricas ópticas, técnicas de moiré com deslocamento de fase, determinação de volume em sólidos e reconstituição tridimensional de sólidos*

INTRODUÇÃO

A utilização das técnicas de *moiré* é de grande importância para diversos segmentos, como na Engenharia Agrícola, envolvendo vários problemas associados ao estudo da topografia de superfícies, o comportamento mecânico de materiais biológicos, controle da qualidade na operação de preparo do solo baseado na determinação do micro relevo, relações mecânicas máquina–planta, etc. Em função da oportunidade de gerar conhecimento da aplicabilidade das técnicas de *moiré* em atividades ligadas a Engenharia Agrícola, motivou-se o desenvolvimento desta pesquisa, demonstrando assim, que a técnica de moiré pode ser aplicada com resultados satisfatórios na geração de Modelos Digitais de Elevação de superfícies regulares e irregulares, gerando a reconstituição de sólidos ou superfícies em três dimensões [5], juntamente, com a obtenção de medição volumétrica.

A pesquisa aborda as variações nos tipos e frequências das grades, demonstrando comparações nos resultados obtidos, bem como as vantagens e desvantagens de cada uma, comprovando que a sensibilidade depende principalmente do período do reticulo da grade.

Em pesquisas anteriores não foi constatada nenhuma evidencia de que o tipo de grade influenciava na reconstituição tridimensional e na medição volumétrica. A Técnica de *moiré* com Deslocamento de Fase (Phase shiffing) é uma técnica muito simples, não possui peças móveis e é de baixo custo [10]. Além disso, tem alta

grid period [1]. A variation of that method was developed, by projecting onto the body surface a sinusoidal grid pattern with codified RGB colors, obtaining, that way, the DEM by phase shifting, requiring not more of one image.

The results can be influenced by color of the object being tested, indicating that the method is recommended for bodies of neutral colors [1, 14, 15]. [3] reports the application of the RisingSun Moiré program to calculate the phases, generating the wrapped phase image, as well as to obtain the unwrapped image to generate the DEM of a pear fruit model. [8] and [9] developed algorithms for the MATLAB program to calculate the phases and the unwrapping procedures, eliminating the steps by adding or subtracting π values and by comparing a pixel with its neighboring one the differences with that value, positive or negative, respectively are found.

[11] described the Phase Shifting Method applied to Shadow Moiré, emphasizing the need of 04 images of Moiré fringes. At each image, the object is approximated or distanced from the reference grid (Rg), displacing the Moiré fringes by 1/2π, 1π and 3/2π of phase. However, when 04 images are employed and displaced by π/2, the light intensity at each one of these images is described by the following equation.

precisão e facilidade de adaptação a objetos de vários tamanhos e texturas apenas variando o período das franjas projetadas [1]. Para melhorar e contornar este problema, foi desenvolvida uma variação desta técnica em que se projeta padrão de grades senoidais com cores codificadas no espectro RGB, de modo que, com apenas uma imagem, e aplicando a técnica de deslocamento de fase obtive-se o MDT dos objetos.

Porém os resultados podem ser influenciados pela coloração do objeto, sendo, portanto indicada apenas para objetos com coloração neutra [1, 14, 15]. [3], utilizou um programa computacional específico (RisingSun Moiré) para fazer o cálculo das fases, gerando o mapa de fases empacotadas, e também para o desempacotamento de fases gerando o MDT de uma modelo de pera feito de cera [8] e [9], desenvolveram algoritmos para programa MATLAB, com a finalidade de fazer o cálculo das fases e o desempacotamento isto é, elimina os degraus, pela soma ou subtração de valores de π, e comparando um "pixel"com o seu vizinho encontra-se diferenças com esse valor, negativos ou positivos respectivamente.

[11], descrevendo o Método de Mudança de Fase aplicado à técnica de *moiré* de Sombra informa que são necessárias 4 imagens das franjas de *moiré*. Em cada uma delas as o objeto é aproximado ou afastado do Retículo de referencia (Rr) de maneira a produzir deslocamentos das franjas de *moiré* 1/2π, 1π e 3/2π de fase. Quando se usa 4 imagens deslocadas de π/2, a intensidade luminosa em cada uma das imagens é descrita pelas equações:

$$I_1(x,y) = a(x,y) - b(x,y)\cos\phi(x,y) \quad (1)$$

$$I_2(x,y) = a(x,y) - b(x,y)\cos[\pi/2 + \phi(x,y)] \quad (2)$$

$$I_3(x,y) = a(x,y) - b(x,y)\cos[\pi + \phi(x,y)] \quad (3)$$

$$I_4(x,y) = a(x,y) - b(x,y)\cos[3\pi/2 + \phi(x,y)] \quad (4)$$

Where $a(x,y)$ stands for light intensity of the background at each image point, $b(x,y)$ stands for modulation intensity at image point and ϕ stands for the phase to be determined. [13] demonstrated that phase term, $\cos\phi$, for each point of the image comes from the simultaneous solution of these 4 equations

Onde $a(x,y)$ é a intensidade luminosa do fundo em cada ponto da imagem, $b(x,y)$ é a intensidade de modulação em cada ponto da imagem, ϕ é a fase a ser determinada. [13], demonstra que resolvendo as 4 equações simultaneamente, pode se obter o termo fase ($\cos\phi$) para cada ponto da imagem:

$$\phi(x,y) = \arctan\left[\frac{(I_4(x,y)) - (I_2(x,y))}{(I_1(x,y)) - (I_3(x,y))}\right] \quad (5)$$

For each 3 images displaced by π /3, the phase term can be obtained through the Equation 6.

Para 3 imagens deslocadas de π /3, o termo fase pode ser obtido pela equação 6.

$$\phi(x,y) = \arctan\left[\frac{(I_3(x,y)) - (I_2(x,y))}{(I_1(x,y)) - (I_2(x,y))}\right] \quad (6)$$

For the 5 images displaced by π /5 the phase term can be obtained through the Equation 7.

E Para 5 imagens deslocadas de π /5, o termo fase pode ser obtido pela equação 7.

$$\phi(x,y) = \arctan\left[\frac{2(I_2(x,y)) - (I_4(x,y))}{2(I_3(x,y)) - (I_5(x,y)) - (I_5(x,y))}\right] \quad (7)$$

[2, 8, 9, 11] reported the application of phase shift method to the shadow Moiré with 4 images At each image, the object is approximated or distanced from the reference grid (Rg), displacing the Moiré fringes by 1/2π,

[2, 8, 9, 11] aplicando o método de deslocamento de fase à técnica de *moiré* de sombra utilizaram 4 imagens das franjas de *moiré*. Em cada uma delas o objeto é aproximado ou afastado do retículo de referencia (Rr) de maneira a produzir

1π and 3/2π of phase.

[13] emphasizes some advantages of these techniques when compared to the techniques supported by this one: high precision, quickness, good results even with low contrast.

MATERIAL AND METHODS

Volume measurement through the Moiré technique included a PC, a LCD projector, a CCD camera coupled to a Data Translation model DT313 data capturing board and the Global Lab Image2 of the Data Translation for image capturing. Six rubber cylinders and resin made fruit models for volume tests. Two types of grids, Ronchi and sinusoidal with 100 and 200 lines per millimeter, projected a distance of 1 meter. Four images were captured displaced of 90º. Four images of Moiré fringes were captured, referred as I1, I2, I3 and I4, displacing the grid in the **Z** direction from the reference grid which generated displacement from the fringes of 0. 1/4π, 1/2 π and 3/4π. From these images, the "RISING-SUN *MOIRÉ*" software generated the wrapped phase. The phase unwrapping produced the digital model of the fruit. The obtained image is qualified as a "raster" which color varies from zero to 255, i.e. 256 color levels corresponding to **Z** values**.** The measure by immersion is based on the volume of liquid displaced by the testing body as shown on Figure 1. Two types of optical grids were applied, the sinusoidal grid and the Ronchi grid.

gerar das franjas de *moiré* deslocadas1/2π, 1π e 3/2π de fase.

[13] cita algumas vantagens dessas técnicas, quando comparadas às técnicas às quais essas auxiliam, as quais são: alta precisão, rapidez e bons resultados mesmo com baixo contraste das franjas.

MATERIAL E MÉTODOS

O arranjo experimental foi constituído por um computador com processador Core 2 Duo, de 2,2GHz, com 1GB de memória RAM, ao qual foi acoplado um projetor LCD e uma câmera CCD. Sendo o projetor da marca NEC, modelo VT560, com resolução de 1024 colunas por 768 linhas. A câmera CCD, marca SAMSUNG, modelo SDC-312, em cores, com resolução de 640 colunas por 480 linhas, acoplada a uma placa de captura de imagens marca Data Translation, modelo DT313. Para a captura e tratamento das imagens utilizou-se o software Global Lab Image2 da Data Translation. Foram feitas projeções de dois tipos de grades: a senoidal e Ronchi, com duas variações de frequências cada, sendo-as de 100 linhas por mm e 200 linhas por mm. Foram obtidas quatro imagens das franjas de *moiré* (I1, I2, I3 e I4). Entre elas, a grade é deslocada na direção Z (afastada do retículo de referência) distâncias que produzam deslocamentos das franjas de *moiré* de 0, 1/4π, 1/2 π e 3/4π. O modelo final é uma imagem do tipo "raster" onde as cores variando de 0 a 255, isto é, 256 níveis de cores ou tons de cinza, correspondem às cotas ou aos valores de z.

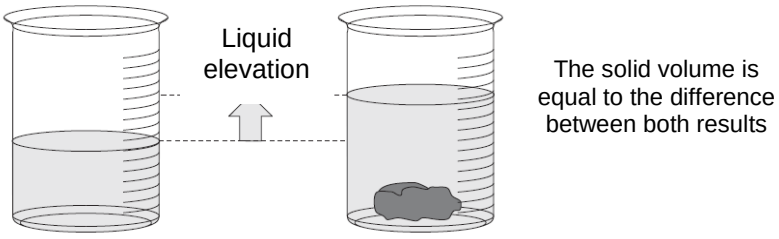

Fig. 1 – Volume Determination Method by Fluid Displacement

RESULTS AND DISCUSSIONS

Figure 2, (a), (b), and (c) shows the projected grid onto a the surface of an apple fruit model, the topographic view expressed in gray scale and digital elevation model, respectively. Table 01 shows the volume values as generated by the immersion technique. Table 02 shows the fruit volumes as obtained by the phase displacement Moiré method and processed by the Scilab. These volume values include the mean error obtained by means of calibrating object of regular geometry. The fluid displacement technique also generated the error calculation. Errors were applied to correct the sample dimensions.

RESULTADOS E DISCUSSÃO

Foi utilizado o método de deslocamento de fluido, onde foram obtidos os seguintes valores volumétricos encontrados na Tabela 1. Utilizando o software Scilab através de rotinas foram calculados os volumes do fruto conforme mostrados na Tabela 02 e comparados com os medidos através do deslocamento de fluido. Sendo que os valores obtidos no item TM são valores diretos obtidos Através da técnica de *moiré* por deslocamento de fase e tratados no scilab obtendo o volume da amostra, o valor do erro médio utilizado é obtido através de um objeto que foi utilizado como calibrador cujas dimensões são conhecidas e que posteriormente foram utilizadas para calcular a variação sendo similar ocorrido com a medição de volume por deslocamento de fluido onde o valor do erro médio utilizado é também o do objeto calibrador que posteriormente foi utilizado para calcular a variação e corrigindo os valores das amostras.

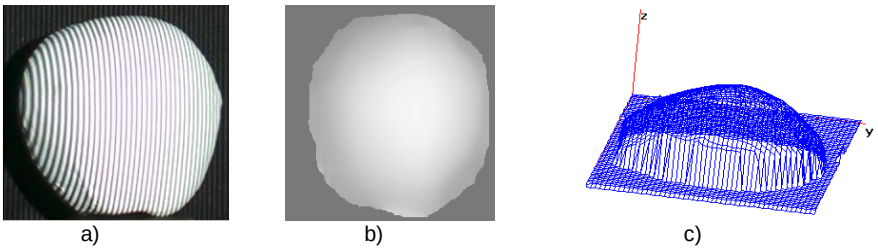

a) b) c)

Fig. 2 - (a) projection of fringes in the sample, (b) increase in MDE, (c) three-dimensional model

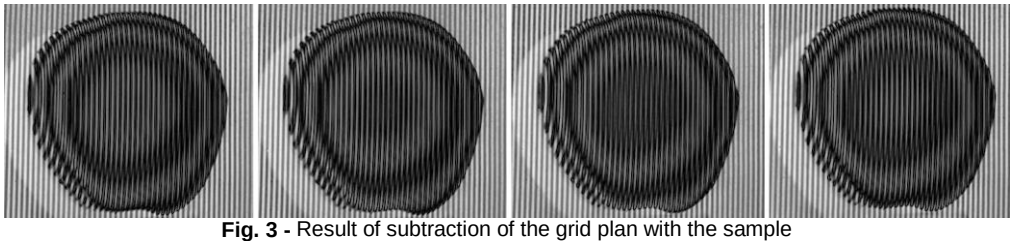

Fig. 3 - Result of subtraction of the grid plan with the sample

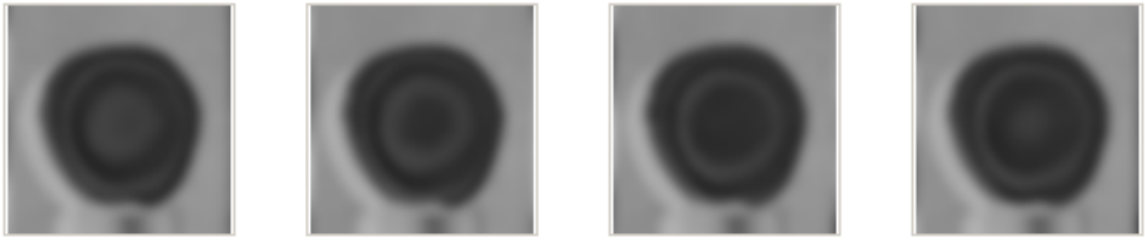

Fig. 4 - Result of subtraction of the grid plan with filtered sample image

Table 1

Volume obtained by immersion

Replication 1 (ml)	Replication 2 (ml)	Replication 3 (ml)	Replication 4 (ml)	Replication 5 (ml)	Mean (ml)	Mean (mm³)
400	380	400	390	390	392	392000

Table 2

Volume of the fruit model obtained through the Moiré method

Fruit Model	100lines/mm Ronchi (mm³)	100lines/mm Senoidal (mm³)	200lines/mm Ronchi (mm³)	200ines/mm Senoidal (mm³)	Mean (mm³)
TM	392201.520	389125.730	388780.070	386896.520	389250.960
Mean error (%)	3.91	2.21	1.86	0.61	1.340
Variation	15335.079	8599.679	7231.309	2360.069	5215.963
Corrected value	**37866.441**	**380526.051**	**381548.761**	**38.536.451**	**384034.997**
Displaced fluid volume	392000,000	392000,000	392000,000	392000,000	392000,000
Mean error (%)	1.9	1.9	1.9	1.9	1.9
Variation	7448	7448	7448	7448	7448
Corrected value	**384552,000**	**384552,000**	**384552,000**	**384552,000**	**384.552,000**

Variation between Methods	**7685.559**	**4025.949**	**3003.239**	**15.549**	**517.003**
% of variation after correction	**1.998574817**	**1.046919177**	**0.780970923**	**0.004043347**	**0.1344429**

The adjustment of variation between methods led to a value of 0.13 in percentage. Figures 5, 6 and 7 refer to the three-dimensional reconstitution of the apple fruit model as obtained by grid variation.

Foi aferida a variação entre os métodos obtendo-se um índice de 0,13 pontos percentuais médio entre as técnicas. Logo a seguir tem-se a reconstituição tridimensional da maçã utilizando as quatro variações sendo-as de tipos de grade e espessura.

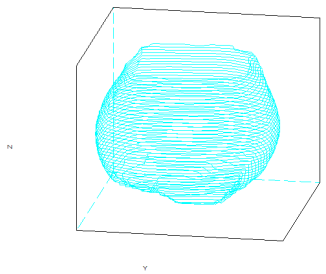

Fig. 5 – Three-dimensional reconstruction of the fruit model by the 100 lines/mm Ronchi grid

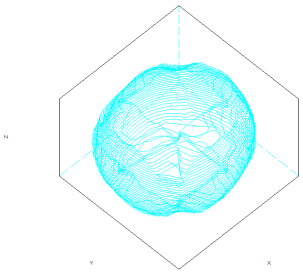

Fig. 6 – Three-dimensional reconstruction of the fruit model model by the 100 lines/mm with sinusoidal grid

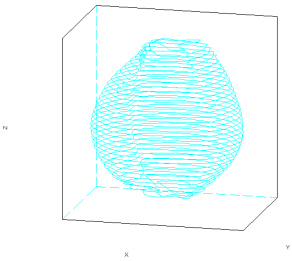

Fig. 7 - – Three-dimensional reconstruction of the fruit model by the 100 lines/mm Ronchi grid of 200 linhas/mm

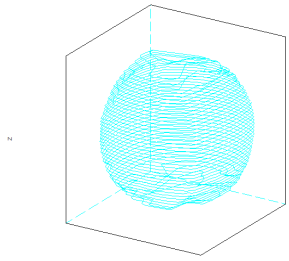

Fig. 8 - Three-dimensional reconstruction of the fruit model by the 200 lines/mm with sinusoidal grid

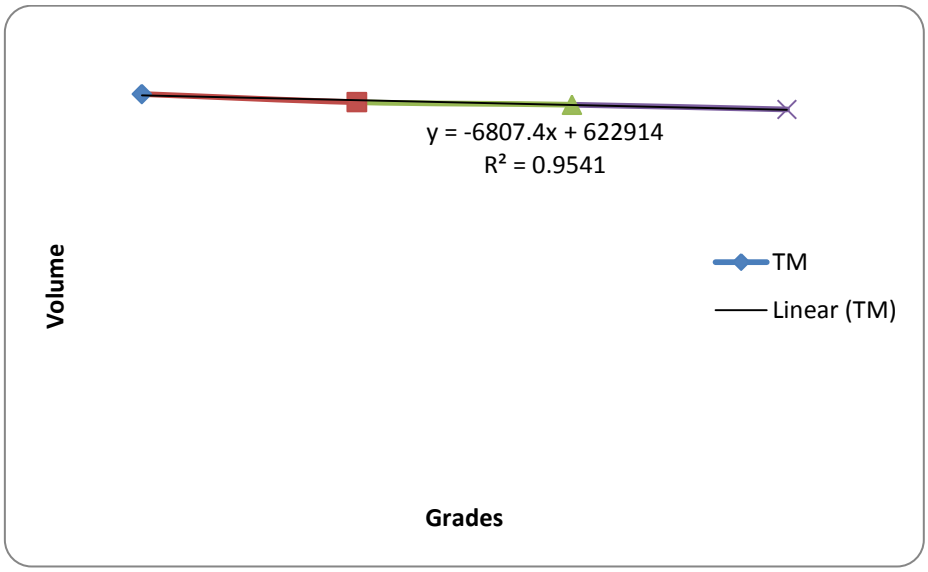

Fig. 9 - Correlation between the measured values

Referring to three-dimensional reconstitution the obtained results were shown to be satisfactory and useful to determine fruit volume. The application of different grids indicated the sinusoidal grid to generate better results.

CONCLUSIONS

Based on what it has been exposed before it can be concluded that Moiré method yields satisfactory results in determining fruit topography. These techniques allowed the determination of surface digital models; however they require specific computer programs. Sinusoidal grid with greater line density yielded better three-dimensional reconstruction. The Moiré method with phase displacement was noted to be of quick execution, causing no bruising on the testing material, mainly the results generated by the sinusoidal grid of higher density.

REFERENCES

[1]. Huang P.S., Feng J., Fu-Pen C. (1999) - *Quantitative evaluation of corrosion by a digital fringe projection technique*, Optics and Lasers in Engineering, vol. 31, pg. 331-380;
[2]. Lino A.C.L., Sanches J., Dal Fabbro I.M. (2008) - *Image processing techniques for lemons and tomatoes classification*, Bragantia, Campinas, vol. 67, no.3, pg. 785-789;
[3]. Lino A.C.L. (2002) - *Application of Moiré Optical Techniques* for the Study of Irregular Surface, 86pg, Master Thesis in Agricultural Engineering. Faculty of Agricultural Engineering, State University of Campinas, SP, Brazil;
[4]. Lino A.C.L., Dal Fabbro I.M., Rodrigues S. (2006) - *Fourier Transform Assisted Phase Shift Moiré Technique*, International Conference on Information Systems in Sustainable Agriculture, Agroenvironment and Food

Os resultados da reconstrução tridimensional obtidos mostraram ser satisfatórios e úteis na determinação do volume de frutas. Quanto a aplicação de diferentes tipos de grades ópticas, a grade sinusoidal gerou melhores resultados.

CONCLUSÕES

Baseado no que foi acima exposto, as seguintes conclusões podem ser emitidas.A introdução das TM de deslocamento de fase determinou satisfatoriamente a topografia de um fruto. Estas técnicas permitiram a geração de modelos digitais da superfície das amostras utilizadas. A TM com deslocamento de fase é bastante rápida, reconhece automaticamente picos e vales, mas necessita do uso de programas computacionais específicos. Foi possível reconstruir as amostras tridimensionalmente sem qualquer dano ao material amostrado com detalhamento de pontos, sendo esses mais perceptíveis utilizando grade senoidal com maior número de linhas/mm.

REFERÊNCIAS

[1]. Huang P.S., Feng J., Fu-Pen C. (1999) - *Avaliação Quantitativa de Corrosão po Meio de Projeção de Franjas Digitais*, Optics and Lasers in Engineering, vol. 31, p. 331-380;
[2]. Lino A.C.L., Sanches J., Dal Fabbro I.M. (2008) - *Técnicas de Processamento de Imagens para Classificação de Limões e Tomates*, *Bragantia*, Campinas, v.67, n.3, p.785-789;
[3]. Lino A.C.L. (2002) - *Técnica óptica de moiré visando a aplicação no estudo de superfícies irregulares*, 86 p., Dissertação (Mestrado em Engenharia Agrícola), Universidade Estadual de Campinas. Campinas;
[4]. Lino A.C.L., Dal Fabbro I.M., Rodrigues S. (2006) -. *Aplicação da Transformada de Fourier na Técnica de Moiré cm Deslocamento de Grade*, Anais da Conferencia Internacional em Sistema de Informação

Technology (HAICTA 2006), 2006, Volos. Annals of the International Conference on Information Systems in Sustainable Agriculture, Agroenvironment And Food Technology (HAICTA 2006). Volos: University of Thessaly, vol. 3. pg. 784-791;
[5]. Noordam J.C. (2010) - *Innovative Applications in the Agro and Food industry*, http://greenvision.wur.nl/, 20 de junlo;
[6]. Post D., Han B., Ifju P. (1994) - *High sensitivity Moiré: experimental analysis for mechanics and materials*, New York: Spring-Verlag.
[7]. Quan C., He X.Y., Wang C.F., Tay C.J, Shang H.M. (2001) - *Shape measurement of small objects using LCD fringe projection with phase shifting*, Optics Communication, vol. 189, pg. 21-29;
[8]. Smith Neto P., Fonseca E.A., Freitas G.H.F. (2006) - *Applicaton of Digital Shadow Moiré to Measurements of Human Body Perfilometry*, 5th International Conference on Mechanics and Materials in Design, 2006, Porto. Mechanics and Materials in Design, Leça do Balio, Portugal: INEGI - Instituto de Engenharia Mecânica e Gestão Industrial, vol. 1 pg. 63-71;
[9]. Smith Neto P., Magalhães Junior P.A.A. (2006) - *Determination of human body profile using digital shadow Moiré experimental technique*, Iberian Latin America Congress on Computational Methods in Engineering, 27 Cilamce, Belém-Pará. Cilamce2006. Belém, Pará: Universidade Federal do Pará;
[10]. Vecchio S.D., Campos I.L.P., Pinotti M., Sesselmann M. (2007) - *Measurement of three-dimensional profile free from the projection Moiré technique contours*, CONEM 2006. IV National Congress of Mechanical Engineering, Recife - PE, Proceedings of the IV National Congress of Mechanical Engineering. Rio de Janeiro - RJ. Brazilian Association of Mechanical Sciences and Engineering - ABCM, CDROM;
[11]. Wang Y. (2008) - Shadow Moiré sensitivity increase by fringe shifting: phase-stepping, <http://www.warpfinder.com/ hase.html>, 03/09/2008.
[12]. Winterle P. (2000) - *Vectors and analytic geometry*, São Paulo, Makron Books, ISBN 85-346-1109-2;
[13]. Wyant J.C. (2000) - *Phase-Shifting Interferometry*, http://www.optics.arizona.edu/jcwyant/Short_Courses/SPIE OpticalTesting/Part2.pdf, 20/05/2008;
[14]. Zhang Z., Towers C.E., Towers D.P. (2007) - *Phase and colour calculation in colour fringe projection,* J. Opt. A: Pure Appl. Opt., vol. 9, S81–S86;
[15]. Zhang Z., Towers C.E., Towers D.P. (2006) - *Time efficient color fringe projection system for 3D shape and color using optimum 3-frequency Selection*, Optics Express. vol. 14, pg. 6444 - 6455.

em Agricultura Sustentável, Ambiente Agrícola e Tecnologia de Alimentos. (HAICTA 2006), 2006, Volos. (HAICTA 2006), Volos: University of Thessaly, v. 3. p. 784-791;
[5]. Noordam J.C. (2010) - *Aplicações Inovativas na Industria Agrícola e de Alimentos*, http://greenvision.wur.nl/, 20 de junho;
[6]. Post D., Han B., Ifju P. (1994) - *Moiré de Alta Sensibilidade: Analise Experimental para Mecânica dos materias*, New York: Spring-Verlag;
[7]. Quan C., He X.Y., Wang C.F., Tay C.J, Shang H.M. (2001) - *Medida de Formas de Objetos Pequenos com Aplicação Projeção de Franjas com LCD com Mudança de Fase*, Optics Communication. v. 189, p. 21-29;
[8]. Smith Neto P., Fonseca E.A., Freitas G.H.F. (2006) - *Aplicação da Técnica de Moiré de Sombra Digital na Medição do Perfil do Corpo Humano*, Quita Conferencia Internacional em Mecânica e Materiais em Projeto, Porto. Leça do Balio, Portugal: INEGI - Instituto de Engenharia Mecânica e Gestão Industrial, v. 1. p. 63-71;
[9]. Smith Neto P., Magalhães Junior P.A.A. (2006) -. *Determinação do Perfil do Corpo Humano com Aplicação da Tecnica de Moiré de Sombra*, Congresso Ibero Latino Americano em Métodos Computacionais em Engenharia. - 27 Cilamce, Belém-Pará, Cilamce2006. Belém, Pará: Universidade Federal do Para;
[10]. Vecchio S.D., Campos I.L.P., Pinotti M., Sesselmann M. (2007) - *Medição do perfil tridimensional de contornos livres a partir da técnica de moiré de projeção*, CONEM 2006. IV Congresso Nacional de Engenharia Mecânica, Recife – PE, Anais do IV Congresso Nacional de Engenharia Mecânica. Rio de Janeiro – RJ. Associação Brasileira de Engenharia e Ciências Mecânicas - ABCM, CDROM;
[11]. Wang Y. (2008) - *Aumento da Sensibilidade da Técnica de Moiré de Sombra Através de Mudança de Franja e Incremento de Fase*, http://www.warpfinder.com/ phase.html, 03/09/2008;
[12]. Winterle P. (2000) - *Vetores e geometria analítica*, São Paulo, Makron Books, ISBN 85-346-1109-2;
[13]. Wyant J.C. (2000) - *Interferometria de Mudança de Fase*, http://www.optics.arizona.edu/jcwyant/Short_Courses/SPIE OpticalTesting/Part2.pdf, 20/05/2008;
[14]. Zhang Z., Towers C.E., Towers D.P. (2007) - *Calculo de Fase e Cor em Projeção de Franjas Coloridas*. J. Opt. A: Pure Appl. Opt. v. 9, S81–S86, 2007.
[15]. Zhang Z., Towers C.E., Towers D.P. (2006) - *Sistema de Projeção de Franjas Coloridas para Determinação de Forma e Cor com Aplicação Otimizada de Três Frequências Selecionadas*. Optics Express. v. 14, v. 14, p. 6444 - 6455.

FREE SURFACE EQUATION OF BEER WORT IN A ROTAPOOL
/
ECUAŢIA SUPRAFEŢEI LIBERE A MUSTULUI DE BERE ÎN ROTAPOOL

Prof. PhD. Eng. Biriş S.Şt.[1)], PhD. Eng. Vlăduţ V.[2)], As. PhD. Stud. Eng. Ungureanu N.[1)], Lect. Ph.D. Eng. Begea M.[1)], As. PhD. Stud. Eng. Ionescu M.[1)]
[1)] Polytechnic University Bucharest, Faculty of Biotechnical Systems Engineering / Romania
[2)]INMA Bucharest / Romania
Tel: 0744756832; E-mail: biris.sorinstefan@gmail.com

Abstract: *In this paper is presented a mathematical model that allows an analytical description of the free surface of the beer wort in a rotapool. The free surface of the beer wort in the rotapool has the equation of a rotation paraboloid. The developed mathematical model has allowed, using the Microsoft Excel program, plotting variation graphs after radial direction of the liquid height, for different supply conditions of beer wort and different typo-dimensional vessels.*

Keywords: *mathematical model, rotapool, free surface, beer wort, hydrodynamic process*

INTRODUCTION

Beer wort boiled with hops contains hops draff in suspension and precipitates formed during wort boiling, which is called ”hot trub”, with particles of 30-80 µm, containing a quantity of 40-80 g d.s./hl of wort [11, 13].

The study of the wort, yeast and beer fermentation, its manufacturing technology, have been studied in numerous papers [1, 2, 3, 5, 6, 8, 9] in order to determine if the new equipment can influence the flavor of beer [4], if the baker's yeast influence the formation of fungi [7] or if the wort fermentation by increased gravity has an influence on the metabolism [10, 12].

Hot trub can be separated by sedimentation, centrifugation, filtration or, more commonly, by a process of complex hydrodynamic separation in a vessel called rotapool (Fig. 1), cylindrical-shaped and closed, into which the hot wort is introduced tangentially at velocities of up to 5 m/s through a connection (nozzle) 1, located in the lower third of the vessel. The vessel body and bottom are isolated, in order to maintain a high temperature 6 of the wort in the process of trub separation, through isolation 2.

Rezumat: *În cadrul acestei lucrări, este prezentat un model matematic care permite descrierea analitică a suprafeţei libere a mustului de bere în rotapool. Suprafaţa liberă a mustului de bere în rotapool are ecuaţia unui paraboloid de rotaţie. Modelul matematic elaborat a permis, folosind programul Microsoft Excel, trasarea graficelor de variaţie după direcţia radială a înălţimii lichidului, pentru diverse condiţii de alimentare cu must de bere şi diverse tipo-dimensiuni de vase.*

Cuvinte cheie: *model matematic, rotapool, suprafaţa liberă, must de bere, proces hidrodinamic*

INTRODUCERE

Mustul de bere fiert cu hamei conţine în suspensie borhotul de hamei şi precipitate formate în timpul fierberii mustului, care poartă denumirea de ”trub la cald”, având particule de 30-80 µm, fiind în cantitate de 40-80 g s.u. / hl must [11, 13].

Studiul mustului, drojdiei şi fermentarea berii, tehnologia de fabricare a acesteia, au fost studiate în numeroase lucrări [1, 2, 3, 5, 6, 8, 9] pentru a se determina dacă echipamentele noi pot influenţa aroma berii [4], dacă drojdia din brutării influenţează formarea ciupercilor [7] sau ce influenţa asupra metabolismului o are fermentarea mustului prin gravitaţie ridicată [10, 12].

Trubul la cald se poate separa prin sedimentare, centrifugare, filtrare sau, cel mai adesea, printr-un procedeu de separare hidrodinamică complexă, într-un vas numit rotapool (Fig. 1), care este de formă cilindrică, închis, în care mustul fierbinte este introdus tangenţial cu viteze de până la 5 m/s printr-un racord (duză) 1, situată în treimea inferioară a vasului. Corpul şi fundul vasului sunt izolate, pentru a menţine temperatura ridicată a mustului 6 în procesul de separare a trubului, prin intermediul unei izolaţii 2.

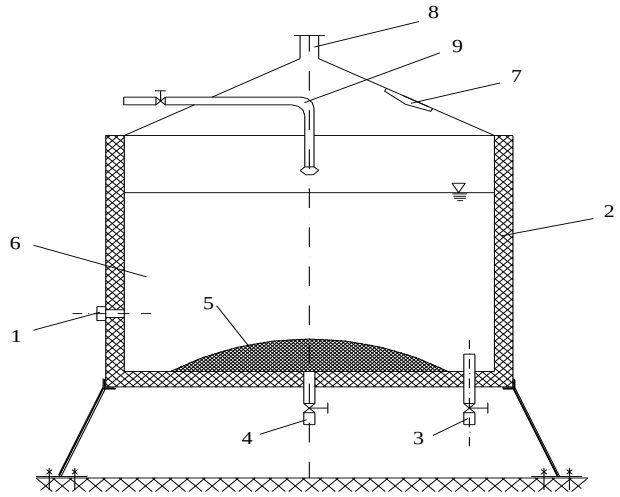

Fig. 1 – Vessel for hydrodynamic separation of hot trub from the beer wort

After 20-40 minutes, as long as it takes the separation process [11, 13], the wort is discharged through the connection 3, while trub 5 accumulated at the bottom of the vessel is discharged through the connection 4, mixed with the washing water introduced into the vessel through the connection 9. The vessel is also fitted with a basket 8 for secondary steam evacuation and a sight 7.

Due to the complex hydrodynamic process taking place in the rotapool, the free surface of beer wort is not plane, having the shape of a rotation paraboloid.

The isolation of the vessel walls must cover entirely the contact surface between wort and walls, in order to reduce heat exchange with the outside environment and to maintain a high temperature of the wort in the vessel. But, during the working process, the height of the liquid on the lateral walls increases, so, due to that fact, at present, isolation width remains constant up to the top of the vessel.

Deducting the free surface equation of the liquid in the rotapool, the maximum height of the liquid in the vessel walls can be inferred, from which the above no longer requires an isolation of the same consistency.

MATERIALS AND METHOD

The equation defining the shape of the free surface of beer wort in the rotapool can be deduced based on the following assumptions:

- the effect of beer wort viscosity is neglected;
- the velocity of beer wort is maximum near the wall, being directly proportional with the horizontal component of liquid input velocity in the vessel;
- the study refers to the final stage of trub separation process, when the volume of liquid in the vessel reaches the nominal value.

The wort is placed in the lower third of the vessel, tangential to its body, with velocity v_l=2-5 m/s and an angle α = 15°, supply that prints a rotation movement of the liquid in the vessel, forming upward currents in the central area of the vessel and descending currents at the periphery, transporting and deposing trub particles in the central area of the vessel bottom (Fig. 2).

După 20-40 minute, cât durează procesul de separare [11, 13], mustul este evacuat prin racordul 3, iar trubul 5 depus pe fundul vasului, este evacuat prin racordul 4, în amestec cu apa de spălare introdusă în vas prin racordul 9. Vasul mai este prevăzut cu un coş 8 pentru evacuarea aburului secundar şi cu un vizor 7.

Datorită procesului hidrodinamic complex care se desfăşoară în rotapool, suprafaţa liberă a mustului de bere nu este plană, ci este de forma unui paraboloid de revoluţie.

Izolaţia pereţilor vasului trebuie să acopere întreaga suprafaţă de contact dintre must şi pereţi, pentru a reduce schimbul de căldură cu mediul înconjurător şi pentru a menţine temperatura ridicată a mustului în vas. Dar, în procesul de lucru, înălţimea lichidului pe pereţii laterali creşte şi de aceea, în prezent, vasele au izolaţii cu aceeaşi grosime până la partea superioară a vasului.

Deducându-se ecuaţia suprafeţei libere a lichidului în rotapool se va putea deduce care este înălţimea maximă a lichidului pe pereţii vasului, de la care în sus nu se mai impune o izolaţie de aceeaşi consistenţă.

MATERIALE ŞI METODĂ

Ecuaţia care defineşte forma suprafeţei libere a mustului de bere în rotapool se deduce pe baza următoarelor ipoteze:

- se neglijează efectul vâscozităţii mustului de bere;
- viteza mustului de bere în zona peretelui este maximă, fiind direct proporţională cu componenta orizontală a vitezei de introducere a mustului în vas;
- studiul se referă la etapa finală a procesului de separare a trubului, când volumul de lichid din vas ajunge la valoarea nominală.

Mustul este introdus în vas în treimea inferioară, tangenţial la corpul acestuia, cu viteza v_l=2-5 m/s şi sub un unghi α = 15°, alimentare care imprimă o mişcare de rotaţie a lichidului în vas, luând naştere curenţi ascensionali la partea centrală a vasului şi coborâtori la periferie, care transportă şi depun particulele de trub în partea centrală a fundului vasului (Fig. 2).

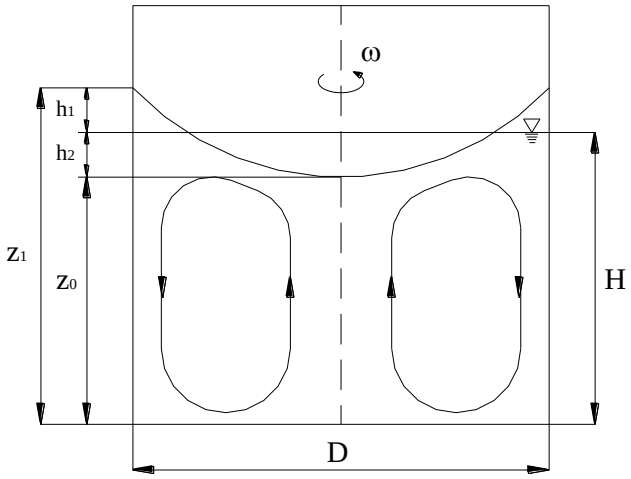

Fig. 2 – Calculus model for the free surface of the wort in the rotapool

Theoretical tangential velocity of the liquid in the vessel, on its periphery, is calculated from velocity v_l, angle α and a decrease coefficient of the velocity in the vessel k=0,3-0,5, with the equation:

Viteza teoretică tangenţială a lichidului în vas, la periferia acestuia, se calculează în funcţie de viteza v_l, de unghiul α şi un coeficient de scădere a vitezei lichidului în vas k=0,3-0,5, cu relaţia:

$$v = k \cdot v_l \cdot \cos\alpha = R \cdot \omega \quad (1)$$

from which it results the angular velocity of the liquid in

din care rezultă viteza unghiulară a lichidului în vas:

the vessel:

$$\omega = \frac{k \cdot v_l \cdot \cos\alpha}{R} \quad (2)$$

On the free surface of the beer wort (Fig. 3) are acting the centrifugal force F_c and weight G:

Pe suprafaţa liberă a mustului de bere (Fig. 3) acţionează forţa centrifugă F_c şi greutatea G:

$$F_c = m \cdot r \cdot \omega^2 \quad (3)$$

$$G = m \cdot g \quad (4)$$

with the resultant N normal to the surface (Fig. 3).

care au rezultanta N normală la suprafaţă (Fig. 3).

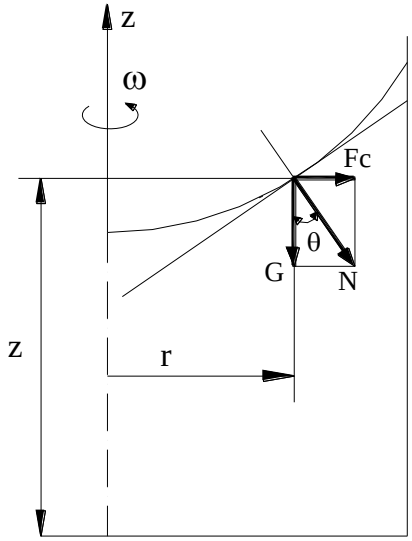

Fig. 3 – Force components

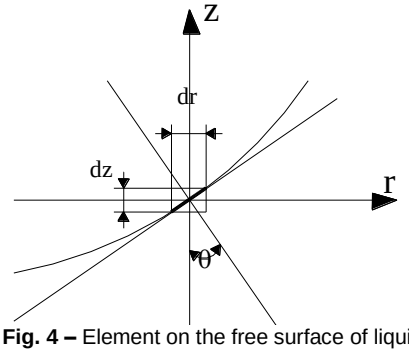

Fig. 4 – Element on the free surface of liquid

From figures 3 and 4, equation (5) can be written:

Analizând figurile 3 şi 4 se poate scrie relaţia:

$$tg\theta = \frac{F_c}{G} = \frac{m \cdot r \cdot \omega^2}{m \cdot g} = \frac{r \cdot \omega^2}{g} = \frac{dz}{dr} \quad (5)$$

Considering that the velocity distribution is linear:

Considerând distribuţia de viteze liniară:

$$v = r \cdot \omega \quad (6)$$

it results:

rezultă:

$$dz = \frac{r \cdot \omega^2}{g} \cdot dr \quad (7)$$

By integrating relation (7) it results:

Prin integrarea relaţiei (7) rezultă:

$$\int dz = \int \frac{r \cdot \omega^2}{g} \cdot dr = \frac{\omega^2}{g} \cdot \int r \cdot dr \quad (8)$$

respectively:

respectiv:

$$z - z_0 = \frac{r^2 \cdot \omega^2}{2 \cdot g} \tag{9}$$

so the free surface equation of the beer wort in the rotapool has the following form:

din care rezultă ecuaţia suprafeţei libere a mustului de bere în rotapool sub forma:

$$z = z_0 + \frac{\omega^2}{2 \cdot g} \cdot r^2 \tag{10}$$

equivalent to the equation:

care este echivalentă cu ecuaţia:

$$z = z_0 + \frac{\omega^2}{2 \cdot g} \cdot \left(x^2 + y^2\right) \tag{11}$$

z_0 can be deduced from the following conditions:

Valoarea z_0 se deduce punând condiţiile:

$$r = R \implies z = H + h_1 = z_0 + \frac{\omega^2}{2 \cdot g} \cdot R^2 \tag{12}$$

$$r = 0 \implies z = z_0 = H - h_2 \tag{13}$$

$$h_1 = h_2 \tag{14}$$

it results:

din care rezultă:

$$z_0 = H - \frac{\omega^2}{4 \cdot g} \cdot R^2 \tag{15}$$

Given the relation (15), equations (10) and (11) will have the final form:

Ţinând cont de relaţia (15), ecuaţiile (10) şi (11) vor avea forma finală:

$$z = H - \frac{\omega^2 \cdot R^2}{4 \cdot g} \cdot \left(1 - 2 \cdot \frac{r^2}{R^2}\right) \tag{16}$$

$$z = H - \frac{\omega^2 \cdot R^2}{4 \cdot g} \cdot \left(1 - 2 \cdot \frac{x^2 + y^2}{R^2}\right) \tag{17}$$

RESULTS

The mathematical model developed in this paper has allowed obtaining data which were processed in Microsoft Excel and plotting variation graphs after radial direction of the height of the points on the free surface of beer wort, for various supply conditions of beer wort and various typo-dimensional vessels.

Three different vessels were studied, with diameters of 3 m, 2 m and 1 m, for which, in all cases, the liquid height H was 1 m. The liquid input velocity in the vessel was 3m/s, 4 m/s and 5 m/s.

Variations in liquid height after radial direction in the three vessels, for three different input velocities of beer wort in the rotapool, are shown in figures 5 and 6.

REZULTATE

Modelul matematic elaborat în cadrul prezentei lucrări a permis obţinerea unor date care au fost prelucrate în Microsoft Excel şi au permis trasarea graficelor de variaţie după direcţia radială a înălţimii punctelor de pe suprafaţa liberă a mustului de bere, pentru diverse condiţii de alimentare cu must de bere şi diverse tipo-dimensiuni de vase.

Au fost studiate trei vase diferite, având diametru de 3m, 2 m şi 1 m, la care, în toate cazurile, înălţimea H a lichidului a fost de 1 m. Viteza de introducere a lichidului în vas a fost de 3 m/s, 4 m/s şi 5 m/s.

Variaţia înălţimii lichidului după direcţia radială în cele trei vase studiate, pentru cele trei viteze diferite de introducere a mustului de bere în rotapool, este prezentată în figurile 5 şi 6.

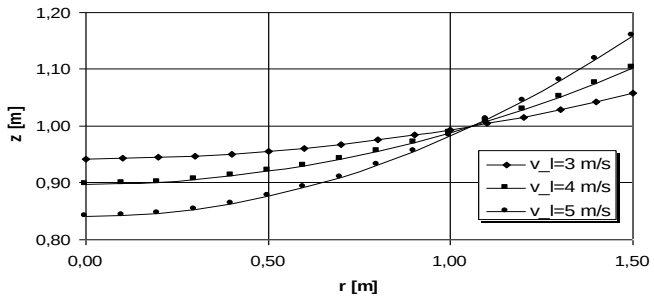

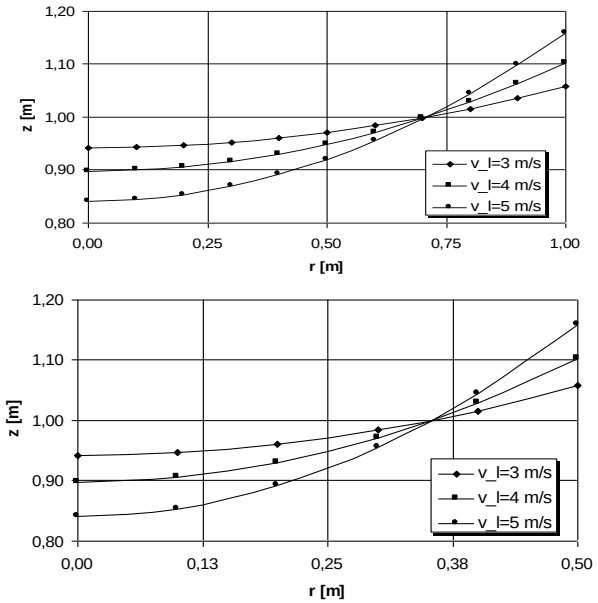

Fig. 5 – Variation in liquid height after radial direction in vessels of radius R=1,5 m, R=1 m, R=0,5 m, for three velocities v_l

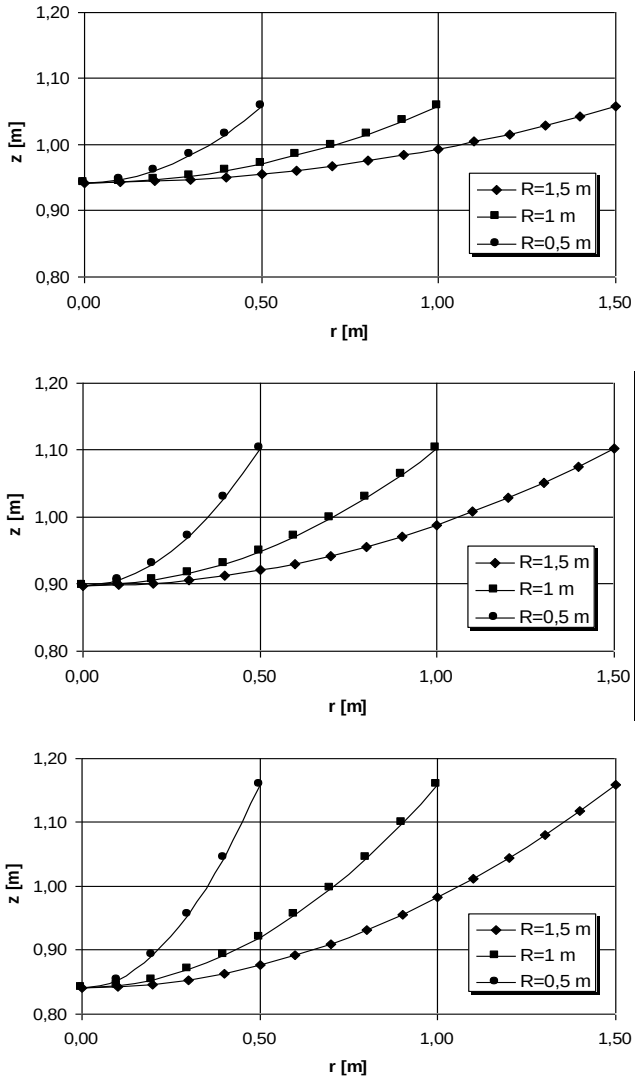

Fig. 6 – Variation in liquid height after radial direction, after entering the vessel with velocities v_l=3 m/s, v_l=4 m/s, v_l=5 m/s, for three radius R

CONCLUSIONS

The free surface equation of beer wort in the rotapool, deduced in this paper, has the expressions (16), respectively (17), representing a rotation paraboloid.

Figures 5 and 6 show that regardless of the vessel diameter, for the same liquid height H and the same liquid input velocity in the vessel vl, the maximum beer wort height in the rotapool is the same.

REFERENCES

[1]. Boulton C, Quain DE. (2001) - *Brewing yeast and fermentation*, Oxford: Blackwell Science Ltd.;
[2]. Briggs D.E., Chris A. Boulton, Peter A., Stevens B. and Stevens R. (2004) - *Brewing Science and Practice*, Woodhead Publishing Limited, Abington Hall, Abington, Cambridge CB1 6AH, England;
[3]. Kiselev P.G., (1988) - *Directory for hydraulic calculations*, Technical Publishing House, Bucharest;
[4]. Meilgaard M. (2001) - *Effects on flavour of innovations in brewery equipment and processing: A review*, Journal of The Institute of Brewing 107:271–86;
[5]. Narziβ L., (1980) - *Technologies brewing*, Ferdinand Enke Verlag, Stuttgart;
[6]. Pădureanu V. (2001) - *Equipment for brewing*, "Transilvania" University Brasov Publishing;
[7]. Reynolds TB, Fink GR. (2001) - *Baker's yeast, a model for fungal biofilm formation*, Science 291:878–81;
[8]. Rus, Fl. (2001) - *Separation operations in the food industry*, Editura Universităţii Transilvania, Braşov;
[9]. Rus, Fl. (2001) - *Bazele operaţiilor din industria alimentară,* "Transilvania" University Brasov Publishing;
[10]. Stewart GG. (2001) - *Fermentation of high gravity worts – its influence on yeast metabolism and morphology*, Proceedings European Brewery Convention Congress, Chapter 36;
[11]. Stroia I., Biriş S.Şt., Begea M., (1998) - *Equipment for malt and beer*, CISON Publishing House, Bucharest;
[12]. Verstrepen KJ, Derdelinckx G, Verachtert H, Delvaux FR. (2003) - *Yeast flocculation: what brewers should know,* Applied Microbiology and Biotechnology 61:197–205;
[13]. *** (1999) - *Handbook of Food Engineer*, Vol. 2, Technical Publishing House, Bucharest.

CONCLUZII

Ecuaţia suprafeţei libere a mustului de bere în rotapool, dedusă în cadrul prezentei lucrări, are expresia (16) respectiv (17), reprezentând un paraboloid de rotaţie.

Din figurile 5 şi 6 rezultă că indiferent de diametrul vasului, pentru aceeaşi înălţime H a lichidului şi aceeaşi viteză de introducere a lichidului în vas vl, înălţimea maximă a mustului de bere în rotapool este aceeaşi.

BIBLIOGRAFIE

[1]. Boulton C, Quain DE. (2001) - *Drojdia şi fermentarea berii*, Oxford: Blackwell Science Ltd.;
[2]. Briggs D.E., Chris A. Boulton, Peter A., Stevens B. and Stevens R. (2004) - *Ştiinţa şi practica fabricării berii*, Editura Woodhead Limited, Abington Hall, Abington, Cambridge CB1 6AH, England;
[3]. Kiselev P.G., (1988) - *Îndreptar pentru calcule hidraulice*, Editura Tehnică, Bucureşti;
[4]. Meilgaard M. (2001) - *Efectele asupra aromelor ale inovaţiilor în echipamentele si procesarea berii*: O sinteză, Jurnalul Institutului de Bere 107:271–86;
[5]. Narziβ L., (1980) – *Tehnologii de fabricare a berii*, Ferdinand Enke Verlag, Stuttgart;
[6]. Pădureanu V. (2001) - *Utilaje pentru fabricarea berii*, Editura Universităţii "Transilvania" Braşov;
[7]. Reynolds TB, Fink GR. (2001) - *Drojdia din brutării, un model pentru formarea ciupercilor biofilm*, Ştiinţă 291:878–81;
[8]. Rus, Fl. (2001) - *Operaţii de separare în industria alimentară*, Editura Universităţii Transilvania, Braşov;
[9]. Rus, Fl. (2001) - *Bazele operaţiilor din industria alimentară,* Editura Universităţii Transilvania, Braşov;
[10]. Stewart GG. (2001) - *Fermentarea mustului prin gravitaţie ridicată – influenţa sa asupra metabolismului şi morfologiei drojdiei,* Lucrările Convenţiei Congresului European de fabricare a berii, Capitol 36;
[11]. Stroia I., Biriş S.Şt., Begea M., (1998) - *Utilaje pentru industria malţului şi a berii*, Editura CISON, Bucureşti;
[12]. Verstrepen KJ, Derdelinckx G, Verachtert H, Delvaux FR. (2003) - *Floculaţia berii: ce trebuie să ştim despre fabricarea berii,* Microbiologie şi biotehnologie aplicată 61:197–205;
[13]. *** (1999) - *Manualul inginerului de industrie alimentară*, Vol. 2, Editura Tehnică, Bucureşti.

RESEARCHES ON HORTICULTURAL PRODUCTS DECONTAMINATION DESIGNED TO FRESH CONSUMPTION, USING NON-IONIZING UV-C ULTRAVIOLET RADIATION
/
CERCETARI PRIVIND DECONTAMINAREA PRODUSELOR HORTICOLE DESTINATE CONSUMULUI IN STARE PROASPATA, UTILIZAND RADIATIA NEIONIZANTA ULTRAVIOLETA UV-C

PhD. Eng. Sorică C.[1)], Prof. PhD. Eng. Pirnă I.[1)], PhD. Stud. Eng. Matache M.[1)], PhD. Stud. Eng. Voicea I.[1)], Eng. Grigore I.[1)], Eng. Bolintineanu Gh.[1)], PhD. Stud. Eng. Cujbescu D.[1)], PhD. Stud. Eng. Sorică E.[1)], PhD. Eng. Kabas O.[2)]

[1)]INMA Bucharest / Romania; [2)] Batı Akdeniz Agricultural Research Institute, Antalya / Turkey

E-mail: cri_sor2002@yahoo.com

Abstract: *Consumed in fresh-state, horticultural products can be carriers of some optional pathogenic microorganisms: bacteria, yeasts, molds. These microorganisms can cause either loss of horticultural products in the storage process, due to the post harvest decay process or food-borne diseases with direct effects on consumer human health. In this context, the paper presents experimental researches on the possibility of using non-ionizing ultraviolet radiation UV-C within the conditioning technologies of horticultural products, by investigating the capability of an experimental model of installation for the decontamination of external surfaces of horticultural products, to apply the minimum dosage recommended for the destruction of the most representative pathogens.*

Keywords: *post harvest treatment,, UV-C radiation, fruits and vegetable, shelf-life*

INTRODUCTION

Fruits and vegetables play an important role in the human nutrition. The nutritive value of horticultural products consumed in fresh-state, is given especially by large quantities of vitamins which they synthesize. Vitamins are biocatalysts of life processes, essential for life, their absence from the human metabolism causing serious functional disorders. The failure of keeping the vitamins into the body, implies the need for a permanent intake in daily food components. For the continuos supply of fresh fruits and vegetables, it is necessary to extend the shelf-life of these products, to eliminate the seasonality of consumption, to get closer the production areas to the consumption ones, to reduce as much as possible the loss due to the degradation of perishable food products.

Consumed in fresh-state, horticultural products can be carriers of some optional pathogenic microorganisms: bacteria, yeasts, molds. These microorganisms can cause either loss of horticultural products in the storage process, due to the post harvest decay process or food-borne diseases with direct effects on consumer human health. Losses of horticultural products, due to the post-harvest decay process, are at the level of 10-50% depending on the degree of development of the area and the facilities for temporary storage. In order to limit these losses, there have been used synthetic fungicide substances. Residues of these substances, which remain on the surface of horticultural products, after treatment, are considered a potential threat to consumer health and especially children [9].

Rezumat: *Consumate în stare proaspătă, produsele horticole pot fi purtatoare ale unor microorganisme facultativ patogene: bacterii, drojdii, mucegaiuri. Aceste microorganisme pot provoca fie pierderi de produse horticole la pastrare, datorate procesului de descompunere postrecoltare, fie îmbolnăviri sau toxinfecţii alimentare cu efecte directe asupra sanatatii consumatorului uman. In acest context, lucrarea prezinta cercetari experimentale privind posibilitatea de utilizare a radiatiei ultraviolete neionizante UV-C in cadrul tehnologiilor de conditionare a produselor horticole, prin investigarea capabilitatii unui model experimental de instalatie pentru decontaminarea suprafetelor exterioare ale produselor horticole, de a aplica dozele minime de radiatie recomandate pentru distrugerea celor mai reprezentativi agenti patogeni.*

Cuvinte cheie: *tratament post recoltare, radiatie UV-C, fructe si legume, perioada de valabilitate*

INTRODUCERE

Fructele si legumele joacă un rol important în alimentaţia umana. Valoarea nutritivă a produselor horticole consumate în stare proaspătă este dată în special de cantităţile importante de vitamine pe care le sintetizează. Vitaminele sunt biocatalizatori ai proceselor vitale, indispensabile vieţii, absenţa lor din metabolismul uman producând grave tulburări funcţionale. Imposibilitatea de păstrare în organism a vitaminelor, implică necesitatea unui aport permanent în componentele alimentare zilnice. Pentru aprovizionarea continuă cu fructe si legume proaspete, este necesar să se prelungească durata de păstrare a acestor produse, să se elimine cât mai mult caracterul sezonier al consumului, să se apropie zonele producătoare de cele consumatoare şi să se reducă într-o măsură cât mai mare pierderile prin degradarea produselor alimentare perisabile.

Consumate în stare proaspătă, produsele horticole pot fi purtatoare ale unor microorganisme facultativ patogene: bacterii, drojdii, mucegaiuri. Aceste microorganisme pot provoca fie pierderi de produse horticole la pastrare, datorate procesului de descompunere postrecoltare, fie îmbolnăviri sau toxinfecţii alimentare cu efecte directe asupra sanatatii consumatorului uman. Pierderile de produse horticole, datorate procesului de descompunere postrecoltare, se situeaza la nivelul a 10-50 % in functie de gradul de dezvoltare al zonei respective si facilitatile de pastrare temporara. In vederea limitarii acestor pierderi, s-au utilizat substante fungicide sintetice. Reziduurile acestor substante, care raman pe suprafata produselor horticole

Alternative methods to fungicide treatments have been studied in order to prevent horticultural products losses in the post harvest phase. Within these methods the applications of biological control agents, plant bioactive compounds and physico-chemical methods showed interesting results but still far from a practical application in Europe. Despite the substantial progress obtained with biological control agents, the use of them is limited due to their insufficient and inconsistent performance. The use of plant bioactive compounds has shown that the treatment conditions (concentration, form of application, time of treatment, etc.) can deeply influence their efficacy. A barrier to use the plant bioactive compounds may not be the efficacy, but rather the off-odours caused in horticultural products and/or the phytotoxicity. Physico-chemical methods include heat, ionising radiation, ultraviolet UV-C radiation and food additives which induce the resistance to pathogens [13].

Conventional thermal methods of food sterilizarion are unsuitable for fruits and vegetable destined for fresh consumption because of the heat which causes inevitable changes of color, smell, flavor and a loss of nutritional value [12].

Recent research has identified a number of energy-based alternative technologies to improve the safety of fresh and fresh-cut fruits and vegetables: ultraviolet radiation, electron-beam irradiation, technology with pulsed visible light and technology with cold plasma. In some cases, such as UV light, these technologies have a substantial database of information regarding the use in other domains, and can be adapted to use with fresh produce. In other cases, such as with electron-beam irradiation, advances in technology need new researches. Other technologies, such as pulsed visible light and cold plasma, are newer areas of research that hold promise as antimicrobial processes which can reduce the viability of bacterial pathogens on fresh products.

Within the methods earlier mentioned, a special potential has the use of non-ionizing ultraviolet radiation UV-C. The wavelength range that varies between 200 and 280 nm, which is considered lethal to most types of microorganisms, affects the DNA replication of these microorganisms [3], [4]. Non-Ionizing UV radiation can cause breaks of molecular chemical bonds and can induce photochemical reactions. The biological effects of UV radiation depend on the wavelength and the exposure time. UV-C ultraviolet radiation is already successfully used in various fields such as medicine (decontamination of air and medical instruments), environment (wastewater treatment), packaging industry (decontamination of packaging for various food products) etc. Worldwide, there are initiatives in using this method for decontaminating the outer surfaces of food products. As a postharvest treatment on fresh produce, UV-C irradiation has been proven beneficial to reduce respiration rates, control rot development, and delay senescence and ripening in different whole or fresh-cut fruits and vegetables, such as apples, citrus, peaches,

dupa tratare, sunt considerate o amenintare potentiala la adresa sanatatii consumatorilor si in mod special a copiilor [9].

Au fost studiate, de asemenea, metode alternative la tratamentele cu fungicide, in vederea prevenirii pierderilor de produse horticole in perioada postrecoltare. In cadrul acestor metode, utilizarea agentilor de control biologic, compusilor bioactivi obtinuti din plante si metodelor fizico-chimice au obtinut rezultate interesante dar inca departe de o aplicare practica in Europa. In ciuda progresului substantial obtinut in privinta agentilor de control biologic, utilizarea acestora este limitata datorita performantelor insuficiente si inconsistente obtinute. Utilizarea compusilor bioactivi obtinuti din plante a aratat faptul ca eficienta lor poate fi infuentata de conditiile de tratament (concentratie, forma de aplicare, timp de tratament etc.). Un obstacol in calea aplicarii nu este reprezentat de eficienta metodei ci de mirosurile nespecifice si/sau fitotoxicitatea induse materialului horticol. Categoria metodelor fizico-chimice include utilizarea caldurii, radiatiei ionizante, radiatiei ultraviolete UV-C si aditivilor alimentari ce induc rezistenta la agentii patogeni [13].

Metodele termice conventionale de decontaminare sunt improprii utilizarii pentru fructe si legume destinate consumului in stare proaspata datorita caldurii care produce modificari permanente ale culorii, mirosului, aromelor si pierderi ale valorii nutritionale [12].

Cercetarile recente au identificat o serie de tehnologii alternative bazate pe energie pentru a imbunatati siguranta fructelor și legumelor proaspete și proaspăt tăiate: radiatia ultravioleta, iradierea cu fascicul de electroni, tehnologia cu impulsuri de radiatie luminoasa vizibilă și tehnologia cu plasmă rece. In unele cazuri, cum ar fi radiatia ultravioleta, aceste tehnologii au o baza de date substanțiala de informații privind utilizarea in alte domenii, și pot fi adaptate pentru a fi utilizate pentru produsele proaspete. În alte cazuri, cum ar fi iradierea cu fascicul de electroni, progresele tehnologice necesita cercetari noi. Alte tehnologii, cum ar fi tehnologia cu impulsuri de radiatie luminoasa vizibilă și cu plasmă rece, sunt domenii noi de cercetare care promit a fi utilizate ca procese antimicrobiene ce pot reduce viabilitatea agenților patogeni bacterieni in cazul produselor proaspete.

In cadrul metodelor enumerate anterior, un potential deosebit il are utilizarea radiatiei neionizante ultraviolete UV-C. Lungimea de unda cuprinsa intre 200 si 280 nm, care este considerata letala pentru majoritatea tipurilor de microorganisme, afecteaza replicarea AND-ului microorganismelor patogene [3], [4]. Radiaţiile UV neionizante pot produce ruperi de legături chimice moleculare şi pot induce reacţii fotochimice. Efectele biologice ale iradierii cu ultraviolete depind de lungimea de undă şi de timpul de expunere. Radiatia ultravioleta UV-C este deja utilizata cu succes in diverse domenii precum medicina (decontaminarea aerului si a instrumentarului medical), ecologie (epurarea apelor uzate), industria ambalajelor (decontaminarea ambalajelor pentru diverse produse alimentare) etc. Pe plan mondial exista preocupari in domeniul utilizarii acestui procedeu pentru decontaminarea suprafetelor exterioare ale produselor alimentare. Ca si tratament postrecoltare al produselor horticole, iradierea cu radiatie ultravioleta UV-C s-a dovedit benefica in diminuarea ratei

watermelon, grape berries, tomatoes, lettuce, baby spinach and mushrooms [5], [10], [1], [2], [6], [8], [7], [11].

The researches undertaken and presented in this paper, focus on the following approaches:

- performing experimental researches on the possibility of using non-ionizing ultraviolet radiation UV-C within the conditioning technologies of horticultural products;
- investigating the capability of an experimental model of installation for the decontamination of external surfaces of horticultural products, to apply the minimum dosage recommended for the destruction of the most representative pathogens.

MATERIAL AND METHOD

The most common microorganisms that can contaminate horticultural products, with adversely affect on storage or human health, are shown in table 1. For the destruction of these potentially pathogenic microorganisms, it is recommended to apply certain doses of UV-C radiation.

de respiratie, controlul deprecierii produselor si in intarzierea proceselor de maturare si coacere la diferite fructe si legume, intregi sau maruntite, precum mere, citrice, piersici, pepene, boabe de struguri, rosii, salata verde, spanac si ciuperci [5], [10], [1], [2], [6], [8], [7], [11].

Cercetarile intreprinse si prezentate in aceasta lucrare, se focalizeaza pe urmatoarele abordari:

- realizarea de cercetari experimentale privind posibilitatea de utilizare a radiatiei ultraviolete neionizante UV-C in cadrul tehnologiilor de conditionare a produselor horticole;
- investigarea capabilitatii unui model experimental de instalatie pentru decontaminarea suprafetelor exterioare ale produselor horticole, de a aplica dozele minime de radiatie recomandate pentru distrugerea celor mai reprezentativi agenti patogeni.

MATERIAL ŞI METODĂ

Cele mai frecvente microorganisme care pot contamina produsele horticole, cu efecte directe asupra pastrarii sau sanatatii consumatorului uman, sunt prezentate in tabelul 1. Pentru distrugerea acestor microorganisme potential patogene, se recomanda aplicarea anumitor dose de radiatie UV-C.

Table 1

Potentially pathogenic microorganisms and recommended UV-C radiation doses [14]

Microorganism	UV-C radiation dose [mWs/cm^2] necessary for the destruction of	
BACTERIA	90 %	99 %
Bacillus anthracis	4.52	8.70
Clostridium tetani	13.00	22.00
Escherichia coli	3.00	6.60
Mycobacterium tuberculosis	6.20	10.00
Salmonella enteritidis	4.00	7.60
Shigella dyseteriae	2.20	4.20
Staphylococus aureus	2.60	6.60
MOLDS		
Aspergillus flavus	60.00	99.00
Penicillium expansum	13.00	22.00
Rhizopus nigricans	111.00	220.00
YEASTS		
Saccharomyces spores	8.00	17.60

Considering the data presented above, the experimental researches on the possibility of using non-ionizing ultraviolet radiation UV-C within the conditioning technologies of horticultural products, have focused on investigating the capability of applying the minimum dosage recommended for the most representative pathogens. In this respect, it was experimented a new technical equipment (fig. 1) - Installation for the decontamination of external surfaces of horticultural products, IDPH. The main technical characteristics of the decontamination installation are presented in table 2.

The installation is proposed to be used for the decontamination of external surfaces of horticultural products, as preliminary stage for the temporary storage phase itself. The main characteristic of the transport system is that it performs not only the transportation of the product along the installation but also the rotation of it around an axis perpendicular to the direction of advance. This characteristic assures a homogenous distribution of the UV-C radiation upon the exterior surfaces of the products.

Avand in vedere datele prezentate mai sus, cercetarile experimentale privind posibilitatea de utilizare a radiatiei ultraviolete neionizante UV-C in cadrul tehnologiilor de conditionare a produselor horticole, s-au focalizat pe investigarea capabilitatii de a aplica dozele minime de radiatie recomandate pentru distrugerea celor mai reprezentativi agenti patogeni. In acest sens, a fost experimentat un echipament tehnic nou (fig. 1) – Instalatie pentru decontaminarea suprafetelor exterioare ale produselor horticole, IDPH. Principalele caracteristici tehnice ale instalatiei de decontaminare sunt prezentate in tabelul 2.

Instalatia este propusa a fi utilizata pentru decontaminarea suprafetelor exterioare ale produselor horticole, ca etapa preliminara pentru faza de pastrare temporara propriuzisa. Principala caracteristica a sistemului de transport este aceea ca realizeaza nu numai transportul produsului de-a lungul instalatiei dar si rotirea acestuia in jurul unei axe perpendiculare pe directia de deplasare. Aceasta caracteristica permite o distributie omogena a radiatiei UV-C asupra suprafetelor exterioare ale produselor.

Fig. 1 - Installation for the decontamination of external surfaces of horticultural products, IDPH

Table 2

The main technical characteristics of the decontamination installation

Dimensions (LxWxH)	3420x1215x1340 mm
Length of the transport system	1500 mm
UV Generator type	discharge lamps at low pressure mercury vapor
The wavelength of the emitted radiation	253.7 nm (UV-C)
Power of the UV-C lamps	55 W / pcs.
Number of UV-C lamps	5 pcs.

The experimentation was aimed to determine the energetic indices and qualitative working indices of the decontamination installation. For this purpose, there were taken into account the following parameters:
- The minimum and maximum rotational speed of the driving system of the conveyor - there were determined by varying the frequency of the supply current of the gear-motor, through the frequency converter currently existing within the automation installation;
- The minimum and maximum transport time - there were determined by measuring the time needed for a product subjected to decontamination, to pass a length of the transport system, in terms of maximum and minimum rotational speed of the driving system.

In order to determine the intensity of non-ionizing ultraviolet radiation UV-C, there were performed measurements using a set of tools, sglux brand, Germany, comprising of the following elements: an intensity sensor for ultraviolet radiation, calibrated for the UV-C spectrum (UV Sensor "UV-Water-D"), a communication interface between the sensor and the laptop ("DIGIBOX" - CAN-to-USB converter) and a data acquisition software for the radiation intensity and air temperature, based on LabView programming environment ("DigiLog").

Experimentarea a avut ca obiectiv determinarea indicilor energetici si indicilor calitativi de lucru ai instalatiei de decontaminare. In acest scop, s-au luat in considerare urmatorii parametri:
- turatia minima si maxima a sistemului de actionare a transportorului - s-au determinat prin varierea frecventei curentului de alimentare a motoreductorului, prin intermediul convertizorului de frecventa existent in cadrul instalatiei de automatizare a echipamentului tehnic;
- timpul minim si maxim de transport - s-au determinat prin masurarea duratei in care un produs supus decontaminarii, parcurge o lungime a sistemului de transport, in conditii de turatie maxima si minima a sistemului de actionare;

In vederea determinarii intensitatii radiatiei neionizante ultraviolete UV-C, s-au realizat masuratori utilizand un pachet de instrumente de masura (fig. 2) marca *sglux*, Germania, avand in componenta urmatoarele echipamente: un senzor de intensitate a radiatiei ultraviolete, calibrat pentru spectrul UV-C (UV Sensor „UV-Water-D”), o interfata de comunicatie intre senzor si laptop („DIGIBOX” – CAN-to-USB converter) si un software pentru achizitia datelor privind intensitatea radiatiei si temperatura aerului, bazat pe mediul de programare LabView („DigiLog”).

Fig. 2 - Measuring instruments for UV-C radiation intensity

There were performed determinations at different distances from the source of radiation (50 mm, 75 mm, 100 mm and 125 mm), under a lamp and also in the space between two adjacent UV-C lamps. The first objective of the research was to investigate if the radiation intensity is homogenous, as well under the lamps, as between the two adjacent lamps, with or without the aluminium deflector for the lamps (a semicylindrical aluminium sheet). The second objective was to highlight the influence of the distance on the intensity of emitted UV-C radiation. Also, there were calculated the UV-C radiation doses, according to the measured radiation intensity and its duration of application, using the equation (1). The durations of application for the UV-C radiation were considered to be the minimum and maximum time that a product needs to pass through the transport system of the installation.

S-au efectuat măsurători la diferite distante fata de sursa de radiatie (50 mm, 75 mm, 100 mm si 125 mm), sub o lampa si de asemenea, in spatiul dintre doua lampi UV-C alaturate. Primul obiectiv al cercetarii sa se investigheze daca intensitatea radiatiei este omogena, atat sub lampi cat si intre doua lampi alaturate, cu sau fara deflectorul din aluminiu, pentru lampi (o tabla semicilindrica din aluminiu). Al doilea obiectiv a fost punerea in evidenta a influentei distantei asupra intensitatii radiatiei UV-C emise. De asemenea, s-au calculat dozele de radiatie UV-C, conform intensitatii masurate a radiatiei si duratei de aplicare, folosind ecuatia (1). Durata de aplicare a radiatiei UV-C s-a considerat a fi timpul minim si timpul maxim de care are nevoie un produs pentru a parcurge sistemul de transport al instalatiei.

$$D = I \cdot t \text{, [mWs/cm}^2\text{]} \quad (1)$$

RESULTS

After carrying out experimental researches on the installation for decontamination, there were achieved a series of results regarding the energetic indices and qualitative indices of the decontamination installation (tables 3, 4 and 5).

REZULTATE

Dupa efectuarea cercetarilor experimentale asupra instalatiei de decontaminare, s-au obtinut o serie de rezultate privind indicii energetici si indicii calitativi ai instalatiei de decontaminare (tabelele 3, 4 si 5).

Table 3

Energetic indices of the decontamination installation IDPH /

No.	Parameter	Measure unit	Parameter values determined from tests
1.	The length of the transport system	*mm*	1620
2.	The minimum rotational speed of the driving system of the conveyor	*rpm*	5.5
3.	The maximum transport time	*s*	45
4.	The minimum transport speed	*m/s*	0.036
5.	The energy consumption of the whole installation at minimum transport speed	*kWh*	0.335
6.	The maximum rotational speed of the driving system of the conveyor	*rpm*	72
7.	The minimum transport time	*s*	2.93
8.	The maximum transport speed	*m/s*	0.55
9.	The energy consumption of the whole installation at maximum transport speed	*kWh*	0.643

Table 4

The influence of aluminium deflector on the intensity of UV-C radiation

No.	Distance from the source of radiation [mm]	The intensity of UV-C radiation [W/m^2]			
		Under the lamp		Between two adjacent lamps	
		Without deflector	With deflector	Without deflector	With deflector
1.	50	37.66	64.01	59.51	64.04
2.	75	31.42	57.40	37.72	57.41
3.	100	27.16	55.52	31.46	55.53
4.	125	25.32	51.95	26.43	53.78

Table 5

Qualitative indices of the decontamination installation

No.	Parameter	Measure unit	Parameter values determined from tests			
1.	The distances from the source of radiation	*mm*	125	100	75	50
2.	The intensity of UV-C radiation	*W/m^2*	52.87	55.53	57.41	64.03
3.	The minimum UV-C radiation dose, according to the minimum transport time	*mWs/cm^2*	15.45	16.26	16.82	18.75
4.	The maximum UV-C radiation dose, according to the maximum transport time	*mWs/cm^2*	238.05	249.75	258.30	288.00

The radiation intensity values from table 5 represent the average of the values obtained with deflector, under the lamp and between the lamps. The minimum and maximum doses at various distances from the source of UV-C radiation were calculated based on relation (1), considering the minimum and maximum time that a product needs to pass through a length of the transport system.

Figures 3, 4 and 5 show the influence of the aluminium deflector on the intensity of UV-C radiation, under the lamp and between lamps.

Figure 6 shows the variation of the radiation intensity with the distance from the source.

Valorile intensitatii radiatiei din tabelul 5 reprezinta media valorilor obtinute, in prezenta deflectorului, sub lampa si intre lampi. Dozele minima si maxima la diferite distante fata de sursa de radiatie UV-C au fost calculate pe baza relatiei (1), tinand seama de timpul minim si timpul maxim de care are nevoie un produs pentru a parcurge lungimea sistemului de transport.

Figurile 3, 4 si 5 prezinta influenta deflectorului de aluminiu asupra intensitatii radiatiei UV-C, sub lampa si intre lampi.

Figura 6 prezinta variatia intensitatii radiatiei cu distanta fata de sursa.

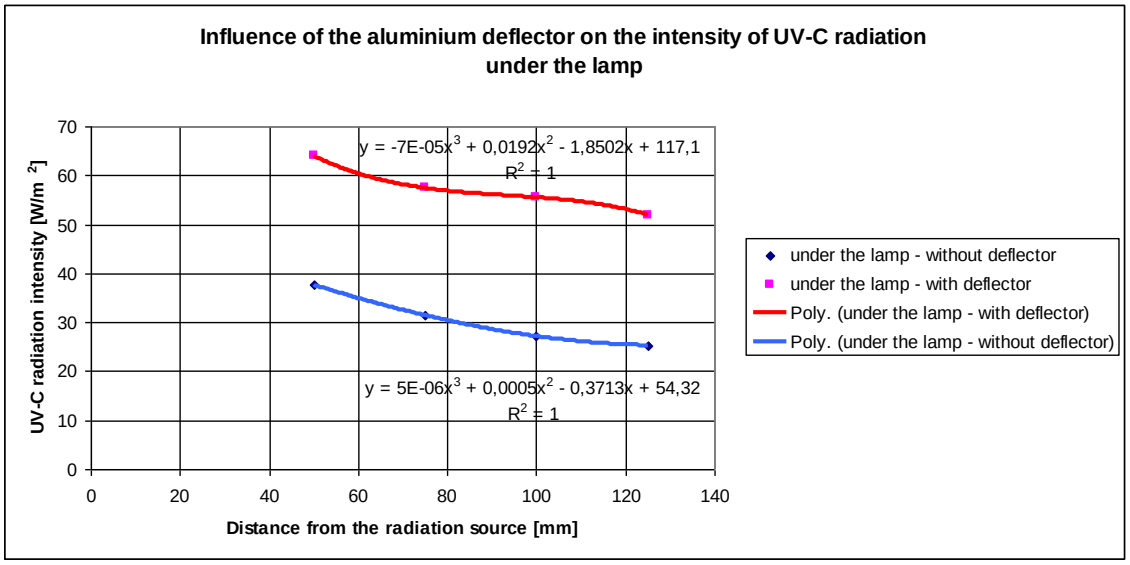

Fig. 3 - Influence of the deflector on the intensity of UV-C radiation under the lamp

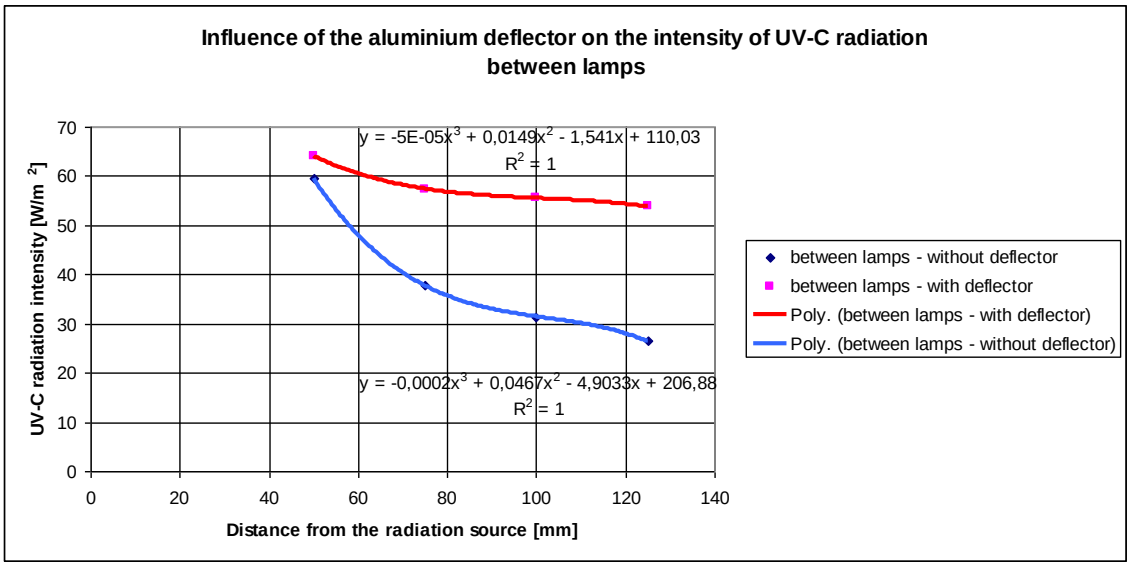

Fig. 4 - Influence of the deflector on the intensity of UV-C radiation between lamps

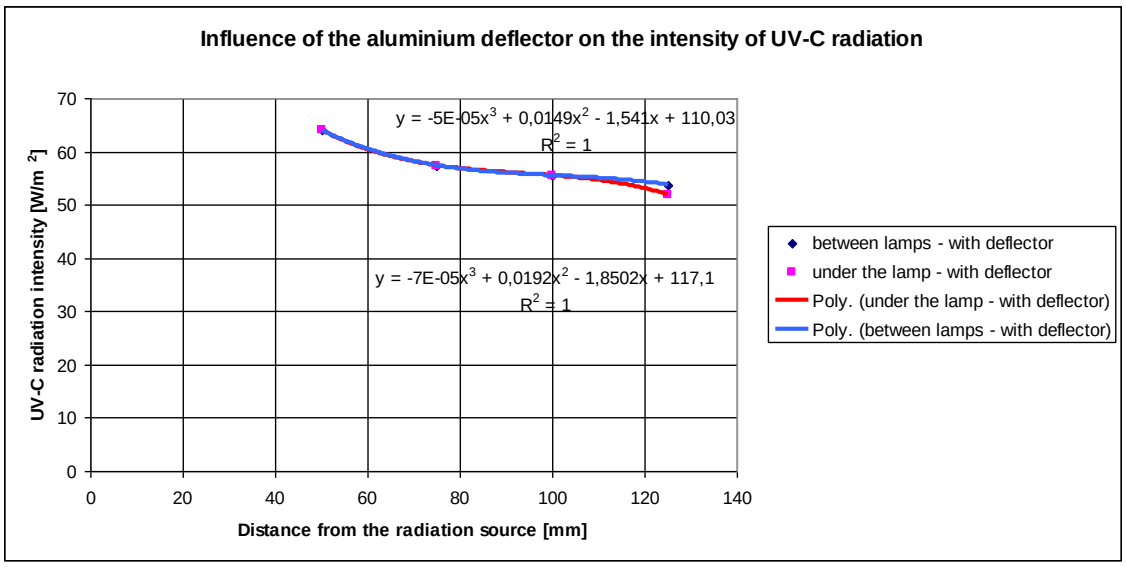

Fig. 5 - Influence of the deflector on the intensity of UV-C radiation

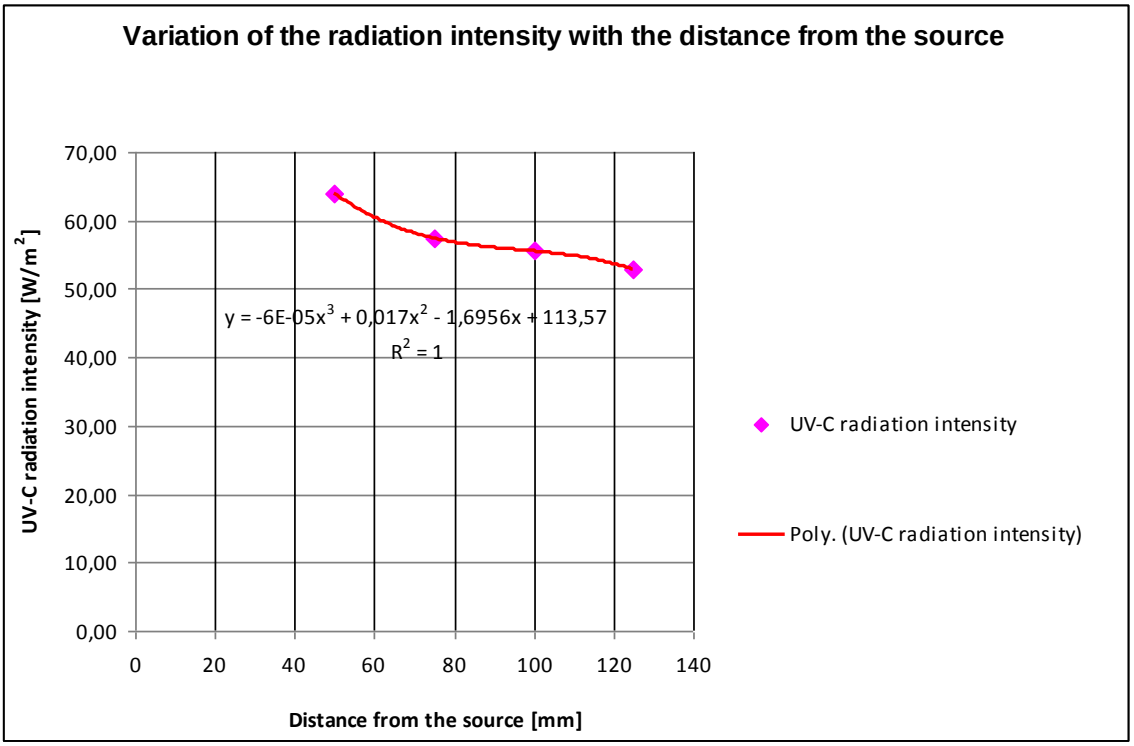

Fig. 6 - Variation of the radiation intensity with the distance from the source

Linear regression performed using Excel, allowed the identification of a third degree polynomial function, which estimates the variation of the radiation intensity depending on the distance from the source, with a maximum coefficient of determination.

Figure 7 shows the variation of minimum and maximum dose of UV-C radiation with the distance from the source of radiation.

Regresia liniara realizata cu ajutorul programului Excel, a permis identificarea unei functii polinomiale de gradul 3 care estimeaza variatia intensitatii radiatiei in functie de distanta fata de sursa, cu un coeficient de determinare maxim.

In figura 7 se prezinta variatia dozei minime si maxime de radiatie UV-C cu distanta fata de sursa de radiatie.

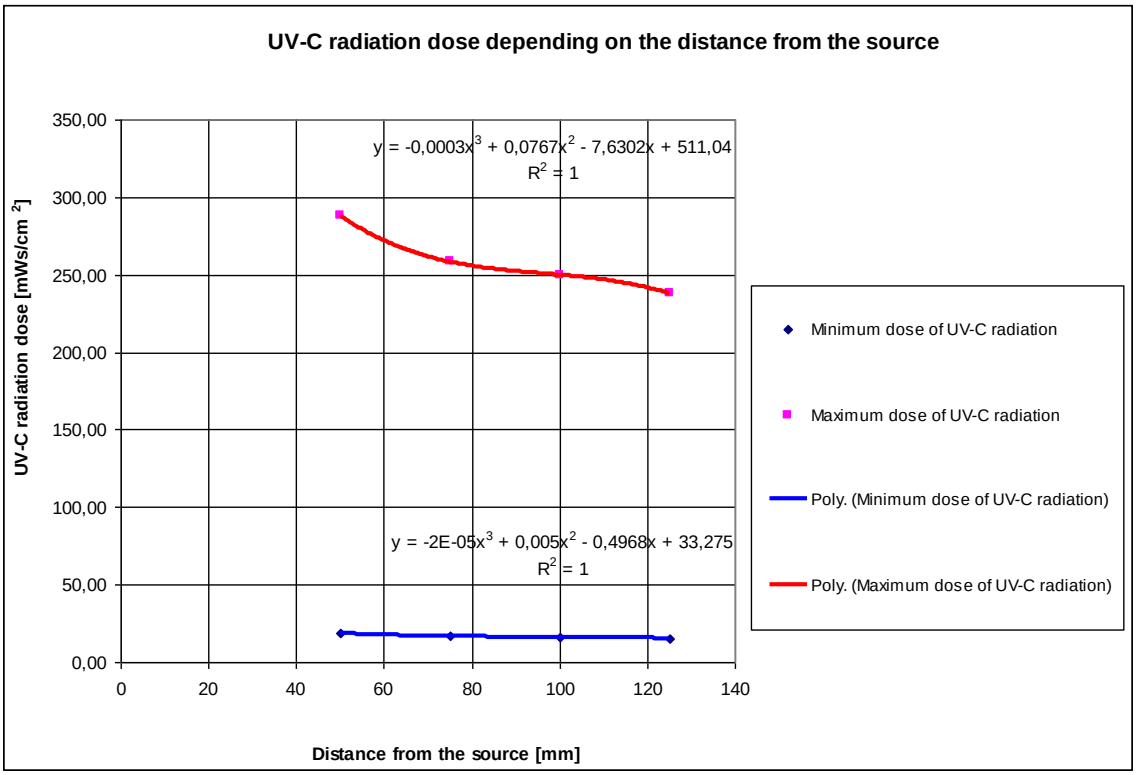

Fig. 7 - Variation of minimum and maximum dose of UV-C radiation with the distance from the source

Also, using linear regression was identified a third degree polynomial function, which estimates the variation of UV-C radiation dose depending on the distance from the source, with a maximum coefficient of determination.

Some aspects during the determination of the energy indices and qualitative indices of the decontamination installation, are shown in figures 8 and 9.

De asemenea, cu ajutorul regresiei liniare s-a identificat o functie polinomiala de gradul 3 care sa estimeze variatia dozei de radiatie UV-C in functie de distanta fata de sursa, cu un coeficient de determinare maxim.

Cateva aspecte din timpul determinarii indicilor energetici si indicilor calitativi ai instalatiei de decontaminare, sunt prezentate in figurile 8 si 9.

Fig. 8 - The determination of the energy indices of the decontamination installation

Fig. 9 - The determination of the qualitative indices of the decontamination installation

CONCLUSIONS

Analyzing the data obtained, regarding the use of aluminium deflector for the UV-C lamps, it is found that its use increases the radiation intensity by 70 % - 105 % under the lamp and by 8 % - 103 % between lamps. Also it conducts to the obtaining of a homogenous distribution of UV-C radiation on the working width of the installation, with a variation index of the intensity between 0.01 % and 2.45 %.

Following the analysis of the obtained experimental data and the data contained in table 1, regarding the UV-C radiation doses recommended for the destruction of the most common potentially pathogenic microorganisms existing on the exterior surfaces of the horticultural products, it is found that the experimented decontamination installation has the capability to achieve quality indices superior to the recommendations in table 1. However, although the installation is able to provide radiation doses higher than those shown in table 1, the product subjected to decontamination receives only half the dose, relative to its entire surface. This statement was set forth taking into account the simplifying assumption that, at a certain moment in time, only the upper half of the product will be exposed to UV-C radiation, the other half being shadowed. Considering this hypothesis, the installation still achieves a destruction rate of 90% of the most resistant pathogens presented in table 1, even in a single pass, adjusted at 125 mm distance from the radiation source, without having to repeat the exposure to UV-C radiation. For a destruction rate of 99 %, the installation is able to provide the necessary radiation doses for almost all the pathogens in the table 1, except for *Rhizopus nigricans* which needs a higher dose. The next phase of the research will be directed towards the measurement of the microbial count existing on the exterior surfaces of horticultural products.

Given the results obtained, the use of UV-C ultraviolet non ionizing radiation may be a viable solution as post harvest treatment method, in order to decrease the microbiological load from the exterior surfaces of horticultural products.

CONCLUZII

Analizand datele obtinute, in ceea ce priveste utilizarea deflectorului de aluminiu pentru lampile UV-C, s-a constatat faptul ca utilizarea acestuia creste intensitatea radiatiei cu 70 % - 105 % sub lampa si cu 8% - 103 % intre lampi. De asemenea, conduce la obtinerea unei distributii omogene a radiatiei UV-C pe latimea de lucru a instalatiei, cu un indice de variatie a intensitatii cuprins intre 0,01% si 2,45%.

In urma analizei datelor experimentale obtinute si a datelor continute in tabelul 1, in ceea ce priveste dozele de radiatie UV-C recomandate pentru distrugerea celor mai frecvente microorganisme potential patogene existente pe suprafetele exterioare ale produselor horticole, s-a constatat ca instalatia de decontaminare experimentata are capabilitatea de a atinge indici de calitate superiori recomandarilor din tabelul 1. Totusi, desi instalatia poate furniza dose de radiatie mai mari decat cele prezentate in tabelul 1, produsul supus decontaminarii receptioneaza numai jumatate de doza, raportat la intreaga sa suprafata. Aceasta afirmatie a fost enuntata luand in considerare ipoteza simplificativa conform careia la un anumit moment de timp, numai jumatatea superioara a produsului va fi expusa la radiatia UV-C, cealalta jumatate fiind umbrita. Luand in considerare aceasta ipoteza, instalatia inca poate atinge o rata de distrugere de 90 % a celor mai rezistenti agenti patogeni prezentati in tabelul 1, chiar dintr-o singura trecere, reglata la o distanta de 125 mm fata de sursa de radiatie, fara a fi nevoie sa se repete expunerea la radiatia UV-C. Pentru o rata de distrugere de 99 %, instalatia poate furniza dozele necesare pentru aproape toti agentii patogeni din tabelul 1, cu exceptia *Rhizopus nigricans* care necesita doze mai ridicate. Urmatoarea etapa a cercetarii va fi directionata catre determinarea numarului de microorganisme existente pe suprafetele exterioare ale produselor horticole.

Avand in vedere rezultatele obtinute, utilizarea radiatiei ultraviolete neionizante UV-C poate fi o solutie viabila ca si metoda de tratare post recoltare, in scopul micsorarii incarcaturii microbiene de pe suprafetele exterioare ale produselor horticole.

REFERENCES

[1]. Allende A., Selma M.V., López-Gálvez F., Villaescusa R. and Gil M.I. (2008). *Role of commercial sanitizers and washing systems on epiphytic microorganisms and sensory quality of fresh-cut escarole and lettuce*. Postharvest Biol. Technol. 49: 155–163;

[2]. Artés-Hernández F., Robles P., Gómez P., Tomás-Callejas A. and Artés F. (2010). *Low UV-C illumination for keeping overall quality of fresh-cut watermelon*. Postharvest Biol. Technol. 55: 114–120;

[3]. Bintsis T., Litopoulou-Tzanetaki E. and Robinson R. (2000). *Existing and potential applications of ultraviolet light in the food industry – a critical review*. J. Sci. Food Agric. 80: 637–645;

[4]. Char C., Mitilinaki E., Guerrero S. and Alzamora S.M. (2010). *Use of high intensity ultrasound and UV-C light to inactivate some microorganisms in fruit juices*. Food Bioprocess Technol. 3: 797–803.

[5]. De Capdeville G., Wilson C.L., Beer S.V. and Aist J.R.. (2002). *Alternative disease control agents induce resistance to blue mold in harvested 'red delicious' apple fruit*. Phytopathology 92: 900–908;

[6]. Escalona V.H., Aguayo E., Martínez-Hernández G.B. and Artés F. (2010). *UV-C doses to reduce pathogen and spoilage bacterial growth in vitro and in baby spinach*. Postharvest Biol. Technol. 56: 223–231;

[7]. Fava J., Hodara K., Nieto A., Guerrero S., Alzamora S. and Castro M. (2011). *Structure (micro, ultra, nano), color and mechanical properties of Vitis labrusca L. (grape berry) fruits treated by hydrogen peroxide*, UV-C irradiation and ultrasound. Food Res. Int. 44: 2938–2948;

[8]. Jiang T., Jahangir M., Jiang Z., Lu X. and Ying T. (2010). *Influence of UV-C treatment on antioxidant capacity, antioxidant enzyme activity and texture of postharvest shiitake (Lentinus edodes) mushrooms during storage*. Postharvest Biol. Technol. 56: 209–215;

[9]. Kasim M.U. and Kasim R. (2007). Tarim Bilimleri Dergisi-Journal of Agricultural Sciences. 3: 413-419;

[10]. Lamikanra O., Kueneman D., Ukuku D. and Bett-Garber K.L. (2005). *Effect of processing under ultraviolet light on the shelf life of fresh-cut cantaloupe melon*. J. Food Sci. 70: C534–C539;

[11]. Manzocco L., Da Pieve S. and Maifreni M. (2011). *Impact of UV-C light on safety and quality of fresh-cut melon*. Inn. Food Sci. Emerg. Technol. 12: 13–17;

[12]. Perni S., Liu D.W., Shama G. and Kong M.G. (2008). *J. Food Prot*. 71: 302;

[13]. Mari M., Neri F. and Bertolini P. (2010). *Postharvest pathology* - Book Series: Plant Pathology in the 21st Century, 119-135;

[14]. http://www.midasexpert.com;

BIBLIOGRAFIE

[1]. Allende A., Selma M.V., López-Gálvez F., Villaescusa R. si Gil M.I. (2008). *Rolul echipamentelor de dezinfectie si a sistemelor de spălare comerciale asupra microorganismelor epifite și a calității senzoriale a produselor proaspăt tăiat de escarole și salata verde*. Postharvest Biol. Technol. 49: 155–163;

[2]. Artés-Hernández F., Robles P., Gómez P., Tomás-Callejas A. si Artés F. (2010). *Iluminare scazuta cu UV-C pentru păstrarea calității pepenelui verde proaspat taiat.* Postharvest Biol. Technol. 55: 114–120;

[3]. Bintsis T., Litopoulou-Tzanetaki E. si Robinson R. (2000). *Aplicații existente și potențiale ale razelor ultraviolete din industria alimentară - o analiză critică.* J. Sci. Food Agric. 80: 637–645;

[4]. Char C., Mitilinaki E., Guerrero S. si Alzamora S.M. (2010). *Utilizarea de ultrasunete de mare intensitate ș lumină ultravioleta UV-C pentru a inactiva unele microorganisme din sucurile de fructe*. Food Bioprocess Technol. 3: 797–803.

[5]. De Capdeville G., Wilson C.L., Beer S.V. si Aist J.R.. (2002). *Agenți alternativi de control a imbolnavirii induc rezistență la mucegaiul albastru în fructele de mere 'red delicious' recoltate.* Phytopathology 92: 900–908;

[6]. Escalona V.H., Aguayo E., Martínez-Hernández G.B. si Artés F. (2010). *Dozele UV-C pentru a reduce dezvoltarea bacteriilor patogene și alterarea in vitro și pe spanac*. Postharvest Biol. Technol. 56: 223–231;

[7]. Fava J., Hodara K., Nieto A., Guerrero S., Alzamora S. si Castro M. (2011). *Structura (micro, ultra, nano), culoarea și proprietățile mecanice ale fructelor de Vitis labrusca L. (boabe de struguri) tratate cu peroxid de hidrogen.* UV-C irradiation and ultrasound. Food Res. Int. 44: 2938–2948;

[8]. Jiang T., Jahangir M., Jiang Z., Lu X. si Ying T. (2010). *Influența tratamentului cu UV-C asupra capacitatii antioxidante, activitatii enzimelor antioxidante și textura dupa recoltare a ciupercilor Shiitake (Lentinus edodes) în timpul depozitării*. Postharvest Biol. Technol. 56: 209–215;

[9]. Kasim M.U. si Kasim R. (2007). Tarim Bilimleri Dergisi-Journal of Agricultural Sciences. 3: 413-419;

[10]. Lamikanra O., Kueneman D., Ukuku D. si Bett-Garber K.L. (2005). *Efectul procesarii in camp de lumina ultravioleta asupra perioadei de valabilitate a pepenelui galben proaspat taiat*. J. Food Sci. 70: C534–C539;

[11]. Manzocco L., Da Pieve S. si Maifreni M. (2011). *Impactul luminii ultraviolete UV-C lumină asupra siguranței și calitatii pepenelui galben proaspat taiat*. Inn. Food Sci. Emerg. Technol. 12: 13–17;

[12]. Perni S., Liu D.W., Shama G. si Kong M.G. (2008). J. *Food Prot.* 71: 302;

[13]. Mari M., Neri F. si Bertolini P. (2010). *Postharvest pathology* - Book Series: Plant Pathology in the 21st Century, 119-135;

[14]. http://www.midasexpert.com;

ANALYSIS OF INFLUENCE OF SPEED VARIATION OF HIGH SPEED BALL BEARINGS ON CAGE DYNAMIC PERFORMANCE
/
高速球轴承转速变化对保持架动态性能影响分析

Ass. Prof. Ph.D. Eng. Ye Zhenhuan[1, 2], Prof. Ph.D. Eng. Wang Liqin[*2] , Ph.D. Eng. Zhang Chuanwei [2, 3]
[1] School of Engineering, Zunyi Normal College, Zunyi / China; [2] School of Mechatronics Engineering, Harbin Institute of Technology, Harbin / China; [3] Nano-Tribology of Discrete Track Recording Media, University of California, San Diego, La Jolla / United States
Tel: +8645186402012; Email: lqwanghit@gmail.com

Abstract: *With the aim of increasing the stability of high-speed ball bearings in the transmission system of agricultural machinery, taking a type 7004 high speed angular contact ball bearings as the research material, a dynamic model of high speed ball bearings was built based on the geometry and force relationship of bearing elements. The integration method used by Runge-Kutta and Newton-Raphson is proposed to efficiently solve the nonlinear equations. The accuracy of the dynamic model constructed in this paper was verified by the testing and computation results studied by Gupta. A computation program is developed and the cage stability at different bearing rotation speeds is studied. The results shown that the increase of bearing rotation speed has improved both the cage stability and cage sliding ratio. In addition, the impact between the cage pocket and the ball has a serious effect on cage stability when the bearing is in the starting process. This study provides support for the design of working conditions and failure analysis of ball bearings, as well as a theoretical basis for analysis of the system stability of transmission systems in agricultural machinery.*

Keywords: *High speed ball bearings; Dynamic; Cage stability; Static condition; Transitional condition*

摘要: *针对农机传动系统中高速球轴承的稳定性问题，根据高速球轴承内部的几何位置关系以及相互作用力关系，以 7004 型高速角接触球轴承作为研究对象，建立了高速球轴承的动力学模型。采用 Runge-Kutta 法和 Newton-Raphson 法混合求解的思想对模型非线性方程组进行了高效求解。采用 Gupta 的实验和仿真结果验证了本文模型和方法的可靠性。从轴承稳态和瞬态过渡两种工况角度研究了轴承转速变化对保持架动态性能的影响规律，结果表明轴承转速增加有利于保持架的稳定但同时也增大了保持架滑动率；变速过程中，保持架在启动阶段产生的兜孔和滚动体频繁冲击对其稳定性影响较大。研究结果为高速球轴承在设计计算以及失效分析等方面提供有力的支持，并为传动系统的系统稳定性分析提供了理论基础。*

关键词: *高速球轴承；动力学；保持架振动；稳态工况；瞬态过渡工况*

INTRODUCTION

With developments in modern agricultural machinery moving toward lightweight and intelligent designs, the reliability and stability of agricultural machinery transmission systems has gradually become an area of focus [13,14,16]. Over the years, many researchers have studied the rolling bearings in the transmission systems of agricultural machinery in terms of two aspects: a detection technique for bearing faults [4,11,22] and predictions and simulations which focus on the influence of bearing structure on performance [1,2,5,21]. However, those simulation analyses only consider the loading properties of the bearing and rarely involve the dynamic stability of the bearings.

The dynamic performance of high-speed rolling bearings in these transmission systems not only affect their own life and stability, but also relates to the vibration and reliability of the rotor system. In order to understand the dynamic performance of the bearings during operation, a fully dynamic analysis of the bearings is needed. Over the years, much research has been done on the dynamic characteristics of high-speed ball bearings. In particular, with regard to the force and motion analysis of cage, Gupta developed the influence of cage clearance on bearing stability [7], while Weinzapfel et al. [17] also analyzed and compared the effects of rigid and flexible cage on bearing stability. In addition, Bai [3] and Liu [19] also studied the dynamic characteristics of the bearings in terms of the waviness and cage clearance ratio of angular contact bearings.

However, previous studies on high-speed rolling bearings in these transmission systems are limited to the

引言

随着现代农业机械朝着轻量化和智能化方向的发展，农机传动系统的可靠性和稳定性逐渐成为农机设计和使用的重点关注内容[13,14,16]。多年来，许多学者对农机传动系统中的滚动轴承进行了研究，一方面是集中在针对轴承故障进行检测技术的研究[4,11,22]，另一方面集中在轴承结构对性能影响的仿真预测分析[1,2,5,21]，但是仿真分析多考虑到轴承承载性能而很少涉及到轴承动态稳定性。

农机传动系统中高速滚动轴承的动态性能不仅影响其自身的寿命和稳定性，还关系到转子系统的振动和可靠性。为了清楚的研究轴承在工作过程中的动态性能必须对轴承进行完全动力学分析。多年来，国内外的众多学者在高速球轴承的动力学方面做了大量的研究工作，特别是针对保持架受力运动分析 Gupta 专门讨论了保持架间隙对轴承稳定性的影响[7]，Nick Weinzapfel 等[17]还分析对比了保持架刚性和柔性对轴承稳定性的影响。国内的白长青[3]、刘秀海[19]等也针对角接触球轴承的波纹度、保持架间隙比等情况研究了轴承的动态特性。但是通过分析可以发现，对于农机传动系统高速滚动轴承的研究基本都局限于不同稳态工况下的动态性能分析，对于农机传动系统在

basic dynamic performance analysis of different steady state conditions and have rarely ever investigated the dynamic properties of the bearing in the variable transition process. Frequent impact of the cage and the rolling elements during transmission operation directly affects the dynamic stability of the cage and ultimately influences the stability and reliability of transmission systems in agricultural machinery.

In this paper, through the establishment of a dynamic analysis model and development of an efficient dynamics program, the effect of velocity changes of high-speed ball bearings on the dynamic performance of the cage was analyzed and discussed. The results support the improvement of the design computation and failure analysis of high-speed rolling bearings in agricultural machinery transmission systems.

变工况过渡过程中高速轴承的动态性能研究较少，而轴承在工况变化过程中保持架和滚动体的频繁冲击直接影响着保持架的动态稳定性，进而影响到整个农机传动系统的稳定性和可靠性。

本文通过建立球轴承的动力学分析模型，开发高效的动力学程序，对高速球轴承转速变化对保持架动态性能的影响进行分析和讨论，为农机传动系统高速球轴承在设计计算以及失效分析等方面提供有力的支持。

MATERIAL AND METHOD

Research materials

7004 angular contact ball bearings are used in this paper as the research material, their material and geometry parameters being shown in Table 1 and Table 2. The lubrication oil type MIL-L-7808 is used. The axial load F_x and radial load F_z on the bearings are 2000 N and 400 N, respectively.

材料与方法

研究材料

本文将以 7004 型角接触球轴承作为研究材料进行分析，具体的结构参数和材料参数如表 1 和表 2 所示，润滑采用 MIL-L-7808 型润滑油。轴承承受轴向载荷和径向载荷分别为 2000N 和 400N。

Table 1

Material parameters of ball bearings [7]

Elements	Density [kg/m3]	Elastic modulus [GPa]	Poisson's ratio [-]
Ball	3200	310	0.260
Rings	7750	200	0.250
Cage	1500	1.73	0.300

Table 2

Geometry parameters of ball bearings [7]

Geometry parameter	u.m.	Value
Pitch diameter	[mm]	31
Ball diameter	[mm]	8
No. of balls	[-]	6
Contact angle	[°]	24
Inner curvature factor	[-]	0.56
Outer curvature factor	[-]	0.52
Cage inner diameter	[mm]	30
Cage outer diameter	[mm]	35
Cage pocket clearance	[mm]	0.1
Cage guiding clearance	[mm]	0.25

Analysis Method

The contact load Q between the raceways and the balls are calculated by the Hertz contact theory [10], so the contact load between the j^{th} rolling element and the raceways is expressed as:

分析方法

套圈滚道和滚动体之间的接触载荷 Q 采用赫兹接触理论计算[10]，第 j 个滚动体和滚道之间的接触载荷表示为：

$$Q_j = K_j \delta_j^{3/2} \tag{1}$$

where the stiffness K is calculated according to the study by Johnson [10], and the contact deformation δ is determined by the positional relationship between the rolling element and the raceway as shown in Fig. 1. Thus, the contact deformation δ_j between the j^{th} rolling element and the raceway is expressed by the vector $\mathbf{O_{rj}O_{bj}}$ which means that the center of the raceway to the center of the ball, the groove curvature coefficient f of the ring, and the diameter of the ball D_w are expressed as:

式中的刚度 K 根据文献[10]计算，接触变形 δ 根据如图 1 所示的滚动体和套圈滚道之间的位置关系确定，其中第 j 个滚动体和套圈滚道之间的接触变形 δ_j 由套圈圈滚道中心到球中心的矢量 $\mathbf{O_{rj}O_{bj}}$、套圈的沟曲率系数 f 表示和滚动体直径 D_w 表示为：

$$\delta_j = (f - 0.5) \cdot D_w - \left|\mathbf{O_{rj}O_{bj}}\right| \tag{2}$$

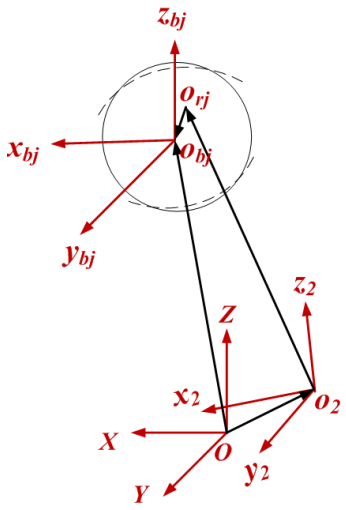

Fig. 1 - The sketch of the displacement of raceway and ball

The traction force F_μ of the contact area is equal to the traction coefficient μ multiplied by the contact load Q. The traction coefficient formula [20] is:

接触区的拖动力 F_μ 等于拖动系数 μ 和接触载荷 Q 的乘积，拖动系数公式为[20]：

$$\mu = \left(A + Bs\right)e^{-Cs} + D \tag{3}$$

where s is the slip-roll ratio which could be obtained from the kinematic analysis. Coefficients A, B, C, and D are calculated according to the formula in the study by Wang [20].

Fig. 2 shows the relative position relationship between the rolling element and the cage pocket. According to the vector $\mathbf{O_{pj}O_{bj}}$ between the cage pocket and the center of the ball bearing and the initial clearance between the cage pocket and the ball bearing Δ_{bp}, the minimum clearance δ_{bp} can be expressed as follows:

式中 s 为滑滚比，由运动学分析计算得到，系数 A、B、C、D 按文献[20]中公式计算。

图 2 所示为滚动体和保持架兜孔之间的相对位置关系，根据保持架兜孔中心到球心的向量 $\mathbf{O_{pj}O_{bj}}$ 和保持架兜孔和滚动体之间的初始间隙 Δ_{bp}，最小间隙 δ_{bp} 可以表示为：

$$\delta_{bp} = \Delta_{bp} - \left|\mathbf{O_{pj}O_{bj}}\right| \tag{4}$$

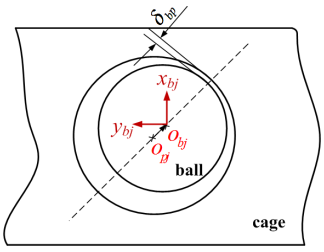

Fig. 2- The sketch of the displacement of the cage pocket and the ball bearing

According to the amplitude of the clearance between the cage pocket and the ball bearing δ_{bp}, taking into consideration both the roughness of the ball bearing ε_b and the cage ε_p, two interaction models are used:

根据球和保持架兜孔间的间隙 δ_{bp}，考虑球的粗糙度 ε_b 和保持架兜孔的粗糙度 ε_p，将滚动体和保持架兜孔的位置关系归纳为以下两个模型：

$$d_{bp} \pounds \sqrt{e_b^2 + e_p^2} \tag{5a}$$

$$d_{bp} > \sqrt{e_b^2 + e_p^2} \tag{5b}$$

If the inequality (5a) is true, the interaction is assumed to be Hertz contact. The normal load between the cage pocket and ball bearing is calculated by Hertz point contact theory [10], and the tangential load between cage pocket and the ball bearing equals the normal load multiplied by the friction coefficient.

Otherwise, if the inequality (5b) is true, the interaction is assumed to be hydrodynamic lubrication. Reynolds equations [9] are used to calculate the interaction force. The interactions in two directions, shown as Fig. 3, are assumed to be independent of each other.

若滚动体和保持架兜孔满足（5.a）模型，二者之间的相互作用为赫兹接触。根据赫兹点接触理论[10]计算二者间的法向力，二者间的切向力等于法向力乘以摩擦系数。

若滚动体和保持架兜孔满足（5.b）模型，二者之间的相互作用为流体动压。根据雷诺方程[9]计算二者间的作用力，其中如图 3 所示的两个方向的流体动压作用假设为不相干函数。

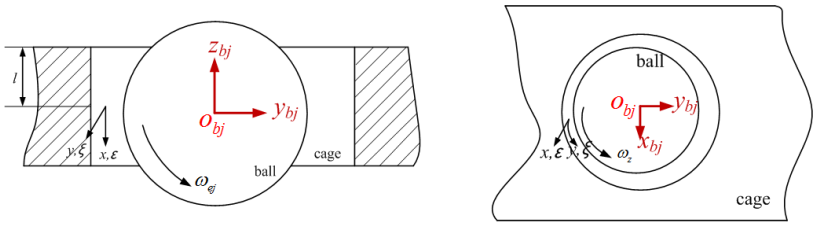

a) rotating by axis x_b b) rotating by axis z_b

Fig. 3- Hydrodynamic effect between ball bearing and cage pocket

Fig. 4 shows the interaction between the cage and the guiding ring, and the force between the two can be approximated as the fluid dynamic pressure of the journal bearing. As the contact surface of the ring flange and cylinder surface of the cage is relatively small, the short journal bearings model [18] is adopted.

图 4 所示为保持架和引导套圈之间的作用，套圈挡边引导面与保持架引导面间的作用力可以近似为滑动轴承计算中的流体动压力，由于挡边与保持架柱面间的作用面比较小，故通常采用短滑动轴承模型[18]。

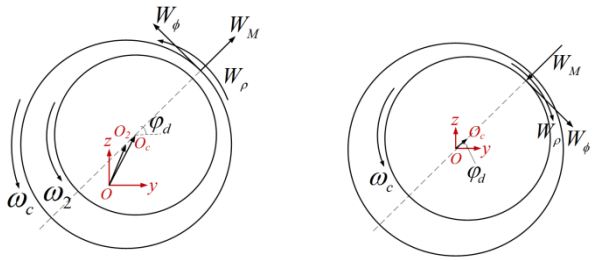

a) inner race guidance b) outer race guidance

Fig. 4- The interaction between cage and guiding ring

$$W_M = \pm\frac{\eta R_g B_g^{\,3}}{C_g^{\,2}}\frac{\varepsilon^2}{(1-\varepsilon^2)^2}(\omega_{1,2}+\omega_c)$$
$$W_\phi = \pm\frac{\pi\eta R_g B_g^{\,3}}{4C_g^{\,2}}\frac{\varepsilon}{(1-\varepsilon^2)^{3/2}}(\omega_{1,2}+\omega_c) \quad (6)$$
$$W_\rho = \frac{2\pi\eta R_g^{\,3} B_g}{C_g}\frac{1}{\sqrt{1-\varepsilon^2}}(\omega_{1,2}-\omega_c)$$

Where:

W_M, W_Φ, and W_ρ are the normal force, tangential force, and moment between the cage and the guiding ring. η is the viscosity of the oil. R_g and B_g are the radius and the width of the guiding surface. C_g is initial clearance of the bearings. ε is the eccentricity ratio of the cage center. ω is that rotational speed of the element. Subscripts *1*, *2*, and *c* represent the outer ring, inner ring, and cage, respectively. The sign of the equations is negative while the cage with outer race guidance.

According to the interaction angle between the cage and the ring φ_d, the interaction force could be expressed as equation (7) through a coordination transformation.

式中，W_M、W_Φ 和 W_ρ 分别代表保持架和套圈引导面之间的法向力、切向力以及转矩。η 为润滑油粘度。R_g 和 B_g 代表引导面直径及宽度。C_g 为轴承初始游隙。ε 为保持架的偏心率。ω 是轴承元件的转速。下标 *1*、*2* 和 *c* 分别代表外圈、内圈和保持架。若保持架由外圈引导，计算式前取负号，否则取正号。

根据保持架和套圈引导面之间的作用角 φ_d，通过坐标变换将二者之间的作用力变换为固定坐标系下的表达形式，如式（7）所示。

$$\begin{bmatrix} F_{ly} \\ F_{lz} \\ M_l \end{bmatrix} = \begin{bmatrix} \cos\varphi_d & -\sin\varphi_d & 0 \\ \sin\varphi_d & \cos\varphi_d & 0 \\ 0 & 0 & 1 \end{bmatrix} \begin{bmatrix} W_M \\ W_\phi \\ W_\rho \end{bmatrix} \tag{7}$$

Solution method

In addition to the interaction force, the bearing lubricant retarding force F_D and retarding moments M_e, which can be calculated by Schlichting's fluid theory [15], should also be taken into consideration. Forces of the loaded rolling element are shown in Figure 5. In the figures, M_μ and M_{bp} are the traction moment between the raceway and the rolling element and friction moment between the cage and the rolling element, respectively. The motion equation of the j^{th} rolling element centroid and of its revolving around the centroid is determined by its resultant force and the moment as shown in equation (8).

求解方法

轴承套圈、保持架以及滚动体除了相互作用力，还需要考虑轴承中润滑油的阻滞力 F_D 和阻滞力矩 M_e，根据 Schlichting 的流体理论进行计算[15]。考虑所有载荷的滚动体受力情况如图 5 所示，其中 M_μ 和 M_{bp} 分别为滚道/滚动体之间拖动力矩及保持架/滚动体之间摩擦力矩。第 j 个滚动体质心的运动方程和绕质心的运动方程分别根据第 j 个滚动体所受的合力和合力矩确定，如式（8）所示：

$$\begin{aligned} F_{\mu j} - F_{Dj} + F_{bpjy} &= m_b r_{bj} \ddot{\theta}_j \\ M_{bpjx} - M_{ejx} + M_{\mu jx} &= I_b \dot{\omega}_{xj} \\ M_{bpjy} - M_{ejy} + M_{\mu jy} &= I_b \dot{\omega}_{yj} \\ M_{bpjzx} - M_{ejz} + M_{\mu jz} &= I_b \dot{\omega}_{zj} \end{aligned} \tag{8}$$

where, m_b *and* I_b are the mass and rotary inertia of ball. r_b is the revolution radius of ball. θ *is the azimuth angle of ball and* ω *is the rotation speed of ball.* Subscript j represents the parameter j^{th} ball. Subscripts x, y, and z represent the components in each of the three directions.

式中 m_b，I_b 分别表示球的质量和转动惯量，r_b 表示球的公转半径，θ 表示球的方位角，ω 表示球的转速。下标 j 表示第 j 个滚动体；下标 x、y、z 表示 x、y、z 三个坐标方向的分量。

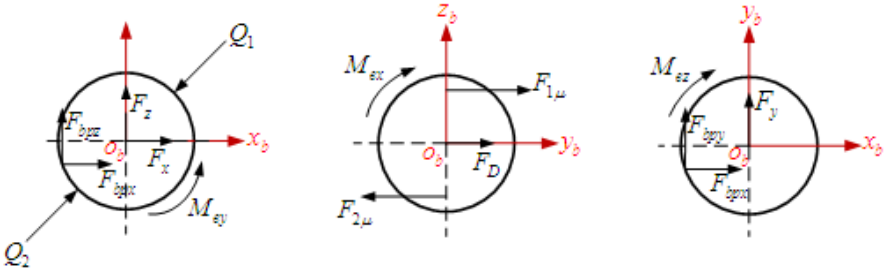

Fig. 5 - Forces and moments acting on ball.

To eliminate high-frequency vibrations generated by contact between a ball bearing and rings, a balance constraint is adopted for the contact between the ball and the ring. First, nonlinear equilibrium equations with the quasi-dynamic method are established, and the Newton-Raphson method is used to solve the equations [12].

Similarly, based on the force condition, the differential equations of the cage can be listed as equation (9). Where, n is the ball number. m_c and I_c are mass and rotary inertia of cage. x_c, y_c and z_c are displacement of cage mass center on direction x, y and z. θ_c is the relative rotation angle between cage mass center and bearing center.

为消除球和套圈接触产生的高频振动，球和套圈之间接触采用平衡约束，通过拟动力学的分析方法建立非线性平衡方程组并采用 Newton—Raphson 方法求解 [12]。

同理，对于保持架可以根据其受力情况列出其运动微分方程如式（9）所示，其中 n 表示球数，m_c 和 I_c 表示保持架质量和转动惯量，x_c、y_c 和 z_c 表示保持架质心在 x、y 和 z 方向的位移，θ_c 表示保持架质心相对轴承中心的转角。

$$\begin{aligned} &\sum_{j=1}^{n}(-F_{bpjx}) = m_c \ddot{x}_c \\ &F_{ly} + \sum_{j=1}^{n}(-F_{bpjy}\cdot\cos\theta_j - F_{bpjz}\cdot\sin\theta_j) = m_c \ddot{y}_c \\ &F_{lz} + \sum_{j=1}^{n}(-F_{bpjy}\cdot\sin\theta_j - F_{bpjz}\cdot\cos\theta_j) = m_c \ddot{z}_c \\ &\sum_{j=1}^{n}\left(-F_{bpjy}\cdot\frac{D_c}{2}\right) + M_l = I_c \ddot{\theta}_c \end{aligned} \tag{9}$$

Based on simultaneous motion differential equations of the ball bearing and cage, one should use non-dimensional quantities to the parameters of the equation in formula (10), and resolve the non-dimensional differential equations with the adaptive step size fourth-order Runge-Kutta method. A stationary solution is obtained by the quasi-dynamic method as the initial values of whole solution process. The calculation procedure is shown in Fig. 6.

基于保持架和球的运动微分方程，根据式(10)对微分方程中的参数进行无量纲化处理，采用自适应步长的四阶 Runge—Kutta 方法求解无量纲的微分方程组。动力学求解启动初值由拟动力学结果提供。球轴承动力学模型的求解流程如图 6 所示。

$$\bar{F}=\frac{F}{F_x} \quad \bar{m}=\frac{m}{m_b} \quad \bar{r}=\frac{r}{D_w/2} \quad \bar{t}=\frac{t}{\sqrt{m_b\cdot D_w/(2F_x)}} \tag{10}$$

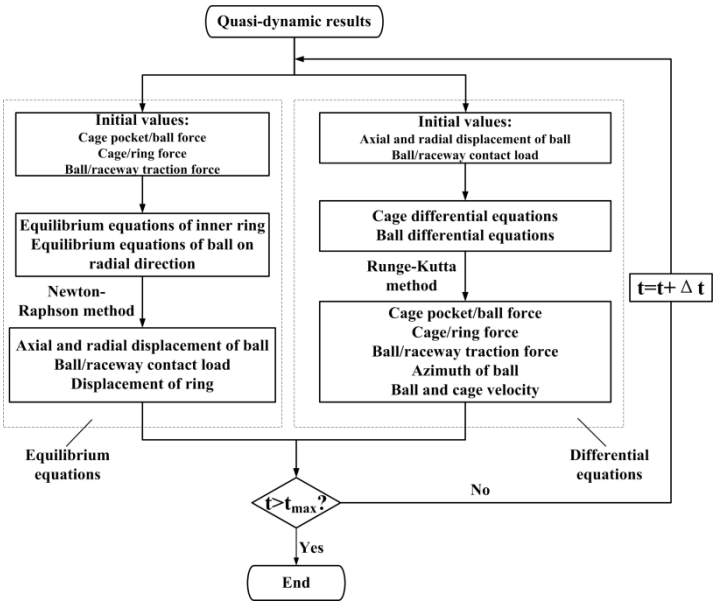

Fig. 6 - Calculation flow chart of dynamic equations

Model validation method

Taking a certain type of angular contact ball bearings as used in Gupta's experiment, the reliability verification on the bearing dynamic model is carried out. The axial load of the bearing is 4448 N, the working velocity is 20000rot/min, and other specific parameters are those used in the reference [8].

Fig. 7 shows the results of the cage mass center orbit simulated by Gupta's experimental and theoretical work. Fig. 8 shows the results of the cage mass center orbit and the ratio of the cage epicycle speed and bearing speed simulated in this study.

模型验证方法

以 Gupta 实验的某型角接触球轴承为算例，对建立的轴承动力学模型进行可靠性验证。轴承承受轴向负荷 4448N，工作转速 20000r/min，其他具体参数见文献[8]。

图 7 所示为 Gupta 实验和仿真获得的保持架涡动轨迹，图 8 所示为本文模型仿真获得的保持架涡动轨迹以及保持架质心涡动速比。

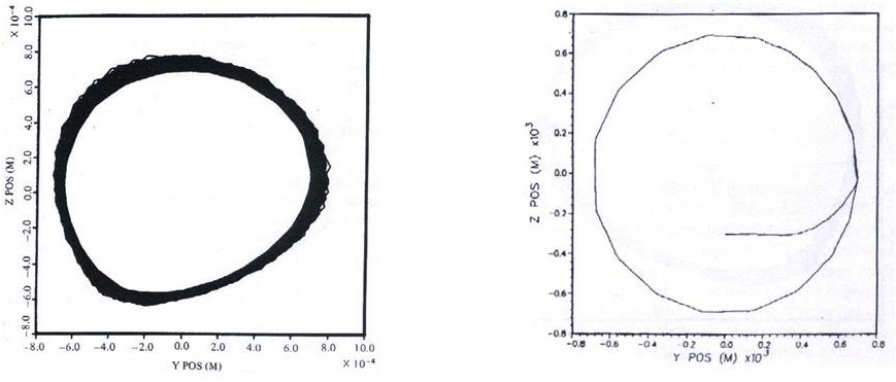

a) Determined by experiment b) Predicted by simulation

Fig. 7- Cage mass center orbit determined by Gupta [8]

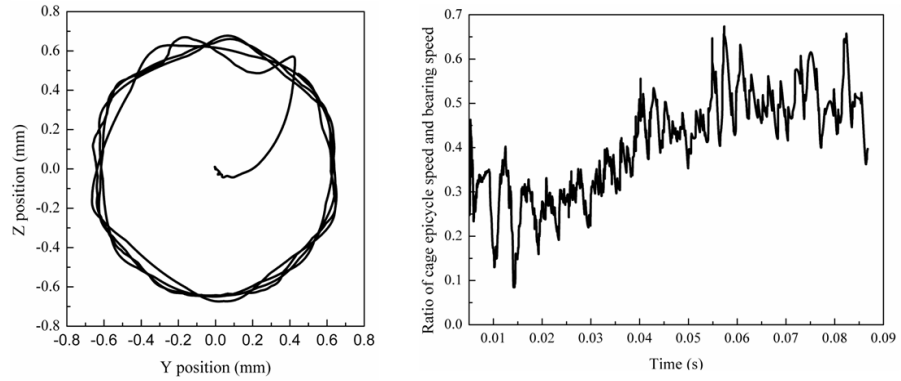

a) Cage mass center orbit b) Ratio of cage epicycle speed and bearing speed

Fig. 8 - Cage mass center orbit and cage speed ratio predicted in this study

It can be seen that there is good agreement between the shape of the experimental orbit and the theoretical prediction. In addition, according to the ratio of cage epicycle speed and bearing speed simulated in this study, the range of the cage speed ratio is 0.4-0.65 when the cage whirl tends to be stable. Also, the range of the cage speed ratio determined by Gupta's experiment and theory is 0.37-0.50 and 0.31-0.35, respectively [10]. It can be seen that errors exist between the experimental work and theoretical work on the ratio of the cage epicycle speed and bearing speed, but the errors are in the acceptable range.

RESULTS AND DISCUSSIONS

Effect of bearing velocity on the dynamic performance of the cage

Fig. 9 shows the cage whirl track when the velocity of the bearing is 30000 r/min, 60000 rot /min, 80000 r/min, and 120000 r/min. In the figure, axes indicate dimensionless displacement, which is defined as the ratio of actual displacement of the cage mass to the guiding clearance of the cage. As shown in the figure, with the increase in the revolving velocity of the inner ring, the whirl track of the cage becomes regular.

从涡动轨迹上看，本文模型仿真结果与 Gupta 实验及仿真获得的结果较为一致。从本文仿真得到的保持架质心涡动速度比可以看出，保持架涡动趋于稳定时的速度比变化范围在 0.4~0.65 之间，而 Gupta 通过实验以及仿真获得的保持架质心涡动速度比变化范围分别为 0.37~0.50 以及 0.31~0.35[10]。比较可知，仿真结果和实验结果之间存在误差，但是在可接受的范围内。

结果分析与讨论

不同轴承转速对保持架动态性能影响

图 9 所示为轴承在 30000r/min、60000r/min、80000r/min、120000r/min 四种不同转速下保持架的质心涡动轨迹，坐标轴表示无量纲位移，定义为保持架质心实际位移值除以保持架引导间隙值。从图中可以看出，随着内圈转速的增大，保持架质心的涡动轨迹逐渐规则。

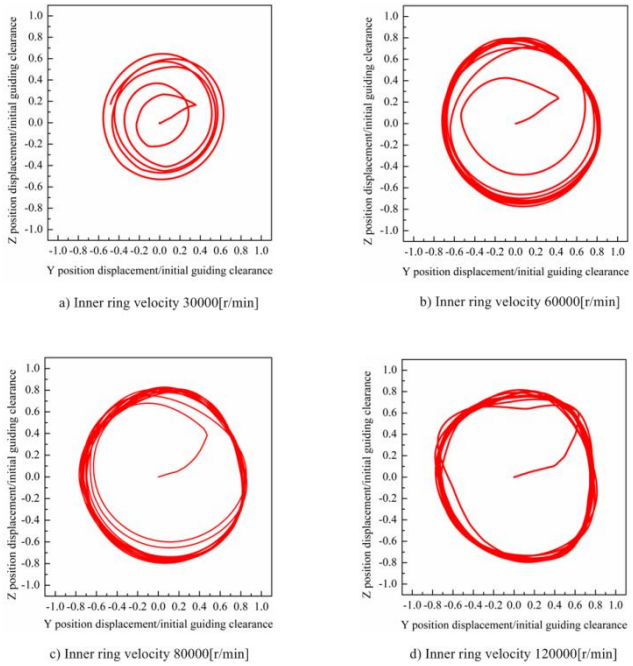

a) Inner ring velocity 30000[r/min] b) Inner ring velocity 60000[r/min]

c) Inner ring velocity 80000[r/min] d) Inner ring velocity 120000[r/min]

Fig. 9 - Cage whirl motion at different bearing operation speeds

According to the criteria of Ghaisas et al. [6], cage instability can be determined by the calculation of the deviation ratio σ of the whirl velocity which is defined as the ratio between the standard deviation value and average value of the velocity vector as shown in eq. (11).

根据 Ghaisas 等人的判断标准[6]，保持架质心涡动的不稳定性可以通过计算保持架的涡动速度偏差比 σ 来进行量化判定，速度偏差比定义为速度向量的标准偏差值与其平均值之比：

$$\sigma = \frac{\sqrt{\sum_{i=1}^{N}(v_i - v_m)^2 / N}}{v_m} \tag{11}$$

Where, N is the number of sampling. v_m is the average speed of cage mass center.

Figure 10 shows the deviation ratio of cage whirl velocity at four different velocities. A comparison shows that with the increase of the rotational velocity of the bearings, the deviation ratio of cage whirl velocity reduces, indicating the gradual stability of the cage. The main reason for this stability is that the increase in velocity causes the cage to be pushed against the guide surface of the ring quickly under the force of the rolling element, during which the cage reaches a new balance. Meanwhile, the increase in velocity also helps to enhance the centrifugal force, which gradually increases the guiding force of the ring to the cage. Therefore, the cage whirl track tends to be stabilized.

式中，N 表示采样的点数，v_m 表示保持架质心运动的平均速度。

图 10 所示为四种不同转速下的保持架涡动速度偏差比，比较可知，随着轴承转速的提高，保持架的涡动速度偏差比逐渐减小，说明保持架的稳定性逐渐增强。其主要原因为转速的上升促使保持架在滚动体的作用下被迅速推向套圈引导面获得新的平衡，另外随着转速增加带来的离心力升高促使套圈引导面对保持架的引导作用也逐渐增强，这两方面同时促使保持架质心涡动趋于稳定。

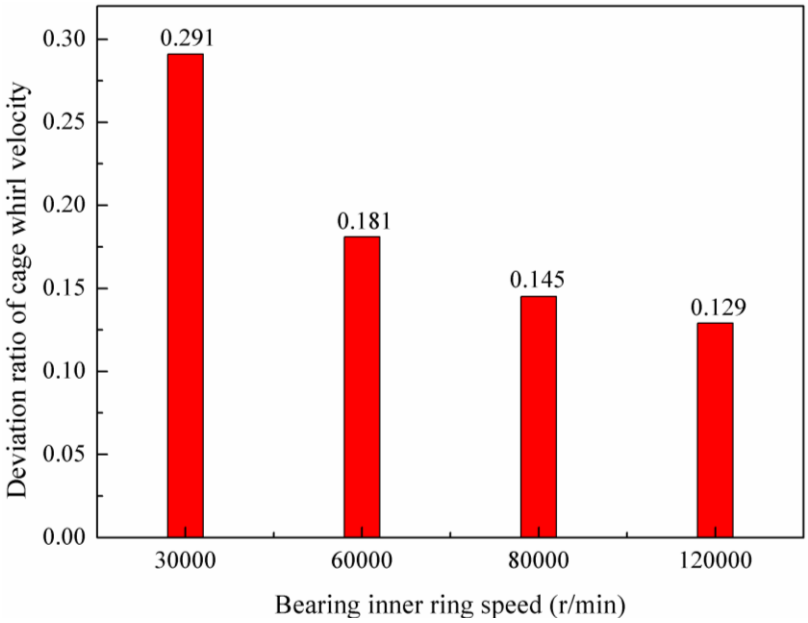

Fig. 10 - Stability of cage at different bearing operation speeds

The vibration spectrum of cage mass center at four different bearing velocities is shown in Figure 11. A comparison of the vibration frequency and the characteristic frequency of the cage mass center shows that whirl frequency of the cage mass center is always near to its revolving frequency. Also, with the increase in the bearing velocity, the whirl frequency of the cage mass center is higher than its revolving frequency at first and then gradually decreases. Therefore, to avoid having the contact between the cage and the guiding ring restricted in only one place or several places which would cause rapid wear of the cage, the relationship between the vibration frequency of cage mass center and the main frequency, the sub-frequency, and the multi-frequency of the cage revolution must be known.

在四种不同轴承转速下的保持架质心振动频谱如图 11 所示。将保持架质心振动频率和保持架特征频率进行对比可知，保持架质心涡动频率始终处于保持架转动频率附近，且随着转速的升高保持架质心涡动频率逐渐从大于保持架转动频率变为小于保持架转动频率。因此，为了避免保持架和引导套圈的接触发生在同一点或少数几点而导致保持架快速磨损，随着轴承工作转速的提升，必须关注保持架质心振动频率和保持架转动主频、分频及倍频的关系。

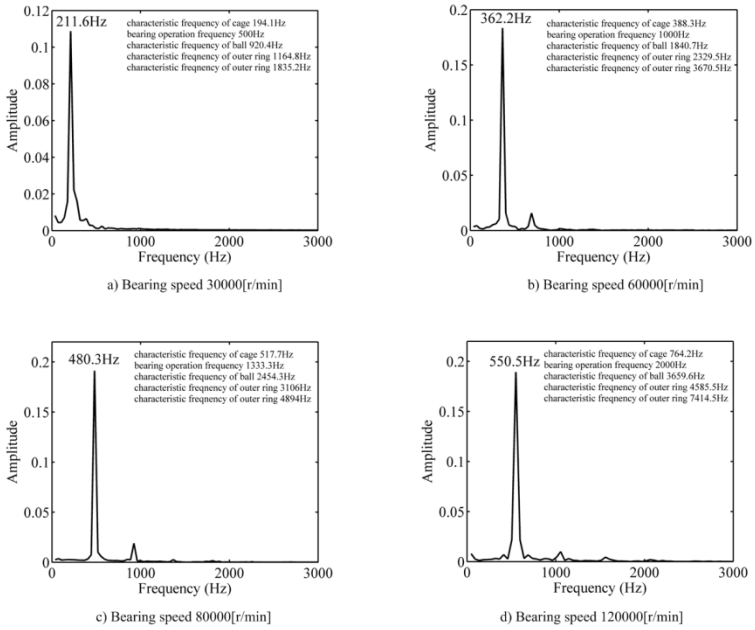

Fig. 11 - The spectrum of the cage center vibration at different bearing operation speed

Effect of changing bearing velocity on the dynamic performance of cage

According to the analysis results of the impact of different velocities on dynamic performance of the cage in the last section, it is clear that for different initial velocity, the changing processes of the bearing starting and the velocity increasing should be treated differently in terms of their impact on the dynamic performance of the cage.

Figure 12 shows the speeds of bearing elements during the starting process. It is indicated that the range of the speed of the rolling elements during the starting process follows the same trend of the speed ranges of the inner ring which shows a linear acceleration. However, there is stagnation and fluctuation of the cage speed within 6 ms while the bearing is started. This phenomenon can be ascribed by the fact that the cage speed relies entirely on the promotion of the rolling elements during the short period in which the bearing is started, and the relatively long interaction cycle between the cage and the rolling elements under the low velocity determines some delay of the cage starting. Meanwhile, the difference of speed between the rolling elements and the cage on the sudden start-up condition causes reciprocating collision between the cage pocket and the rolling element, leading to momentary velocity fluctuations of the cage during start-up.

转速变化过程对保持架动态性能影响

根据上一节不同转速对保持架动态性能影响的分析结果可知，轴承启动和轴承提速两个变化过程对保持架动态性能的影响由于初始转速不同需要区别对待。

图 12 所示为轴承启动过程中各元件的转速变化情况。从图中可见，轴承启动加速过程中滚动体的转速变化与轴承内圈速度变化趋势一致，呈现线性加速状态。但是保持架转速在轴承启动的 6ms 内存在停滞和波动现象，这是因为在轴承启动的短时内保持架的运动加速完全依靠滚动体的推动作用，而低转速下滚动体和兜孔之间较长的相互作用周期决定了保持架的启动会出现一定的延迟，同时，突然启动的保持架与滚动体之间的速度差使得保持架兜孔和滚动体之间出现往复碰撞，使得刚启动的保持架出现短时的速度波动。

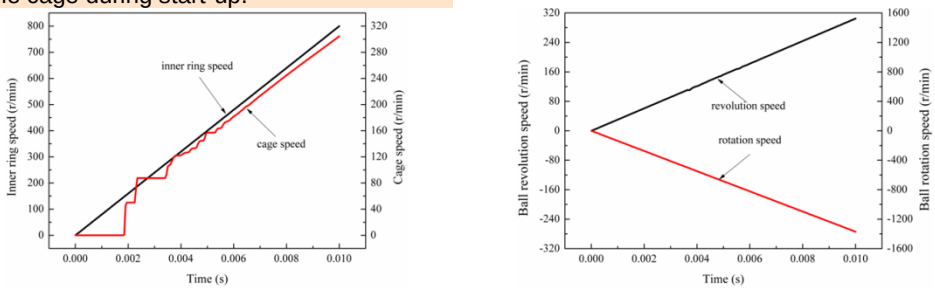

Fig. 12- Speed of the bearing elements during the beginning of their movement

Figure 13 shows the time response of the cage during the bearing starting process. According to Figure 13a, the impact of the cage pocket and the rolling element appears mainly in the short period when the cage is

图 13 所示为轴承启动过程中保持架的受力情况。据图 13a)可知，保持架兜孔和滚动体的冲击主要出现在保持

starting-up, and the driving force of the rolling element to the cage weakens gradually with time, with the cage eventually reaching a stable stage. Meanwhile, it can be seen from Figure 13b that the impact of the guiding surface of the ring on the cage increases gradually, indicating that under the force of the rolling element, the cage is getting close to the guiding surface of the ring to achieve a new balance.

架启动的很短时间内，滚动体对保持架的推动力随着时间逐渐减弱，最终使得保持架启动进入平稳阶段。同时，从图 13b)可以看出，套圈引导面对保持架的作用逐渐增强，说明保持架在滚动体的作用下会向套圈引导面靠近从而寻找新的平衡。

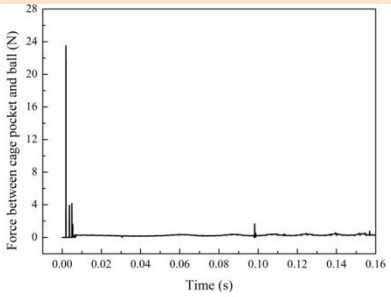

a) Time response of the cage pocket/ball force

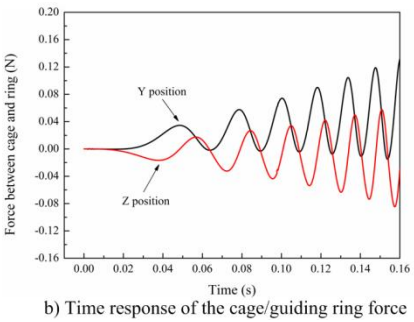

b) Time response of the cage/guiding ring force

Fig. 13 - Load vibration of cage in the bearing starting process

Fig. 14 shows the speed of bearing elements when the speed of inner ring ranges from 80000 - 85000 rot/min. As the figure shows, when the velocity of the bearing is accelerated under high-speed operation, the velocity of the rolling elements and the cage shows a fluctuating rising state, which is different from that of the bearing starting process. The main reasons that are the frequent collision of the rolling element and the cage pocket under a high velocity as well as the centrifugal force generated at a high velocity have an influence on the internal load distribution of the bearings which causes a difference among the traction force of the rolling elements at different azimuths.

图 14 所示为轴承内圈从 80000r/min 加速到 85000r/min 的过程中各元件的转速变化情况。从图中可以看出，轴承在高速运转情况下进一步加速时滚动体和保持架的转速都呈现波动上升的状态，与轴承启动加速过程中的情况不同。这是因为滚动体和套圈兜孔在高速情况下发生碰撞接触的频率增大，同时高速产生的离心力对轴承内部载荷分布的影响导致滚动体在不同方位下受到的套圈拖动力存在差异，二者的共同作用最终导致滚动体在加速过程中出现不规则的速度波动。

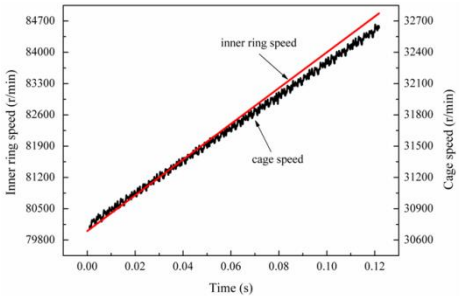

a) Cage speed

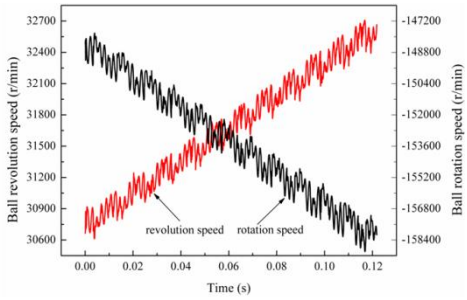

b) Ball speed

Fig. 14 - Speed of bearing element in bearing acceleration process

Fig. 15 shows the spectra of the interaction between the cage and the rolling element as well as the interaction between the cage and the guiding ring during the bearing acceleration process.

图 15 给出了提速过程中保持架和滚动体以及套圈间相互作用的频谱。

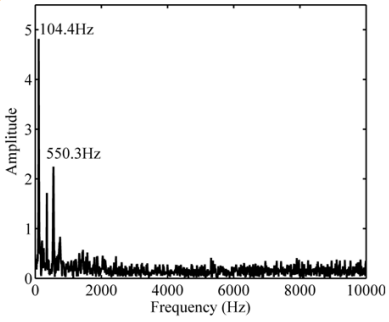

a) Spectrum of the cage pocket/ball force

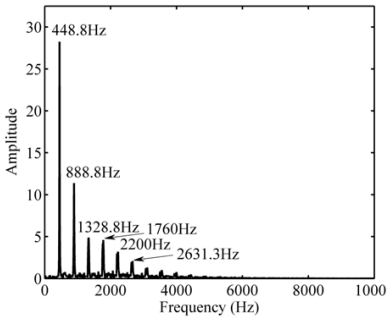

b) Spectrum of the cage/guiding ring force

Fig. 15 - Load spectra of cage in bearing acceleration process

As shown in Fig. 15, despite the spectral peaks appearing in the force spectrum of the interaction between the cage and the rolling element, broadband noise still exists. Therefore, there is a random impact process in the interaction between the cage and the rolling element in the bearing acceleration conditions with high speed. Meanwhile, multi-cycle vibration characteristics occur in the interaction between the cage and the guiding ring, indicating that the guiding effect of the ring to the cage is obvious when the bearing is accelerated.

CONCLUSIONS

In this paper, a dynamics analysis model of high-speed ball bearings is established, the reliability of which is verified by using the experimental examples of Gupta. The model can be used for the steady and transitional dynamic analysis for bearings under different working conditions, which provides a theoretical tool for the design of working conditions and failure analysis of high-speed ball bearings in the transmission systems of agricultural machinery. Though analysis of the effects of velocity changes on the stability of the dynamic performance of high-speed ball bearings, there are some conclusions that have been reached:

(1) As the velocity increases, the vibrational frequency of the cage mass center changes from being higher than the cage rotation frequency to be lower than it. Thus, in order to avoid the contact between the cage and the guiding ring being restricted in only one place or several places which would cause rapid wear of the cage, the relationship between the cage whirl frequency and the main frequency, the sub-frequency, the multi-frequency of the cage must be analyzed during actual operation.

(2) The cage suffers from periodic impact of the rolling elements during the startup phase of the bearing, which causes the cage to be in an unstable state. However, when the bearing is moving high-speed, bearing acceleration has no significant effect on the stability of the cage.

ACKNOWLEDGEMENT

The work has received support from the National Natural Science Foundation of China (51375108), Science and Technology Foundation of GuiZhou Province of China (Qian Ke He J Zi [2014]2172) and Natural Science Research Project of Education Department of GuiZhou Province of China (Qian Jiao He KY Zi [2014]294).

REFERENCES

[1]. Baomin Wang, Xuesong Mei, Chibing Hu, Zaixin Wu., (2008) – *Contact Angular Calculation and Analysis of High-Speed Angular Contact Ball Bearing,* Transactions of the Chinese Society for Agricultural Machinery, vol.39, no.9, pp.174-178;

[2]. Bing Fang, Lei Zhang, Xingtian Qu, Ji Zhao., (2012) – *Dynamic Modeling and Experiment of Angular Contact Ball Bearing*, Transactions of the Chinese Society for Agricultural Machinery, vol.43, no.6, pp.215-219;

[3]. Changqing Bai, Qingyu Xu., (2006) - *Dynamic Model of Ball Bearings with Internal Clearance and Waviness*, Journal of Sound and Vibration, vol.294, pp.23-28;

[4]. Chendong Duan, Yan Guo., (2008) – *An Envelop Analysis Approach for Ball Bearing Based on Lifting Wavelet Packet Transform*, Transactions of the Chinese Society for Agricultural Machinery, vol.39, no.5, pp.192-196;

从图 15 可以看出，保持架兜孔和滚动体之间的作用力频谱虽然出现了频谱峰值但是周围存在宽频噪声，所以高速提速情况下保持架和兜孔之间的作用依然存在随机的冲击过程。保持架和套圈引导面之间的作用呈现多周期振动的特点，说明在提速情况下套圈引导面对保持架的引导作用明显。

结论

本文建立了高速球轴承的动力学分析模型并采用 Gupta 实验算例验证了本文模型的可靠性，模型可针对不同工况条件下轴承的稳态及瞬态过渡进行动力学分析，为农机传动系统中高速球轴承的设计以及失效分析提供了理论工具。通过分析转速变化对高速球轴承动态性能稳定性影响，得出以下结论：

(1) 随着转速的升高，保持架质心振动频率逐渐从大于保持架转动频率变为小于保持架转动频率，为避免保持架和引导套圈的接触发生在同一点或少数几点而导致保持架快速磨损，在实际工作中必须对保持架质心振动频率与保持架转动主频、分频及倍频的关系进行分析。

(2) 轴承在加速启动阶段保持架受到滚动体周期性的冲击，使保持架处于不稳定状态，而当轴承处于高速阶段时转速的提升对保持架的稳定性没有明显的影响。

致谢

本文的研究获得了国家自然科学基金项目(51375108)，贵州省科学技术基金（黔科合 J 字[2014]2172），贵州省教育厅自然科学研究项目（黔教合 KY 字[2014]294）的资助。

参考文献

[1]. 王保民, 梅雪松, 胡赤兵, 邬再新. (2008) – *高速角接触球轴承接触角计算与影响因素分析*, 农业机械学报, 第 39 卷, 第 9 期, 174-178;

[2]. 方兵, 张雷, 曲兴田, 赵继. (2012) – *角接触球轴承动力学建模与实验*, 农业机械学报, 第 43 卷, 第 6 期, 215-219;

[3]. 白长青, 许庆余. (2006) - *带有内部游隙和表面波纹度的球轴承动力学模型*, 声音与振动, 第 294 卷, 23-28;

[4]. 段晨东, 郭研. (2008) – *基于提升小波包变换的滚动轴承包络分析诊断方法*, 农业机械学报, 第 39 卷, 第 5 期, 192-196;

[5]. 赵春江, 崔国华, 王国强, 黄庆学, 张芳萍. (2008) – *轴向*

[5]. Chunjiang Zhao, Guohua Cui, Guoqiang Wang, Qingxue Huang, Fangping Zhang., (2008) – *Precise Definition of Contact Angle Field on High Speed Angular-Contact Ball Bearing under Axial Load,* Transactions of the Chinese Society for Agricultural Machinery, vol.39, no.12, pp.153-156;
[6]. Ghaisas N., Wassgren C. R., Sadeghi F., (2004) - *Cage Instabilities in Cylindrical Roller Bearings,* Journal of tribology, vol.126, pp.681-689;
[7]. Gupta, P. K., (1991) - *Modeling of Instabilities Induced by Cage Clearances in Ball Bearings*, Tribology Transactions, vol.34, no.1, pp.93-99;
[8]. Gupta P. K., (1984) - *Advanced Dynamic of Rolling Elements,* Springer-Verlag, New York;
[9]. Hamrock B. J., Dowson D., (1981) - *Ball Bearing Lubrication:The Elastohydrodynamics of Elliptical Contacts*, John Wiley, New York;
[10]. Johnson K. L., (1992) - *Contact Mechanics,* Cambridge University Press, Cambridge;
[11]. Jun Zhang, Senlin LU, Weixing He, Yishun Wang, Tianbo Li., (2007) – *Vibration Diagnosis of Rolling Bearings Based on Wavelet Packet Energy Feature*, Transactions of the Chinese Society for Agricultural Machinery, vol.38, no.10, pp.178-181;
[12]. Liqin Wang, Li Cui, Dezhi Zheng, Le Gu., (2007) - *Analysis on Dynamic Characteristics of Aero-Engine High-Speed Ball Bearings,* Acta Aeronautica et Astronautica Sinica, vol.28, no.6, pp.1461-1467;
[13]. Mingming Li, (2013) – *Upgrade Path of China Agricultural Industry (Continued 1)*, Farm Machinery, no.22, pp. 48-56;
[14]. Preda I., Ciolan Gh., (2013) – *Algorithm to Define the Speed Ratios of the Tractor Complex Geartrains,* INMATEH–Agricultural Engineering, vol.41, no.3, pp.77-84;
[15]. Schlichting, H., Translated by Kestin, J. (1979) - *Boundary-Layer Theory*, McGraw-Hill Inc., New York;
[16]. Villa D., Gazzola J., Dal Fabbro I. M., Silva M. V.G. (2014) – *Moir Supported Stress Distribution Study on Gears,* INMATEH – Agricultural Engineering, vol.44, no.3, pp.157-164;
[17]. Weinzapfel, N., Sadeghi, F., (2009) - *A Discrete Element Approach for Modeling Cage Flexibility in Ball Bearing Dynamics Simulations*, Journal of Tribology, vol.131, no.2: 021102;
[18]. Xianqi Yang, Wenxiu Liu, Xiaoling Li, (2002) – *Dynamic Analysis on Cage of High Speed Roller Bearing,* Bearing, no.7, pp.1-5;
[19]. Xiuhai Liu, Sier Deng, Hongfei Teng, (2011) - *Dynamic Stability Analysis of Cages in High-Speed Oil-Lubricated Angular Contact Ball Bearings,* Transactions of Tianjin University, vol.17, no.1, pp.20-27;
[20]. Yanshuang Wang, Boyuan Yang, Liqin Wang, Peibin Zheng, (2004) - *Traction Behavior of 4106 Aviation Lubricating Oil*, Tribology, vol.24, no.2, pp.156-159;
[21]. Yaobin Zhuo, Xiaojun Zhou, (2013) – *Analysis of Effect of Clearance on Static Mechanical Behavior for Double Row Self-Aligning Ball Bearing and Control of Clearance,* Transactions of the Chinese Society of Agricultural Engineering, vol.29, no.19, pp.63-70;
[22]. Yonggang Xu, Zhipeng Meng, Ming Lu, (2013) – *Fault Diagnosis of Rolling Bearing Based on Dual-Tree Complex Wavelet Packet Transform*, Transactions of the Chinese Society of Agricultural Engineering, vol.29, no.10, pp.49-56;

受载的高速角接触球轴承接触角域的精确确定, 农业机械学报, 第 39 卷, 第 12 期, 153-156;
[6]. Ghaisas, N., Wassgren, C. R., Sadeghi, F. (2004) – *援助滚子轴承的保持架不稳定性分析,* 美国摩擦学报, 第 126 卷, 681-689;
[7]. Gupta, P. K. (1991) -*保持架间隙导致球轴承不稳定的分析模型*, 美国摩擦学会会刊, 第 34 卷, 第 1 期, 93-99;
[8]. Gupta, P. K. (1984) – *滚动轴承高等动力学,* 施普林格出版社, 纽约;
[9]. Hamrock, B. J., Dowson, D. (1981) – *球轴承的润滑:椭圆接触的流体动压润滑*, 约翰威立出版社, 纽约;
[10]. Johnson, K. L. (1992) – *接触力学,* 剑桥大学出版社, 剑桥;
[11]. 张军, 陆森林, 和卫星, 王以顺, 李天博. (2007) – *基于小波包能量法的滚动轴承故障诊断*, 农业机械学报, 第 38 卷, 第 10 期, 178-181;
[12]. 王黎钦, 崔立, 郑德志, 古乐. (2007) - *航空发动机高速球轴承动态特性分析*, 航空学报, 第 28 卷, 第 6 期, 1461-1467;
[13]. 李明明. (2013) – *中国农机工业的升级路（续 1）*, 农业机械, 第 22 期, 48-56;
[14]. Preda I., Ciolan Gh. (2013) – *拖拉机复杂齿轮系速度比定义的算法*, INMATEH – 农业工程, 第 41 卷, 第 3 期, 77-84.
[15]. Schlichting, H.著, Kestin, J.翻译 (1979) – *边界层理论*, 麦格劳-希尔出版社, 纽约;
[16]. Villa D., Gazzola J., Dal Fabbro I. M., Silva M. V.G. (2014) – *齿轮莫尔支承应力分布研究*, INMATEH – 农业工程, 第 44 卷, 第 3 期, 157-164.
[17]. Weinzapfel, N., Sadeghi, F. (2009) – *球轴承柔性保持架动力学仿真的离散单元法*, 美国摩擦学报, 第 131 卷, 第 2 期, 021102;
[18]. 杨咸启, 刘文秀, 李晓玲. (2002) - *高速滚子轴承保持架动力学分析*, 轴承, 第 7 期, 1-5;
[19]. 刘秀海, 邓四二, 腾弘飞. (2011) – *高速油润滑角接触球轴承的保持架动态稳定性分析,* 天津大学学报, 第 17 卷, 第 1 期, 20-27;
[20]. 王燕霜, 杨伯原, 王黎钦, 郑培斌. (2004) – *4106 航空润滑油拖动特性研究*, 摩擦学学报, 第 24 卷, 第 2 期, 156-159;
[21]. 卓耀彬, 周晓军. (2013) – *游隙对双列调心球轴承静力学性能影响及游隙控制分析*, 农业工程学报, 第 29 卷, 第 19 期, 63-70;
[22]. 胥永刚, 孟志鹏, 陆明. (2013) – *基于双树复小波包变换的滚动轴承故障诊断*, 农业工程学报, 第 29 卷, 第 10 期, 49-56.

MULTI-SYSTEM COUPLING VIBRATION OF A DISTRIBUTED ELECTRIC-DRIVE AGRICULTUAL VEHICLE
/
分布式电传动农用汽车多系统耦合振动研究

Ph.D. Jin C.[1)], Ms. Wei J.[1)], Ph.D. Stud. Sun H.[1)], Ph.D Stud Yin Y.[2)]
[1)]School of Mechanical Engineering, University of Science and Technology Beijing, Beijing / China,
[2)] Department of Mechanical and Industrial Engineering, Concordia University / Canada
Tel:010-82375949; E-mail: jinjinbit@163.com

Abstract: *To ensure riding comfort, vibration generated by engine, drive system and ground need to be considered in designing an agricultural vehicle. This study examines multi-body dynamics model of an agricultural vehicle, and focuses on the distributed electric-drive agricultural vehicle. To simulate the response of an electric-drive agricultural vehicle to vibrations excited by the drive motors, engine and road roughness, this study proposes a vibration model of a distributed electric-drive agricultural vehicle that has 11 degrees of freedom and coupled excitation sources. The model was derived from vehicle dynamics equations and solved numerically employing fast Fourier transform. The model was validated in experiments on a real distributed electric-drive agricultural vehicle. Simulations and experiments showed that the amplitude of low-frequency vibration of the cab was increased by simultaneous excitations, which could not be ignored. This result is useful for the design of the suspension component and overall design of agricultural machinery.*

Keywords: *Electric drive; Agricultural vehicle; Riding comfort; Vibrations; Multiple systems*

INTRODUCTION

An electric-drive agricultural vehicle is energetically efficient, environmentally friendly and convenient. It is increasingly being used for transportation work in farm lands. However, because of road roughness, simultaneous shocks generated by farming land and vehicle systems have a significant effect on the health of the driver and the reliability of the vehicle. A distributed electric-drive agricultural vehicle is powered by hybrid of diesel engine and battery. Compared with the traditional mechanical transmission, the vehicle is specially designed for farming lands with in-motor wheel, and deleting the gearbox, driveshaft, final drive, differential, so the vehicle has advantages of simple structure, small space requirement, easy high torque performing, convenient feedback control and continuous speed change. Thus, the wheel electric drive has great application potential for agricultural vehicles. However, an electric-drive agricultural vehicle has a significant unsprung load. Additionally, the connection of the hydro-pneumatic spring and wheel rim drive unit generates interacting vibrations from the engine and drive motor and reduces the ride comfort. Thus, the relationship between ride comfort and the structure of the distributed electric-drive agricultural vehicle should be examined.

Present studies on the effects of drive motor vibration on vehicle power and riding comfort usually focus on passenger cars, and the drive motor is typically designed as a sprung load [1,5,7,14,17]. Researchers have analyzed the vibration of a switched reluctance

摘要：*为确保行驶平顺性，农用汽车设计需综合考虑动力、传动系统及地面冲击产生的振动。论文以分布式电传动农用汽车为研究对象，提出了十一自由度发动机激振—电动机激振—路面不平度耦合振动模型。推导出整机动力学方程，并利用快速傅立叶变换方法得到了数值计算结果。通过实车试验与耦合振动模型进行对比，结果表明在考虑驱动电机及发动机激振影响下驾驶室振动的低频段振幅明显增大，在发动机及驱动电机激振力频率段影响明显，不可忽略。通过分析实测数据验证了耦合激励模型在实车中的有效性.耦合激励模型对农用汽车悬架及整车平顺性设计具有指导意义。*

关键词：*电驱动；农用汽车；平顺性；振动；多系统*

引言

电传动农用汽车具有节能、环保、便捷等优势，目前，在农耕地上承担越来越多的运输及装卸工作。但是，农业耕地属于非公路，其路面不平度产生的冲击和车辆本身的振动对驾驶员的健康及车辆的可靠性有很大影响。分布式电传动农用汽车动力系统采用柴油机与蓄电池混合动力。其传动方式不同于传统的机械传动，牵引电动机直接驱动车轮，省去了变速箱、传动轴、主减速器、差速器等传动部件，牵引力大、结构简单、可靠性高，同时便于实现反馈控制和无级变速平稳运行，具有良好的应用前景。但是，该传动方式以轮边驱动单元作为驱动桥，非簧载质量大，悬架下端与轮边驱动单元相连接，牵引电动机与发动机共同作为激振源引起车辆平顺性恶化。因此，对分布式电传动结构形式带来的整车平顺性问题的研究是十分有必要的。

牵引电动机振动对车辆动力性及平顺性能的影响，目前研究多集中于乘用车[1,5,7,14,17]。有学者以开关磁阻驱动电机的振动为例分析，表明电机激振力对悬架系统的影响较大而不能忽略[9]；谭迪以 1/4 车辆简化模型探讨非簧载质量增加对平顺性影响[12]；李朝峰等针对四轮乘用车

motor and pointed out that the effect of motor excitation on the suspension cannot be ignored [9]. Tan [12] built a ¼ vehicle model and discussed the effect of increasing the unsprung load on the riding comfort. Li, using road excitation as the main source of motivation, established a nonlinear model of riding comfort with 11 degrees of freedom (DOFs) for a passenger car [6]. The analysis of riding comfort by Wellman and Wang showed that the powertrain and road excitation cannot be ignored [15, 16]. However, few studies on riding comfort have investigated the coupled excitation effects of the in-wheel motor, engine and road for a distributed electric-drive agricultural vehicle. This paper initiates modeling and discussion on this topic.

Taking the distributed electric-drive agricultural vehicle as the study object, this paper proposes a method of describing the coupled vibration generated by multiple systems of the vehicle and builds a vibration model with 11 DOFs. Moreover, the riding comfort of the vehicle travelling on random surfaces is simulated by employing white-noise filtering. The model and simulation are validated in experiments on a real vehicle undergoing coupled vibration.

建立了 11 自由度非线性车辆平顺性模型，模型主要取路面激励为主要的激励来源[6]；Wellman Thomas 和王登峰针对动力总成振动对整车行驶平顺性展开分析，表明动力总成和路面激励在平顺性分析中不可忽略[15,16]。分析常见车辆平顺性研究，以分布式电驱动车辆为研究对象的论文较少，激励源往往没有同时考虑驱动电机激励、发动机激振、路面不平度的影响，本文正是基于以上问题展开建模和讨论。

本文以分布式电驱动农用汽车为研究对象，提出了兼顾电机激振、发动机振动路面不平度来描述整车多系统耦合运动的方法，建立整车十一自由度的振动模型。采用白噪声滤波法模拟时域内的随机路面进行平顺性仿真。通过联立运动方程分析振动特性并进行了实车现场测试，探究在耦合激励下整车平顺性的影响。

MATERIALS AND METHODS

材料与方法

Vibration subsystem analysis of the electric-drive agricultural vehicle

分布式电驱动农用汽车振动子系统分析

An engine vibration system has a variety of vibration forms. The dominant vibration is the oscillation of the whole machinery, which is much stronger than the vibration of an axle or local vibration [2].

As mentioned, the road roughness, engine vibration and in-wheel electric motor vibration are excitation sources of vibration. The vibration subsystem includes the engine vibration system and in-wheel electric motor vibration system. The electric-drive agricultural vehicle studied in this paper has a Cummings engine. The vibration of the engine is mainly due to the unbalanced forces and torques produced in operating the engine. According to the characteristics of the engine, the excitation frequency is [4]:

发动机系统运转时，机体上存在各种激振力。产生的整机振动主要指机体跳动，这类振动对机体的结构影响较大,而轴系振动、局部振动影响较小[2]。

如前所述，系统振动的激励源包括：路面不平度，发动机振动以及轮边电机振动激励。整机振动子系统包括发动机振动系统和轮边电机振动系统。本文所研究的分布式电驱动农用汽车采用康明斯发动机，发动机振动主要来自于发动机运转过程中产生的不平衡力和力矩，根据发动机自身的工作特性可知，发动机的激励频率为 [4]：

$$f = \frac{n\lambda Z}{60\tau} \tag{1}$$

Where, τ—the stroke number, n—the engine speed (r/min), Z—the cylinder number, and λ—the incentive order.

式中：τ—冲程数，n—发动机转速（r/min），Z—气缸数，λ—激励阶数。

The engine exciting force is mainly generated by the imbalance torque and moment produced by the running of the engine. According to the working characteristics of the four-cylinder engine, a cycle of crank shaft rotation has two instances of torque fluctuation. Based on the traditional dynamic analysis formula, two reciprocating inertia force expressions are [18]:

发动机激振力主要来自于发动机运转过程中产生的不平衡力和力矩根据发动机自身的工作特性可知：在四缸发动机中曲轴每转一周就会产生两次转矩波动。按照传统的动力学分析公式 二次往复惯性力表达式为[18]：

$$P_j = -4\lambda m_j r w^2 \cos(2\alpha) = -4\lambda m_j r w^2 \cos(wt + \varphi) \tag{2}$$

$$m_j = m_{hz} + m_A \tag{3}$$

Where, P_j—twice the reciprocating inertia force, λ—the link ratio, r—the radius of the crank, m_{hz}—the quality of the piston assembly, and m_A—the quality of the small end of the link.

In the experiment conducted in this study, the engine speed measured using a controller area network was 1500 rpm when the vehicle speed reached 30 km/h.

式中：P_j—二次往复惯性力；λ—连杆比；r—曲柄半径；m_{hz}—活塞组件的质量，m_A—双质量系统代换得到的连杆小头的质量。

后续试验过程中车速为 30km/h 时，CAN 数据采得发动

Using equation (1), we calculated the first-order excitation frequency of the engine as 37.5 Hz and the force as 25.3 kN. These results are consistent with data provided by the engine manufacturer.

机转速 n 为 1500 r/min，代入式（1）可得理论的发动机一阶激励频率为 37.5Hz，采得大小为 25.3kN，这与发动机厂家提供数据一致。

The drive motor vibration comprises electromagnetic vibration, mechanical vibration and pneumatic vibration [3]. The electromagnetic vibration is generated by the interaction of the magnetic field in the air gap, and varies with time and space. It is also a major vibration source [8]. The main frequency of the drive motor is twice the power frequency. For a synchronous motor, the relation between the revolving speed and power frequency is) [11]:

对于电动机系统振动分别由电磁振动、机械振动、气体振动三部分组成[3]。电磁振动是由气隙中磁场的相互作用而产生，且随时间和空间变化，电磁振动为主要振动源[8]。电动机振动力主波频率为二倍电源频率。对于同步电机，转速与供电电源频率关系如下[11]：

$$n' = \frac{60f'}{p} \tag{4}$$

Where, *f'*—the power frequency, *p*—the number of drive motor pole pairs, *n'*—the drive motor speed (r/min).

式中：*f'*—供电频率；*p*—电动机极对数；*n'*—电动机转速（r/min）。

The Maxwell stress tensor is used to calculate the electromagnetic exciting force acting on the stator. Here, the magnetic field strength on the surface of the strain object is H, the object is surrounded by air and the electromagnetic force acting on the object is[10]:

定子上受到的电磁激振力可用麦克斯韦应力张量法计算，假设受力物体表面 S 上的磁场强度为 H，并且这个物体外部被空气所包围，则这个物体受到的电磁力[10]为：

$$\hat{F} = \int_s \left[-\frac{\mu_0}{2} H^2 \hat{n} + \mu_0 \left(\hat{n} \cdot \hat{H} \right) \hat{H} \right] ds \tag{5}$$

The force can be decomposed into x (vertical) and y (horizontal) directions:

将力分解在 x（垂直）和 y（水平）方向，则:

$$F_x = \int_s \mu_o H_x H_y ds \tag{6}$$

$$F_y = \int_s \frac{\mu_o}{2} (H_y^2 - H_x^2) ds \tag{7}$$

Where, μ_0—the permeability of air, *n*—a unit vector normal to the surface S, and H_x and H_y are the magnetic strength in the *x* and *y* directions respectively. The magnetic field distribution of the motor can be obtained by employing the finite element method (FEM). The electromagnetic force and road excitation are input into differential equations to calculate the system response.

式中：μ_o—空气中的磁导率，$\hat{n}$—沿表面 S 法方向上的单位矢量，H_x 和 H_y 分别为受力物体表面 S 上 x 和 y 方向上的磁场强度。电动机各处磁场分布可以通过有限元方法求得。将得到的电磁力与路面激励带入整个系统微分方程组求解系统响应。

In the experiment, the revolving speed of the electric motor in stable operation was 1200 r/min. The excitation force of the electric motor was calculated as 15.6 kN by employing the FEM software ANSOFT. The equation shows that the excitation frequency is approximately 120 Hz. The frequency in other segments can be similarly estimated.

所研究的分布式电驱动农用汽车试验电机稳定段运行转速为 1200r/min。电动机激振力可通过有限元软件 Ansoft 分析得出，激振力大小为 15.6kN，带入公式（3）可知激振力频率约为 120Hz。不同段频率可依此估计。

Establishment of a three-dimensional vibration model

三维整机振动模型建立

To control the torque of the in-wheel drive motor and monitor the revolving speed of the wheel, a dynamic model of a distributed electric-drive agricultural vehicle that can be used to analyze the force between the vehicle and ground surface was constructed. Three DOFs in the vertical, horizontal and transverse directions were adopted for the whole vehicle.

建立整车动力学模型来分析车辆与地面的作用力关系，达到控制轮边牵引电机转矩和监测电机转速的目的。选取纵向、侧向和横摆三个自由度，建立整车动力学模型。

The following preconditions were proposed to be taken into consideration for the dynamic model [13].

从研究问题的需要出发，针对所研究的分布式电驱动农用汽车的特点提出以下前提[13]：

(1) The vehicle speed is less than 30 km/h; thus, the unbalanced excitations of tires and transmission shaft can be ignored;

(2) The frame stiffness is sufficiently high, so the vibration generated by elastic deformation of the frame is ignored;

(3) The articulated body has no effect on the vertical vibration of the vehicle, and the DOF of steering is ignored;

(4) The non-suspended load is simplified as having a single DOF. Only the vertical DOF is considered in this model because it is significantly more influential than other DOFs of the load;

(5) Under the excitation of the engine, wheel electric motor and ground, the vibrations are only slightly near the equilibrium position. Therefore, the linear vibration of the vehicle bar centered on the horizontal plane and the angular vibration of the vehicle around the z-axis can be ignored.

Under these preconditions, an 11-DOF model of an agricultural vehicle is built as shown in Fig 1. In the figure, the front suspension is a hydro-pneumatic suspended structure and the rear suspension is a balanced beam structure. The vertical vibration, because of its effect on riding comfort, is the only factor considered for the engine vibration and drive motor vibration. The excitations from the road roughness, engine vibration and drive-motor vibration are considered. The vertical, roll and pitch DOFs of the engine are also introduced to reflect the effects of the stiffness and damping of the four mounts at the front and rear of the engine.

The 11 DOFs are listed as follows:

Z_a—barycentre displacement of the sprung mass in the vertical direction;

A—displacement of the pitch angle of the vehicle sprung mass around the bary centre;

θ_1 and θ_2—roll angular displacements of front and rear frames, respectively;

Z_e—engine displacement in the vertical direction;

α_e—pitch angular displacement around the barycentre;

θ_e—engine roll angle displacement around the centre of mass of the engine;

Z_1 and Z_2—displacements of the vehicle's front wheels in the vertical direction;

β_1 and β_2—angular displacements of the rear suspensions ;

Other parameters in the model are described as follows. Z_{11}–Z_{61}—the input displacements of the road that act on the six wheels, F_{d1}–F_{d6}—the input forces given by the vibrations of the six drive motors, F_{de}—the input force arising from engine vibration, Z_1 and Z_2—the vertical displacements of the hydro-pneumatic springs, Z_3–Z_6—the vertical displacements of middle- and rear-axle tires, K_1 and K_2—the stiffness coefficients of the hydro-pneumatic springs, K_7–K_{12}—the stiffness coefficients of the tires, C_1 and C_2—the damping coefficients of the hydro-pneumatic springs, C_7–C_{12}—the damping coefficients of the tires, L_1—the horizontal distance between a front wheel and the vehicle centre of mass, L_2 —the distance between a middle wheel and the centre of mass, L_3—the distance between middle and rear wheels, L_4—the distance between front wheels, L_5—the distance between rear wheels, L_6—the horizontal distance between the cab and the vehicle's centre of mass, L_8—the distance between the rear engine and barycentre of the cab, L_9—the length of

（1）在低速情况下工作，故忽略轮胎和传动轴不平衡的激励；

（2）机身和车架刚度很大，忽略车身弹性引起的振动；

（3）铰接体对机身的垂直振动没有影响，不考虑铰接体转向自由度；

（4）非悬挂质量简化为单自由度质量系统，只考虑对整机振动影响较大垂向振动自由度；

（5）在发动机、轮边电机以及路面激励作用下，整车在平衡位置附近作微幅振动，车身质心在水平面内的振动忽略不计，机身绕 Z 轴的角振动忽略不计。

本文将车辆简化为 11 自由度三维整机模型（如图 1）。图中，前悬架为油气悬架，后悬架为平衡梁结构。影响乘坐舒适性的唯一因素是由发动机振动和电机振动引起的垂向振动。模型考虑了路面不平度激励，发动机振动和轮边驱动电机振动。发动机前后悬置的刚度和阻尼由发动机的垂向、侧倾以及俯仰三个自由度来描述。

模型 11 个自由度分别为：

Z_a —整车簧载质量质心垂直方向位移；

A —整车簧载质量绕质心的俯仰角位移；

θ_1、θ_2 —前后车体分别绕前后车体质心的侧倾角位移

Z_e —发动机垂直方向位移；

α_e —发动机绕其质心的俯仰角位移；

θ_e —发动机绕其质心的侧倾角位移；

Z_1、Z_2 —前轮垂直方向位移；

β_1、β_2 —两平衡梁绕铰接处的角位移；

模型中其他参数如下：Z_{11}~Z_{61}—路面对六轮的输入位移；F_{d1}~F_{d6}—六个电机振动的输入力；F_{de}—发动机振动的输入力；Z_1、Z_2—油气弹簧与簧载质量连接点处的垂直位移；Z_3~Z_6—中后桥轮胎中心处的垂直位移；K_1、K_2—油气弹簧的刚度系数；K_7~K_{12}—轮胎的刚度系数；C_1、C_2—油气弹簧的阻尼系数；C_7~C_{12}—轮胎的阻尼系数；L_1—前轮距整机质心的水平距离；L_2—中轮到质心的水平距离；L_3—中后轮间的水平距离；L_4—前轮距；L_5—后轮距；L_6—驾驶室质心距整机质心的水平距离；L_8—发动机尾部距驾驶室质心距离；L_9—发动机长度；L_f—发动机前

engine, L_f—the distance between front suspensions, L_r—the distance between rear suspensions, M_0—the sprung mass of the vehicle, M_{01} and M_{02}—the sprung masses of front and rear frames respectively, M_1–M_6—the unsprung masses of the six wheels, M_e—the engine mass, and I_1—the longitudinal moment of inertia of the sprung mass that turns around the vehicle centre of mass. I_2—the horizontal inertia moment of the sprung load of the front frame, I_3—the horizontal inertia moment of the sprung load of the rear frame, I_{e1}—the inertia moment produced by the rotation of the engine around its longitudinal axis, and I_{e2}—inertia moment produced by the rotation of the engine around its horizontal axis.

悬之间的距离；L_r—发动机后悬之间的距离；M_0—整车簧载质量；M_{01}、M_{02}—前后车体簧载质量；M_1~M_6—六个车轮的非簧载质量；M_e—发动机质量；I_1—整车簧载质量绕质心纵向转动惯量；I_2—前车体簧载质量横向转动惯量；I_3—后车体簧载质量横向转动惯量；I_{e1}—发动机绕其质心纵向转动惯量；I_{e2}—发动机绕其质心横向转动惯量。

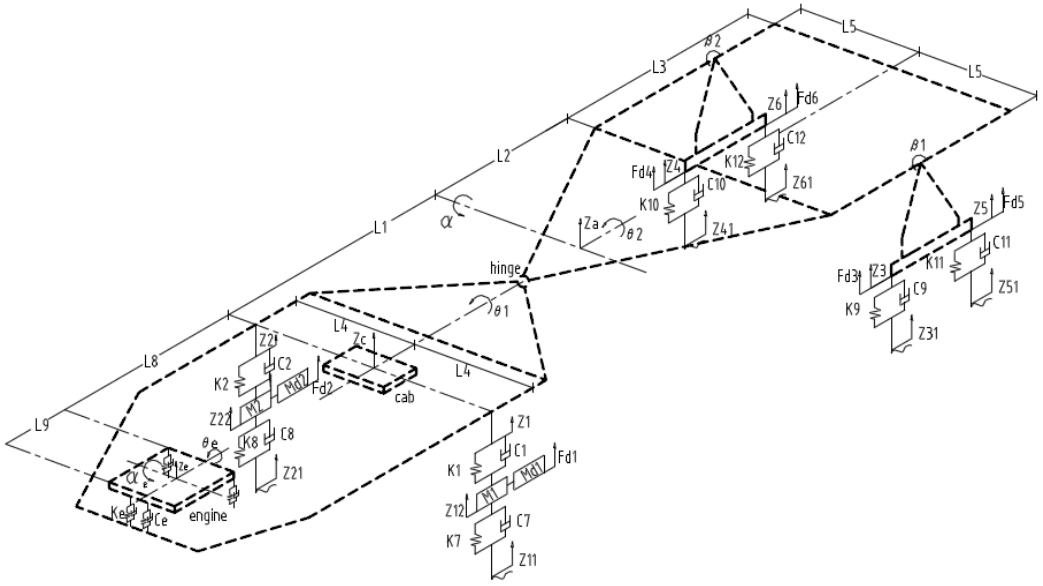

Fig.1- Model of an agricultural vehicle with 11 DOFs

The equations that govern the micro-vibration of the machinery are:

整机微分振动的动力学方程如下：

$$\begin{aligned}&M_0\ddot{Z}_a = C_1(\dot{Z}_{12}-\dot{Z}_1)+K_1(Z_{12}-Z_1)+C_2(\dot{Z}_{22}-\dot{Z}_2)+K_2(Z_{22}-Z_2)+C_{11}(\dot{Z}_{31}-\dot{Z}_3)+K_{11}(Z_{31}-Z_3)\\&+C_{12}(\dot{Z}_{41}-\dot{Z}_4)+K_{12}(Z_{41}-Z_4)+C_{13}(\dot{Z}_{51}-\dot{Z}_5)+K_{13}(Z_{51}-Z_5)+C_{14}(\dot{Z}_{61}-\dot{Z}_6)+K_{14}(Z_{61}-Z_6)\\&-K_e(Z_{e5}+Z_{e6}+Z_{e7}+Z_{e8})-C_e(\dot{Z}_{e5}+\dot{Z}_{e6}+\dot{Z}_{e7}+\dot{Z}_{e8})+F_{d1}+F_{d2}+F_{d3}+F_{d4}+F_{d5}+F_{d6}\end{aligned} \tag{8}$$

$$\begin{aligned}&I_1\ddot{a} = (L_2+L_3/2)[C_{11}(\dot{Z}_{31}-\dot{Z}_3)+K_{11}(Z_{52}-Z_5)+C_{12}(\dot{Z}_{41}-\dot{Z}_4)+K_{12}(Z_{51}-Z_5)+C_{13}(\dot{Z}_{51}-\dot{Z}_5)\\&+K_{13}(Z_{51}-Z_5)+C_{14}(\dot{Z}_{61}-\dot{Z}_6)+K_{14}(Z_{61}-Z_6)+F_{d3}+F_{d4}+F_{d5}+F_{d6}]-L_1[C_1(\dot{Z}_{12}-\dot{Z}_1)\\&+K_1(Z_{12}-Z_1)+C_2(\dot{Z}_{22}-\dot{Z}_2)+K_2(Z_{22}-Z_2)+F_{d1}+F_{d2}]-K_e[(Z_{e7}+Z_{e8})(L_1+L_8)\\&+(Z_{e5}+Z_{e6})(L_1+L_8+L_9)]-C_e[(\dot{Z}_{e7}+\dot{Z}_{e8})(L_1+L_8)+(\dot{Z}_{e5}+\dot{Z}_{e6})(L_1+L_8+L_9)]\end{aligned} \tag{9}$$

$$I_2\ddot{q}_1 = L_4[C_1(\dot{Z}_{12}-\dot{Z}_1)+K_1(Z_{12}-Z_1)-C_2(\dot{Z}_{22}-\dot{Z}_2)-K_2(Z_{22}-Z_2)]+I_{e2}\ddot{q}_e \tag{10}$$

$$\begin{aligned}&I_3\ddot{\theta}_2 = L_5[C_{11}(\dot{Z}_{31}-\dot{Z}_3)+K_{11}(Z_{31}-Z_3)+C_{13}(\dot{Z}_{51}-\dot{Z}_5)+K_{13}(Z_{51}-Z_5)+F_{d3}+F_{d5}\\&-C_{12}(\dot{Z}_{41}-\dot{Z}_4)-K_{12}(Z_{41}-Z_4)-C_{14}(\dot{Z}_{61}-\dot{Z}_6)-K_{14}(Z_{61}-Z_6)-F_{d4}-F_{d6}]\end{aligned} \tag{11}$$

$$M_1\ddot{Z}_{12} = C_7(\dot{Z}_{11}-\dot{Z}_{12})+K_7(Z_{11}-Z_{12})+C_1(\dot{Z}_1-\dot{Z}_{12})+K_1(Z_1-Z_{12})+F_{d1} \tag{12}$$

$$M_2\ddot{Z}_{22} = C_8(\dot{Z}_{21}-\dot{Z}_{22})+K_8(Z_{21}-Z_{22})+C_2(\dot{Z}_2-\dot{Z}_{22})+K_2(Z_2-Z_{22})+F_{d2} \tag{13}$$

$$I_4\ddot{b}_1 = L_3/2\cdot[C_{13}(\dot{Z}_{51}-\dot{Z}_5)+K_{13}(Z_{51}-Z_5)+F_{d5}-C_{11}(\dot{Z}_{31}-\dot{Z}_3)-K_{11}(Z_{31}-Z_3)-F_{d3}] \tag{14}$$

$$I_5\ddot{\beta}_2 = L_3/2\cdot[C_{14}(\dot{Z}_{61}-\dot{Z}_6)+K_{14}(Z_{61}-Z_6)+F_{d6}-C_{12}(\dot{Z}_{41}-\dot{Z}_4)-K_{12}(Z_{41}-Z_4)-F_{d4}] \tag{15}$$

$$M_e\ddot{Z}_e = K_e(Z_{e5}+Z_{e6}+Z_{e7}+Z_{e8})+C_e(\dot{Z}_{e5}+\dot{Z}_{e6}+\dot{Z}_{e7}+\dot{Z}_{e8})+F_e \quad (16)$$

$$I_{e1}\ddot{\alpha}_e = [K_e(-Z_{e5}-Z_{e6}+Z_{e7}+Z_{e8})+C_e(-\dot{Z}_{e5}-\dot{Z}_{e6}+\dot{Z}_{e7}+\dot{Z}_{e8})]\cdot L_9/2 \quad (17)$$

$$I_{e2}\ddot{\theta}_e = K_e[(Z_{e7}-Z_{e8})L_r+(Z_{e5}-Z_{e6})L_f]+C_e[(\dot{Z}_{e7}-\dot{Z}_{e8})L_r+(\dot{Z}_{e5}-\dot{Z}_{e6})L_f] \quad (18)$$

In the preceding equations, Z_{e5}–Z_{e8} are the engine mount vertical displacements. The following dynamic equation can be obtained by solving the preceding equations:

其中：Z_{e5}~Z_{e8} 为发动机微幅振动是发动机悬置垂向位移。联立上述方程可以解出整机的动力学方程：

$$M\ddot{Y}+C\dot{Y}+KY = K_t Q+C_t\dot{Q}+A_d F_d+A_e F_e \quad (19)$$

Where, ***M***—an 11 × 11 mass matrix, ***C***—an 11 × 11 stiffness matrix, ***K***—an 11 × 11 damping matrix, C_t—an 11 × 6 stiffness matrix of the tires, K_t—an 11 × 6 damping matrix of the tires, A_d—the drive motor excitation coefficient matrix, A_e—the excitation coefficient matrix of the engine, ***Q***—the excitation matrix of the ground surface, F_d—the excitation matrix of the drive motor, and F_e—the excitation matrix of the engine. These matrices are expressed as:

其中，***M***—11×11 阶质量矩阵；***C***、***K***—11×11 阶阻尼矩阵和刚度矩阵；***Ct*** 和 ***Kt***—11×6 阶轮胎阻尼矩阵和轮胎刚度矩阵；A_d—电机激励系数矩阵；A_e—发动机激励系数矩阵；***Q***—路面激励矩阵；F_d—电机激励矩阵；F_e—发动机激励。各矩阵表示为以下形式：

$$\mathbf{Y}=[Z_a \quad \alpha \quad \theta_1 \quad \theta_2 \quad Z_{12} \quad Z_{22} \quad \beta_1 \quad \beta_2 \quad Z_e \quad \alpha_e \quad \theta_e]^T, \qquad \mathbf{Q}=[Z_{11} \quad Z_{21} \quad Z_{31} \quad Z_{41} \quad Z_{51} \quad Z_{61}]^T$$

$$\mathbf{F_d}=[F_{d1} \quad F_{d2} \quad F_{d3} \quad F_{d4} \quad F_{d5} \quad F_{d6}]^T, \qquad \mathbf{A_e}=[0 \quad 0 \quad 0 \quad 0 \quad 0 \quad 0 \quad 0 \quad 0 \quad 1 \quad 0 \quad 0]^T$$

$$\mathbf{A_d}=\begin{pmatrix} 0 & 0 & 1 & 1 & 1 & 1 \\ 0 & 0 & L_2+L_7 & L_2+L_7 & L_2+L_7 & L_2+L_7 \\ 0 & 0 & 0 & 0 & 0 & 0 \\ 0 & 0 & L_5 & -L_5 & L_5 & -L_5 \\ 1 & 0 & 0 & 0 & 0 & 0 \\ 0 & 1 & 0 & 0 & 0 & 0 \\ 0 & 0 & -L_7 & 0 & L_7 & 0 \\ 0 & 0 & 0 & -L_7 & 0 & L_7 \\ 0 & 0 & 0 & 0 & 0 & 0 \\ 0 & 0 & 0 & 0 & 0 & 0 \\ 0 & 0 & 0 & 0 & 0 & 0 \end{pmatrix} \quad \mathbf{C_t}=\begin{pmatrix} 0 & 0 & C_9 & C_{10} & C_{11} & C_{12} \\ 0 & 0 & C_9(L_2+L_7) & C_{10}(L_2+L_7) & C_{11}(L_2+L_7) & C_{12}(L_2+L_7) \\ 0 & 0 & 0 & 0 & 0 & 0 \\ 0 & 0 & C_9L_5 & -C_{10}L_5 & C_{11}L_5 & -C_{12}L_5 \\ C_7 & 0 & 0 & 0 & 0 & 0 \\ 0 & Cs & 0 & 0 & 0 & 0 \\ 0 & 0 & -C_9L_7 & 0 & C_{11}L_7 & 0 \\ 0 & 0 & 0 & -C_{10}L_7 & 0 & C_{12}L_7 \\ 0 & 0 & 0 & 0 & 0 & 0 \\ 0 & 0 & 0 & 0 & 0 & 0 \\ 0 & 0 & 0 & 0 & 0 & 0 \end{pmatrix}$$

$$\mathbf{M}=\begin{pmatrix} M_0 & 0 & 0 & 0 & 0 & 0 & 0 & 0 & 0 & 0 & 0 \\ 0 & I_1 & 0 & 0 & 0 & 0 & 0 & 0 & 0 & 0 & 0 \\ 0 & 0 & I_2 & 0 & 0 & 0 & 0 & 0 & 0 & 0 & 0 \\ 0 & 0 & 0 & I_3 & 0 & 0 & 0 & 0 & 0 & 0 & 0 \\ 0 & 0 & 0 & 0 & M_1 & 0 & 0 & 0 & 0 & 0 & 0 \\ 0 & 0 & 0 & 0 & 0 & M_2 & 0 & 0 & 0 & 0 & 0 \\ 0 & 0 & 0 & 0 & 0 & 0 & I_4 & 0 & 0 & 0 & 0 \\ 0 & 0 & 0 & 0 & 0 & 0 & 0 & I_5 & 0 & 0 & 0 \\ 0 & 0 & 0 & 0 & 0 & 0 & 0 & 0 & M_e & 0 & 0 \\ 0 & 0 & 0 & 0 & 0 & 0 & 0 & 0 & 0 & I_{e1} & 0 \\ 0 & 0 & 0 & 0 & 0 & 0 & 0 & 0 & 0 & 0 & I_{e2} \end{pmatrix} \quad K_t=\begin{pmatrix} 0 & 0 & K_9 & K_{10} & K_{11} & K_{12} \\ 0 & 0 & K_9(L_2+L_7) & K_{10}(L_2+L_7) & K_{11}(L_2+L_7) & K_{12}(L_2+L_7) \\ 0 & 0 & 0 & 0 & 0 & 0 \\ 0 & 0 & K_9L_5 & -K_{10}L_5 & K_{11}L_5 & -K_{12}L_5 \\ K_7 & 0 & 0 & 0 & 0 & 0 \\ 0 & Ks & 0 & 0 & 0 & 0 \\ 0 & 0 & -K_9L_7 & 0 & K_{11}L_7 & 0 \\ 0 & 0 & 0 & -K_{10}L_7 & 0 & K_{12}L_7 \\ 0 & 0 & 0 & 0 & 0 & 0 \\ 0 & 0 & 0 & 0 & 0 & 0 \\ 0 & 0 & 0 & 0 & 0 & 0 \end{pmatrix}$$

The analytic solution can be obtained by putting the experimental parameters into the above equations. Given that road roughness is an important excitation for

根据上述方程组，可带入实车参数进行求解析解。另外路面不平度是设备行驶时最主要的激励，在进行汽车平顺

a moving vehicle, the input model of road excitation with accurate road information must be built before the vehicle riding comfort simulation and performance assessment is conducted. The road excitation is built by employing harmonic superposition as [19]:

性仿真研究和性能评价时，要获得足够准确的路面信息，建立路面激励的输入模型。本文用谐波叠加法建立路面输入模型。分别将每个小区间的正弦波叠加，即可得到用谐波叠加法模拟道路的时域模型，如下所示[19]：

$$q(t)=\sum_{i=1}^{n}\sqrt{2S_q(n_{mid-i})\Delta n_i}\sin(2\pi n_{mid-i}ut+\theta_i) \quad (20)$$

Where, θ_i is an independent random variable distributed uniformly in the range of 0 to 2π, $S_q(n)$ is the power spectral density (PSD) of the road roughness, and the spatial frequency n ranges from n_1 to n_2 (n_1 = 0.011 m^{-1}, n_2 = 2.83 m^{-1}). The spatial frequency n is divided into multiple intervals between n_1 and n_2, and the centre frequency of each interval is expressed as n_{mid-i} (i = 1, 2,…, n).

The random displacement of the road at the front left wheel $q_1(t)$ and that at the front right wheel $q_2(t)$ can be determined by assigning corresponding values to θ_i The random displacements of the road at the rear wheels can be deduced from those of the front wheels according to a time delay as:

式中，θ_i 为[0,2π]上均匀分布的相互独立的随机变量。其中 S_q（n）为路面不平度 PSD，空间频率范围为 n_1< n< n_2(n_1=0.011m^{-1}, n_2=2.83m^{-1})。将 n_1< n< n_2 的空间频率区间划分为 n 个小区间，设 n_{mid-i}(i=1,2,…,n)为每个小区间的中心频率。

在上式中 θ_i取不同值可以得出左前轮和右前轮的路面随机位移输入 q_1（t）、q_2（t），左中后轮和右中后轮可由时间延迟得出：

$$q_3(t)=q_1(t+(L_1+L_2)/u),\ q_5(t)=q_1(t+(L_1+L_2+L_3)/u),$$

$$q_4(t)=q_2(t+(L_1+L_2)/u),\ q_6(t)=q_2(t+(L_1+L_2+L_3)/u),$$

According to the Chinese National Standard GB7031-1986, roads are classified into eight levels based on road roughness. The road condition in the experiment corresponds to the standard level D. Employing harmonic superposition, the excitation of the road roughness on the left and right of the travelling vehicle at a speed of 30 km/h is simulated (see Fig. 2 for the excitation of the front left wheel of the vehicle).

In a test conducted to verify the coupled vibration model, a vehicle travelled along a random road on which two pieces of wood were placed. Figure 3 shows the road roughness excitation when the machinery travelled at 10 km/h on the B grade standard pavement.

国标 GB7031-1986 根据路面不平度系数 $G_q(n_0)$的大小，将路面分为 8 级，试验路面情况一般，应选用较为平整但碎石较多的 D 级路面模型建模。本文用谐波叠加法编写了速度为 30km/h D 级标准路面得到车辆实际行驶过程中左右车辙的路面不平度激励如图 2 所示。

在随机路面的基础上加入两个高度分别为 H_1、H_2 的木块，其宽度分别为 b_1、b_2，间距为 S_1，仿真时车辆以速度 v 均速驶过木块。图 3 为速度为 10km/h，B 级标准路面下得到车辆实际行驶过程中左右车辙的路面不平度激励。

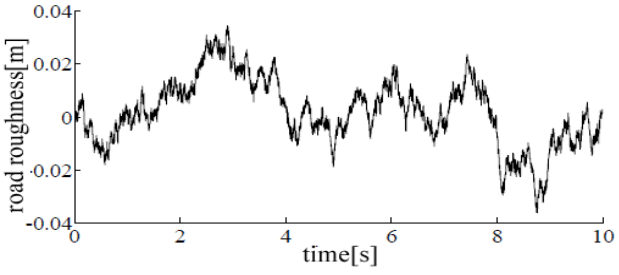

Fig.2- Road excitation of machinery's front left wheel

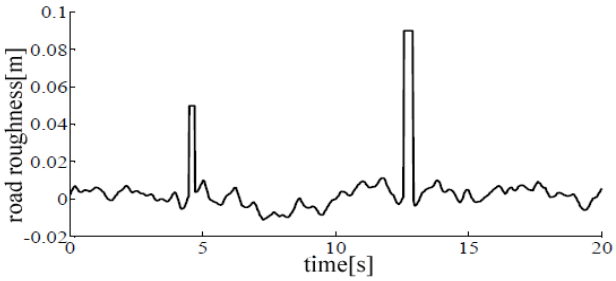

Fig.3- Simulation of road roughness

RESULTS

Simulation results

A simulation of an idling machinery moving at a speed of 30 km/h on a road corresponding to ISO level D was performed. The coupled vibration was simulated by inputting the structural parameters, excitation of random roads, engine excitation and drive-motor excitation into the model established in the previous section. A time-domain plot and the PSD of the vertical vibration of the cab are shown in Figs. 4 and 5

结果

耦合振动仿真分析

将模型各参数数值、路面随机激励、发动机与电机激励理论值代入模型中可得仿真结。这里，以空载情况下速度 30km/h，ISO D 级路面为例进行分析。图 4 表示仿真分析后驾驶室垂向振动加速度时域图，图 5 为驾驶室垂向振

respectively. For comparison, the results obtained when ignoring the excitations of the engine and drive motor are also shown.

The simulation started from a static state. Figure 4 reveals that the maximum acceleration is 2.5 m/s^2 when the excitations of the engine and drive motor are included. After 1 s, a state of stable vibration is reached regardless of whether the excitations of the engine and drive motor are included or not. The maximum acceleration is 0.5 m/s^2 when the excitations of the engine and drive motor vibration are included, whereas it is only 0.4 m/s^2 when the excitations are excluded. The trend is seen more clearly when the result is converted to the frequency domain by Fourier transformation as shown in Fig 5.

动加速度功率谱密度，进行了耦合振动模型仿真，及忽略电动机与发动机振动影响下的仿真。

图 4 仿真是从静止状态开始的，可以看出在考虑发动机和电机振动激励的条件下，最大加速度可以达到 2.5 m/s^2，在 1s 后二者都进入平稳振动阶段，平稳振动阶段耦合振动模型加速度峰值为 0.5 m/s^2 左右，而在忽略发动机和电动机振动的仿真模型结果中，平稳阶段振动加速约为 0.4 m/s^2。为了便于分析，通过傅里叶变换得到频域图如图 5 所示。

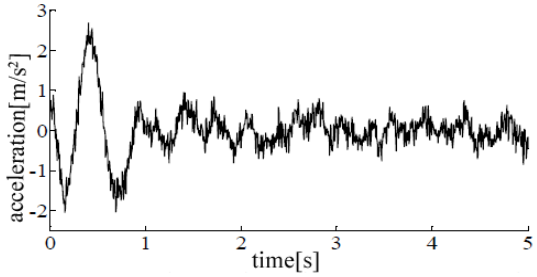

(a) Including the vibration of the engine and drive motor

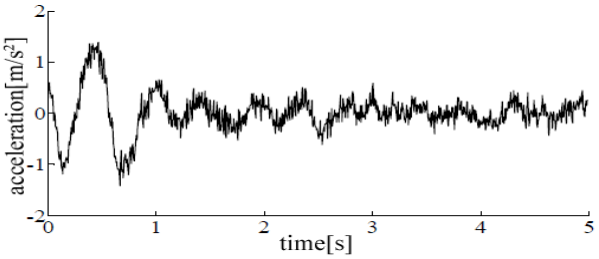

(b). Excluding the vibration of the engine and drive motor

Fig.4 - Vertical acceleration of the cab vibration

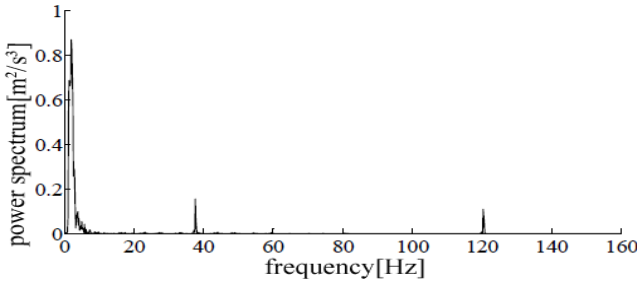

(a) Including the vibration of the engine and drive motor

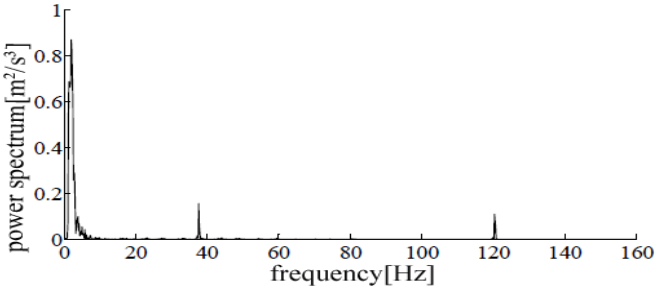

(b) Excluding the vibration of the engine and drive motor

Fig.5 - Vertical acceleration PSD of the cab vibration

The comparison of Fig. 5 (a) and (b) shows that the power at low frequency is affected by the engine and drive motor. The maximum power increases from 0.6 m^2/s^3 to 0.85 m^2/s^3 after the inclusion of the excitations from the engine and drive motor. Additionally, obvious spikes in the power spectrum appear at the frequency of the engine (37.5 Hz) and at the frequency of the drive motor (120 Hz). Significant power increases in the frequency domain analysis cannot be ignored.

Experimental validation

To validate the coupled vibration model, an experiment was conducted using an agricultural vehicle. The machinery was controlled by six-wheel-drive motors independently. Acceleration sensors were placed on fixed surfaces of the cab, the rear frame, the left suspension, the right suspension and a drive motor as shown in Fig. 6. The signals of vibration acceleration were measured using a data capture card. The signals

通过图 5 对比，总体可见耦合振动模型下驾驶低频段功率明显增加，其最大值为 0.85 m^2/s^3，远大于简化模型结果，忽略发动机及电动机振动模型得到的功率谱最大值只为 0.6 m^2/s^3，同时在发动机 37.5Hz 激振力处，电动机两倍供电频率 120Hz 处，在频域分析中存在明显功率，不可忽略。

整车平顺性试验

采用实车进行了实验以验证耦合振动模型，该车辆是由 6 个轮边驱动电机独立驱动。加速度传感器被安置在驾驶室的固定表面上，后车架以及前后悬架，如图 6 所示。通过采集卡采集传感器安装位置的振动加速度信号，通过 CAN 总线采集发动机以及电机转速信号，其中电机上方

of the engine and drive motor speeds were collected using a controller area network (CAN) bus device. Acceleration signals of motor vibration at low frequency were filtered to remove the vibration excitation of the road. The sampling frequency of each sensor was 2560 Hz, which was appropriate for signal analysis.

振动加速度数据需要进行滤波去掉低频段路面的振动激励。每个传感器的采样频率为适合数据分析的 2560Hz。

Fig.6 - Sensors placed on the vehicle

The experiment was conducted on a fine-gravel road corresponding to ISO level D. The vehicle was driven at an even speed of 30 km/h with relative error less than ±5%. The mean value was calculated for three repetitions of the experiment. The vertical vibration acceleration of the cab at the stage of stable running is shown in Fig. 7. Figure 8 presents the vertical vibration PSD after fast Fourier transformation. Fig 9 clearly shows the PSD of the drive motor at high frequency by focusing on the data range of 0–0.2 m^2/s^3.

设备的实验在相当于 ISO D 级的细砂石路面上进行，以 30km/h 速度匀速行驶，车速变化不大于±5%，且同一工况条件下的试验重复三次，结果取其平均值。平稳运行阶段实测驾驶室垂向振动加速度如图 7。经 FFT 变换后为图 8，即驾驶室垂向振动加速度功率谱密度，为了清晰展示高频段的电动机功率谱可截取 0~0.2 m^2/s^3 段功率谱进行分析，得到图 9。

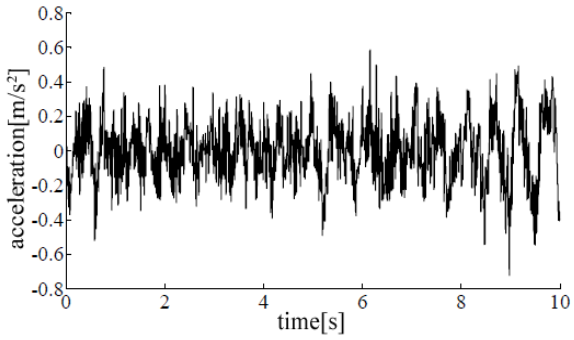

Fig.7 - Measured vertical vibration acceleration of the cab

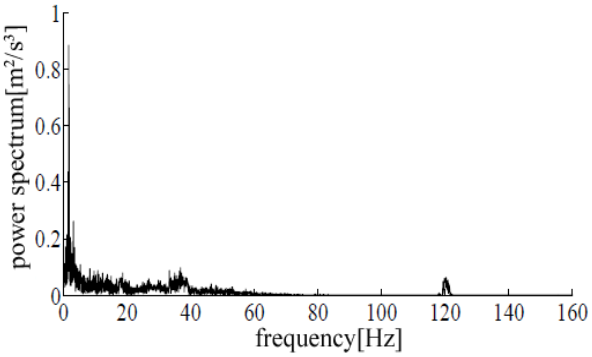

Fig.8 - PSD of the vertical vibration acceleration of the cab

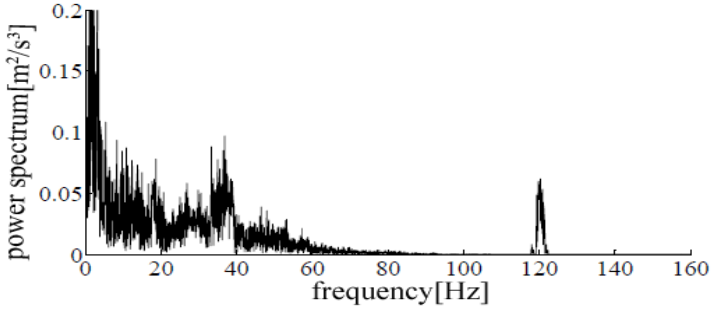

Fig.9 - PSD of the vertical vibration acceleration of the cab within 0–0.2 m^2/s^3

Comparison of the acceleration time-domain curves and PSD curves of the cab obtained in the experiment with the simulation results reveals that the coupled vibration model and experimental results are basically consistent. The power spectrum obtained in the experiment mainly ranged from 1 Hz to 20 Hz and had a peak value of 0.85 m^2/s^3 at 2 Hz. Additional peaks at the excitation position of the engine and drive motor were found in both simulation and experiment. Figure 9 shows that the PSD had a second peak of 0.06 m^2/s^3 near the excitation frequency of the drive motor, 120 Hz. Another obvious peak value of 0.09 m^2/s^3 was recorded at a frequency of approximately 37 Hz. The result obtained excluding the vibrations of the engine and drive motors showed a peak value of only 0.6 m^2/s^3, which was obviously lower than the value when these two vibrations were included. The good match of simulation and experimental results shows that the multisystem coupled vibration model including the excitations of the engine and drive motors can be used to simulate the vibrations and riding comfort of the cab.

We next consider the vehicle running at a speed of 10 km/h over two blocks with heights of 0.06 m and 0.09 m and spaced 10 m. Table 1 provides the root mean square of the vibration acceleration in both simulation and experiment.

将试验得出驾驶室的振动加速度时域曲线以及功率谱密度曲线与三维整车模型得出仿真结果作比较，耦合振动模型与实测模型加速度功率谱基本一致，主要出现在低频段 1-20hz 以内，在 2Hz 左右出现约为 0.85 m^2/s^3 的峰值，在发动机和电动机激振频率处都有明显峰值。图 9 表明在高频段电动机激励力频率 120 Hz 附近驾驶室出现第二个峰值，驾驶室峰值大小为 0.06 m^2/s^3，在 37Hz 左右还有一个明显峰值，大小为 0.09 m^2/s^3。而忽略了电动机和发动机的模型结果，在低频段整体峰值较低，最高值只有 0.6 m^2/s^3，且在别处再无明显峰值出现。仿真和实验结果基本保持一致表明包括发动机和驱动电机激励的多系统耦合振动模型可用于模拟驾驶室的振动和行驶舒适性。

接下来考虑车辆以 10km/h 通过在两个高为 0.06m 和 0.09m 木块的情况。表一给出了在仿真和实验时振动加速度的均方根。

Table 1

Root mean square of vibration acceleration under pulse excitation (m/s)

Measuring point	Test value	Simulation value
Cab	0.2801	0.2967
Upper fulcrum of the left suspension	0.3124	0.3019
Rear frame	0.4933	0.5123
Upper fulcrum of the left motor	0.7123	0.7506

The acceleration results obtained under the impulse excitation are similar to those obtained for the random road. The experimental acceleration (Fig. 11) differs from the simulation acceleration (Fig. 10) by only less than 10%, and the trends of the acceleration are consistent between simulation and experiment.

在脉冲激励下获得的加速度结果与在随机路面上获得的结果类似。实验加速度（图 11）略小于仿真加速度（图 10），但不超过 10%。实验和仿真加速度的变化趋势是一致的。

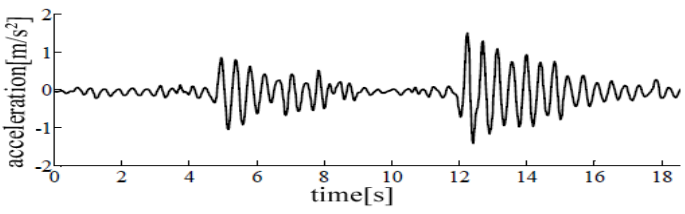

Fig.10 - Vibration acceleration in simulation

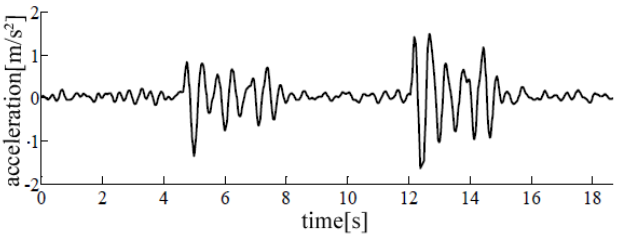

Fig.11 - Vibration acceleration in experiment

Fig 10 and Fig 11 reveal obvious fluctuations in acceleration near 4.5 s. The instantaneous acceleration reached 0.93 m/s^2 and 1.29 m/s^2 in the experiment and simulation, respectively. Then, under the effect of suspension damping, the acceleration began to attenuate. At 12 s, a second obvious fluctuation occurred, with the instantaneous acceleration reaching 1.41 m/s^2 in the experiment and 2.06 m/s^2 in the simulation. The acceleration then gradually decayed.

由图 10 和图 11 可以看出仿真与试验的加速度值均在 4.3s 附近第一次发生明显波动，试验瞬时加速度大小达到 0.93m/s^2，仿真瞬时加速度大小达到 1.29m/s^2，之后在悬架阻尼的作用下开始衰减，在 11s 时仿真与试验的加速度值出现第二次明显波动之后，试验瞬时加速度大小达到 1.41m/s^2，仿真瞬时加速度大小达到 2.06m/s^2，之后逐渐衰减并恢复正常。

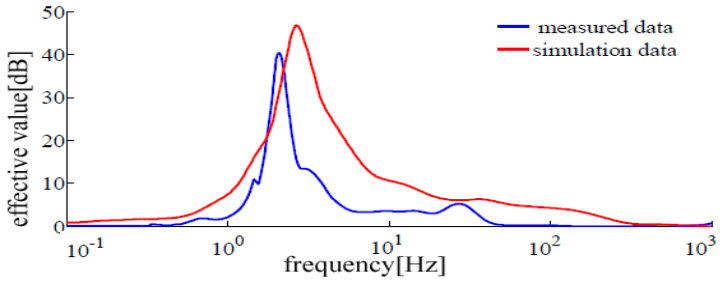

Fig.12 - Power spectrum of the vibration acceleration of the cab

Figure 12 shows the power spectra of the vibration acceleration of the cab in the experiment and simulation. The peak value is 40.26 dB at 1.75 Hz in the experiment and 46.1 dB at 1.98 Hz in the simulation, showing good agreement. Both power spectra are concentrated at low frequency within 1-5 Hz. Owing to the differences between the model and the real machinery, the acceleration of cab vibration is higher in the simulation than in the experiment, but the acceleration fluctuation time and trend of acceleration are roughly the same. The same results are observed in the frequency domain as in the time domain, further verifying the accuracy of the single-point contact model of a machinery.

CONCLUSION

A model was constructed to analyze the vibration response of a distributed electric-drive agricultural vehicle considering coupled excitations of the road roughness, engine and drive motors. The conclusions are shown as follows:

(1) The experiment result shows that the 11-DOF vibration model built in consideration of the coupled excitations of the road can accurately describe the vibration characteristics of the distributed electric-drive agricultural vehicle.

(2) The excitation forces of the engine and drive motors increased the PSD of the vehicle acceleration, and obvious PSD peaks registered at the excitation frequency. Therefore, the excitation forces of the road roughness, drive motors and engine must all be considered to ensure the riding comfort and reliability of the distributed electric-drive agricultural vehicle.

Compared with the research on a passenger vehicle, that on the riding comfort of agricultural vehicle has obvious differences. Air suspension with variable stiffness can improve riding comfort and has a good application prospect in the field of agricultural vehicle.

ACKNOWLEDGEMENT

This study was supported by the National High Technology Research Program (2011AA060404).

REFERENCES

[1]. Ackermann, J Robust. (1993) –*Yaw damping of cars with front and rear wheel steering,* Transactions on Control Systems Technology, vol.1, no.1, pp.15-20;

[2]. Gao Yanlei, Zhou Yanpei, Sun Xiaoning. (2014) –*Engine Vibration Certification*, Procedia Engineering, vol.80, pp.1-9;

[3]. Gu Yu, Li Shaoxiong, Li Rui, Li Qiang. (2013) –*The numerical simulation and finite-element analysis of the motor vibration problem based on the base anchor softening layer, Advanced Materials Research*, vol.815, pp.860-867;

图 12 表示仿真和实验所得驾驶室振动加速度的功率谱密度。两种功率谱都集中在 1-5Hz 的低频范围内，实验加速度功率谱密度在 1.75Hz 出现最大值 40.26dB，仿真加速度功率谱密度在 1.98Hz 出现最大值 46.1dB，仿真数据与实验数据基本保持一致。由于所建模型与实车之间的差异，仿真的加速度值要高于比实验得到的加速度值，但是其波动时间和趋势基本一致。频域和时域分析得到了相同的结果，进一步验证了车辆单点接触模型的准确性。

结论

论文提出了考虑路面不平度和电动机、发动机耦合激振来分析实车系统振动响应的方法。分析了考虑耦合激振后系统响应的差别，主要结论如下：

(1)所建立电机激振力、发动机振动及路面激励的十一自由度整机三维振动系统模型经实车试验验证结果表明，该模型能够准确的反应分布式农用汽车的振动特性。

(2)电动机和发动机振动激励力会整体增大整机加速度功率谱，在激励力频率处会出现明显峰值，不可忽略。为提高电动车辆的平顺性及可靠性，需兼顾电机激振力和路面激励，耦合激励模型对农用机械的悬架及整车平顺性设计有指导意义。

农用机械的行驶平顺性研究与乘用车相比具有一定的差距，采用可变刚度的空气弹簧可提高整机的平顺性，是论文下一步研究的方向。

致谢

国家高技术研究发展计划(2011AA060404)。

参考文献

[1]. Ackermann, J Robust. (1993) –*前后轮转向时的侧偏阻力研究*. 控制系统技术学报, 第1卷, 第1期, 15-20;

[2]. 高艳蕾, 周艳培, 孙晓宁. (2014) –*发动机振动检测*, 能源工程, 第 80 卷, 1-9;

[3]. 谷雨, 李少雄, 李锐, 李强. (2013) –*基于基础垫软化层的电机垂向振动问题的数值模型和有限元分析*, 先进材料研究, 第815期, 860-867;

[4]. Hu Baoyang, Zhang Qiang, Li Qiangqiang.(2013) –*Analysis of Coach Vibration Based on Engine Excitation*. Agricultural Equipment and Vehicle Engineering. vol.51, no.4, pp30-34,
[5]. Liu Weixin. (2001) –*The Automobile Design*. Beijing: Tsinghua University Press;
[6]. Li Chaofeng, Wang Degang. (2009) –*Study and Application of 11-DOF Nonlinear Riding comfort Model for Vehicle.* Journal of Northeastern University, vol.30, no.6, pp.857-861;
[7]. M Canale, L Fagiano, M Milanese. (2007) –*Robust vehicle yaw control using an active differential and IMC techniques*. Control Engineering Practice, vol.21, no.15, pp.923-941;
[8]. Meng Fanwei, Liu Chengying, Li Zhijun, Wang Liping. (2013) –Linear motor vib*ration suppression using current oversampling, Qinghua Daxue Xuebao, vol.53, no.3, pp.307-312;*
[9]. Perez, Pinal F, CervantesI, Emadi A. (2009) –*Stability of an Electric Differential for Traction Applications*, IEEE Transactions on Vehicular Technology, vol.58, no.7, pp.76-82;
[10]. Paulo Cezar, Jorge Nei Brito. (2013) –*Detection of Electrical Faults in Induction Motors Using Vibration Analysis*, Journal of Quality in Maintenance Engineering, vol.194, pp.85-92;
[11]. Song Jianqing. (2014) –*The Technology of Driving AC Servo Motor Based on FPGA, Shang Dong University,*
[12]. Tan Di. (2013) –*Dynamics and Structure Optimi-zation of the In-wheel Motor System with Rubber Bushing*. South China University of Technology;
[13]. Umesh Kumar Rout, Rabindra Kumar Sahu, Sidhartha Panda. (2013) –*Design and Analysis of Differential Evolution Algorithm Based Automatic Generation Control for Interconnected Power Sys-tem,* Electric Engineering, vol.13, no.4, pp.409-421;
[14]. Wang Junnian, Wang Qingnian, Song Chuanxue. (2010) –*Co-simulation and Test of Differential Drive Assist Steering Control System for Four-wheel Electric Vehicle*. Transaction of the Chinese Society for Agricultural Machinery, vol.1, no.6, pp.8-13;
[15]. Wang Dengfeng, Li Wei, Chen Shuming. (2011) –*Transfer Path Analysis of Power Train Vibration on Vehicle Riding comfort,* Journal of Jilin University(Engineering and Technology Edition), vol.41, no.2, pp.92-98;
[16]. Wellman Thomas, Govindswamy Kiran. (2007) –*Aspects of driveline integration for optimized vehicle NVH characteristics,* SAE Technical Paper Series;
[17]. Yu Houyu, Huang Miaohua. (2011) –*Experimental Research of Electronic Differential Control for In-wheel Motor Drive Electric Vehicle*, Journal of Wuhan University of Technology, vol.33, no.5, pp.148-151;
[18]. Zhang Guangrong, Yu Dejie. (2010) –*Study on Automotive Interior Structural Noise Excited by Engine,* Vibration and Noise Control, vol.1 No.1, pp45-47,
[19]. Zhang Daisheng, Li Wei. (2002) –*Simulation for Slip Ratio of An Automobile Antilock-braking System Based on Fuzzy Logic Control Method*, Transaction of the Chinese Society for Agricultural Machinery, vol.33, no.2, pp.29-31,

[4]. **胡宝洋，张强，李锵强**.(2013)-***基于发动机激励的客车振动分析***. **农业装备与车辆工程**.**第**51**卷**, **第**4**期**，30-34,
[5]. 刘惟信. (2001) –*汽车设计*. 北京: 清华大学出版社;
[6]. 李朝峰, 王得刚. (2009) –*11自由度非线性车辆平顺性模型的研究及应用*, 东北大学学报(自然科学版), 第06期, 857-860;
[7]. M Canale, L Fagiano, M Milanese. (2007) –*基于主动差速器和IMC技术的车身横摆控制*, 控制工程实践, 第21卷, 第15期, 923-941;
[8]. 孟凡伟, 刘成英, 李志军, 王丽萍. (2013) –*电流采样法对线性电机振动抑制*, 清华大学学报, 第53卷, 第3期, 307-312;
[9]. Perez, Pinal F, Cervantes I, Emadi A. (2009) –*电子差速器牵引稳定性研究*. IEEE车辆技术学报, 第58卷, 第7期, 76-82;
[10]. Paulo Cezar, Jorge Nei Brito. (2013) –*应用垂向振动分析感应电机的电气故障*, 质量维修工程日报, 第194期, 85-92;
[11]. 宋建庆.（2014）–*基于FPGA的交流伺服电机驱动技术*. 山东大学,
[12]. 谭迪. (2013) –*内置悬置的轮毂电机驱动系统动力学特性及结构优化*. 华南理工大学;
[13]. Umesh Kumar Rout, Rabindra Kumar Sahu, Sidhartha Panda. (2013) –*用于互联电力系统自动发电控制的差分进化算法的设计与分析*, 电子工程, 第4期, 409-421;
[14]. 王军年, 王庆年, 宋传学. (2010) –*四轮驱动电动汽车差动助力转向系统联合仿真与试验*, 农业机械学报, 第41卷, 第6期, 8-13;
[15]. 王登峰, 李未, 陈书明. (2011) –*动力总成振动对整车行驶平顺性的传递路径分析*, 吉林大学学报(工学版), 第S2期, 92-97;
[16]. Wellman Thomas, Govindswamy Kiran. (2007) –*基于 NVH 特性的车辆传动系统的集成优化*, SAE 技术论文系列;
[17]. 喻厚宇, 黄妙华. (2011) –*电动轮车电子差速控制的试验研究*, 武汉理工大学学报, 第33卷, 第5期, 148-151;
[18]. 张光荣,于德介.(2010) –*发动机激励引起的车内结构噪声研究*, 噪声与振动控制, 第1卷, 第1期, 45-47,
[19]. 张代胜, 李伟. (2002) –*基于滑移率的汽车防抱模糊控制方法与仿真*, 农业机械学报, 第 33 卷, 第 2 期, 29-31.

A COMPARISON BETWEEN DIESEL AND FUEL OBTAINED FROM RECICLED WASTE PLASTICS USED FOR FUELED DIESEL ENGINES
/
COMPARAREA MOTORINEI CU COMBUSTIBILI OBŢINUŢI DIN MASE PLASTICE RECICLATE UTILIZABILI LA ALIMENTAREA MOTOARELOR DIESEL

Assist. Ph.D. Eng. Popescu G.L.[1)], Prof. Ph.D. Eng. Filip N.[1)], Prof. Ph.D. Eng. Popescu V.[2)]
[1)] Technical University of Cluj Napoca, Faculty of Mechanical Engineering / Romania
[2)] Technical University of Cluj Napoca, Faculty of Materials and Environmental Engineering / Romania
Tel: 0743174196; E-mail: george.popescu@chem.utcluj.ro; georgepopescu60@gmail.com

Abstract: *The paper presents the possibility of obtaining some fuels resulted from plastic materials waste recycling, the determination of some physicochemical properties of these fuels and a comparison of the obtained results with those specific to commercial diesel fuels. This concept of recycling is a priority in countries with an important technological breakthrough and having at the same time major concerns related to environment protection. If processing is rigorously controlled by the pyrolysis of plastic polymeric materials [1, 2, 3, 4, 9, 10, 11, 12], following the thermal degradation reaction one can obtain at the final:*

- *a gaseous blend which contains saturated and unsaturated hydrocarbons;*
- *a liquid that contains a mixture of saturated and unsaturated hydrocarbons;*
- *a solid residue that contains mainly carbon;*
- *the liquid phase having properties close to the diesel fuel, that can be used as fuel for Diesel engines.*

Keywords: *plastic materials, fuels, properties, viscosity, calorific power, diesel engine.*

INTRODUCTION

Low density polyethylene (LDPE) waste is heated at temperatures of about 500^{o}C in a pyrolysis installation [1, 2, 3, 4]. According to specialty literature, thermal degradation of polyethylene takes place in two stages, namely after the first one viscous products are obtained (C_5 C_{43}, ~87% weight percent), while following the second one liquid hydrocarbons are formed (~74% weight percent) [1, 2, 9, 10, 12].

Figure 1 presents the experiments diagram followed in order to obtain the fuel from LDPE, data acquisition regarding those processes and both the analysis of experimental data and of the resulted products, including their characterization [5, 6, 7, 8].

A superior recovery of plastic materials wastes, such as the production of fuels resembling diesel fuel has an important role in natural resources conservation [11].

MATERIAL AND METHOD

The experimental stand and the description of laboratory equipment used for fuel obtaining

A pyrolysis installation has been performed on a laboratory stand using a heating mantle Raypa X-250 with thermosetting stage system, with a maximum temperature heating stage of 450^{o}C (fig. 2).

In order to determine with the best accuracy the conversion yield of solid LDPE in liquid phase, the parts used for installation have been weighted previously with a KERN EMB 200-3 weighting scale with a resolution of 1 mg and an analytical balance Precisa XT-220A with resolution of 0.1 mg. The temperature control during pyrolysis process has been made using a digital thermometer HI-95350 with a resolution of 0.1^{0}C.

Rezumat: *Lucrarea prezintă posibilitatea obţinerii unor combustibili rezultaţi din reciclarea deşeurilor de mase plastice, determinarea unor proprietăţi fizico-chimice ale acestora şi compararea rezultatelor obţinute cu cele specifice motorinei comerciale. Acest concept de reciclare este o prioritate în unele ţări cu un avans tehnologic important şi care au în acelaşi timp preocupări majore legate de protecţia mediului. Dacă procesarea prin metoda pirolizei a materialelor plastice polimerice este atent controlată [1, 2, 3, 4, 9, 10, 11, 12], în urma reacţiilor de degradare termică se obţine în final:*

- *un amestec gazos care conţine hidrocarburi saturate şi nesaturate;*
- *un lichid care conţine un amestec de hidrocarburi saturate, nesaturate şi aromatice;*
- *un reziduu solid care conţine în principal carbon;*
- *faza lichidă având proprietăţi apropiate motorinelor, ea putând fi utilizată ca şi combustibil la alimentarea motoarelor Diesel.*

Cuvinte cheie: *mase plastice, combustibili, proprietăţi, viscozitate, putere calorifică, motor diesel.*

INTRODUCERE

Deşeurile de polietilenă de joasă densitate (LDPE) sunt încălzite la temperaturi de cca. 500ºC într-o instalaţie de piroliză [1, 2, 3, 4]. Conform literaturii de specialitate, degradarea termică a polietilenei are loc în două etape, după prima etapă se obţin produşi viscoşi (C_5 C_{43}, ~87% procente de masă), iar după a doua rezultă hidrocarburi lichide (~74% procente de masă) [1, 2, 9, 10, 12].

În figura 1 este prezentată diagrama experimentelor desfăşurate pentru obţinerea combustibilului din LDPE, achiziţionarea datelor legate de aceste procese şi analiza atât a datelor experimentale cât şi a produşilor rezultaţi, incluzând aici şi caracterizarea acestora [5, 6, 7, 8].

O valorificare superioară a deşeurilor de mase plastice, cum ar fi producerea de combustibili asemănători motorinelor, are un rol important în conservarea resurselor naturale [11].

MATERIAL ŞI METODĂ

Standul experimental şi descrierea echipamentelor de laborator utilizate la obţinerea combustibilului

Pe un stand de laborator s-a realizat o instalaţie de piroliză încălzită electric cu ajutorul unui cuib de încălzire Raypa X-250 cu termostatare în trepte, cu o temperatură maximă de încălzire de 450^{o}C (fig. 2).

În vederea determinării cât mai corecte a randamentului de conversie din LDPE solidă în fază lichidă, componentele utilizate la alcătuirea instalaţiei au fost cântărite în prealabil cu ajutorul unui cântar KERN EMB 200-3 cu rezoluţia de 1 mg şi o balanţă analitică Precisa XT-220A având o rezoluţie de 0,1 mg. Controlul temperaturii în procesul de piroliză s-a făcut utilizând un termometru digital HI-95350 cu o rezoluţie de 0,1^{0}C.

For cooling and controlling temperature from condensation area, a recirculation thermostatic bath model DC-1006 with the temperature range between -10°C....95°C and a resolution of 0.05°C, will be used. As cooling agent it was used antifreeze with the recommended concentration for -20°C.

Pentru răcirea şi controlul temperaturii din zona de condensare s-a utilizat o baie de apă termostatată cu recirculare model DC-1006 cu domeniul de păstrare al temperaturii între -10°C....95°C şi cu o rezoluţie de 0,05°C. Ca agent de răcire s-a folosit lichid antigel cu concentraţia recomandată pentru -20°C.

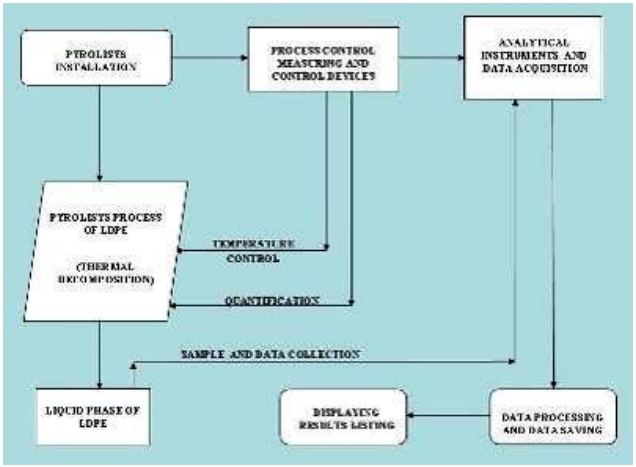

Fig. 1 - Pyrolysis process diagram, its control, data acquisition and data processing

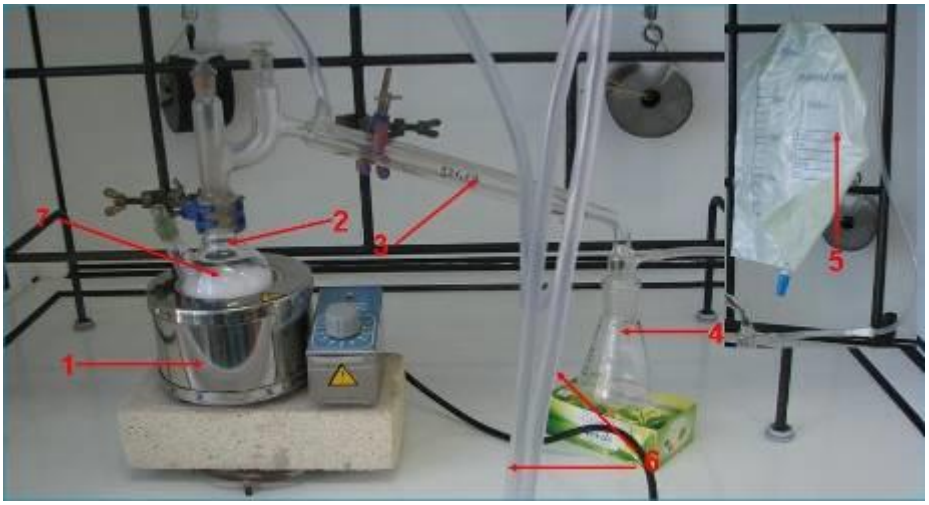

Fig. 2 - The electrically heated pyrolysis installation used [6]
1. Heating mantle; 2. Pyrolysis Flask; 3. Condenser; 4. Erlenmeyer flask; 5. Pyrolysis gas recovery bag; 6. Hose coolant; 7. Polyethylene waste

In the first stage the conversion yield of solid LDPE into liquid phase, residues and gases was calculated. The following are the initial values of the masses obtained by weighing the pyrolysis installation components and LDPE granules on which the yield was determined after conversion to the different phases of pyrolysis products [6].

- condenser initial weight G_{ic} = 221.8 g
- Erlenmeyer glass initial weight G_{ie} = 122.6 g
- pyrolysis flask initial weight G_{if} = 122.8 g
- LDPE granules weight G_{LDPE} = 100.015 g

The weighting made at the final stage of pyrolysis process conducted to the following values:

- condenser final weight G_{fc} = 222.3 g
- Erlenmeyer glass final weight G_{fe} = 211.9 g
- pyrolysis flask final weight G_{ff} = 127.4 g

Making the difference between the final weights and the initial ones and knowing at the same time the weight of LDPE subjected to pyrolysis we will obtain the final conversion yield in liquid phase, by relation (1),

În prima fază s-a calculat randamentul de conversie din fază solidă a granulelor de LDPE în fază lichidă, reziduuri solide şi gaz. In continuare sunt prezentate valorile iniţiale ale maselor obţinute prin cântărirea componentelor instalaţiei de piroliză şi a granulelor de LDPE pe baza cărora s-a determinat ulterior randamentul de conversie pentru diferitele faze ale produşilor de piroliză [6].

- masa iniţială refrigerent G_{ir} = 221,8 g
- masa iniţială pahar Erlenmeyer G_{ie} = 122,6 g
- masa iniţială balon piroliză G_{ib} = 122,8 g
- masa granule LDPE G_{LDPE} = 100,015 g

Cântărirea făcută la finalul procesului de piroliză ne dă următoarele valori:

- masa finală refrigerent G_{fr} = 222,3 g
- masa finală pahar Erlenmeyer G_{fe} = 211,9 g
- masa finală balon de piroliză G_{fb} = 127,4 g

Făcând diferenţele dintre masele finale şi cele iniţiale, cunoscând totodată masa de LDPE supusă procesului de piroliză vom obţine în final randamentul de conversie în fază lichidă, cu relaţia (1),

Where:

Unde:

$G_{fr} - G_{ir} = 0.5$ g

$G_{fe} - G_{ie} = 89.3$ g

$$\eta_{liquid} = \left[\frac{[(G_{fc} - G_{ic}) + (G_{fe} - G_{ie})]}{G_{LDPE}}\right] * 100 \quad [\%] \qquad (1)$$

it results the yield of conversion in liquid phase:

$\eta_{liquid} = 89.787$ [%]

Applying the mass conservation law, based on the data presented previously taking into account the solid weight the conversion yield in solid residue and gaseous phase has been also determined.

For solid residue we use relation (2):

Where:

de unde rezultă randamentul de conversie în fază lichidă:

$\eta_{lichid} = 89,787$ [%]

Aplicând legea conservării masei, însumând la cele enumerate anterior şi masa reziduurilor solide am determinat randamentul de conversie în reziduu solid şi în fază gazoasă.

Pentru reziduul solid folosim relaţia (2):

Unde:

$G_{ff} - G_{if} = 4,6$ g

$$\eta_{res} = \frac{G_{ff} - G_{if}}{G_{LDPE}} * 100 \quad [\%] \qquad (2)$$

$\eta_{res} = 4,599$ [%]

The quantity of gas was determined by relation (3), making the difference between the quantity of LDPE introduced into the pyrolysis installation and the sum of the liquid and solid residue resulted from the process.

Cantitatea de gaz se determină cu relaţia (3), făcând diferenţa dintre cantitatea de LDPE introdusă în instalaţia de piroliză şi suma cantităţilor de lichid şi reziduu solid rezultate în proces.

$$\eta_{gas} = \left[\frac{[(G_{fc} - G_{ic}) + (G_{fe} - G_{ie}) + (G_{ff} - G_{if})]}{G_{LDPE}}\right] * 100 \ [\%] \qquad (3)$$

$\eta_{gas} = 5.614$ [%]

Based on the measurements and the calculus performed it resulted a superior conversion yield in liquid phase of LDPE, comparing to the one found in the literature [5, 6], the most probable cause being the low temperature maintained into the condensation installation.

Pe baza măsurătorilor făcute şi a calculelor efectuate a rezultat un randament superior la conversia în fază lichidă a LDPE, faţă de cel găsit în literatura de specialitate [5, 6], cauza cea mai probabilă fiind menţinerea zonei de condensare a instalaţiei la temperaturi mai coborâte.

RESULTS

The determination of the density and the calculation of the relative density of the obtained fuel

The volume V occupied by the liquid phase measured with a measuring cylinder at ambient temperature t_a = 27.6°C was of 114 ml, and in this case the density of liquid phase has been calculated with relation (4):

REZULTATE

Determinarea densităţii şi calculul densităţii relative a combustibilului obţinut

Volumul V ocupat de faza lichidă măsurat cu cilindrul gradat la temperatura ambientală t_a = 27,6 °C a fost de 114 ml, în acest caz densitatea fazei lichide a fost calculată cu relaţia (4):

$$\rho = \frac{[(G_{fc} - G_{ic}) + (G_{fe} - G_{ie})]}{V} \ [kg/m^3] \qquad (4)$$

$\rho = 783.33$ [kg/mc] or else $\rho_4^t = 0.78333$ [kg/l]

Because the temperature at which the determination has been made is higher than 20°C it has been calculated the relative density of liquid phase obtained from LDPE by pyrolysis with relation (5).

Deoarece temperatura la care s-a făcut determinarea pentru calculul densităţii este mai mare de 20°C s-a calculat densitatea relativă a fazei lichide obţinute din LDPE prin piroliză cu relaţia (5).

$$\rho_4^{15} = \rho_4^t + c(t - 15) \qquad (5)$$

Where:

ρ_4^t - represents the relative density at the temperature of the measurement;

t – is the working temperature;

c – is the correction coefficient

$$\rho_4^{15} = 0,7933$$

în care:

ρ_4^t - reprezintă densitatea relativă la temperatura la care s-a efectuat determinarea;

t - este temperatura de lucru;

c - este coeficientul de corecţie a temperaturii

$$\rho_4^{15} = 0,7933$$

Comparing the density obtained in this way with the density presented in table 1, we were able to estimate that the density of liquid phase obtained from LDPE by pyrolysis is situated between the density of gasoline and diesel fuels.

Comparând densitatea obţinută prin metoda de calcul arătată anterior, cu densităţile prezentate în tabelul 1 am putut estima că densitatea fazei lichide obţinute din LDPE prin piroliză se încadrează între densitatea benzinelor şi a motorinelor.

Table 1

The relative density values of some fuels.

Fuel	The relative density [kg/l]
Gasoline	0.682 – 0.767
Diesel	0.820 – 0.910

Experimental determination of density and viscosity

For experimental determination of the density and viscosity we used the SVM viscometer, an apparatus that measures the dynamic and kinematic viscosity of fuels and oils respectively, and the results are provided as tables.

The determinations were made in the same conditions for diesel fuel as for the liquid pyrolysis product from LDPE, namely atmosphere pressure of $P_a = 9.74 \cdot 10^4$ [Pa] and environment temperature of $t_{ma} = 27,6^oC$.

The results obtained following the measurements for dynamic and kinematic viscosity for diesel fuel and the fuels from LDPE are presented in figure 3 and 4. The variation of the density of the studied fuels depending on temperature, including the density calculated for 15°C for the obtained fuel by LDPE pyrolysis is presented in figure 5.

Determinarea experimentală a densităţii şi viscozităţii

Pentru determinarea experimentală a densităţii şi viscozităţii s-a folosit viscozimetrul SVM 3000, aparatul măsoară viscozitatea dinamică şi densitatea combustibililor, respectiv a uleiurilor, iar rezultatele le redă tabelar.

Determinările s-au efectuat în aceleaşi condiţii pentru motorină şi faza lichidă a produsului obţinut prin piroliză din LDPE, adică presiunea atmosferică de $P_a = 9,74 \cdot 10^4$ [Pa] şi temperatura mediului ambiant $t_{ma} = 27,6^oC$.

Rezultatele obţinute în urma măsurătorilor pentru viscozităţile dinamice şi cinematice ale motorinei şi combustibilului din LDPE sunt prezentate în figurile 3 şi 4. Variaţia densităţii combustibililor studiaţi în funcţie de temperatură, inclusiv a densităţii calculate la 15°C pentru combustibilul obţinut prin piroliză din LDPE, este redată în figura 5.

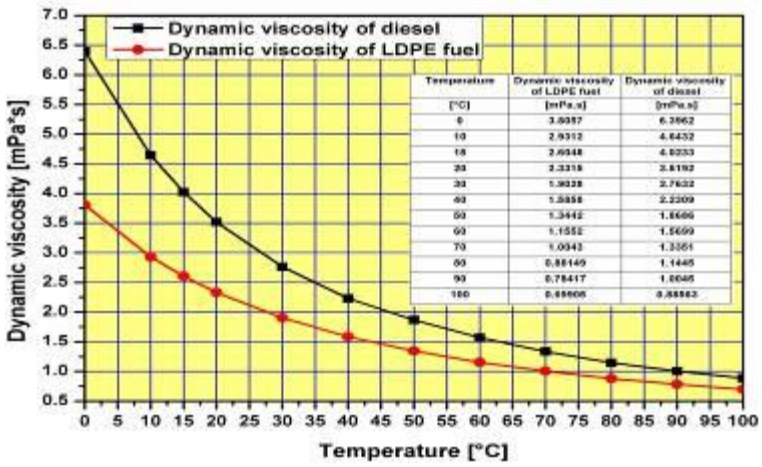

Fig. 3 - Variation of dynamic viscosity of fuels analyzed by temperature [6].

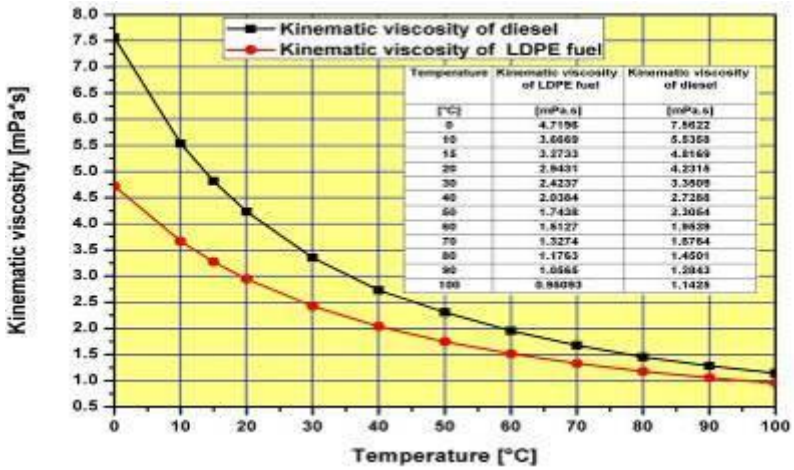

Fig. 4 - Variation of kinematic viscosity of fuels analyzed by temperature [6].

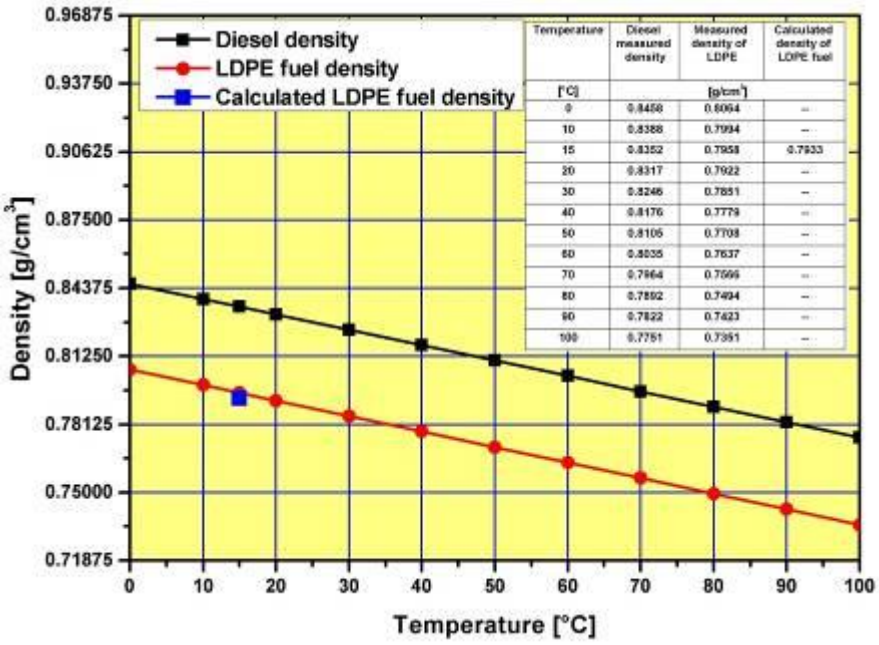

Temperature	Diesel measured density	Measured density of LDPE	Calculated density of LDPE fuel
[°C]	[g/cm³]		
0	0.8458	0.8064	--
10	0.8388	0.7934	--
15	0.8352	0.7958	0.7933
20	0.8317	0.7922	--
30	0.8246	0.7851	--
40	0.8176	0.7779	--
50	0.8105	0.7708	--
60	0.8035	0.7637	--
70	0.7964	0.7566	--
80	0.7892	0.7494	--
90	0.7822	0.7423	--
100	0.7751	0.7351	--

Fig. 5 - Fuel density variation analyzed by temperature [6]

Experimental determination of the flash point (Penski-Martens)

For the determination of this parameter it was used Automated Pensky Martens Closed Cup Flash Point Analyzer HFP 339. The determination was made according to ISO 2719A norms. If during the measurements the atmospheric pressure differs from101.3 kPa (760 mmHg), it is necessary a correction of the determined values with the relation (6):

Determinarea experimentală a temperaturii de inflamabilitate (Pensky-Martens)

Pentru determinarea acestei mărimi s-a utilizat analizorul cu creuzet închis HFP 339, aparatul funcţionând după metoda Persky-Martens. Determinarea s-a făcut conform normelor ISO 2719A. Dacă pe durata efectuării determinărilor presiunea atmosferică este diferită de 101,3 kPa (760 mmHg), este necesară corectarea valorii determinate cu relaţia (6):

$$T_{inf} = T_{inf\ mas} + 0{,}25 \cdot (101{,}3 - p_{atm}) \quad (6)$$

where:

$\mathbf{T}_{inf\ mas}$ is the measured inflammability temperature, in Celsius degrees.

$\mathbf{p}_{atm}$ is the atmospheric pressure, expressed in kPa.

After the recalculation of the flash point in this way, the resulted values will be rounded by 0.5 ^{o}C.

Table 2 presents the data resulted following the measurements and data correction.

unde:

$\mathbf{T}_{inf\ mas}$ este temperatura de inflamabilitate măsurată, în grade Celsius;

$\mathbf{p}_{atm}$ este presiunea atmosferică exprimată în kPa.

După recalcularea în acest mod a temperaturii de inflamabilitate, valorile rezultate se vor rotunji cu o precizie de 0,5 ^{o}C.

În tabelul 2 sunt prezentate datele rezultate în urma măsurătorilor şi datele corectate.

Table 2

The values obtained for flashpoint

Tested fuel	Flash point measured [^{o}C]	Atmospheric pressure [kPa]	Flash point corrected [^{o}C]
Diesel fuel	55	97,3	56,5
LDPE fuel	44	97,3	45,5

Experimental determination of cetane number

Experimental determination was made with the help of the stand for the evaluation of cetane number WAUKESHA CFR-F5**,** according to norms ASTM D613 and ISO 5165, namely the standards for the determination of cetane number of fuels for Diesel engines. Cetane number (CN) determined for the fuel obtained by LDPE pyrolysis is:

CN=66

The diesel engines function well with diesel fuel with CN varying in the range 40 and 55. A higher cetane number means a faster self-ignition that allows the realization of engines with higher speed rate or, which at the same speed rate, offer longer time for burning completion, resulting smaller noxious emissions.

Determinarea experimentală a cifrei cetanice

Determinarea experimentală s-a făcut cu ajutorul standului pentru evaluarea cifrei cetanice WAUKESHA CFR-F5, în conformitate cu normele ASTM D613 şi ISO 5165, acestea fiind standardele de determinare a cifrei cetanice din combustibilii pentru motoarele Diesel.

Cifra cetanică (CC) determinată a combustibilului obţinut prin piroliza din LDPE este:

CC=66

Motoarele diesel funcţionează bine cu motorină cu CC cuprinsă între 40 şi 55. O cifră cetanică mai mare înseamnă o autoaprindere mai rapidă, ceea ce permite sau realizarea unor motoare cu turaţii mai mari, sau, la aceeaşi turaţie, oferă mai mult timp pentru completarea arderii, rezultând emisii de noxe mai mici.

Experimental determination of sulphur content

For the determination of sulphur content from the fuel resulted following the pyrolysis process of LDPE it was used the UV-fluorescence (UVF) Antek 9000 Analyzer.

The used method is based on pyrochemiluminescence. In this case, the apparatus measures the content of sulphur in very small quantities in gasoline, diesel fuel, light oils and other light hydrocarbons, including GPL, according to ASTM D-5453, ASTM D-4629 şi SR EN ISO 20846-04. The sulphur quantity determined in the analyzed product was:

S = 2 [mg/kg] sau 2 [ppm]

Experimental determination of Cold Filter Plugging Point

For this determination it was used the apparatus FPP 5Gs, which provides results according to the testing methods EN 116, 309 IP şi ASTM D 6371. The value obtained for cold filter plugging point:

$CFPP_{LDPE}$ = +4 [^{0}C]

Experimental determination of calorific power

For the determination of calorific power of the analyzed fuel it was used the calorimeter with mantle maintained at constant temperature, model PARR CALORIMETER 6200. Following the measurements for the determination of calorific power for the fuel obtained from LDPE the resulted value was obtained:

$Q_{s\ LDPE}$ = 45735,35 [kJ/kg]

For diesel fuel, the usual value of calorific power is:

$Q_{s\ M}$ = 44800 [kJ/kg]

Table 3 presents the results for the determinations undertaken for the fuel resulted by the pyrolysis of LDPE comparing to some quality specifications of diesel fuel.

Determinarea experimentală a conţinutului de sulf

Pentru determinarea conţinutului de sulf din combustibilul rezultat în urma procesului de piroliză din LDPE s-a folosit analizorul de sulf prin fluorescenţa UV ANTEK 9000.

Metoda folosită fiind piro-chemiluminescenţă, aparatul măsoară conţinutul de sulf în concentraţii foarte mici în: benzină, motorină, uleiuri uşoare şi alte hidrocarburi uşoare, inclusiv în GPL, în concordanţă cu ASTM D-5453, ASTM D-4629 şi SR EN ISO 20846-04. Cantitatea de sulf determinată în produsul analizat a fost:

S = 2 [mg/kg] sau 2 [ppm]

Determinarea experimentală a temperaturii limită de filtrabilitate

Pentru această determinare s-a folosit aparatul FPP 5Gs, care livrează rezultatele în conformitate cu metodele de testare EN 116, 309 IP şi ASTM D 6371. Temperatura limită de filtrabilitate obţinută pentru combustibilul LDPE a fost:

TLF_{LDPE} = +4 [^{0}C]

Determinarea experimentală a puterii calorifice

La determinarea puterii calorifice a combustibilului analizat s-a folosit calorimetrul cu mantaua menţinută la temperatură constantă PARR CALORIMETER 6200. În urma măsurătorilor efectuate pentru determinarea puterii calorifice a combustibilului obţinut din LDPE a rezultat valoarea:

$Q_{s\ LDPE}$ = 45735,35 [kJ/kg]

Pentru motorină valoarea uzuală a puterii calorifice este:

$Q_{s\ M}$ = 44800 [kJ/kg]

În tabelul 3 sunt prezentate rezultatele determinărilor efectuate pentru combustibilul rezultat prin piroliza LDPE comparativ cu unele specificaţii de calitate ale motorinei.

Table 3

The specifications of diesel fuel compared with those of the LDPE fuel analyzed [6].

Properties	UM	Value			
		Diesel fuel		LDPE fuel	
Density @ 15˚C	kg/m3	820 ÷ 845		793,3	
Cetane number, min.	-	51,0		66	
Cetanic index, min.	-	46,0		-	
Cold Filter Plugging Point	˚C	Classes (summer) A B C +5 0 -5	Classes (winter) D E -10 -15	Classes (summer) A B C +4------	Classes (winter) D E
Flash point (Pensky-Martens), min.	˚C	> 55		> 44	
Sulphur content, max.	mg/kg	10		2	
Viscosity @ 40 ˚C	mm^2/s	2.00 ÷ 4.50		2,0384	
Copper strip corrosion (3 h @ 50 ˚C)	class	1		(1)	

CONCLUSIONS

The most used method for obtaining liquid fuels from plastic materials waste, and from LDPE is pyrolysis in the absence of oxygen using or not the catalysts.

Following the experiments there were obtained liquid fuels with properties close to the fuels used in internal combustion engines.

The obtained yield of conversion in liquid phase obtained by the reduction and the control of the temperature from the condensation area is superior comparing to the data from scientific literature.

The calculated and corrected density to the relative density of fuel is fitted between the specific density of gasoline and diesel fuel.

CONCLUZII

Metoda cea mai utilizată pentru obţinerea combustibililor lichizi din deşeurile de mase plastice, implicit şi din LDPE, este piroliza în absenţa oxigenului cu utilizarea sau nu a catalizatorilor.

În urma experimentelor s-au obţinut combustibili lichizi cu proprietăţi apropiate de ale combustibililor utilizaţi în motoarele cu ardere internă.

Randamentul de conversie în fază lichidă obţinut prin reducerea şi controlul temperaturii din zona de condensare este superior datelor întâlnite în literatura de specialitate.

Densitatea calculată şi corectată la densitatea relativă a combustibilului obţinut se încadrează între densităţile specifice benzinei şi motorinei.

The calorific power of the new fuel is higher than the one of diesel fuel by 935.35 kJ/kg, due to the presence in the fuels from LDPE of light hydrocarbons specific to gasoline with higher energetic power and to hydrocarbon with carbon number between C_{24} - C_{35} which increase the concentration of carbon that enters the combustion process.

The determinations and measurements undertaken have put into evidence the fact that this fuel obtained in the laboratory can be used in Diesel engines.

The production of the fuels from plastic material waste saves the stocks of fossil fuels and reduces the emissions of carbon in the case of the utilization of those materials to the obtaining of alternative fuels.

ACKNOWLEDGEMENT

This paper was supported by the Post-Doctoral Programme POSDRU/159/1.5/S/137516, project co-funded from European Social Fund through the Human Resources Sectoral Operational Program 2007-2013.

REFERENCES

[1]. Achilias D.S., Antonakou E., Roupakias C., Megalokonomos P., Lappas A. (2008) - *Recycling Techniques of Polyolefins From Plastic Wastes*, Global NEST Journal, vol. 10, no. 1, ISSN 1790-7632, pg. 114-122;

[2]. Aguado J., Serrano D. P., San Miguel G. (2007) - *Analysis of Products Generated from the Thermal and Catalytic Degradation of Pure and Waste Polyolefins using Py-GC/MS*, J Polym Environ, 15, p. 107;

[3]. Gobin K, Manos G (2004) - *Polymer degradation to fuels over microporous catalysts as a novel tertiary plastic recycling method*, Polymer Degradation and Stability, 83 (2), pg. 267;

[4]. Mikulec J., Vrbova M. (2008) - *Catalytic and thermal cracking of selected polyolefins,* Clean Technologies Environ Policy, 10, 2008, pg. 121;

[5]. Popescu G.L., Filip N., Popescu V. (2011) - *Research on the implementation of alternative fuels obtained from polymeric materials for agricultural tractors*, Actual tasks on agricultural engineering, Vol.39, p. 39;

[6]. Popescu G.L. (2012) - *Studies and research on the fuels obtaining from waste plastics and polluting emissions determination when is used to fuelled the compression ignition engines*, PhD dissertation, Technical University of Cluj-Napoca, Romania;

[7]. Popescu V., Vasile C., Brebu M., Popescu G.L., Moldovan M., Prejmerean C., Stănuleţ L., Trişcă-Rusu C., Cojocaru I. (2009) - *The characterization of recycled PMMA*, Journal of Alloys and Compounds 483, pg. 432;

[8]. Popescu V., Popescu G.L., Cojocaru I. (2009) - *Waste treatment in mechanical biological treatment (MBT) units*, Science USAMV papers - Horticulture Series-Iasi, Vol.52/2009, pg. 1163;

[9]. Scheirs J., Kaminsky W. (2006) - *Feedstock Recycling and Pyrolysis of Waste Plastics: Converting Waste Plastics into Diesel and Other Fuels*, Ed. "John Wiley & Sons Ltd.", ISBN-13:978-0-470-02152-1, West Sussex, Great Britain;

[10]. Saito K. (1992) - *Kogaku to Kagyo*, Osaka, Vol. 66, pg. 438;

[11]. Şuteu D. (2007) - *Management, Treating and Valorisation of Wastes*, Publishing Politehnium, Iaşi;

[12]. Takuma K, Uemichi Y, Ayame A (2000) - *Product distribution from catalytic degradation of polyethylene over H-gallosilicate,* Applied Catalysis A: General, 192, (2), pg. 273;

Puterea calorifică a noului combustibil este mai mare decât cea a motorinelor cu 935,35 kJ/kg, cauzele cele mai probabile fiind prezenţa în compoziţia combustibilului din LDPE a hidrocarburilor uşoare specifice benzinelor cu valoare energetică mai mare şi a hidrocarburilor cu număr de carbon cuprins între C_{24} - C_{35} care măresc concentraţia carbonului intrat în procesul arderii.

Determinările şi măsurătorile făcute evidenţiază faptul că acest combustibil obţinut în laborator poate fi utilizat în motoarele Diesel.

Producţia combustibililor din deşeuri de mase plastice conservă stocurile de combustibili fosili şi reduc emisiile de carbon în cazul utilizării acestora la obţinerea de combustibili alternativi.

MULŢUMIRI

Această lucrare a beneficiat de suport financiar prin programul Post-Doctoral POSDRU/159/1.5/S/137516, proiect cofinanţat din Fondul Social European prin Programul Operaţional Sectorial Dezvoltarea Resurselor Umane.

BIBLIOGRAFIE

[1]. Achilias D.S., Antonakou E., Roupakias C., Megalokonomos P., Lappas A. (2008) – *Tehnici de reciclare apoliolefinelor din reziduurile de mase plastice*, Global NEST Journal, vol. 10, nr. 1, ISSN 1790-7632, pag. 114-122;

[2]. Aguado J., Serrano D. P., San Miguel G. (2007) - *Analiza Produselor Generate din Degradarea Termala si Catalitica a Poliofelinelor Pure si din Reziduuri folosind Py-GC/MS*, J Polym Environ, 15, pag. 107;

[3]. Gobin K., Manos G. (2004) – *Degradarea polimerilor pentru combustibilii lichizi prin catalizatori microporosi ca o noua metoda de reciclare tertiara ay plasticelor*, Polymer Degradation and Stability, 83 (2), pag. 267;

[4]. Mikulec J., Vrbova M. (2008) – *Cracarea catalitica si termica a poliolefinelor selectate*, Clean Technologies Environ Policy, 10, 2008, pag. 121;

[5.] Popescu G.L., Filip N., Popescu V. (2011) – *Cercetarea privind implementarea combustibililor alternativi obtinuti din materiale polimerice pentru tractoarele agricole,* Actual tasks on agricultural engineering, Vol.39, pag. 39;

[6]. Popescu G.L. (2012) - *Studii şi cercetări privind obţinerea de combustibili din deşeuri de mase plastice şi determinarea emisiilor poluante la utilizarea în alimentarea motoarelor cu aprindere prin comprimare*, Teză de doctorat, Universitatea Tehnică din Cluj-Napoca, România;

[7]. Popescu V., Vasile C., Brebu M., Popescu G.L., Moldovan M., Prejmerean C., Stănuleţ L., Trişcă-Rusu C., Cojocaru I. (2009) - *Caracterizarea PMMA reciclat*, Journal of Alloys and Compounds 483, pag. 432;

[8]. Popescu V., Popescu G.L., Cojocaru I. (2009) - *Waste treatment in mechanical biological treatment (MBT) units*, Science USAMV papers - Horticulture Series-Iasi, Vol.52, p. 1163;

[9]. Scheirs J., Kaminsky W. (2006) - *Reciclarea materiei prime si piloriza reziduurior plastice in diesel si alti combustibili*, Ed. "John Wiley & Sons Ltd.", ISBN-13:978-0-470-02152-1, West Sussex, Great Britain;

[10]. Saito K. (1992) - *Kogaku to Kagyo*, Osaka, Vol. 66, p.438;

[11]. Şuteu D. (2007) - *Managementul, Tratarea şi Valorificarea Deşeurilor,* Ed. Politehnium, Iaşi;

[12]. Takuma K., Uemichi Y., Ayame A. (2000) – *Distribuirea produselor provenite dindegradarea catalitica a polietilenei peste H-gallosilicate*, Applied Catalysis A: General, 192, (2), pag. 273;

[13]. *** (2005), *Feedstock recycling of plastics, Third International Symposium on Feedstock Recycling of Plastics & Other Innovative Plastics Recycling Techniques*, Karlsruhe, Germany, September 25-29;
[14]. *** (2006) - *Feedstock Recycling and Pyrolysis of Waste Plastics: Converting Waste Plastics into Diesel and Other Fuels*, Publishing John Wiley & Sons Ltd, West Sussex;
[15].***(2009) http://eur-lex.europa.eu/LexUriServ/ exUriServ. do?uri=CELEX:32009 L0028:EN:NOT; Directive 2009/28/ EC of 23 April 2009 on the promotion of the use of energy from renewable sources;
[16]. *** http://www.lukoil.ro/pdf/EuroLuk.pdf;
[17]. *** http://www.lukoil.ro/pdf/EuroLDiesel.pdf.

[13]. *** (2005), *Reciclarea materiei prime din mase plastice, Al 3-lea simpozion international al reciclarii materiilor prime din plastice & alte tehnici inovative de reciclare a maselor plastice,* Karlsruhe, Germany, Sept.25-29;
[14]. *** (2006) – *Reciclarea materiei prime si piroliza reziduurilor plastice : Convertrea reziduurilor plastice in Diesel si alti combustibili lichizi*, Ed. John Wiley & Sons Ltd, West Sussex;
[15] *** (2009) - http://eur-lex.europa.eu/LexUriServ/LexUriServ. do?uri=CELEX:32009 L0028:EN:NOT;- Directive 2009/28/ EC of 23 April 2009 on the promotion of the use of energy from renewable sources;
[16] *** http://www.lukoil.ro/pdf/EuroLuk.pdf;
[17] *** http://www.lukoil.ro/pdf/EuroLDiesel.pdf.

MECHANICAL PROPERTIES OF ENERGETIC PLANT STEMS - REVIEW
/
PROPRIETĂŢILE MECANICE ALE TULPINILOR PLANTELOR ENERGETICE - REVIEW

PhD. Eng. Moiceanu G.[1)], Prof. PhD. Eng. Voicu Gh.[1)], Prof. PhD. Eng. Paraschiv G.[1)], Lect. PhD. Eng. Dinca M.[1)], PhD. Stud. Eng. Chitoiu M.[1)], PhD. Eng. Vlădut V.[2)]
[1)]University POLITEHNICA of Bucharest / Romania; [2)]INMA Bucharest / Romania
Tel: 0745.201.365; E-mail: moiceanugeorgiana@gmail.com

Abstract: *An important component of modern society is represented by renewable energy. This type of energy can be obtained through energetic plant processing, wind energy, solar energy, etc. Taking into consideration the potential of energetic plants regarding ensuring a sustainable future from an energetic point of view, this paper presents a review on the way in which mechanical properties influence the processing stage. Considering that the equipment used for this process is in continuing development, knowing the energetic plant stem mechanical properties is a major component in creating and developing these machines. Energetic plant mechanical properties are important data for mathematical modelling of the processes to which the stems are subjected to. Studying shearing resistance, compression/stretching resistance, cutting resistance, as well as the elasticity module, we can see that all the data lead to creating an adequate design for the equipment. The main objective of this paper is to create a synthesis regarding energetic plant mechanical properties.*

Keywords: *mechanical properties, mathematical modelling, energetic plants*

INTRODUCTION

Nowadays, fossil fuels as gas, coal, etc. represent the main source of energy in the world. Studies regarding the quantities of these resources and the use by consumers show that in approximately 40-50 years they will considerable diminish, some will even drain. Also, these energy sources produce annually environment degradation through acid rains, global warming, air pollution, etc. Regarding the lowering of this constant degradation, more and more countries have analysed the possibility to replace fossil fuels with renewable energy sources that do not have the same negative impact on the environment. [12]

The varied number of energetic plants nowadays imposes to the researchers extensive studies regarding their characteristics within the use for technological processes. Among these characteristics both biological characteristics influenced by culture conditions [13, 28] as well as physical properties that greatly influence processing stages, were identified.

The study of this paper is focused on presenting energetic plant stem mechanical properties and the influence that they have on these processes.

MATERIAL AND METHOD

Outlining physical properties of energetic plant stems was the focus of many researchers, this current paper showing research papers and studies from speciality sites, ASABE, articles published in journals from international data base (ScienceDirect, Springerlink, etc.) or volumes of some national and international conferences which had as an interest this theme, and are presented as bibliographical sources.

Rezumat: *O componentă foarte importantă a societăţii moderne este reprezentată de energia regenerabilă. Acest tip de energie poate fi obţinut prin procesarea plantelor energetice, energie eoliană, energie, solară etc. Luând în considerare potenţialul plantelor energetice privind asigurarea unui viitor sustenabil din punct de vedere energetic în această lucrare este prezentat un review privind modul în care proprietăţile mecanice ale acestora influenţează procesul de prelucrare. Având în vedere faptul că echipamentele utilizate sunt în continuă dezvoltare, cunoaşterea proprietăţilor mecanice ale tulpinilor plantelor energetice este o componentă importantă în crearea şi dezvoltarea acestor utilaje. Proprietăţile mecanice ale plantelor energetice constituie date importante în modelarea matematică a proceselor la care sunt supuse tulpinile. Studiind rezistenţa la forfecare, rezistenţa la compresiune/întindere, rezistenţa la tăiere, rezistenţa la încovoiere, rezistenţa la mărunţire precum si modulul de elasticitate, se constată că toate datele acumulate conduc la crearea unui design adecvat al echipamentelor. Obiectivul principal al acestei lucrări este acela de a alcătui o sinteză cu privire la proprietăţile mecanice ale plantelor energetice.*

Cuvinte cheie: *proprietăţi mecanice, modelare matematică, plante energetice*

INTRODUCERE

In prezent, combustibili fosili precum gazele, carbunii etc. reprezintă principala sursa de energie din lume. Studii privind cantitatea acestor resurse şi utilizarea lor de către consumatori prezintă faptul că în aproximativ 40 - 50 de ani se vor diminua considerabil, unele chiar vor seca. Totodată, aceste surse de energie utilizate în prezent produc anual degradarea mediul înconjurător prin provocarea de ploi acide, încalzire globală, poluarea aerului etc. In vederea diminuării acestei degradări constante din ce în ce mai multe ţări au analizat posibilitatea de a înlocui combustibilii fosili cu surse de energie regenerabila care nu au acelaşi impact asupra mediului [12]

Numărul variat al plantelor energetice din zilele noastre impune cercetătorilor un studiu amănunţit asupra caracteristicilor acestora pentru utilizarealor în cadrul diferitelor procese tehnologice. Între aceste caracteristici se indentifică atât caracteristicile bilogice influenţate de condiţiile de cultură [13, 28], cât şi proprietăţile fizice care influenţează în mare parte procesele de prelucrare

Studiul acestei lucrări se concentrează pe prezentarea proprietăţilor mecanice ale tulpinilor plantelor energetice şi influenţa pe care aceastea o au asupra acestor procese.

MATERIALE ŞI METODA

Evidenţierea proprietăţilor mecanice ale tulpinilor plantelor energetice a fost studiată de numeroşi cercetări, în lucrarea de faţă fiind prezentate lucrări de cercetare şi studii preluate de pe site-uri de specialitate, ASABE, articole publicate în jurnale din baze de date internaţionale (ScienceDirect, Springerlink, etc.) sau volume ale unor conferinţe naţionale si internaţionale care au avut ca interes aceasta tematică şi utilizate ca surse bibliografice.

RESULTS AND DISCUTIONS

According to scientific papers [1...28], the processing state of energetic plants and its optimisation can be realised through establishing the mechanical properties of plants used to yield biogas.

Determining mechanical properties of energetic plants is a part of a complex process, mainly because of the composite structure of plants being different from one plant to another [3].

Generally the most used procedure in determining mechanical properties is performed in lab conditions where each component can be analysed individually. Data taken during lab trials can be used as input data inside mathematical models used to determine parameters that affect energy consumption during the processing stage [4]. An example in this purpose can be given by the difference between the energy associated to the obtained product after breaking and the energy associated to the raw material, which is equal with the consumed energy for the breaking process.

The theory of free mincing can be expressed through the relation:

REZULTATE ŞI DISCUTII

Conform lucrărilor ştiinţifice [1...28], procesul de prelucrare al plantelor energetice precum şi optimizarea acestuia pot fi realizate prin stabilirea proprietăţilor mecanice ale plantelor utilizate în vederea obţinerii de biogaz.

Determinarea proprietăţilor mecanice ale plantelor energetice face parte dintr-un proces complex, mai ales datorită faptului ca structura compozită a plantelor este diferită de o plantă la alta [3].

În general cea mai utilizată procedură de determinare a proprietăţilor mecanice se realizează în condiţii de laborator unde fiecare componentă poate fianalizată individual. Datele preluate din cadrul încercărilor de laborator pot fi utilizate ca date de intrare în cadrul modelelor matematice folosite pentru a determina parametrii care afectează consumul de energie în timpul procesului de prelucrare [4]. Un exemplu în acest sens poate fi dat de diferenţa dintre energia asociată produsului obţinut după mărunţire şi energia asociată materiei prime, care este egală cu energia consumată pentru procesul de mărunţire.

Teoria liberei mărunţiri se poate transpune în relaţia:

$$E_p - E_m = \eta \cdot E_c \quad (1)$$

Where

E_p – mincing energy;
E_m – raw material energy;
E_c – consumed energy by the breaking equipment;
η - equipment energetic efficiency.

unde:

E_p - energia produsului de mărunţire;
E_m - energia materiei prime;
E_c - energia consumată de utilajul de mărunţire;
η - randamentul energetic al utilajului.

Table 1

Different biomass types mechanical and physical properties

Nr. crt.	Plant type	Moisture content, [%wb]	Bulk density, [kg/m^3]	True density [kg/m^3]	Specific energy, [kN/m]	Ash content, [%]	Paper no.
1	Wheat straw	8.30	108	1210	15	8.32	[25]
2	Switchgrass	8	151	1090	86.5	5.49	[26, 27
3	Corn stover	11 - 15	148	1280	31.5	7.46	[26, 27]
4	Barley straw	6.98	98	1100	53k Wh/t	10.72	[25]
5	Miscanthus	8.5	1170	1080	4.4 kW	2.3	[7]

Resistance at shearing and bending

During outlining plant behavior at different processes in the paper [14], the authors had studied shearing and bending resistance for saffron stems as well as their elasticity module.

Thus, considering the fact that the cutting/grinding process is made out of processes like compression, shearing, bending, stretching and friction [15, 23] the authors have tested saffron stems at different values of humidity content. For determining the shearing resistance the equation was:

Rezistenţa la forfecare şi încovoiere

În vederea evidenţierii comportamentului plantelor în timpul diferitelor procese în lucrarea [14] autorii au studiat rezistenţa la forfecare şi încovoiere a tulpinilor de şofran precum şi modulul de elasticitate al acestora.

Astfel, considerând faptul că procesul de tăiere/tocare este format din procese precum compresiune, forfecare, încovoiere, întindere şi frecare [15, 23] autorii au testat tupinile de şofran la valori diferite ale conţinutului de umiditate. Pentru determinarea rezistenţei de forfecare ecuaţia utilizată a fost:

$$\tau_S = \frac{F_S}{2A} \quad (2)$$

Where:

τ_s – shearing resistance;
F_s – shearing force during disposal (N);
A – Area of the stem surface subjected to shearing (mm^2).

Also, using the same equipment stems have been subjected to bending tests by placing them on a metallic support, than applying force in the center at a load rate of 1mm/min (similar to the shearing test). Calculus formula for bending resistance was:

unde:

τ_s - rezistenţa la forfecare;
F_s - forţa de forfecare în momentul cedării (N);
A - aria suprafeţei tulpinii supuse forfecării (mm^2.

Totodată, folosind acelaşi echipament tulpinile au fost supuse testelor de încovoiere prin plasarea lor pe un suport metalic, apoi aplicându-se forţa în centrul probelor la o rată de încărcare de 10 mm/min (similară testului de forfecare). Formula de calcul pentru rezistenţa la încovoiere a fost:

$$\tau_b = \frac{F_b \cdot y \cdot l}{4 \cdot l} \quad (3)$$

where:

σ_b – bending resistance (MPa);
F_b – bending force (N);
y – distance from de neutral axe to the most distant point (mm);
l – distance between the two supports used during experimentation (50mm);

Using statistical data analysis ANOVA the conclusions referring to shearing resistance values have outlined a rise together with a rise in humidity from 4 to 8.46Mpa, results which were also confirmed in the paper [1,2,17], when the bending resistance dropped along with a rise in stem humidity content.

The average values of the bending stress, Young's modulus, shear stress, and shear energy varied from 50.59 to 26.91 MPa, 2.52 to 1.22 GPa, 4.00 to 4.00 MPa, and 231.45 to 730.02 mJ, respectively, as the moisture content increased from 8.61 to 37.16%.

Also a study about shearing resistance is presented in paper [24], where the authors have used as raw material rice stems. Their conclusions showed a rise in shearing resistance together with a rise in stem humidity content.

This effect of stem height on shearing energy was also reported by [2] for alfalfa stem and [18] for barley stem.

unde:

σ_b - rezistenţa la încovoiere (MPa);
F_b - Forţa de încovoiere (N);
y - distanţa de la axa neutră la cel mai depărtat punct (mm);
l - distanţa dintre cele două suporturi folosite în cadrul încercărilor experimentale (50 mm).

Folosind ca metodă de prelucrare a datelor analiza statistică a datelor ANOVA concluziile referitoare la valorile rezistenţei la forfecare au evidenţiat o creştere odată cu creşterea conţinutului de umiditate de la 4 la 8.46 MPa, rezultate confirmate şi în lucrarea [1, 2, 17] pe când rezistenţa la încovoiere a scăzut odată cu creşterea conţinutului de umiditate al tulpinilor.

Valorile medii ale tensiunii la incovoiere, modulul lui Young, tensiunea la forfecare, si energia de forfecare a variat intre 50.59 la 26.91 MPa, 2.52 la 1.22 GPa, 4.00 la 4.00 MPa, si 231.45 la 730.02 mJ, respectiv, umiditatea de la 8.61 la 37.16%.

Tot un studiu efectuat în vederea prezentării rezistenţei la forfecare este prezentat în lucrarea [24] unde autorii au utilizat ca materie primă tulpini de orez. Concluziile cercetărilor experimentale au evidenţiat creşterea rezistenţei la forfecare odată cu creşterea conţinutului de umiditate al tulpinilor.

Acest efect al inaltimii tulpinii asupra energiei forfecarii a fost de asemenea raportat de catre [2] pentru tulpini de alfalfa si [18] pentru tulpini de orz.

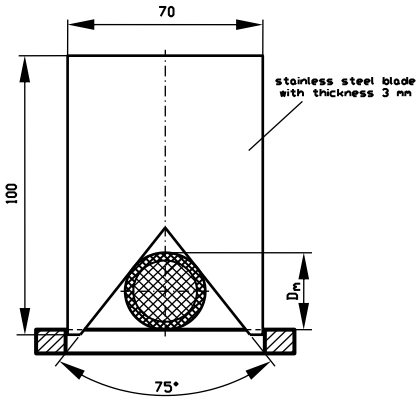

Fig. 1 – Miscanthus stem shearing cutting scheme

Similarly to papers presented earlier, in [21], the authors have subjected Miscanthus Giganteus to shearing tests. These tests had as a basis subjecting stem samples at repeated shearing stresses after which rupture point, bioflow point and the proportionality limit (characteristic of stem elasticity on a transversal section) were determined, from the force-deformation curve. Samples were put on the support frame so that the applied force on the shearing frame will be at the half of the sample. During application the shearing frame goes through an orifice until the moment of rupture point detection. During tests the Hounsfield mechanical trail apparatus was accessorised with metallic shearing plates of 100x70x3 dimensions (fig.1), and the shearing angle (plate opening) was different, of 30, 50, 60 and 75^o.

Because the material probes had variations in large diameter limits, their mass and the weight of the

Similar lucrărilor prezentate anterior, în [21], autorii au supus testelor de forfecare tulpini de Miscanthus x Giganteus. Testele au constat in supunerea epruvetelor din tulpini de Micanthus la solicitări de forfecare repetate în urma cărora s-au determinat punctul de rupere, punctul de biocurgere şi limita de proporţionalitate (caracteristică a elasticităţii tulpinilor pe secţiunea transversal) de pe curba forţă-deformaţie. Probele de material au fost aşezate pe placa de sprijin astfel încât forţa aplicată prin placa de forfecare să se afle la jumătatea epruvetei. În momentul aplicării testelor placa de forfecare trece printr-o fantă până în momentul în care era detectat de către aparat punctul de rupere. În cadrul testelor aparatul de încercări mecanice Hounsfield a fost prevăzut cu plăci metalice de forfecare de dimensiuni 100x70x3 (fig.1), iar unghiul de forfecare (deschidere a plăcilor) a fost diferit, şi anume 30, 50, 60 şi 75^o.

Deoarece probele de material au avut variaţii în limite largi ale diametrului, masei acestora şi grosimii învelişului lignocelulozic, variaţiile forţelor de rupere, atât

lignocellulose layer, variation of rupture forces, both to crushing, and shearing, regardless of plate angle, as well as necessary energy at shearing and the bioflow point corresponding force are between large limits. Still, it was observed that the shearing energy variation with Miscanthus plant diameter has an exponential variation rising from 0.308 J for 4.29mm diameter, at 2.315J for 7.95mm. Nevertheless, the results are similar to other papers on experimental testing.

Cutting resistance and cutting energy

Also, in the paper [19] the authors analysed the cutting resistance of sugarcane stems. During testing the plants were dried in natural conditions, at 25 degrees and 55% humidity. Testing the plants at different values of the humidity content, stems have been brought at wanted values through saturation or drying. Cutting blade of the Instron Universal Testing Machine had an inclination angle of 30^o and the angle of cutting blade of 60^o. In accordance with the humidity content and area of cutting section, the cutting resistance and cutting energy of sugarcane stems were determined. Conclusions of these tests showed an optimum cutting resistance when the humidity content was between 50-75%.

Using a similar knife, *V* shaped, in [20] Miscanthus stems cutting resistance was determined.

la strivire, cât şi la forfecare, indiferent de unghiul plăcii de lucru, precum şi ale energiei necesare la forfecare sau ale forţei corespunzătoare punctului de biocurgere se încadrează în limite destul de largi. Totuşi, s-a constat că variaţia energiei de forfecare cu diametrul plantelor de miscanthus are o variaţie exponenţială crescând de la 0.308 J pentru diametrul de 4.29 mm, la circa 2.315 J pentru diametrul de 7.95 mm. Cu toate acestea datele rezultate sunt similare lucrărilor utilizate ca model în efectuarea testelor experimentale.

Rezistenţa la tăiere şi energia de tăiere

De asemenea, in lucrarea [19] autorii au analizat rezistenta la tăiere a tulpinilor de trestie de zahăr. În vederea efectuării testelor experimentale plantele au fost uscate în condiţii naturale si anume la aproximativ 25 de grade si 55% umiditate. Testând plantele la diferite valori ale conținutului de umiditate tulpinile au fost aduse la valorile dorite prin saturare sau uscare. Lama de tăiere a echipamentului Instron Universal Testing Machine (Instron UTM/SMT-5, SANTAM Company, Tehran, Iran) utilizat a avut un unghi de înclinare de 30^o şi unghiul de lamei tăietoare 60^o. În funcţie de conţinutul de umiditate şi aria secţiuni tăiate s-a determinat rezistenta la tăiere şi energia la tăiere a tulpinilor trestiei de zahăr. Concluziile testelor au evidenţiat o rezistenţă la tăiere oprimă atunci când avem un conţinut de umiditate cuprins între 50- 75%.

Folosind un cuţit similar, în formă de *V*, în [20] s-a determinat rezistenţa la tăiere a tulpinilor de Miscanthus.

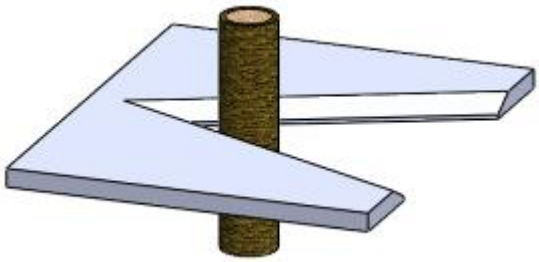

Fig. 2 - Miscanthus stem cutting V shaped blade [20]

Cutting blades (shearing) had an opening angle of 30^o, and different sharpening angles (i=10, 20, 30, 40, 50^o). It was observed that the cutting force drops from the base to the top of the plant, together with a drop in average stem diameter, curve of cutting variation presenting a decreasing exponential variation.

Similarly, using a cutting blade with a 50 ^{o} opening angle in [10] the authors realized experimental researches regarding miscanthus plant cutting resistance. Conclusions of the tests have showed a drop in cutting force values until the angle of 30-40 ^{o}, after which the force rises for cutting angles of over 40 ^{o}.

In paper [5] the authors have determined a cutting resistance of reed stalks using 6 knives with different blade inclination angles.

Lamele de tăiere (forfecare) au avut un unghi de deschidere de 30^o, si unghiuri de ascuţire diferite (i=10, 20, 30, 40 50^o). S-a constat că forţa de tăiere scade de la bază spre vârful plantei, odată cu scăderea diametrului mediu al tulpinii, curba de variaţie a forţei de tăiere prezentând o variaţie exponenţială descrescătoare.

Similar folosind o lamă de tăiere cu un unghi de deschidere de 50^o în [10] autorii au realizat cercetări experimentale privind rezistenţa la tăiere a plantelor de miscanthus. Concluziile testelor au evidenţiat o scădere a valorilor forţei de tăiere a plantelor de miscanthus până la un unghi de 30 – 40^o, după care forţa creşte pentru unghiuri de ascuţire de peste 40^o.

In lucrarea [5] autorii au derminat rezistenta la tăiere a tulpinilor de stuf folosind 6 cuţite cu diferite unghiuri de înclinare a lamei.

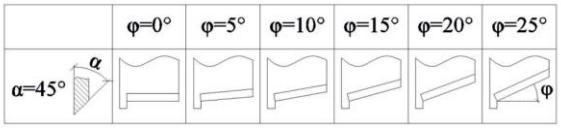

Fig. 3 – Knives with different blade cutting angles [5]

Conclusions refer to the fact that the consumed energy values during the moment of cutting operation have not presented large variations for different cutting blades [5].

Similarly, in [6] the authors used hemp stems for testing. Cutting resistance presented values between 11.8 and 19.4 N/mm^2. Also, the lowest energy value consumed was for the blade angles of 25 and 45 ^{o}. For all knives used during experimental testing the maximum cutting force dropped with 40% for knives inclined from 0 to 20°.

Other studies determined that the cutting speed and the blade configuration play a critical role in crops harvesting process. Maughan J.D. et al. (2014),[.9.] investigated the effects of cutting speed, blades bevel angle and fixation on the power consumption during Miscanthus harvesting. Authors used a rotary platform with only one cutting end, driven by a hydraulic motor with measuring instruments of stalk bending force and cutting speed. The results indicated that the cutting speed and the blades angle directly influence the power and efficiency of the Miscanthus harvesting machines. Instead it was determined that the way to fix the blade was insignificant.

Compression resistance

Another property of energetic plants analysed by researchers is plant compression resistance. Thus, in paper [11] Miscanthus plant stems were subjected to tests. The Hounsfield apparatus was fitted with an adaptor connected to a loading cell. Data resulted have showed the influence of stem diameter on tests, namely the bigger the diameter of the stem the larger the necessary compression force.

Concluziile evidenţiate fac referire la faptul că valorile energiei consumate în momentul operaţiei de tăiere nu a prezentat variaţii mari pentru diferite lame de tăiere [5].

Similar in [6] autorii au supus testelor de tăiere tulpini de cânepă. Rezistenţa la tăiere a prezentat valori cuprinse intre 11.8 şi 19.4 N/mm^2. De asemenea, cel mai scazut consum de energie s-a constatat a fi pentru lamele cu unghi de tăiere de 25 si 45^o. Pentru toate cuţitele folosite în timpul testelor experimentale forţa maximă de tăiere a scăzut cu aproximativ 40% pentru cuţitele cu lame de tăiere înclinate de la 0 la 20^0.

Alte studii au determinat faptul ca viteza de taiere si configurarea lamelor joaca un rol critic in procesul de recoltare. Maughan J.D. et al. (2014),[.9.] a investigat efectele vitezei de taiere, unghiul lamelor si fixarea de puterea consumata in timpul recoltarii. Autorii au folosit o platform rotativa cu un singur capat de taiere, actionat de un mtor hidrauloc cu instrumente de masura pentru forta de incovoiere a cozilor si viteza de taiere. Rezultatele au aratat ca viteza de taiere si unghiul lamelor influenteaza direct puterea si eficienta echipamentului de recoltat miscanthus. S-a determinat ca metoda de reparare a lamei nu era semnificativa.

Rezistenţa la compresiune

O altă proprietate a platelor energetice analizată de către cercetători face referire la rezistenţa plantelor la compresiune. Astfel, în lucrarea [11] s-au supus testelor de compresiune tulpini de Miscanthus X Giganteus. Aparatul Hounsfield utilizat în timpul experimentelor a fost dotat cu un adaptor conectat la o celulă de încărcare. Datele rezultate au evidenţiat influenţa diametrului tulpinilor asupra testelor, cu cât diametrul tulpinilor era mai mare cu atât şi forţa necesară de compresiune era mai mare.

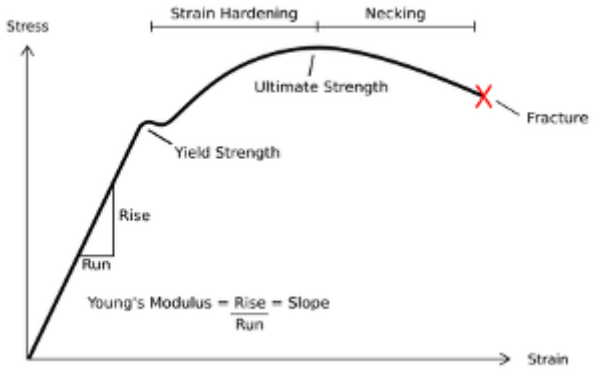

Fig. 4 – A typical stress-strain curve for plants - compression

Other studies [22] showed the miscanthus plant behavior subjected to compression tests through compression stress determinations and Young module. Knowing the loading feed and the contact surface for each loading feed (2 rectangular surfaces, superior and inferior, equal at the sample contact with the apparatus mass and with the pressure plate were considered), the compression stress was determined. Through regression analysis the 2 parameters were determined. Test conclusions as for deformation until crushing at transversal compression stresses are necessary for static loads larger than 2.5 daN.

During the process of transversal compression process the plant deforms, and this deformation keeps a certain value after removing the load pressure. So as a

Alte studii [22] au urmărit evidenţierea comportamentului plantelor de miscanthus supuse testelor de compresiune prin determinarea tensiuni de compresiune şi a modului lui Young. Cunoscand sarcina de încarcare si suprafata de contact a fost determinata tensiunea de compresiune s pentru fiecare sarcina de încărcare (au fost considerate 2 suprafete dreptunghiulare, superioara si inferioara, egale la contactul epruvetei cu masa aparatului si cu placa de presiune). Prin analiză de regresie au fost determinaţi cei doi parametrii. Concluziile testelor ca pentru deformarea pana la strivirea plantelor de miscanthus la solicitari de compresiune tranversale sunt necesare încarcari statice mai mari de 2.5 daN.

În timpul procesului de comprimare transversala planta se deformeaza, deformare care isi pastreaza o oarecare valoare dupa înlaturarea sarcinii de încarcare.

result , the miscanthus plant stem has a plastic-elastic behavior during the process of compression which assumes an energy quantity accumulated in the plant without being transformed in smaller parts, thus without being crushed until rupture, this behavior being showed in [16].

In [8], there were used different compaction speeds for the oak sawdust in the limits of 0.24–5.0 MPa/s. It was concluded that the density of compacted dry material measured at 2 min after compression decreases with the increasing compaction rate up to 3 MPa/s, above this value of the compression speed not being detected any significant influences regarding the density of the compacted material.

CONCLUSIONS

It is necessary to know the mechanical properties of energetic plant due to the influence that it has on the processing stage.

In this purpose, the fact that initial properties are necessary for realizing high performance equipment and with a low energy cost is also mentioned in previous papers. Also, knowing mechanical properties of different types of energetic plants contributes to the design of the machines. Tension and cutting resistance values, compression, shearing, bending differ according to the humidity content of the plants, considerably influencing equipment rotor, the action angle of the shearing/cutting blades, feed flow, applied forces, etc.

It must be mentioned that the physical properties of energetic plants influence the technological process.

ACKNOWLEDGEMENT

The work has been funded by the Sectoral Operational Programme Human Resources Development 2007-2013 of the Ministry of European Funds through the Financial Agreement POSDRU/159/1.5/S/132395 and with the support of the University "Politehnica" from Bucharest.

REFERENCES

[1]. Annoussamy M., Richard G., Recous S. and Guerif J. (2000) - *Change in Mechanical Properties of Wheat Straw Due to Decomposition and Moisture*, Appl. Eng. Agric., 16(6), pg. 657-664;

2]. Nazari Galedar M., Tabatabaeefar A., Jafari A., Sharifi A., O'Dogherty M.J., Rafee S. and Richard G. (2008) - *Effects of Moisture Content and Level in the Crop on the Engineering Properties of Alfalfa Stems*, Biosys. Eng., 101(2), pg. 199-208;

[3]. González M., Muñoz G. (2002) - *Experimental Determination of the Optimal Parameters of the Mechanical Densification Process of Fibrous Material for Animal Feed*, ASAE Annual International Meeting/CIGR XVth World Congress 2002';

[4]. Hepworth D.G. and Bruce D M (2000) – *A method of calculating the mechanical properties of nanoscopic plant cell wall components from tissue properties*, J. Mater. Sci. 35(23), pg. 5861-5865;

[5]. Kronbergs A., Kronbergs E., Siraks E., Dalbins J. (2012) - *Cutting Properties Of Arranged Stalk Biomass* - Renewable Energy and Energy Efficiency, Conditioning of the energy crop biomass compositions, pg. 145 - 149, 2012,

[6]. Kronbergs A., Kronbergs E., Siraks E., Adamovics A. (2011) - *Cutting Properties Of Different Hemp Varieties In Dependence On The Cutter Mechanism*, Conference-Engineering for rural Development, Jelgava, pg 446 – 451;

Rezulta asadar ca tulpinile plantei de miscanthus au o comportarea elasto-plastica în timpul procesului de comprimare ceea ce presupune o cantitate de energie acumulata în planta fara ca acesta sa fie transformata în particule mai mici, deci fara a fi strivita pana la rupere, acest comportament elasto-plastic fiind evidenţiat şi în [16].

In [8], s-au folosit diferite viteze de compactare pentru rumegusul de stejar in limitele 0.24–5.0 MPa/s. A fost concluzionat faptul ca densitatea materialului uscat compactat masurat la 2 min dupa compresie a scazut odata cu cresterea ratei de compactare de pana la 3MPa/s, peste aceasta valoare nu s-au mai detectat alte influente semnificative legate de densitatea materialului compactat.

CONCLUZII

Este necesar a cunoaşte proprietăţile mecanice ale plantelor energetice datorită influenţei pe care acestea o exercită asupra proceselor de prelucrare.

În aceste sens, este menţionat şi în lucrările prezentate anterior faptul că proprietăţile iniţiale ale plantelor sunt necesare pentru realizarea unor echipamente performante şi cu un consum redus de energie. Totodată, cunoaşterea proprietăţile mecanice ale diferitelor tipuri de plante energetice contribuie la designul maşinilor. Valorile tensiunilor şi rezistenţelor la tăiere, comprimare, forfecare, încovoiere diferă în funcţie de conţinutul de umiditate al plantelor, influenţând considerabil turaţia rotorului echipamentului, unghiul de acţiune al lamelor de tăiere/forfecare, feed flow, forţele aplicate etc.

Trebuie menţionat faptul că şi proprietăţile fizice ale plantelor energetice influenţează procesul tehnologic.

MULŢUMIRI

Rezultatele prezentate in acest articol au fost obtinute cu sprijinul Ministerului Fondurilor Europene prin Programul Operational Sectorial Dezvoltarea Resurselor Umane 2007-2013, Contract nr. POSDRU/159/1.5/S/132395 si al Universitatii Politehnica in Bucuresti.

BIBLIOGRAFIE

[1]. Annoussamy M., Richard G., Recous S. and Guerif J. (2000) - *Schimbarea proprietăților mecanice ale tulpinilor de grâu datorita descompunerii si umezelii,* Inginerie Agricola Aplicata, 16(6), pag. 657-664;

[2]. Nazari Galedar M., Tabatabaeefar A., Jafari A., Sharifi A., O'Dogherty M.J., Rafee S. and Richard G. (2008) - *Efectele conținutului de umiditate si a nivelului acestora asupra proprietăților tulpinilor de alfalfa* - Ing. Biosist., 101(2), pag. 199-208;

[3]. González M., Muñoz G. (2002) - *Determinări experimentale privind parametrii optimi ai procesului de densificare al materialelor fibroase pentru hrana animalelor,* Intalnirea anuala ASAE /Al XV Congres Mondial CIGR;

[4]. Hepworth D.G., Bruce D M (2000) – *O metoda de calcul a proprietăților mecanice a componentelor celulelor pereților plantelor din proprietățile țesuturilor*, J. Mater. Sci. 35(23), pag. 5861-5865;

[5]. Kronbergs A., Kronbergs E., Siraks E., Dalbins J. (2012) - *Proprietățile de taiere ale diferitelor tipuri de biomasa* - Energie regenerabila si eficienta energetica, Condiționarea compoziției culturilor de biomasa, pag. 145 - 149;

[6]. Kronbergs A., Kronbergs E., Siraks E., Adamovics A. (2011) - *Proprietățile de taiere ale tulpinilor de cânepa in corelație cu mecanismul de taiere*, Inginerie pentru dezvoltare rurala -, Letonia, pag. 446 – 451;

[7]. Kolowca J., Wróbel M., Baran B. (2009) – *Model mechaniczny źdźbła trawy miscanthus giganteus,* Inżynieria Rolnicza, vol. 6(115), pg. 149 - 154;;
[8]. Li Y., Liu H. (2000) - *High pressure densification of wood residues to form an upgraded fuel*, Biomass and Bioenergy, vol. 19, pg. 177-186;
[9]. Maughan J.D., Mathanker S.K., Fehrenbacher B.M., Hansen A.C. (2014) - *Impact of cutting speed and blade configuration on energy requirement for Miscanthus harvesting*, Applied Engineering in Agriculture, 30(2), pg. 137-142;
[10]. Moiceanu G., Voicu Gh., Paraschiv G., Voicu P. (2013) – *Cutting Resistance of Miscanthus Plants Using V Shaped Blades with Opennig of 50 degrees and diffrent sharpening angles*, 13th International Scientific Conference Engineering for Rural Development, Jelgava, Latvia, pg. 509 – 515;
[11]. G. Moiceanu, Gh. Voicu, G. Ipate, P. Voicu (2011) – *Researches regarding crushing behavior and Mechanical Characteristics of Miscanthus Energetic Plant*; International Commission of Agricultural and Biosystems Engineering. Bioenergy and Other Renewable Energy Technologies and Systems, 33 International Symposiums of Section IV of CIGR, Identifying number OS 212,23, vol. 13, (ISSN 1682-1139);
[12]. Saidura R., Abdelaziza E.A., Demirbasb A., Hossaina M.S, Mekhilefc S. (2011) - *A review on biomass as a fuel for boilers*, Renewable and Sustainable Energy reviews, Elsevier, vol 15 (5), Pg. 2262 - 2289;
[13]. Sorică Cristian, Voicu Emil, Manea Dragoş, Karl Schweighofer (2009) - *Technology For Promotion In Romania Of Energy Crop Miscanthus, As Renewable Resource To Increase Energy Competitiveness In Independence Purposes,*Lucrări Ştiinţifice INMATECH Bucureşti, vol 29, No. 3/2009, pg. 10 - 15;
[14]. Shahbazi F., Nazari Galedar M. (2012) - *Bending and Shearing Properties of Safflower Stalk*, Agricultural Science Technology Journal, vol. 14, pg 743 - 754;
[15]. Shaw, M., Tabil, L. (2006) - *Mechanical Properties of Selected Biomass Grinds*. Agric. Eng. Int.: The CIGR Ejournal, Manuscript FP 07 006. Vol. IX;
[16]. Schubert G., Bernotat S., (2004), *Comminution of non-brittle materials,* International Journal of Mineral Processing, 74S, pg. 19-30;
[17]. Tavakoli, H., Mohtasebi, S.S., Jafari, A. (2009) - *Physical and Mechanical Properties of Wheat Straw as Influenced by Moisture Content*. Int. Agrophysics, vol. 23, pg. 175-181;
[18]. Tavakoli H., Mohtasebi S.S., Jafari A., Galedar M. N. (2009) - *Some engineering properties of barley straw*, Applied Eng. Agric., vol. 25, no. 4, pg. 627-633;
[19]. Taghinezhad J., Alimardani R, Jafari A. (2014) - *Models of mechanical cutting parameters in terms of moisture content and cross section area of sugarcane stalks* - Agricultural Engineering Int. CIGR Journal, Vol. 16 No. 1, pg 280-288;
[20]. Voicu Gh., Moiceanu G., Paraschiv G. (2013) - *Miscanthus Stalk Behavior At Shear Cutting With V Cutting Blades*, At Different Sharpening Angles - U.P.B. Sci. Bull., Series D, Vol. 75, Iss. 3, 2013, ISSN 1454-2358
[21]. Voicu Gh., Moiceanu M., Sandu I.C., Poenaru I.C., Voicu P. (2011) - *Experiments regarding mechanical behaviour of the energetic plant miscanthus to crushing and shear stress,* 10th International Scientific Conference „Engineering for Rural Development", Proceedings, vol.10, Jelgava, Letonia, pg.490-495;
[22]. Voicu Gh., Moiceanu G., Biris S-St., Rusanescu C. (2011) – *Researches regarding Miscanthus Stalk behaviour during crushing stress under small loads,* Proceedings of the 39th International Symposium "Actual

[7]. Kolowca J., Wróbel M., Baran B. (2009) – *Modelarea mecanica a operației de taiere a tulpinilor de miscanthus Inginerie Agricola,* vol. 6(115), pag.149-154;
[8]. Li Y., Liu H. (2000) - *Densificarea sub presiuni ridicate a reziduurilor lemnoase in vederea creării unui combustibil inovator*, Biomasa si bioenergie, vol. 19, pag. 177-186;
[9]. Maughan J.D., Mathanker S.K., Fehrenbacher B.M., Hansen A.C. (2014) - *Viteza de impact la taiere si configurația lame asupra consumului de energie in timpul recoltării plantelor de Miscanthus*, Ingineria aplicata in Agricultura, 30(2), pag. 137-142;
[10]. Moiceanu G., Voicu Gh., Paraschiv G., Voicu P. (2013) – *Rezistenta la taiere a plantelor de miscanthus folosind lame de taiere tip V cu deschiderea de 50 de grade si diferite unghiuri de ascuțire a lamei A* 13 -a Conferinta Stiintifica Internationala, Inginerie pentru Dezvoltare Rurala, Letonia, pp. 509 – 515;
[11]. Moiceanu G., Voicu Gh., Ipate G., Voicu P. (2011) – *Cercetări privind comportamentul la comprimare si caracteristicile mecanice ale plantei energetice Miscanthus,* Comisia internațională de agricultura si ingineria biosistemelor, bioenergie si alte tehnologi de energii regenerabile si sisteme, Al 33-lea Simpozion International, Sectiunea IV a CIGR, Numar de identificare OS 212, vol. 13, (ISSN 1682-1139),
[12]. Saidura R., Abdelaziza E.A., Demirbasb A.,. Hossaina M.S, Mekhilefc S. (2011) - *Un review asupra biomasei ca si combustibil pentru boilere* Energii sustenabile si regenerabile review, Elsevier, vol 15 (5), Pag. 2262 - 2289;
[13]. Sorică C., Voicu Emil, Manea Dragoş, Karl Schweighofer (2009) - *Tehnologie pentru promovarea in Romania a plantei energetice Miscanthus ca sursa regenerabila in scopul creșterii competitivității si securității energetice,* Lucrări Ştiinţifice (INMATEH), vol 29 (3), pag. 10 - 15;
[14]. Shahbazi F., Nazari Galedar M. (2012) - *Proprietățile tulpinilor de floarea soarelui la solicitări de încovoiere si forfecare,* Jurnalul Stiinta Tehnologiei Agricole, vol. 14, pag. 743 - 754;
[15]. Shaw, M., Tabil, L. (2006). *Proprietățile mecanice ale diferitelor tipuri de biomasa*. Agric. Ing. Int.: Ejurnal CIGR, Manuscript FP 07 006. Vol. IX;
[16]. Schubert G. and Bernotat S., (2004), *Mărunțirea materialelor dure*, Jurnalul International de procesare a mineralelor, 74S, pag 19-30;
[17]. Tavakoli, H., Mohtasebi, S. S., Jafari, A. (2009) - *Proprietățile mecanice si fizice ale paielor de grâu sub influenta conținutului de umiditate,* Int. Agrofizica, vol. 23, pag. 175-181;
[18]. Tavakoli H., Mohtasebi S.S., Jafari A., Galedar M. N. (2009) - *Cateva proprietati ale paielor de grau din punct de vedere ingineresc* " Ing. Aplicata in Agr., vol. 25, no. 4, pag. 627-633;
[19]. Taghinezhad J., Alimardani R., Jafari A. (2014) - *Modelarea matematica a parametrilor de tocare in corelație cu aria secțiunii transversale si conținutul de umiditate pentru tulpini de trestie de zahar* - Inginerie Agricola Int. Jurnal CIGR, Vol. 16, No. 1, pag. 280-288;
[20]. Voicu Gh., Moiceanu G., Paraschiv G. (2013) - *Comportarea tulpinilor de miscanthus la procese de taiere cu forfecare folosind cuțite tip V si diferite unghiuri de taiere* - U.P.B. Buletin Stiintific., Seria D, Vol. 75, Iss. 3, pag. 257-270;
[21]. Voicu Gh., Moiceanu G., Sandu M., Poenaru I.C., Voicu P. (2011) - *Cercetări privind comportamentul mecanic al plantei energetice miscanthus la solicitari de compresiune si forfecare,* A 10-a conferința Internationala "Ingineria pentru dezvoltare rurala", vol.10, Jelgava, Letonia, pag.490-495;
[22]. Voicu Gh., Moiceanu G., Biris S-St., Rusanescu C. (2011) – *Cercetări privind comportarea tulpinilor de miscanthus sub actiunea unor solicitari de comprimare*

tasks on agricultural engineering", Opatija, Croatia, pg.153-160;
[23]. Yiljep, Y. D., Mohammed, U. S. (2005). *Effect of Knife Velocity on Cutting Energy and Efficiency during Impact Cutting of Sorghum Stalk.* Agric. Eng. Int.: The CIGR Ejournal, Manuscript PM 05 004. Vol. VII
[24]. Zareiforoush H., Mahdavian A., Hosseinzadeh B. (2012) - *An Approach to Estimate the Shear Strength of Rice Stem using a Fuzzy Logic Model* - Computer Science And Application, Vol. 1 (2), pg. 4-11
[25]. White N.M. and Ansell M.P. (1983) - *Straw - reinforced polyester composites;* Journal of Materials Science 18, pg.1549-1556;
[26]. Wright C.T., Pryfogle P.A, Stevens N.A., Stefler E.D., Hess J.R., Ulrich T.H. (2005) - *Biomechanics of wheat barley straw and corn stover,* Applied Biochemistry and Biotechnology, pg. 121 – 124;
[27]. Womac A.R., Yu M., Igathinathane C., Ye P., Hayes D., Narayan S., Sokhansanj S., Wright L. (2005) – *Shearing Characteristics of Biomass for size Reduction*, ASAE Meeting Presentation, Paper Number 056058, pg.1-8;
[28] *** http://www.miscanthus-rhizome.at/englisch.htm

scazute, A 39-a conferința Internațională "Probleme actuale in ingineria mecanica", Opatija, Croaţia, pag.153-160;
[23]. Yiljep Y.D., Mohammed U.S. (2005) - *Efectul turației cuțitului asupra energiei de taiere si a eficientei la taiere prin impact pentru tulpini de sorg* - Ing. Agr.: CIGR Ejurnal, Manuscript PM 05 004. Vol. VII, pag.1-10;
[24]. Zareiforoush H., Mahdavian A., Hosseinzadeh B. (2012) - *O metoda de estimare a forței de forfecare a tulpinilor de orez folosind un model Fuzzy* - Informatica aplicata, vol. 1 (2), pag. 4-11;
[25]. White N.M. and Ansell M.P. (1983) – *Paiele - compoziția poliesterului,* Jurnalul de Stiina Materialelor, vol 18. pag. 1549-1556;
[26]. Wright C.T., Pryfogle P.A, Stevens N.A., Stefler E.D., Hess J.R., Ulrich T.H. (2005) - *Proprietățile biomecanice alte tulpinilor de grâu si porumb,* Biochimie si Biotehnologie aplicata, pag.121 – 124;
[27]. Womac A.R., Yu M., Igathinathane C., Ye P., Hayes D., Narayan S., Sokhansanj S., Wright L. (2005) – *Proprietățile de forfecare a biomasei in vederea mărunțirii*, Prezentarea ASAE, Numărul lucrării 056058, pag.1-8;
[28]. ***http://www.miscanthus-rhizome.at/englisch.htm

MATHEMATICAL MODEL BASED ON WARNER – BRATZLER ANALYSIS METHOD CONCERNING TENDERIZED PORK BONELESS LOIN IN ORDER TO PRODUCE ROMANIAN TRADITIONAL PRODUCT "*COTLET PERPELIT*" TYPE

/

MODEL MATEMATIC BAZAT PE METODA DE ANALIZĂ WARNER – BRATZLER PRIVIND FRĂGEZIREA COTLETULUI DE PORC ÎN VEDEREA PRODUCERII PRODUSULUI TRADIŢIONAL ROMÂNESC DE TIP "COTLET PERPELIT"

Ph.D.Stud.Eng. Simion A. D., Ph.D.Eng. Cârdei R. P.,
Assist. Prof. Ph. D. Eng. Roşca A., Prof. Ph. D. Eng. Bădescu M., Prof. Ph. D. Eng. Roşca D.
S.C. AVI – GIIS S.R.L. Stuparei, Valcea County / Romania
E-mail: simion_aurel08@yahoo.com

Abstract: *The paper presents a mathematical model to produce Romanian traditional cured-cooked-smoked pork boneless loin product "Cotlet Perpelit" type made after raw meat's mechanical tenderizing. The tenderizing process performed to decrease the duration of cured marinating period consists in passing several times the raw meat among rollers with cutting prongs, and cyclic impulsive pressing of the meat, respectively. The mathematical model is based on force - extension diagrams obtained by using Werner-Bratzler testing method both for raw meat and final product, too, for no tenderized raw meat, and after raw meat mechanical tenderizing. The mathematical model consists in the geometric linear transforming of the characteristic diagrams obtained by using Werner-Bratzler method for the tenderized meat in comparison with the initial no tenderized meat. The model can be used to predict the mechanical characteristics of "Cotlet Perpelit", after raw meat mechanical tenderizing.*

Keywords: *raw meat tenderizing, Cotlet Perpelit, Warner - Bratzler testing method, mathematical model, linear geometric transformation*

INTRODUCTION

In principle, meat's tenderization represents the resultant of dynamic interdisciplinary processes consisting in chemical, biochemical and mechanical phenomena, [8]. To estimate tenderizing machine's and process' performances, is necessary to determine tenderized meat's mechanical characteristics, which could describe the meat qualitative transformations, [1, 18]. Thus, a mathematical model, expressed by a unified system of relationships and variables, could be used to analyze meat's mechanical tenderizing, [1]. For example, Graiver proposed a mathematical model for the absorption of curing salts in pork's meat, [2].

According to previous research papers, the variables parameters of the mathematical model have to be based on experimental research data of meat diagrams determined by using Warner-Bratzler testing method, [9, 10, 11, and 12].

According to Iacob [3], taking into account only the mechanical phenomena, a dynamic system involves different transformations of its internal parts under the action of given external forces. The mathematical models of the meat tenderizing process could be studied in further theoretical researches by applying the automatic systems theory, [4].

SC AVI-GIIS SRL Stuparei is a small enterprise for meat products in Valcea County, which was initially specialized in commercial cured-raw meats and cured - smoked products. In the last years SC AVI-GIIS SRL focused its effort to produce Romanian traditional cured-cooked-smoked pork boneless loin product "*Cotlet Perpelit*" type. In principle, the processing technology of this traditional cured-smoked-cooked product type consists in: wet curing phase of entire pieces of muscle meat in 15-20% curing

Rezumat: *Lucrarea prezintă un model matematic privind prepararea produsului sărat - prăjit - afumat din cotlet de porc dezosat tip "Cotlet Perpelit", după frăgezirea mecanică a materiei prime. Procesul de frăgezire efectuat pentru scăderea duratei de saramurare, constă în trecerea materiei prime de mai multe ori printre valţuri cu role dinţate, respectiv prin presarea ciclică impulsivă a materiei prime. Modelul matematic are la bază diagramele forţă-deformaţie determinate prin metoda de testare Warner-Bratzler atât pentru materia primă, cât şi pentru produsul final, pentru carnea nefrăgezită, cât şi după ce carnea a fost frăgezită. Modelul matematic constă în transformarea geometrică liniară a diagramelor caracteristice obţinute prin metoda Warner-Bratzler pentru carnea frăgezită, în comparaţie cu materia primă nefrăgezită. Modelul matematic poate fi utilizat pentru estimarea caracteristicilor mecanice ale "Cotlet-ului Perpelit", după frăgezirea mecanică a materiei prime.*

Cuvinte cheie: *frăgezirea cărnii, Cotlet Perpelit, metoda de testare Warner-Bratzler, model matematic, transformarea geometrică liniară*

INTRODUCERE

În principiu, frăgezirea cărnii reprezintă rezultanta unor procese dinamice interdisciplinare care constă în fenomene chimice, biochimice şi mecanice, [8]. Evaluarea performanţelor maşinilor şi proceselor de frăgezire este posibilă prin determinarea caracteristicilor mecanice ale cărnii după operaţia de frăgezire, care pot descrie transformările calitative ale cărnii, [1, 18]. Deci un model matematic reprezentat printr-un sistem unficat de relaţii şi variabile, ar putea fi utilizat pentru analiza frăgezirii mecanice a cărnii, [1]. Spre exemplu, Graiver a propus un model matematic al absorbţiei de saramură în carnea de porc, [2].

Conform unor lucrări de cercetare anterioare, parametrii variabili ai modelului matematic trebuie să aibă la bază rezultate experimentale determinate prin testarea cărnii prin metoda Warner-Bratzler, [9, 10, 11, 12].

Conform Iacob [3], avînd în vederea numai fenomenele mecanice, un sistem dinamic presupune diferite transformări interne sub acţiunea unor forţe exterioare cunoscute. Modelul matematic pentru frăgezirea mecanică a cărnii ar putea fi studiat în viitoare cercetări teoretice prin aplicarea teoriei de control a sistemelor automate, [4].

SC AVI-GIIS SRL Stuparei din judeţul Valcea este o firmă mică specializată iniţial pentru realizarea de produse din carne sărate, respectiv sărat - afumate. În ultimii ani, firma şi-a concentrat eforturile pentru producerea sortimentului sărat - prăjit - afumat din cotlet de porc dezosat, tip "*Cotlet Perpelit*". În principiu, procesul tehnologic al acestui produs tradiţional constă în: saramurarea umedă (12-15% concentraţie) a bucăţilor de

salt concentration, during 2-3 weeks; drying / ripening phase in cold air ventilation for 6-8 hours; cold smoke phase (approx. 20°C) for 2-3 days, followed by a short sequence of hot smoke phase (approx. 20°C), for 4-6 hours, [12].

According to international and Romanian legislation, sodium nitrite, sodium or potassium nitrate ($NaNO_2$); $NaNO_3$/ KNO_3), are not permitted in traditional cured-cooked types products usual processing, and no brine injection is allowed, [5, 6, 7, 13].

In order to reduce the wet curing phase, SC AVI-GIIS SRL decided to realize and to test two types of tenderizing machines: *four roller tenderizer machine*, and *cyclic impulsive pressing machine*, [12, 13].

MATERIALS AND METHOD

Experimental method and equipment

In order to determine the influence of mechanical tenderizing method on raw meat (pork boneless loin) tenderness, two different machines were used: *four roller tenderizer machine* and *cyclic impulsive pressing machine.*

Four roller tenderizer machines are designed to increase the effective surface area for the extraction of meat proteins during subsequent compression and stretching processes. In its operation, the machine performs superficial or deep cuts in the piece of meat that passes through two pairs of tenderizer roller. In principle, the machine consists of two pairs of parallel tenderizing rollers (provided with a number of cutting prongs), located at a certain distance, that are rotated in opposite directions by an electro-mechanical transmission (fig. 1), [12, 13].

Cyclic impulsive pressing machine is a semi-continuous meat press machine for meat's pressing before marinating. If meat pieces are pressed with a significant amount of force applied more or less evenly throughout the piece of meat, it will tenderize the meat piece and condition the meat fibers so that marinade will be absorbed into the meat fibers *without the use of a vacuum*, [15, 16, 17, and 19].

Cyclic impulsive pressing machine consists in mechanical - pneumatic equipment, and automated programmable. In principle (fig. 2), the mechanical - pneumatic equipment consists in an electro-pneumatic system (air compressor, solenoid valve), and two pressing plates (a fixed lower plate, and mobile upper plate). To improve the tenderizing process, each of the two plates (covered food grade Teflon pad) has pyramidal (6 · 6 · 6 mm) prongs, [12, 13].

Fig. 1 - Four roller tenderizer machine (with pyramidal cutting prongs)

In order to determine the influence of tenderizing process on pork boneless loin used to produce traditional cured-smoked-cooked product *"Cotlet Perpelit"*, 6 samples (raw meat, and *"Cotlet Perpelit"* final product) were processed

cotlet dezosat timp de 2-3 săptămâni; zvântarea in aer rece ventilat timp de 6-8 ore; afumarea rece (aprox. 20°C) timp de 2-3 zile, urmată de afumarea caldă (aprox. 20°C) timp de 4-6 ore, [12].

În conformitate cu legislaţia internaţională şi din România, la producerea produselor tradiţionale este interzisă utili-zarea nitriţilor, nitraţilor ($NaNO_2$; $NaNO_3$ / KNO_3), precum şi saramurarea prin injectare, [5 ,6, 7, 13].

În vederea reducerii duratei de saramurare umedă, firma SC AVI-GIIS SRL a realizat şi testat a două tipuri de maşini de frăgezire mecanică: *maşina de frăgezire cu două perechi de cilindri profilaţi pentru perforare*, respectiv *maşina de frăgezire prin presare ciclică dinamică*, [12, 13].

MATERIALE ŞI METODĂ

Metodă şi echipament experimental

În vederea determinării influenţei metodei de frăgezire mecanică asupra materiei prime (cotlet de porc dezosat), au fost utilizate două tipuri de maşini: *maşina de frăgezire cu două perechi de cilindri profilaţi pentru perforare*, respectiv *maşina de frăgezire prin presare ciclică dinamică.*

Maşina de frăgezire cu două perechi de cilindri profilaţi pentru perforare este concepută pentru creşterea suprafeţei de extragere a proteinelor din carne, în timpul unor procese succesive de compresiune şi perforare. În timpul acestei operaţii, carnea trece printre două perechi de valţuri rotative cu dinţi profilaţi care realizează perforaţii de anumită adâncime în bucata de carne. În principiu, maşina constă din două perechi de valţuri paralele (prevăzute cu dinţi de perforare), dispuse la o anumită distanţă, care se rotesc în direcţii opuse prin intermediul unei transmisii electromecanice (fig. 1), [12, 13].

Maşina de frăgezire prin presare ciclică dinamică este o maşină pentru presarea discontinuă a cărnii înainte de saramurare. Dacă bucata de carne este presată cu o anumită forţă, aceasta se va frăgezi, iar saramura va fi absorbită de ţesuturile cărnii fără să mai fie necesară vacuumarea, [15, 16, 17, 19].

Această maşină este compusă dintr-un echipament mecano-pneumatic, şi un automat programabil.

În principiu (fig. 2), echipamentul mecano-pneumatic este compus dintr-un sistem electropneumatic (compresor, electroventile, cilindru pneumatic), şi două plăci de presare (inferioară / fixă, respectiv superioară / mobilă). Pentru îmbunătăţirea procesului de frăgezire, fiecare din cele două plăci (cu plăci food grade Teflon) sunt prevăzute cu dinţi piramidali (6 · 6 · 6 mm), [12, 13].

Fig. 2 - Cyclic impulsive pressing machine (food grade Teflon pads with pyramidal prongs)

Pentru determinarea influenţei procesului de frăgezire asupra cotletului de porc dezosat utilizat pentru reali-zarea produsului sărat-afumat-prăjit *"Cotlet Perpelit"*, câte 6 probe (carne crudă, şi produs finit *"Cotlet Perpelit"*) au

according to four methods:
- no tenderized pork boneless loin (NO TEND);
- pork boneless loin tenderized by six times successive passing amongst the cutting prongs of the *Four roller tenderizer machine* (FRT 6x);
- pork boneless loin tenderized by *Cyclic impulsive pressing machine* in 5 pressing cycles, each consisting in 0.5s pressing periods, and 0.5s pauses periods (CIP 5-0,5);
- pork boneless loin tenderized by *Cyclic impulsive pressing machine* in 20 pressing cycles, each consisting in 0.5s pressing periods, and 0.5s pauses periods (CIP 20-0,5).

To produce *"Cotlet Perpelit"* by using no-tenderized pork boneless loin, there were followed certain traditional phases: wet curing phase of entire pieces of muscle meat (12% curing salt concentration), during 2 weeks; drying / ripening phase in cold air ventilation for 6 hours; cold smoke (approx. 20°C) for 10 hours, followed by 4 hours hot smoke (approx. 80°C).

To produce *"Cotlet Perpelit"* by using tenderized pork boneless loin, the tenderized meat was processed in following phases: wet curing (12% curing salt concentration), during *4 days*; drying / ripening phase in cold air ventilation for 6 hours; cold smoke (approx. 20°C) for 10 hours, followed by 4 hours hot smoke (approx. 80°C), [12].

Tenderness evaluation by using Warner-Bratzler method

The most relevant and utilized methods to estimate meat's tenderness are compression test, and Warner - Bratzler shear test method. During Warner-Bratzler test the shear blade achieves simultaneously both compression and slicing / shearing of the product, [5, 7, 14, 15, 16, 17]. To perform interdisciplinary researches concerning general texture and tenderness analysis, universal testing machine *Lloyd Instruments LRXPlus 5* (Unconventional Technologies and Equipment for Agro-Food Industry Laboratory - UTEFIL, within Faculty of Agriculture and Horticulture in Craiova) was used. Due to collaboration between *UTEFIL* and Environmental Eng. Laboratory within Faculty of Electrical Engineering, a *Warner - Bratzler experimental equipment* was made: special rigid frame (food-grade Teflon) that permits fast fitting of inter-changeable Warner - Bratzler shear blades (DIN W1.4571), [9, 10, 11]. During these experiments, 100mm/min cutting speed was used.

Representative Warner - Bratzler test diagrams for pork boneless loin tenderized by using FRT 6x method, and for *"Cotlet Perpelit"* obtained by using this tenderized meat, are presented in fig. 3, and fig. 4, respectively.

fost procesate conform a patru metode:
- cotlet de porc dezosat nefrăgezit (NO TEND);
- cotlet de porc dezosat frăgezit prin trecerea succesivă de 6 ori printre valţurile profilate ale *maşinii de frăgezire cu două perechi de cilindri profilaţi pentru perforare* (FRT 6x);
- cotlet de porc dezosat frăgezit prin 5 cicluri de presare cu *maşina de frăgezire prin presare ciclică dinamică*, fiecare ciclu constând în: 0,5s presare, şi 0,5s pauze (CIP 5-0,5);
- cotlet de porc dezosat frăgezit prin 20 cicluri de presare cu *maşina de frăgezire prin presare ciclică dinamică*, fiecare ciclu constând în: 0,5s presare, şi 0,5s pauze (CIP 20-0,5).

Pentru producerea *"Cotlet-ului Perpelit"* din cotlet de porc dezosat nefrăgezit, au fost parcurse următoarele faze tradi-ţionale: sărarea umedă a bucăţilor de carne în saramură (12% concentraţie), timp de 2 săptămâni; zvântarea în aer rece ventilat, timp de 6 ore; afumarea rece (aprox. 20°C) timp de 10 ore, urmată de 4 ore de afumare fierbinte (aprox. 80°C).

Pentru producerea *"Cotlet-ului Perpelit"* din cotlet de porc dezosat frăgezit, au fost parcurse următoarele faze: sărarea umedă a bucăţilor de carne în saramură (12% concentraţie), timp de *4 zile*; zvântarea în aer rece ventilat, timp de 6 ore; afumarea rece (aprox. 20°C) timp de 10 ore, urmată de 4 ore de afumare fierbinte (aprox. 80°C), [12].

Evaluarea frăgezimii prin metoda Warner-Bratzler

Cele mai relevante şi utilizate metode pentru evaluarea frăgezimii cărnii sunt testul la compresiune, şi metoda de feliere/tăiere Warner-Bratzler. În timpul testului Warner - Bratzler lama de tăiere realizează simultan compresiunea şi felierea/ tăierea produsului, [5, 7, 14, 15 16, 17]. Pentru a efectua cerce tări interdisciplinare privind analiza texturii şi frăgezimii a fost utilizată maşina universală de încercări *Lloyd Instruments LRXPlus 5* (din dotarea Laboratorului pentru Tehnologii şi Echipamente Neconvenţionale pentru Industria AgroAlimentară - UTEFIL, din cadrul Facultăţii de Agricultură şi Horticultură din Craiova). În urma colaborării dintre UTEFIL şi Laboratorul pentru Ingineria Mediului din cadrul Facultăţii de Inginerie Electrică, a fost realizat un echipament experimental Warner-Bratzler: suport rigid (food-grade Teflon) care permite asamblarea rapidă a lamelor interschimbabile de feliere/tăiere Warner-Bratzler (DIN W1.4571), [9,10,11]. În timpul acestor experimente, a fost folosită viteza de tăiere de 100mm/min.

Diagrame Warner - Bratzler representative pentru cotlet de porc dezosat frăgezit prin metoda FRT 6x, şi pentru *"Cotlet -ul Perpelit"* obţinut din această carne frăgezită, sunt prezentate în fig. 3 şi respectiv în fig. 4.

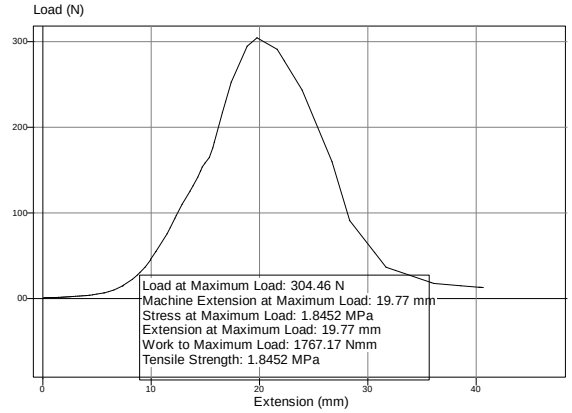

Fig. 3 - Warner-Bratzler test diagram for tenderized pork boneless loin by using FRT 6x

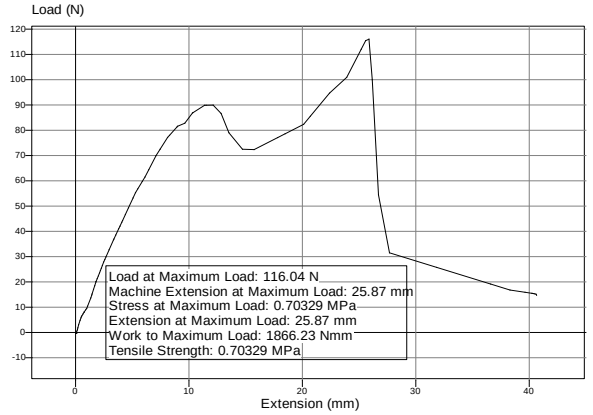

Fig. 4 - Warner-Bratzler test diagram for "Cotlet Perpelit" tenderized by using FRT 6x

RESULTS

Tenderizing mathematical model

The mathematical model for studying the tenderizing effect is based on the hypothesis that any meat's final product material can be characterized by numerical curves obtained by mechanical characteristics experimentally determined for each tenderizing method. Resulting numerical curves could differ more or less from those of no tenderized meat samples.

In fig. 3 and fig. 4 it can be observed the maximum shear force that characterizes each type of pork boneless loin, and *"Cotlet Perpelit"* tenderness'.

Due to the inhomogeneous character of the meat's tissues, the maximum shear force cannot describe all the cutting / shearing process.

Therefore for each un-tenderized / tenderized pork boneless loin sample, and for each *"Cotlet Perpelit"* obtained by using these meat pieces, too, average curves that describe all evolution of the shearing diagrams obtained by using Warner - Bratzler method were numerical determined (fig. 5 and fig. 6).

REZULTATE

Model matematic pentru frăgezire

Modelul matematic pentru studiul efectului frăgezirii are la bază ipoteza că materialul oricărui produs din carne poate fi caracterizat prin curbe numerice obţinute din diagramele caracteristicilor mecanice determinate experimental pentru fiecare tip de metodă de frăgezire. Curbele numerice rezultate pot să difere mai mult sau mai puţin de cele obţinute pentru probele nefrăgezite.

În fig. 3 şi fig. 4 se pot observa valorile maxime ale forţei de tăiere care caracterizează frăgezimea fiecărui tip de cotlet de porc dezosat, şi de *"Cotlet Perpelit"*.

Datorită caracterului neomogen al ţesuturilor cărnii, valoarea forţei maxime de tăiere nu poate descrie întregul proces de tăiere.

De aceea, pentru fiecare probă nefrăgezită / frăgezită de cotlet de porc dezosat, şi pentru fiecare probă de *"Cotlet Perpelit"* obţinut din aceste bucăţi de carne, au fost determinate numeric curbele medii care descriu toată evoluţia diagramei forţei de tăiere obţinută experimental prin metoda Warner - Bratzler (fig. 5 şi fig. 6).

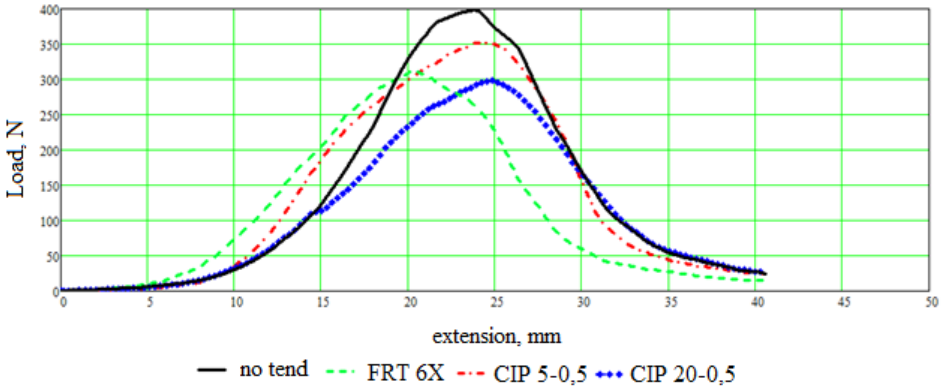

Fig. 5 - Numerical determined average curves of the four types of pork boneless loin samples NO TEND; CIP 5-0,5; CIP 20-0,5; FRT 6x

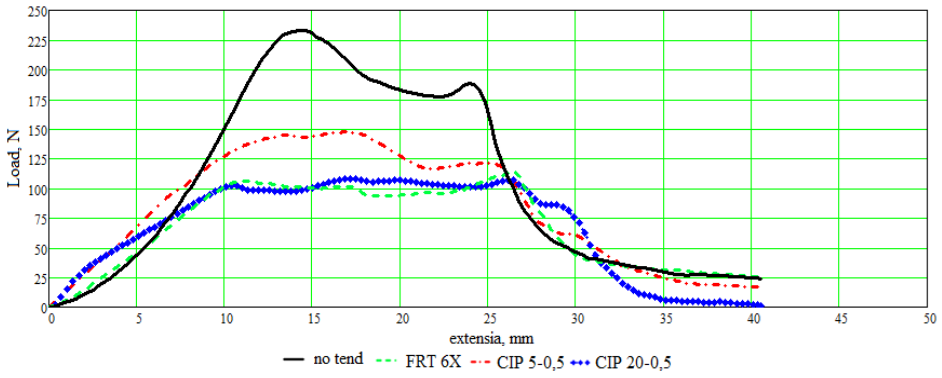

Fig. 6 - Numerical determined average curves of the four "*Cotlet Perpelit*" type samples CP-NO TEND; CP-CIP 5-0,5; CP-CIP 20-0,5; CP-FRT 6x

The proposed mathematical model is based on the hypothesis that the characteristic curve of the sample (no tenderized, or tenderized by using mechanical methods), is obtained as a linear transformation that can be described by the vector equation, [1, 3, 8]:

Modelul matematic propus se bazează pe ipoteza conform căreia curba caracteristică a fiecărei probe (nefrăgezită, sau frăgezită prin metode mecanice), este obţinută ca o transformare liniară care poate fi descrisă de ecuaţia vectorială, [1, 3, 8]:

$$\begin{pmatrix} x' \\ F' \end{pmatrix} = T \begin{pmatrix} x \\ F \end{pmatrix} \quad (1)$$

where: F is the shear force in N, x is the cutting length /extension in mm, before tenderizing (characteristic curve

unde: F este forţa de tăiere în N, x este cursa de tăiere / extensia în mm, înainte de frăgezire (coordonatele curbei

coordinates of the meat sample, before tenderizing); *F'* and *x'* represent the shear force and the cutting lenght / extension of the same meat sample type (characteristic curve coordinates, after tenderizing).

T is the linear transformation given by the matrix:

caracteristice a probei, înainte de frăgezire); *F'* şi *x'* reprezintă forţa de tăiere şi respectiv cursa de tăiere / extensia aceluiaşi tip de probă după frăgezire (coordonatele curbei caracteristice a probei, după frăgezire).

T este transformarea liniară dată de matricea:

$$T = \begin{pmatrix} t_{1,1} & t_{1,2} \\ t_{2,1} & t_{2,2} \end{pmatrix} \quad (2)$$

where t_{ij}, i =1,2; j =1, 2 are real numbers.

It must be noticed that each force *F* is represented by a pair of coordinates (x_i, F_i), i = 1, *N*, and each force *F'* is represented by a pair of coordinates (x'_i, F'_i), i =1, *N*. The matrix elements *T* are calculated considering minimizing condition of the functional:

în care t_{ij}, i =1,2; j =1,2 sunt numere reale.

Trebuie remarcat că fiecare forţă F_i este reprezentată de o pereche de coordotate (x_i, F_i), i = 1, *N*, şi fiecare forţă F_i' este reprezentată de o pereche de coordotate (x'_i,F'_i), i =1, *N*. Elementele matricei *T* sunt calculate prin condiţia de minim a funcţiei:

$$\Im(t_{1,1}, t_{1,2}, t_{2,1}, t_{2,2}) = \sum_{i=1}^{N} \left[\left(t_{1,1} x_i + t_{1,2} F_i - x'_i \right)^2 + \left(t_{2,1} x_i + t_{2,2} F_i - F'_i \right)^2 \right] \quad (3)$$

Based on described linear transformation, for pork boneless loin tenderized by using each method, the matrix *T* elements are:

- pork boneless loin tenderized by *Cyclic impulsive pressing machine* in 5 pressing cycles, each consisting in 0.5s pressing periods, and 0.5s pauses periods, (CIP 5 -0.5).

Pentru cotletul de porc dezosat frăgezit prin fiecare metodă, pe baza transformării liniare descrise, elementele matricei *T* sunt:

- cotletul de porc dezosat frăgezit prin 5 cicluri de presare cu *maşina de frăgezire prin presare ciclică dinamică*, fiecare ciclu constând în: 0,5s presare, şi 0,5s pauze, (CIP 5 - 0,5).

$$T = \begin{pmatrix} 0.998 & 0.000007079 \\ -0.048 & 0.986 \end{pmatrix} \quad (4)$$

- pork boneless loin tenderized by *Cyclic impulsive pressing machine* in 20 pressing cycles, each consisting in 0.5s pressing periods, and 0.5s pauses periods, (CIP 20-0.5).

- cotletul de porc dezosat frăgezit prin 20 cicluri de presare cu *maşina de frăgezire prin presare ciclică dinamică*, fiecare ciclu constând în: 0,5s presare, şi 0,5s pauze, (CIP 20 -0,5).

$$T = \begin{pmatrix} 0.998 & 0.000003448 \\ 0.18 & 0.935 \end{pmatrix} \quad (5)$$

- pork boneless loin tenderized by passing 6 successive times amongst the cutting prongs of the *Four roller tenderizer machine*, (FRT 6x).

- cotletul de porc dezosat frăgezit prin trecerea succesivă de 6 ori printre valţurile profilate ale *maşinii de frăgezire cu două perechi de cilindri profilaţi pentru perforare* (FRT 6x).

$$T = \begin{pmatrix} 0.989 & 0.00004522 \\ -0.326 & 0.773 \end{pmatrix} \quad (6)$$

The numerical tenderizing curves for pork boneless loin obtained by using the mathematical model are presented in fig. 7, fig. 8 and fig. 9, respectively.

In fig. 7, fig. 8 and fig. 9, respectively, it can be observed that the configurations and the maximum amounts of the numerical tenderizing curves are similar with the average curves experimentally determined (fig. 5). All these similarities validate the mathematical model based on proposed linear transformation.

Curbele numerice de frăgezire pentru cotletul de porc dezosat, obţinute prin utilizarea modelului matematic, sunt prezentate în fig. 7, fig. 8, şi respectiv fig. 9.

În fig. 7, fig. 8, şi respectiv fig. 9, se poate observa că atât configuraţia, cât şi valorile maxime ale curbelor numerice de frăgezire, sunt similare cu diagramele medii determinate experimental (fig. 5). Toate aceste similarităţi validează corectitudinea modelului matematic propus bazat pe transformarea liniară.

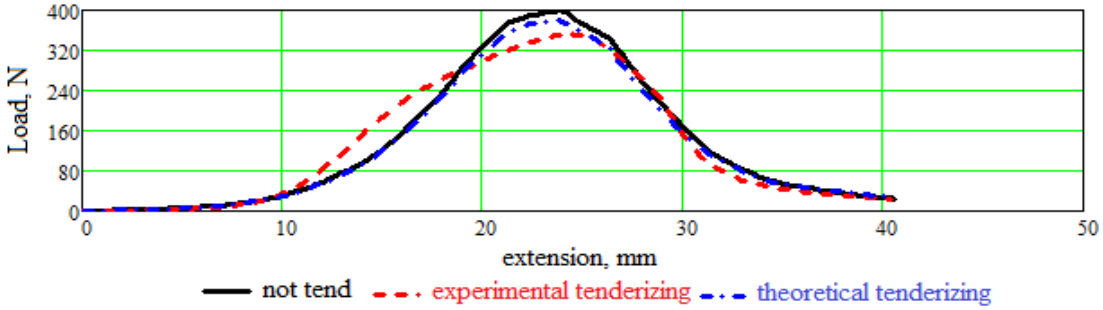

Fig. 7 - Numerical tenderizing CIP 5-0.5 curves obtained by using the mathematical model

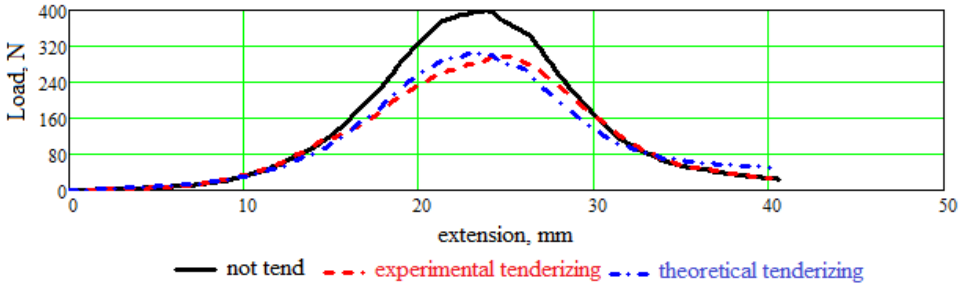

Fig. 8 - Numerical tenderizing CIP 20-0.5 curves obtained by using the mathematical model

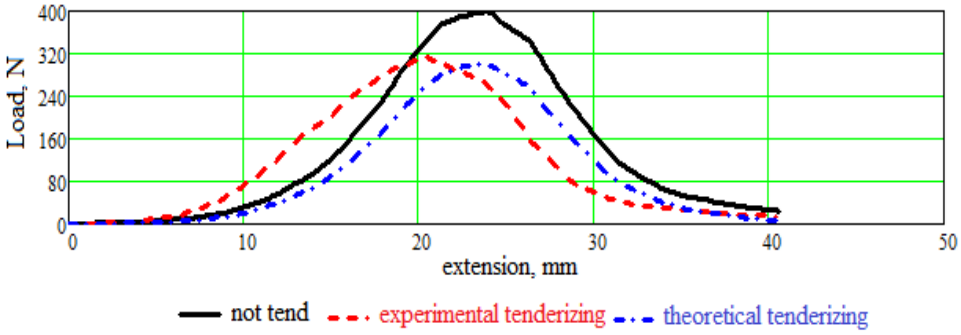

Fig. 9 - Numerical tenderizing FRT 6x curves obtained by using the mathematical model

Based on described linear transformation, for *"Cotlet Perpelit"* tenderized by using each method, the matrix *T* elements are:

- *"Cotlet Perpelit"* tenderized by using *Cyclic impulsive pressing machine* in 5 pressing cycles, each consisting in 0.5s pressing periods, and 0.5s pauses periods, (CP - CIP 5 – 0.5);

Pentru *"Cotlet - ul Perpelit"* obţinut din cotlet de porc dezosat frăgezit prin fiecare metodă, pe baza transformării liniare descrise, elementele matricei *T* sunt:

- *"Cotlet Perpelit"* obţinut după frăgezirea prin 5 cicluri de presare cu *maşina de frăgezire prin presare ciclică dinamică*, fiecare ciclu constând în: 0,5s presare, şi 0,5s pauze, (CP- CIP 5 - 0,5);

$$T = \begin{pmatrix} 1.002 & -0.0002219 \\ -0.048 & 0.689 \end{pmatrix} \quad (7)$$

- *"Cotlet Perpelit"* tenderized by using *Cyclic impulsive pressing machine* in 20 pressing cycles, each consisting in 0.5s pressing periods, and 0.5s pauses periods, (CP - CIP 20 – 0.5);

- *"Cotlet Perpelit"* obţinut după frăgezirea prin 20 cicluri de presare cu *maşina de frăgezire prin presare ciclică dinamică*, fiecare ciclu constând în: 0,5s presare, şi 0,5s pauze, (CP-CIP 20 - 0,5);

$$T = \begin{pmatrix} 0.999 & -0.0005576 \\ 0.331 & 0.534 \end{pmatrix} \quad (8)$$

- *"Cotlet Perpelit"* tenderized by passing 6 successive times amongst the cutting prongs of the *Four roller tenderizer machine* (CP - FRT 6x).

- *Cotlet Perpelit"* obţinut după frăgezirea prin trecerea succesivă de 6 ori printre valţurile profilate ale *maşinii de frăgezire cu două perechi de cilindri profilaţi pentru perforare* (CP-FRT 6x).

$$T = \begin{pmatrix} 1.001 & -0.0005576 \\ 0.696 & 0.478 \end{pmatrix} \quad (9)$$

The numerical tenderizing curves for *"Cotlet Perpelit"* obtained by using the mathematical model are presented in fig. 10, fig. 11 and fig. 12, respectively.

In fig. 10, fig. 11 and fig. 12, respectively, it can be observed that the configurations and the maximum amounts of the numerical tenderizing curves are similar with the average curves experimentally determined (fig. 6).

All these similarities validate the correctness of mathematical model based on proposed linear transformation.

Curbele numerice de frăgezire pentru *"Cotlet Perpelit"*, obţinute prin utilizarea modelului matematic, sunt prezentate în fig. 10, fig. 11, şi respectiv fig. 12.

În fig.10, fig. 11, şi respectiv fig. 12, se poate observa că atât configuraţia, cât şi valorile maxime ale curbelor numerice de frăgezire, sunt similare cu diagramele medii determinate experimental (fig. 6).

Toate aceste similarităţi validează corectitudinea modelului matematic propus bazat pe transformarea liniară.

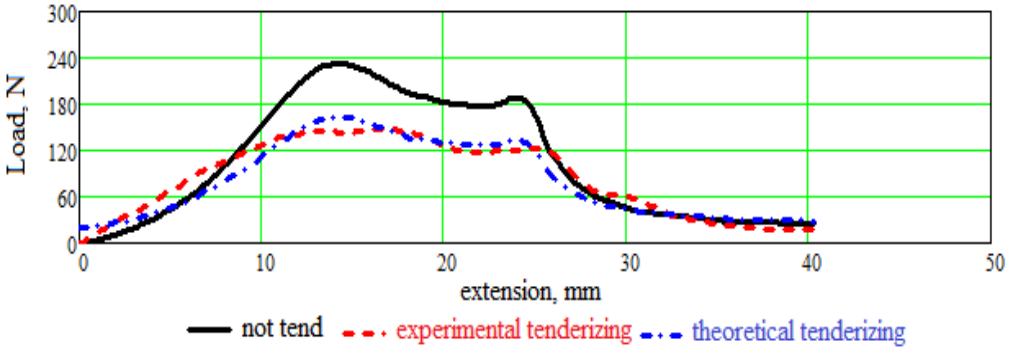

Fig. 10 - Numerical tenderizing CP-CIP 5-0.5 curves obtained by using the mathematical model

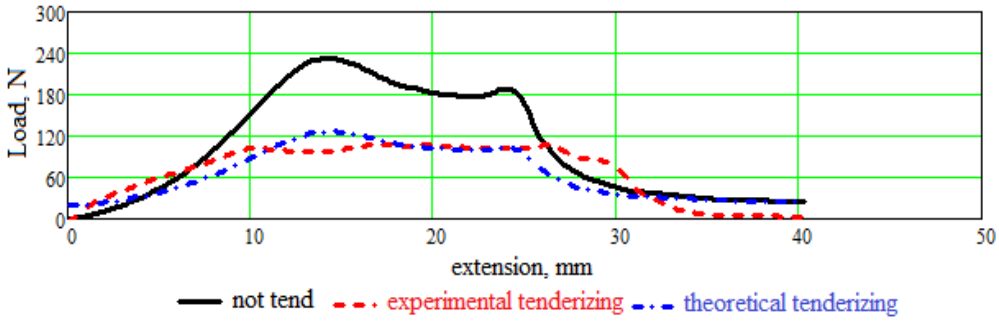

Fig. 11 - Numerical tenderizing CP-CIP 20-0.5 curves obtained by using the mathematical model

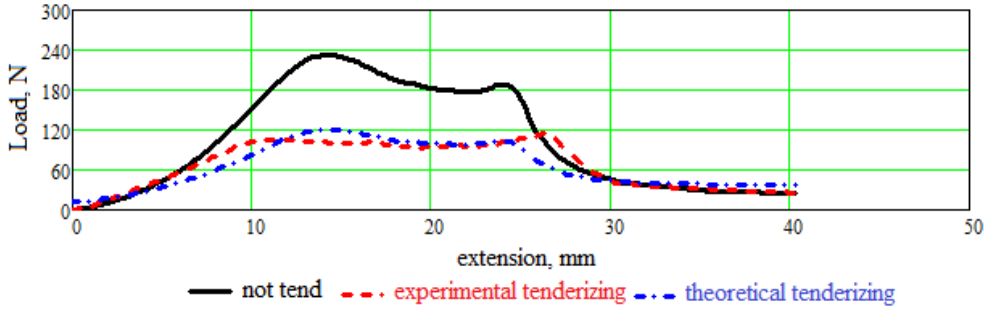

Fig. 12 - Numerical tenderizing CP-FRT 6x curves obtained by using the mathematical model

CONCLUSIONS

Considering physically issues, mechanical tenderizing is a process that has to reduce the meat's mechanical characteristics amounts of the final product. Each tenderizing method produces significant changes of specific strain within the meat's tissues, which determines the tenderness' improvement.

The main conclusion drawn in this paper refers to the correctness of the mathematical model based on proposed linear transformation, proved both by the curves' configurations and the maximum amounts similarities' between the numerical tenderizing curves, too, and the average curves experimentally determined, respectively.

Further general and specific conclusions could be draw after this mathematical model will be applied for other types of meat, before and after the same or other mechanical tenderizing methods.

The data presented in this paper can be important for all the specialists interested in decreasing the wet curring period of the traditional meat products.

REFERENCES

[1]. Bobancu V., Mihaileanu N., Gheorghita S., Brezuleanu A., Stefanescu A., Balanescu T. (1994) - *Dictionary of general mathematics*, Romanian Enciclopedic Publishing, pg. 292-293;
[2]. Graiver N., Pinotti A., Clifano A., Zaritzky N. (2009) -

CONCLUZII

Din punct de vedere fizic, frăgezirea mecanică este un proces care trebuie să reducă valorile caracteristicilor mecanice ale produsului finit. Fiecare metodă de frăgezire produce modificări semnificative a tensiunii specifice din interiorul ţesuturilor cărnii, care determină îmbunătăţirea frăgezimii.

Concluzia principală a acestei lucrări se referă la corectitudinea modelului matematic bazat pe transformarea liniară propusă, dovedită atât prin configuraţia curbelor, şi de asemenea prin similitudinea dintre valorile maxime dintre curbele de frăgezire numerice, şi respectiv curbele medii determinate experimental.

Viitoare concluzii generale şi specifice vor fi formulate după ce acest model matematic va fi aplicat pentru alte tipuri de carne, înainte şi după alte metode de frăgezire mecanică.

Informaţiile prezentate în această lucrare pot fi importante pentru toţi specialiştii interesaţi în reducerea perioadei de sărare umedă a produselor tradiţionale din carne.

BIBLIOGRAFIE

[1]. Bobancu V., Mihaileanu N., Gheorghita S., Brezuleanu A., Stefanescu A., Balanescu T. (1994) – *Dicţionar general de matematică*, Editura Enciclopedică din România, pag. 292-293;
[2]. Graiver N., Pinotti A., Clifano A., Zaritzky N. (2009) -

Mathematical modeling of the uptake of curing salts in pork meat, Journal Food Engineering, vol. 95 (4), pg. 533-540;
[3]. Iacob C., Gheorghita S. I., Soare M., Dragos L. (1980) - *Mechanical Dictionary,* Scientific and Enciclopedical Publishing House, Bucharest;
[4]. Ionescu V., Varga A. (1994) - *Systems Theory*, ALL Publising House, Bucharest;
[5]. Institute of Food Technologists (1981) - *Sensory evaluation guide for testing food and beverage products,* Food Technology, 35 (11), pg. 50-59;
[6]. LAROUSSE *Gastronomique* (2000) - Hamlyn, pg. 1204 (ISBN 0-600-60235-4);
[7]. McGee H. (2004) - *On food and cooking, the science and lore of the kitchen*, Scribner, pg. 155 (ISBN 978-0-684-80001-1);
[8]. Roffel B., Betlem B. (2006) - *Process Dynamics and Control, Modelling for Control and Prediction*, John Wiley & Sons Ltd.;
[9]. Roşca A., Roşca D. (2011) - *Instrumental texture evaluation - An objective measuring method for quality assurance in food industry,* Annals of the University of Craiova, Biology, Horticulture, Food produce processing technology, Environmental engineering Series, vol. XLI (LII), Universitaria Publishing House Craiova, pg. 361-367;
[10]. Roşca A., Roşca D. (2013) - *Instrumental texture evaluation - An objective method to evaluate fresh vegetables quality.* Journal Progress of Cryogenics and Isotopes Separation, ICSI-ICIT Rm. Valcea, Vol. 16 (1), pg. 25 - 30;
[11]. Roşca A. (2014) - *Food industry equipment*. Course Support, Agriculture and Horticulture Faculty, University of Craiova;
[12]. Roşca A., Roşca D., Simion A. D. (2014) - *Tenderizing machines for traditional meat products processing,* Journal Progress of Cryogenics and Isotopes Separation, ICSI-ICIT Rm. Valcea, Vol. 18 (1), pg. 15 - 30;
[13]. Shewfelt R. L. (2000) - *Consumer - friendly specifi - cations to meet the demands of a global market,* Food Australia, vol. 52, pg. 311-314;
[14]. Tyszkiewicz I., Klossowska B.M. (1996) - *Mechanical Tenderization of Pork Meat: Protein and Water Release due to Tissue Damage*. Journal of the Science of Food and Agriculture, Vol. 73(2), pg. 179–185;
[15]. Xargayó M., Lagares J., Fernández E., Borrell D., Sanz D. (2012) - *The impact of tenderization on increased slicing yield*. (http://en.metalquimia.com/upload/document/article);
[16]. Xianzhong Xu, Shaofang Yuan (2011) - *An examination of the force generated from incisor penetration into foods with different textural properties. Part I: Experimental observation,* Journal of Texture Studies, Special Issue, Vol. 42 (3), pg. 228 -235;
[17]. www.lloyd-instruments.co.uk (2013);
[18]. US patent 7578732 B2.

Modelarea matematică a infuzării saramurii în carnea de porc, Jurnalul pt. Inginerie Alimentară, vol. 95 (4), pag. 533-540;
[3]. Iacob C., Gheorghita S. I., Soare M., Dragos L. (1980) - *Dictionar de mecanica,* Editura Stiintifica si Enciclopedica, Bucuresti.
[4]. Ionescu V., Varga A. (1994) - *Teoria sistemelor*, Editura ALL, Bucureşti;
[5]. Institutul pentru Tehnologii Alimentare (1981) - *Ghid de evaluare senzorială a produselor alimentare şi băuturilor.* Tehnologii Alimentare, 35 (11), pag. 50-59;
[6]. LAROUSSE *Gastronomie* (2000) - Hamlyn, pag. 1204 (ISBN 0-600-60235-4);
[7]. McGee H. (2004) - *Despre gătirea alimentelor din carne de pui*, Scribner, pag. 155 (ISBN 978-0-684-80001-1);
[8]. Roffel B., Betlem B. (2006) - *Controlul, modelarea şi predicţia proceselor dinamice*, John Wiley & Sons Ltd.;
[9]. Roşca A., Roşca D. (2011) - *Evaluarea instrumentală a texturii - metodă obiectivă a măsurării pentru asigurarea calităţii in industria alimentară*, Analele Universităţii din Craiova, Seriile Biologie, Horticultură, Tehnologia Pro-duselor Alimentare, Ingineria Mediului, vol. XLI (LII), Editura Universitaria Craiova, pag. 361-367;
[10]. Roşca A., Roşca D. (2013) - *Evaluarea instrumentală a texturii - metodă obiectivă a măsurării pentru asigurarea calităţii produselor vegetale proaspete,* Jurnalul Progrese in Criogenie şi Separare Izotopică, ICSI-ICIT Rm. Valcea, Vol. 16 (1), pag. 25 - 30;
[11]. Roşca A. (2014) - *Utilaje pentru industria alimentară*. Suport de curs, Facultatea de Agricultură şi Horticultură, Universitatea din Craiova;
[12]. Roşca A., Roşca D., Simion A. D. (2014) - *Maşini de frăgezire pentru procesarea produselor tradiţionale din carne*. Jurnalul Progrese in Criogenie şi Separare Izotopică, ICSI-ICIT Rm. Valcea, Vol. 18 (1), pag. 15 -30;
[13]. Shewfelt R. L. (2000) - *Îndeplinirea cerinţelor specifice ale consumatorului din piaţa mondială,* Alimente Australia, vol. 52, pag. 311-314;
[14]. Tyszkiewicz I., Klossowska B.M. (1996) - *Frăgezirea mecanică a cărnii de porc: eliminarea apei şi proteinelor datorită deteriorării ţesuturilor,* Jurnalul de Ştiinţe pentru Alimentaţie şi Agricultură, Vol. 73(2), pag. 179 – 185;
[15]. Xargayó M., Lagares J., Fernández E., Borrell D., Sanz D. (2012) - *Impactul frăgezirii asupra creşterii limitei de feliere*. (http://en.metalquimia.com/upload/document/article);
[16]. Xianzhong Xu, Shaofang Yuan (2011) - *Examinarea forţei de penetrare a dinţilor incisivi în alimente cu diferite texturi. Partea I: Observaţii experimentale,* Jurnalul pentru Studii ale Texturii, Special Issue, Vol. 42 (3), pag. 228 -235;
[17]. www.lloyd-instruments.co.uk (2013);
[18]. US patent 7578732 B2.

WRITING NORMS / *NORME DE REDACTARE*

Article Types

Three types of manuscripts may be submitted:

1. Regular articles: These should describe new and carefully confirmed findings, and experimental procedures should be given in sufficient detail for others to verify the work. The length of a full paper should be the minimum required to describe and interpret the work clearly (max. 8 pages);

2. Short Communications: A Short Communication is suitable for recording the results of complete small investigations or giving details of new models or hypotheses, innovative methods, techniques or apparatus. The style of main sections has not necessarily to be in accordance with that of full-length papers (max. 6 pages);

3. Reviews: Submissions of reviews and perspectives covering topics of current interest are welcome and encouraged (max. 8 pages).

Review Process

All manuscripts are reviewed by the 2 members of the Scientifically Review. Decisions will be made as rapidly as possible, and the journal strives to return reviewers' comments to authors in approx. 3 weeks. The editorial board will re-review manuscripts that are accepted pending revision.

NOTE: Submission of a manuscript implies: that the work described has not been published before (excepting as an abstract or as part of a published lecture, or thesis) that it is not under consideration for publication elsewhere.

1. REGULAR ARTICLES

- All portions of the manuscript must be typed *single-spaced, A4***,** top and bottom: 2 cm; left: 2 cm; right: 2 cm, font: **Arial,** size 9 pt, except the title which will be 11 pt. and explicit figures, which will be 8 pt.
- Text paper will be written in two equal columns of 8.3 cm, 0.4 cm space between them, except the title, authors and their affiliations, tables, figures, graphs and equations to be entered once.
- Text will be written in English in the left column, respectively in native language in the right column.
- The chapter titles are written Uppercase (eg: INTRODUCTION, MATERIAL AND METHODS), between chapters is left a space for 9 pt. At the beginning of each paragraph to leave a tab of 0.5 cm.
- The paper will be written in Word, "Justify" alignment;
- The paper should be transmitted by E-mail.
- There are allowed 2 papers by each first author.

The **Title** should be a brief phrase describing the contents of the paper. PAPER'S TITLE will be uppercase, Bold (the title in English language) and *Bold italic (the title in native language),* center, 11 pt. Under the paper's title, after an space (enter) 9 pt., write *authors' names* (eg: Vasilescu G.). (font: 9 pt., bold) and *affiliations*, the *name of the corresponding author* (next row), (9 pt., regular). Also be passed: the phone, fax and E-mail information, for the first author of paper's (font: 8 pt., italic).
Title should be short, specific and informative. Avoid long titles; a running title of no more than 100 characters is encouraged (without spaces).

The ***Abstract*** should be informative and completely self-explanatory, briefly present the topic, state the scope of the experiments, indicate significant data, and point out major findings and conclusions. The Abstract should be 100 to 300 words in length. Complete sentences, active verbs, and the third person should be used, and the abstract should be written in the past tense. Standard

Tipuri de Articole

Trei tipuri de manuscris pot fi trimise:

1. Articole obişnuite (normale): acestea trebuie să descrie cercetări noi şi confirmate, iar procedurile experimentale să fie descrise pentru a putea fi verificate in detaliu, fără a leza dreptul de proprietate intelectuală. Mărimea unei lucrări trebuie să cuprindă minimul necesar pentru a descrie şi interpreta în mod clar conţinutul (max.8 pagini);

2. Comunicări scurte: o comunicare scurtă este folosită pentru înregistrarea rezultatelor din investigaţii complete de dimensiuni reduse sau pentru a oferi detalii despre modele noi de ipoteze, metode inovative, tehnici sau infrastructuri. Tipul secţiunilor (capitolelor) principale nu trebuie să fie neapărat în concordanţă cu articolele normale (max. 6 pagini);

3. Sintezele: Prezentarea unor comentarii şi perspective acoperind subiecte de interes actual sunt binevenite şi încurajate (maxim 8 pagini).

Procesul de evaluare (recenzie)

Toate manuscrisele sunt evaluate de către 2 membri ai Comitetului Ştiinţific. Deciziile vor fi luate cât mai rapid posibil şi revista va returna comentariile evaluărilor înapoi la autori în aproximativ 3 săptămâni. Conducerea editorială va reevalua manuscrisele care sunt acceptate în vederea publicării în revistă.

Notă: Sunt acceptate numai lucrările care nu au mai fost publicate anterior. În cazul în care autorii trimit spre publicare lucrări ce conţin date, informaţii, capitole, etc., din alte lucrări publicate anterior şi nu se fac referiri la acestea în text, răspunderea aparţine acestora.

1. ARTICOLE OBIŞNUITE

- Toate capitolele manuscrisului trebuie să fie scrise *single-spaced, A4***,** sus şi jos: 2 cm; stânga: 2 cm; dreapta: 2 cm, font: **Arial,** mărime 9 pt, cu excepţia titlului care se scrie cu 11 pt. şi figurile explicite, care se scriu cu 8 pt.
- Textul lucrării va fi scris în două coloane egale de 8,3 cm, 0,4 cm spaţiul dintre ele, exceptând titlul, autorii şi afilierea acestora; tabelele, figurile şi ecuaţiile care nu se scriu pe coloane ci pe toată pagina (vezi modelul ataşat);
- Textul se va scrie în limba engleză în coloana din stânga, respectiv în limba maternă - coloana din dreapta.
- Titlurile capitolelor sunt scrise cu majuscule (ex: INTRODUCERE, MATERIAL ŞI METODE), între capitole se lasă un spaţiu de 9 pt. La începutul fiecărui paragraf se lasă un "tab" de 0.5 cm;
- Lucrarea va fi scrisă în Word, aliniere "Justify".
- Lucrarea trebuie trimisă prin e-mail.
- Sunt permise max. 2 lucrări ca prim autor.

Titlul trebuie să fie o frază scurtă care să descrie conţinutul lucrării. Acesta *va fi scris cu majuscule, centrat*, mărime: 11 pt., bolduit, (titlul in engleză) şi *bolduit italic (titlul în limba maternă)*. Sub titlul lucrării după un spaţiu de 9 pt., se scriu numele autorilor (ex: Vasilescu G.) (9 pt., bold), imediat sub numele autorilor se scrie: afilierea autorilor (9 pt., normal) iar pe următorul rând: telefonul, faxul, e-mailul corespunzător celui care a trimis lucrarea - primului autor (8 pt., italic).
Titlul trebuie să fie scurt, specific şi informativ. Evitaţi titlurile lungi, un titlu de sub 100 caractere este recomandat (fără spaţii).

Rezumatul trebuie să fie informativ şi uşor de înţeles; prezentaţi pe scurt topica, stadiul experimentelor, date semnificative, şi evidenţiaţi descoperirile majore şi concluziile. Rezumatul trebuie să cuprindă între 100 şi 300 cuvinte. Propoziţiile complete, verbele active, şi persoana a III-a trebuiesc folosite (rezumatul să fie scris la timpul trecut). Se va utiliza nomenclatura standard iar abrevierile

nomenclature should be used and abbreviations should be avoided. No literature should be cited (font: 9 pt., the title - *bold italic*; the text of abstract: *italic*).

Following the abstract, about 3 to 10 ***Keywords*** that will provide indexing references should be listed (font: 9, bold italic - the title and 9 pt., *italic* - the text).

A list of non-standard **Abbreviations** should be added. In general, non-standard abbreviations should be used only when the full term is very long and used often. Each abbreviation should be spelled out and introduced in parentheses the first time it is used in the text. Only recommended SI units should be used. Authors should use the Solidus presentation (mg/ml). Standard abbreviations (such as ATP and DNA) need not to be defined.

INTRODUCTION should provide a clear statement of the problem, the relevant literature on the subject, and the proposed approach or solution. It should be understandable to colleagues from a broad range of scientific subjects.

MATERIALS AND METHODS should be complete enough to allow experiments to be reproduced. However, only truly new procedures should be described in detail; previously published procedures should be cited, and important modifications of published procedures should be mentioned briefly. Capitalize trade names and include the manufacturer's name and address. Subheadings should be used. Methods in general use need not be described in detail.

RESULTS should be presented with clarity and precision. The results should be written in the past tense when describing findings in the authors' experiments. Results should be explained, but largely without referring to the literature. Discussion, speculation and detailed interpretation of data should not be included in the Results but should be put into the Conclusions section. Subheadings should be used.

CONCLUSIONS should interpret the findings in terms of the results obtained in this and in past studies on this topic. State the conclusions in a few sentences at the end of the paper. The Results and Discussion sections can include subheadings, and when appropriate, both sections can be combined.

Acknowledgments of people, grants, funds, etc. should be brief (if necessarily).

Tables should be kept to a minimum and be designed to be as simple as possible. Tables are to be typed single-spaced throughout, including headings and footnotes. Each table must be written on the entire width of the page, into the text where reference is made, the columns are broken - one column (see attached sample). Tables should be self-explanatory without reference to the text. The details of the methods used in the experiments should preferably be described in the legend instead of in the text. The same data should not be presented in both table and graph form or repeated in the text. Table's title will be centered bold (in English) and bold italic native language then separated by a slash. In the table, each row will be written in English (Arial, regular, size: 9 pt.) / *native language* (Arial, italic, 9 pt.). The table and its number is written right justified, bold - in English and bold italic - native language, separated by a slash (/).

Figure legends should be typed in numerical order. Graphics should be prepared using applications capable of

trebuiesc evitate. Nu se vor utiliza citări de lucrări în "rezumat" (font: 9 pt., titlu - *bold italic*; textul rezumatului - *italic*).

Cuvinte cheie: ca urmare a rezumatului, între 3 şi 10 cuvinte cheie trebuiesc listate, aceste oferind referinţe de indexare (font: 9 pt., **bold italic** – titlul şi 9 pt., *italic* - textul).

Trebuie adăugată o listă de abrevieri specifice. În general, aceste abrevieri se folosesc atunci când termenul folosit este foarte lung şi des întâlnit în lucrare. Fiecare abreviere ar trebui introdusă în paranteză pentru prima dată când este folosită în text. Doar unităţi din SI trebuiesc folosite. Autorii trebuie să folosească prezentarea Solidus (mg/ml). Abrevierile standard (ca ATP sau ADN) nu trebuiesc definite.

INTRODUCEREA trebuie să ofere o expunere clară a problemei, esenţa relevantă a subiectului şi abordarea propusă sau soluţia. Aceasta trebuie să poată fi înţeleasă de către colegi din diferite domenii ştiinţifice.

MATERIALE ŞI METODE: trebuie să fie suficient de complete pentru a permite experimentelor să fie reproduse. Totuşi, numai metodele cu adevărat noi trebuie descrise în detaliu; metodele publicate anterior trebuie citate; modificările importante ale metodelor publicate trebuie menţionate pe scurt. Scrieţi cu majuscule denumirile comerciale şi includeţi numele şi adresa producătorilor. Subcapitolele trebuie utilizate. Metodele utilizate în general, nu trebuie descrise în detaliu.

REZULTATELE trebuie prezentate cu claritate şi precizie. Acestea trebuie scrise la timpul trecut, atunci când descriu constatările în experimentele autorilor. Rezultatele trebuie să fie explicite, dar în mare măsură, fără a se face referire la literatura de specialitate. Discuţiile, speculaţiile şi interpretarea detaliată a datelor nu trebuie să fie incluse în rezultate, ci trebuie incluse în capitolul Concluzii. Subcapitolele trebuie utilizate.

CONCLUZIILE trebuie să interpreteze constatările în ceea ce priveşte rezultatele obţinute în această lucrare şi în studiile anterioare pe această temă. Concluziile generale vor fi prezentate în câteva fraze la sfârşitul lucrării. Rezultatele şi discuţiile pot include subpoziţii, şi atunci când este cazul, ambele secţiuni pot fi combinate.

Mulţumirile către oameni, cei care au acordat burse, fonduri, etc., trebuie să fie scurte (dacă este necesar).

Tabelele trebuie menţinute la un nivel minim şi să fie proiectate pentru a fi cât mai simple posibil. Tabelele vor fi scrise la un rând, inclusiv titlurile şi notele de subsol. Fiecare tabel trebuie scris pe întreaga lăţime a paginii, între textul în care se face trimitere; coloanele sunt eliminate - o singură coloană (vezi ataşat modelul). Tabelele trebuie să fie auto-explicative, fără referire la text. Detaliile cu privire la metodele utilizate în experimente trebuie să fie, de preferinţă, descrise în legendă şi nu în text. Aceleaşi date nu trebuie prezentate atât în tabel cât şi sub formă grafică (decât dacă este absolut necesar) sau repetate în text. Titlul tabelului va fi scris centrat, bold (în engleză) şi bold italic (în limba maternă), separate de un slash (/). În tabel, fiecare rând va fi scris în limba engleză (9 pt., normal) / limba maternă (9 pt., italic). Tabelul şi numărul acestuia se scrie aliniat la dreapta, bold - în limba engleză şi bold italic în limba maternă, despărţite de un slash (/).

Figurile trebuie scrise în ordine numerică. Grafica trebuie realizată utilizând aplicaţii capabile să genereze JPEG de

generating high resolution JPEG before to introducing in the Microsoft Word manuscript file (Insert - From File - ...jpeg). Use Arabic numerals to designate figures and upper case letters for their parts (Figure 1). Begin each legend with a title and include sufficient description so that the figure is understandable without reading the text of the manuscript. Information given in legends should not be repeated in the text. Each figure must be inserted on the entire width of the page, into the text where reference is made, single columns (see attached sample). Leave a space between the figure and the text of figure, size: 3 pt., figure number is written in **Arial bold**, size: 8 pt., followed by what represent the figure or graph, written with Arial, regular, 8 pt. Left to write in English (regular), followed by a separating slash (/) and text in native language (*Arial italic*). Eg:

Fig 1 - Test stand / *Stand de testare* (size: 8 pt.)

The figures should be "*In line with text*" - Center, not "*Square*"; "*Tight*"; "*Behind text*" or "*In front of text*" (from "*Format picture*" - right mouse button on picture and then "*Layout*".

înaltă rezoluţie, înainte de a introduce în dosarul manuscris Microsoft Word (Insert - From File - ... JPEG). Folosiţi cifre arabe, pentru a desemna cifre şi litere majuscule pentru părţile lor (Figura 1). Începeţi fiecare legendă cu un titlu care să includă o descriere suficientă, astfel încât figura să poată fi înţeleasă, fără citirea textului din manuscris. Informaţiile furnizate în legende, nu trebuie repetate în text. Fiecare figură trebuie introdusă pe întreaga lăţime a paginii, în text, acolo unde se face referire, o singură coloană (vezi ataşat eşantion), centrat. Lăsaţi un spaţiu între figură şi textul figurii, mărimea: 3 pt.; numărul figurii va fi scris cu bold, 8 pct., centrat, urmat de ceea ce reprezintă figura sau graficul, scris cu 8 pt., normal. Prima dată se scrie textul în limba engleză (normal), urmat de un slash (/) apoi textul în limba maternă (italic).

Exemplu:

Fig. 1 - Test stand / *Stand de testare* (mărimea: 8 pt.)

Figurile introduse trebuie să fie "*In line with text*" - Center, nu "*Square*"; "*Tight*"; "*Behind text*" or "*In front of text*" (din "*Format picture*" - butonul dreapta mouse pe figură şi apoi "*Layout*").

Mathematics

Authors must provide instructions on how symbols and equations should be set. Equations should be numbered sequentially in the right-hand side and in parenthesis. They should be referred to in the text as Equation (4) or Eg. (4). Each equation must be written on the entire width of the page, into the text where reference is made, the columns are broken (see attached sample).

Formulele matematice, ecuaţiile: autorii trebuie să furnizeze instrucţiuni privind modul de simbolizare şi de ecuaţii stabilite şi utilizate. Ecuaţiile trebuie numerotate secvenţial, în partea dreaptă şi în paranteze. Ele trebuie menţionate în text ca ecuaţia (4) sau Ex. (4). Fiecare ecuaţie trebuie scrisă pe întreaga lăţime a paginii, în text, acolo unde se face referire, o singură coloană (vezi ataşat model).

REFERENCES: are made in the text; a reference identified by [1], [2], ... [n] is written in the order that was placed at the end of the work - alphabetically.

Example:

[1], [2], [3], ..., [n]

References should be listed at the end of the paper in alphabetical order. Articles in preparation or articles submitted for publication, unpublished observations, personal communications etc. should not be included in the reference list but should only be mentioned in the article text (e.g., A. Danciu, University of Bucharest, Romania, personal communication). Authors are fully responsible for the accuracy of the references.

REFERINŢELE: se fac în text; o referinţă identificată prin intermediul [1], [2], ...[n], se scrie în ordinea în care a fost trecută la sfârşitul lucrării - ordine alfabetică.

Exemplu:

[1], [2], [3], ..., [n]

Referinţele trebuie prezentate la sfârşitul lucrării în ordine alfabetică. Articole în curs de pregătire sau articole trimise spre publicare, observaţiile nepublicate, comunicările cu caracter personal, etc, nu trebuie incluse în lista de referinţă, dar pot fi menţionate în textul lucrării (exemplu, A. Danciu, Universitatea din Bucureşti, România, comunicare personală). Autorii sunt pe deplin responsabil pentru exactitatea referinţelor.

Examples:

Journal / Magazine:

[1]. Nicolescu M.A., (2007) - *Relevant characteristics of alternative liquid fuels aimed at Diesel engines exploitation in polycarburation duty*. INMATEH - Agricultural Engineering, vol. 27, no. 1/2009, ISSN 1583-1019, pg. 50-55;

[2]. Pirna I, Nicolescu M., Marin M., Voicea I., (2009) - *Alternative supply of agricultural tractors with raw oils*. INMATEH - Agricultural Engineering, vol. 29, no. 3/2009, ISSN 1583-1019, pg. 89-92.

Conference / Symposium:

[1]. Bungescu S, Stahli W, Biriş S, Vlăduţ V, Imbrea F, Petroman C., (2009) - *Cosmos programm used for the strength calculus of the nozzles from the sprayers,* Proceedings of the 35 International Symposium on Agricultural Engineering *"Actual Tasks on Agricultural Engineering",* Opatija - Croaţia, ISSN 1333-2651, pg. 177÷184.

Book:

[1]. Vlăduţ V., (2009) - *Studiul procesului de treier în aparatul cu flux axial*, Editura "Terra Nostra", ISBN 973-1888-26-8, Iasi - Romania.

Book Chapter:

[1]. Vlăduţ V., (2009) - Consideraţii şi ipoteze privind modelarea unui proces de treier şi separare. In: *Studiul*

Exemple:

Jurnal / Revistă

[1]. Nicolescu M.A., (2007) - *Proprietăţile relevante ale combustibililor lichizi alternativi vizaţi pentru exploatarea motoarelor Diesel în regim policarburat*, INMATEH - Inginerie Agricolă, vol. 27, nr. 1 / 2009, ISSN 1583-1019, pg. 50-55;

[2]. Pirna I, Nicolescu M., Marin M., Voicea I., (2009) - *Alimentarea alternativă a tractoarelor agricole cu uleiuri vegetale crude,* INMATEH - Inginerie Agricolă, vol. 29, nr. 3 / 2009, ISSN 1583-1019, pg. 89-92.

Conferinţă / Simpozion

[1]. Bungescu S, Stahli W, Biriş S, Vlăduţ V, Imbrea F, Petroman C., (2009) - *Cosmos programm used for the strength calculus of the nozzles from the sprayers,* Proceedings of the 35 International Symposium on Agricultural Engineering *"Actual Tasks on Agricultural Engineering",* Opatija - Croaţia, ISSN 1333-2651, pag. 177÷184.

Carte

[1]. Vlăduţ V., (2009) - *Studiul procesului de treier în aparatul cu flux axial*, Editura "Terra Nostra", ISBN 973-1888-26-8, Iaşi - România.

Capitol din carte

[1]. Vlăduţ V., (2009) - Consideraţii şi ipoteze privind modelarea unui proces de treier şi separare. În: *Studiul*

procesului de treier în aparatul cu flux axial, Editura "Terra Nostra", ISBN 973-1888-26-8, pg. 61-69, Iasi - Romania.

Dissertation / Thesis:

[1]. Constantinescu A., (2010) - *Optimizarea agregatelor formate din tractoare de putere mare cu maşini agricole pentru pregătirea terenului în vederea însămânţării*. PhD dissertation, University of Transylvania Braşov, Romania.

Units, Abbreviations, Acronyms

- Units should be metric, generally SI, and expressed in standard abbreviated form.
- Acronyms may be acceptable, but must be defined at first usage.

2. SHORT COMMUNICATIONS

Short Communications are limited to a maximum of two figures and one table. They should present a complete study that is more limited in scope than is found in full-length papers. The items of manuscript preparation listed above apply to Short Communications with the following differences: (1) Abstracts are limited to 100 words; (2) instead of a separate Materials and Methods section, experimental procedures may be incorporated into Figure Legends and Table footnotes; (3) Results and Conclusions should be combined into a single section.

3. REVIEWS

Summaries, reviews and perspectives covering topics of current interest in the field, are encouraged and accepted for publication. Reviews should be concise (max. 8 pages). All the other conditions are similar with regular articles.

procesului de treier în aparatul cu flux axial, Editura "Terra Nostra", ISBN 973-1888-26-8, pg. 61-69, Iaşi - România.

Disertaţii / Teze de doctorat

[1]. Constantinescu A., (2010) - *Optimizarea agregatelor formate din tractoare de putere mare cu maşini agricole pentru pregătirea terenului în vederea însămânţării*. Teză de doctorat, Universitatea Transilvania Braşov, România.

Unităţi, Abrevieri, Acronime

- unităţile metrice trebuie să fie, în general, SI, şi exprimate în formă prescurtată standard;
- acronimele pot fi acceptate, dar trebuie să fie definite la prima utilizare.

2. COMUNICĂRILE SCURTE

Comunicările scurte sunt limitate la maxim 2 figuri şi un tabel. Acestea trebuie să prezinte un studiu complet, care este mai limitat decât în cazul articolelor normale (de dimensiuni mai mari). Elementele de pregătire a articolelor normale (manuscriselor) enumerate mai sus se aplică şi la comunicările scurte, cu următoarele diferenţe: (1) Rezumatul este limitat la 100 cuvinte; (2) capitolele Materiale şi Metode, Procedurile experimentale pot fi scrise împreună, încorporând figurile şi tabelele; (3) Rezultatele şi Concluziile pot fi combinate într-o singură secţiune.

3. SINTEZELE

Sintezele, comentariile şi perspectivele acoperind subiecte de interes din domeniu sunt încurajate şi acceptate spre publicare. Sintezele trebuie să fie concise şi nu mai mari 8 pagini. Toate celelalte condiţii sunt similare cu cele de la articolele normale (obişnuite), enumerate mai sus.

Edited by: INMA Bucharest
6 Ion Ionescu de la Brad Blvd., sect. 1, Bucharest, ROMANIA
Tel: +4021.269.32.60; Fax: +4021.269.32.73
http://www.inmateh.eu